The Use of GIS and Remote Sensing to Identify Areas at Risk from Erosion in Indonesian Forests: A Case Study in Central Java

A thesis presented in partial fulfilment of the requirements for the degree of Doctor of Philosophy
in Natural Resource Management
at Massey University, Palmerston North,
New Zealand

Endang Savitri

2006

[Since they have become oblivious of God] corruption has appeared on land and in the sea as an outcome of what men's hands have wrought: and so He will let them taste [the evil of] some of their doings, so that they might return [to the right path]

Ar Ruum 30:41

ABSTRACT

Environmental degradation and soil erosion begins when production forests are harvested. Unfortunately, logging cannot be avoided in plantation forests and since this operation can render the land more susceptible to erosion, any negative impacts need to be addressed properly.

Erosion potential is predicted by evaluating the response of land cover, soil and slope to the impact of rainfall and human activities. The role of remote sensing and geographical information systems (GIS) in erosion prediction is to collect information from images and maps; combine and analyse these data so that it is possible to predict the erosion risk.

The objective of this study was to produce a method to identify areas most susceptible to erosion and predict erosion risk. It is intended that the method be used particularly by forestry planners and decision makers so that they can improve forest management, especially during logging.

The study area was within Kebumen and Banjarnegara districts of Central Java, Indonesia. Imagery used included a Landsat 7 satellite image (28th April 2001) and panchromatic aerial photos (5th July 1993). Other data was derived from topographical, soil, and geological maps, and 10 years of daily rainfall data from 17 rainfall stations.

Predicting erosion in this study was done by combining rainfall, slope, geology, and land cover data. The erosion risk was predicted using land cover and soil type and depth. A rainfall map was generated using a thin plate spline method. A slope map was derived from a DEM which was generated by digitizing contours and spot heights from topographic maps. A geological map was derived from Landsat image classification with assistance from a 1:100000 scale geological map; and a land cover map was produced from an interpretation of the Landsat image and aerial photographs.

A stratified classification technique was used to delineate land covers in the study area with an accuracy of 44%. The low accuracy could be attributed to the complexity of the area and the temporal variation in the data acquisition.

The analysis of erosion risk showed that mixed forests and monotype forest experienced high and moderately high erosion risk. This condition supported the contention that harvest plans must incorporate soil conservation measures.

ACKNOWLEDGEMENT

In the name of Allah, the Most Gracious, the Most Merciful. All the praise and thanks to Allah, the Lord of mankind, jinn and all that exists. With His permission, finally, I can finish my work.

I would express my gratitude to all of my supervisors, for all of your supervision, support, encouragements and guidance. To Associate Prof. John D. Holland, thank you so much for sharing your knowledge in "how to do a good research" and managing references, to Mr. Mike P. Tuohy, thank you for your patience, and understanding when it comes to reading my thesis, and last but not least, many warm thanks to Mr. Robert G. Gibb for all of your unexpected questions that help me think for a better solution. Without you all I don't think any of this would be possible.

My appreciation goes to NZAID who awarded me with this scholarship so I can have the opportunity to study in Massey University pleasantly. Recognition goes to Sylvia Hooker and Sue Flynn from International Student Support Offices who help me with my personal and study problems.

Special thanks go to Matthew Irwin who helps me time and time again with the GIS and Remote Sensing and the special lessons on Vegemite. To Robert Murray, Hayden Lawrence, and Mark Coetzee, you guys have made my life more cheerful and happier. To Dr. Ian Yule thank you for allowing me to have a little "taste" of the life in NZCPA.

Many thanks also go to my Indonesian friends: Yuliana Yosaatmaja who was by my side during those bad days. I would also like to extend my deepest gratitude to Erna and Trie Priantoro, Novia and Cahyo Setyawan, Tiara Parahita and Gusrini Tambunan for all of your support, friendship and kindness.

To Prof. Sutikno from Gadjah Mada University in Indonesia, appreciation is given for the brief geological lecture and Mr. Sadhardjo Siswamartana for the information about Perum Perhutani. Many thanks go to Mr. Nugroho S. Priyono and Mr. Irfan B. Pramono for giving the permission to use the secondary data from the study area, Eko Priyanto and other staffs of Watershed Management Technology Center in Solo who

have helped me to collect the data.

To everyone else who were not mentioned here, thank you for everything that you have done for me. It is not that you are unrecognised, but there are too many of you to mention. Without all of your support I will not be like I am today.

Last but not least, I would give my very special thanks to my sister Endang Sasanti who always be by my side in those hard days, who knows how to cheer me up when I am down and laugh with me when I am happy. Thank you for the full supports that are readily given and I would like to dedicate my thesis to you.

ABBREVIATIONS

asl	: above sea level
Bakosurtanal	: *Badan Koordinasi Survey dan Pemetaan Nasional* (National Coordinating Agency for Surveys and Mapping)
CRES	: Centre for Resource and Environmental Studies
DEM	: Digital Elevation Model
DN	: Digital Number
DOS	: Dark Object Subtraction
DPI	: Dot per Inch
ETM	: Enhanced Thematic Mapper
GCP	: Ground Control Point
GIS	: Geographical Information System
IDW	: Inverse Distance Weighted
ISODATA	: Iterative Self-Organizing Data Analysis
ITTO	: International Timber Trade Organization
LAI	: Leaf Area Index
LIPI	: *Lembaga Ilmu Pengetahuan Indonesia* (Indonesian Institute of Sciences)
NDVI	: Normalised Difference Vegetation Index
RGB	: Red – Green – Blue
RMS Error	: Root Mean Square Error
RTGCV	: (Square) Root of Generalised Cross Validation
RTMSE	: (Square) Root of Mean Square Error
SCS	: Sun – Canopy – Sensor
SFM	: Sustainable Forest Management
SJFCSP	: South Java Flood Control Sector Project
SPOT	: *Satellite pour l'Observation de la Terre*

STS	: Sun – Terrain – Sensor
USLE	: Universal Soil Loss Equation
UTM	: Universal Transverse Mercator
WRS	: World Reference System

TABLE OF CONTENTS

LIST OF FIGURES

LIST OF TABLES

INTRODUCTION

1.1 Background

Forests are a specific form of land use in which a complex set of relationships between the flora and fauna exist. This complexity is shown in the many definitions offered from different viewpoints when people consider forests (Convention on Biological Diversity, 2002). The Ministry of Forestry of Indonesia defines 'forest' as 'a relationship between the land and its natural resources -which are dominated by trees- into a non-separated ecosystem' ("UU No. 41 tentang Kehutanan [*The Law Number* 41 *on Forestry*]," 1999). Smith (1993) identified a forest as 'a living collection of various trees growing in a certain place for quite a long time': while a standard definition of forest made by FAO (1999 Annex 2: Definitions) is:

> '...ecosystem with a minimum of 10 percent crown cover of trees and/or bamboos generally associated with wild flora and fauna and natural soil conditions, and not subject to agriculture.'

These definitions show that a forest consists of enough trees to differentiate them from trees planted around houses to mark a property boundary, and also those planted in agricultural areas

Depending on the extent of human interference, forests can be classified as either natural forests or plantation forests. The Forest Stewardship Council International Centre (2000) defines natural forest as 'areas where many principal characteristics and key elements of native ecosystems such as complexity, structure and diversity are present'. Plantation forest is defined as 'a forest established by planting and/or seeding for reforestation or afforestation. It usually consists of even-aged and single species which will be harvested at the same time. Plantation forest is a result of the human activities of planting, sowing or intensive silvicultural treatments' (Forest Stewardship Council International Center, 2000). There is little human interference in a natural forest.

Environmental degradation occur when people harvest natural or plantation forests. Erosion will begin whenever forests are logged. Compared with erosion studies in agricultural areas, erosion research in forested areas is not widespread, however, some work on erosion measurement in natural and plantation forests is being done in Indonesia – Lal (1990b), Kusumandari & Mitchell (1997), and Priyono & Savitri (1998) are some of those who have measured erosion in forests.

Logging is unavoidable in plantation forests and the activity triggers soil erosion and degradation. Indonesia's forestry sector makes a significant contribution to the economy through its creation of between three and four man-years of work each year, and during the last decade forestry accounted approximately 16 percent of all foreign exchange earnings (Nasendi, 2000). Since logging must be done, the negative impact of logging has to be addressed properly. Indonesia's membership of the International Timber Trade Organization (ITTO) means that it must subscribe to the organisation's Sustainable Forest Management (SFM) criteria, one of which is soil and water protection within the forest (Higman *et al.*, 1999). Logging should lead to as little erosion as possible thus requiring that logging companies improve their understanding of the impact of logging on the soil resource.

It is possible to predict areas susceptible to erosion by evaluating indicators such as the slope of land, rainfall, and soil types. The prediction tools, however, need to be sensitive to regional and local environmental characteristics (Renschler, 2000) which means that the available methods have to be adjusted to the local conditions before they can be utilized (Boggs *et al.*, 2001). With some adjustments, the forest planners can better visualise the areas at risk by plotting the predicted erosion sites on a map, and then make the appropriate changes to the planting or harvesting operations.

In reality Indonesia has already adopted some erosion models such as (R)USLE, ANSWERS and AGNPS (Asdak, 2002; Hidayat, 2002; Kusumandari & Mitchell, 1997) with or without modifications. Since those erosion models were developed in the United States or Europe, it is necessary to consider whether it is applicable for Indonesian conditions and if all the parameters for that model need to be taken into account or not. Sometimes a model requires data that is difficult to collect due to lack of equipment. For instance, Hidayat (2002) noted that the application of ANSWERS in

some watersheds in Java have not been successful because of the failure in completing all the required input parameters, due mainly to the unavailability of instruments to measure flow rate and sediment loads. The size of monitoring unit is another problem. AGNPS, for example, works in a grid system, and each grid (0.4 – 1 ha) should be homogeneous (Dillaha *et al.*, 2001). This condition is difficult to be applied in Indonesia since the average size of landownership is 0.4 ha (Central Board Statistics of Kebumen Regency, 2003; Pemerintah Kab. Banjarnegara, 2003).

In addition to the difficulties in applying the available erosion models, Trippett (2002) found that the Indonesian Government does not have up-to-date maps of land-use and forest conditions. This restricts forest planners from building proper afforestation and logging plans.

Taking all these factors into consideration, it is clear that a method of predicting soil erosion during forest operations (especially tracking and logging) is important, and the chosen model should have simple data requirements, and importantly, must be applicable to a variety of regions with minimum calibrations (Renschler & Harbor, 2002). Consequently, there should be a thorough study before a model is implemented for Indonesia's conditions. It means that proposing a method that uses data which are already available will be more likely to succeed rather than choosing a method, then modifying the data.

1.2 Problem Statement

Limited technical and human resources in the forestry sector in Indonesia have contributed to insufficient forestry planning, management and harvesting practices. As a consequence, forest management planners have paid little heed to potential erosion sites and this may have considerable environmental consequences. While erosion prediction forecasting methods are available, there are still problems when it comes to applying them. Therefore, a more reliable method that can use limited data to predict areas at risk of erosion, especially in forest areas in Indonesia, is needed to reduce environmental degradation and support Indonesia's stated objective of wanting to adopt a sustainable forest management strategy.

1.3 Aim and Objectives

The aim of this research is to contribute to Indonesia's SFM Strategy by employing remote sensing and GIS technology to produce a method that identifies areas most at risk from effects of erosion.

Maps resulting from this method could then be used by forestry agencies as auxiliary data to improve their planning, especially logging planning. Using this information they could reduce the impact of erosion caused by logging.

To achieve this aim several objectives have been determined, as follows:

- To compile maps and prepare the available data to comply with the analysis
- To achieve this objective the following is required:
    - The creation of a DEM from topographical maps
    - The creation of rainfall surfaces from daily rainfall data
- To interpret satellite and aerial imagery to be incorporated in a GIS by performing:
    - Atmospheric and topographic corrections
    - The classification of land cover and geological type
- To identify the erosion factors
- To develop a method to determine the areas at risk from erosion by determining:
    - Erosion likelihood
    - Erosion consequence
    - Erosion risk

1.4 Limitations of the Study Area

This study used a Landsat 7 ETM+ satellite image, 1:20000 aerial photographs, 1:100000 soil and geological maps and 1:25000 topographic maps. All of the methods used were developed specifically for the study area. The analysis techniques were applied both to the satellite image (with 30 metre resolution) and the aerial photograph with differing results. The analysis has not yet been tried in other areas; therefore all values used in this study, especially image thresholds, may need to be adjusted to local conditions when applied in other areas.

1.5 Contribution of the Research

The results of this study will be useful to decision makers and planners in the Indonesian forestry sector. By identifying areas prone to erosion, it will give forestry planners the opportunity to include soil conservation practices in their logging plans, thereby reducing erosion and contributing to sustainable timber production in Indonesia.

The method developed in this study to predict areas at risk from erosion will extend the knowledge of predicting erosion. Until recently, the environmental consequence of erosion and erosion risk were seldom taken into account in forest planning in Indonesia. Now erosion risk values are understood to be important considerations when decision makers decide whether a forest is worth logging or not.

Another contribution to knowledge is based on the fact that this method requires minimum data inputs, that are generally available or easily gathered in Indonesia, to predict erosion-prone sites.

1.6 Structure of the Thesis

This thesis consists of seven chapters and is divided into two parts, namely, Preparation and Analysis. The Preparation part consists of compiling the available data and processing the Landsat image to classify the land cover. This part also describes how to prepare the available data to comply with the analysis. The Analysis part describes and discusses the processing to predict areas at risk from erosion, using both Landsat imagery and aerial photos and other auxiliary data. This part also describes how to

surrogate unavailable information from the available data. The chart in Figure 1-1 shows the progression from one chapter to another, and also where the factors influencing erosion were derived and then used for subsequent analysis.

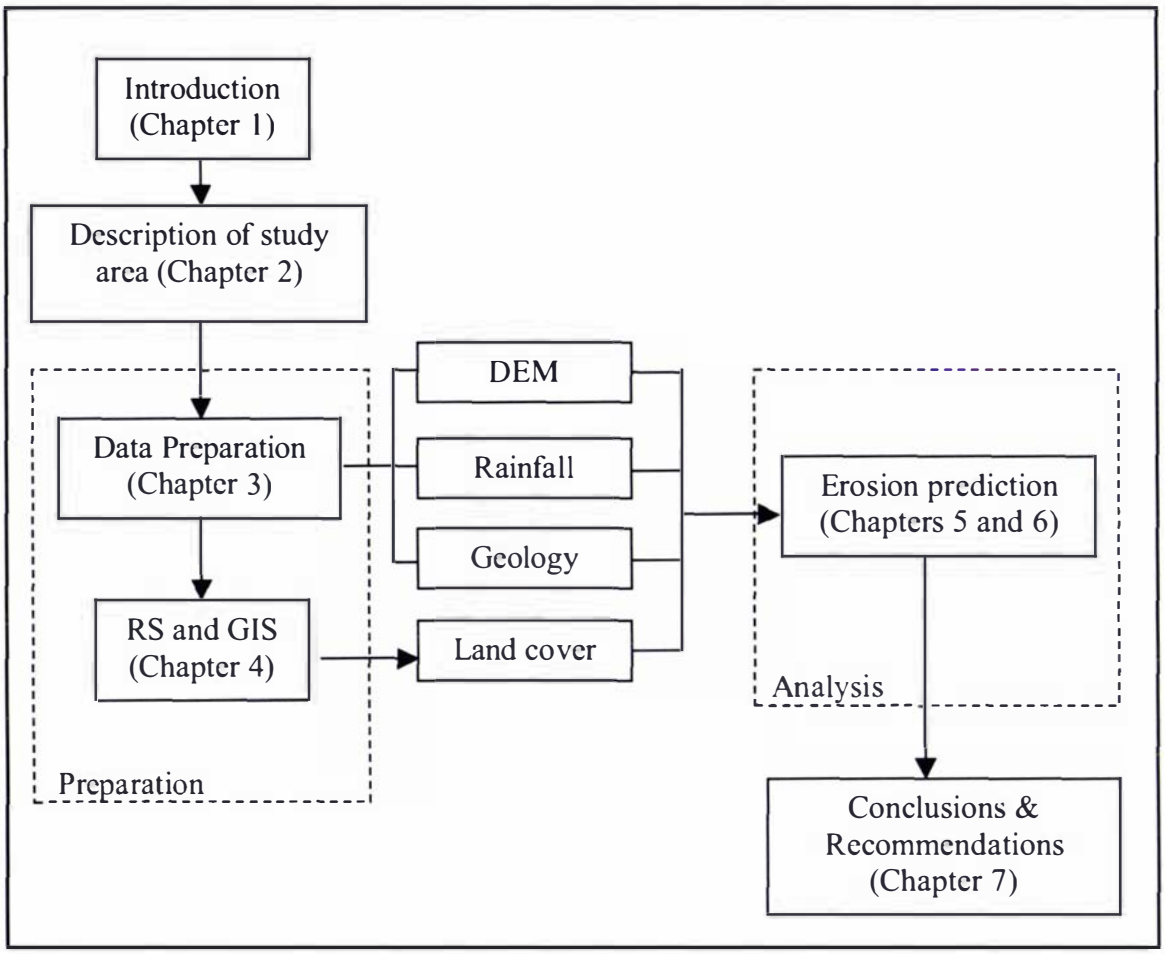

Figure 1-1 The Structure of the Thesis

In **Chapter 1** the background of the study, its limitations and a description of how the thesis is written are presented.

In **Chapter 2** the study area is described in detail. The climate, including precipitation data and the number of rainfall stations, is explained and photographs that show erosion occurring within the study area are also presented.

In **Chapter 3** the imagery and maps that are used are presented. It describes how a DEM was built from contour data and rainfall surfaces were estimated from rainfall data. The DEM and rainfall maps were used for predicting erosion. The rainfall surface

development is discussed intensively by comparing two different methods. This chapter also presents the existing geological map as interpreted by a classification of the Landsat image.

In **Chapter 4** both image processing and Geographical Information Systems methods used to extract land cover by classifying the Landsat image are described. Like Chapter 3, this chapter describes how to prepare land cover information to be used in the analysis in Chapters 5 and 6. The chapter concludes with a discussion of the classification's accuracy when compared with actual conditions as recorded in photographs taken on the ground.

In **Chapter 5** the result of Chapters 3 and 4 are used to predict erosion. A method is developed to predict erosion using a Landsat image and maps as auxiliary data. Unlike more typical erosion prediction methods, environmental values are used to predict the risks of erosion. The implications for forest planning of being able to predict erosion 'hotspots' are also discussed.

Using a similar methodology as described in Chapter 5, in **Chapter 6** two sub-catchments within the study area are studied; an aerial photo is interpreted for the land cover map instead of a Landsat image. The differences between the erosion predicted in Chapter 5 and in this chapter are also discussed.

In **Chapter 7** the conclusions of each chapter are brought together into a general conclusion and recommendations for future work are offered.

DESCRIPTION OF STUDY AREA

2.1 Introduction

The study area covers two districts in the southern part of Central Java in Indonesia, namely Banjarnegara and Kebumen. Banjarnegara is located in the northern part of the study area and Kebumen is situated in the southern part. The total study area is 88,551.6 ha and covers 10% of the Banjarnegara district and 60% of the Kebumen district (Pemerintah Kab. Banjarnegara, 2003; Pemerintah Kab. Kebumen, 2002).

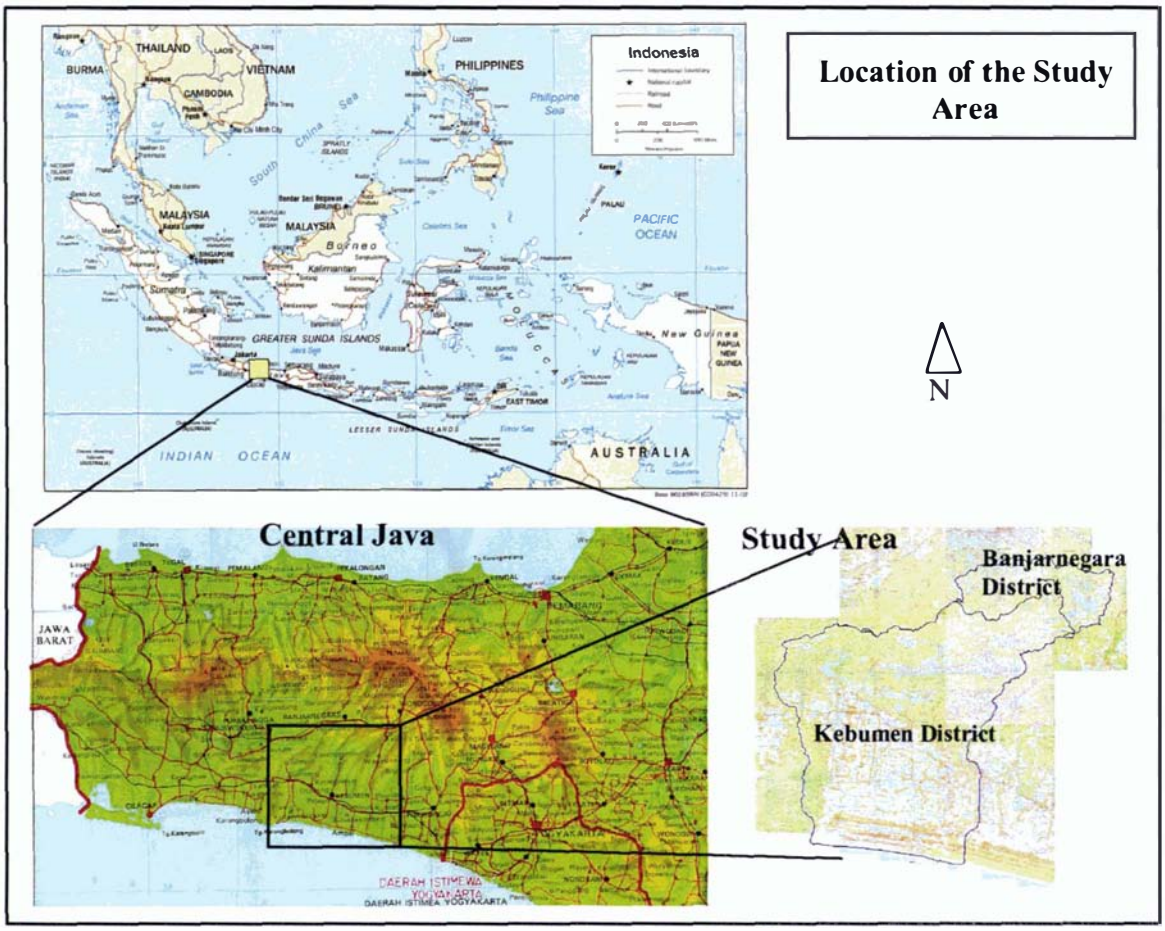

Figure 2-1 Location of the study area

The Kebumen district is relatively flat in the southern part and hilly and mountainous in the northern part, while the Banjarnegara district is steeper and more mountainous. Within Kebumen, there is a complex fault zone with a unique geological structure. Some of the rocks are mined, for example limestone, rock phosphate, bentonite, and

asbestos (Pemerintah Kab. Kebumen, 2002). Furthermore, because the complexity of the geological structure this area has been used as a field laboratory by local universities since 1964. In 2002 this field laboratory became the Centre of Geological Information and Conservation under *Lembaga Ilmu Pengetahuan Indonesia/LIPI* (=Indonesian Institute of Sciences).

The reef limestone and breccias in the southern part of Kebumen were mined extensively with subsequent damage to the environment. To reduce this degradation, the government took control of the allocation of mining rights in 1995 and people now have to ask permission to mine the limestone (Pemerintah Kab. Kebumen, 2002).

The southern part of Banjarnegara, which is located in the northern part of the study area, is hilly with steep slopes and comprised mainly of limestone: it forms part of South Serayu Mountain. Minerals found here include marble, quartz, feldspars, asbestos, andesitic rock, sandstones, limestone, and pebbles (Pemerintah Kab. Banjarnegara, 2003). These minerals contribute to the income of Banjarnegara district.

Kebumen rises from sea-level to 750 metres, while in Banjarnegara the elevation ranges between 40 and 2,300 metres (Pemerintah Kab. Banjarnegara, 2003).

2.2 Population

The populations of Kebumen and Banjarnegara, according to the 2002 data, are 1,193,978 and 864,483, and spread out over 26 and 20 sub-districts respectively (Central Board Statistics of Kebumen Regency, 2003; Pemerintah Kab. Banjarnegara, 2003). The labour force (all persons over 10 years old are called labour units) comprises 67% of the total population in Kebumen. Most work in the agricultural sector, public services, industries, hotels, trades, transportation or communication. The average area of privately owned land in the study area is around 0.4 ha (Central Board Statistics of Kebumen Regency, 2003; Pemerintah Kab. Banjarnegara, 2003).

Transportation and associated infrastructure in both districts is in moderate condition. All villages are connected, although not all roads can be used by cars. The modes of transportation include bicycles, motor cycles, cars, minibuses and buses (Central Board Statistics of Kebumen Regency, 2003; Pemerintah Kab. Banjarnegara, 2003).

2.3 Climate

Average annual rainfall in the study area is 2750 mm. The temperature ranges from 20 °C to 32 °C and relative humidity varies between 70% and 96%. Average sunlight is 5 hours (in the wet season) and 8 hours (in the dry season) and the typical wind velocity is a moderate 0.75 to 2.50 metres/second. Overall, there is not much difference in terms of climate between the dry and wet season in the study area, except that the rainfall during the wet season is higher than the dry season (Central Board Statistics of Kebumen Regency, 2003; Pemerintah Kab. Banjarnegara, 2003; Pemerintah Kab. Kebumen, 2002).

2.3.1 Precipitation

Rainfall is an important contributing factor to erosion. Raindrops and water runoff can detach, transport and then deposit soil particles (Toy *et al.*, 2002). When rainfall is light and the soil dry it does not always lead to erosion. Xie *et al.* (2002) found that 12 mm/hour is the threshold value when rain becomes heavy, turns into runoff and begins to erode the landscape.

In the study area, rainfall data was obtained from thirteen rainfall stations in Kebumen and five stations in Banjarnegara. Each station is located in each sub-district, and the rain gauge usually is placed in the sub-district offices. Most rainfall data has been recorded from the period between 1991 and 2000. Table 2-1 shows the data availability for each rainfall station, their average rainfall and elevation.

Rainfall is a complex process that is influenced by topography and prevailing wind direction (Goovaerts, 2000; Hutchinson, 1998b). Rainfall is influenced by the topography and data from stations at different elevations bear this out. Since information about the exact location of each rain gauge used in this study is needed for further analysis, and there is no information about that exact location, therefore it is assumed that all rain gauges are positioned in the sub-district offices. Using this assumption the coordinates, altitude and aspect of each rain gauge is able to be determined from the Digital Elevation Model (DEM).

Table 2-1 The data availability in each station, average rainfall (mm/year) and associated elevation values (m)

Station	Data availability		Average rainfall (mm)	Elevation (m)
Kebumen				
Adimulyo	10 years	(1991 – 2000)	2659	5
Aliyan	7 years	(1991 – 1997)	2815	39
Gombong	10 years	(1991 – 2000)	3226	22
Karang Anyar	9 years	(1991 – 1997 and 1999 – 2000)	2476	17
Karang Gayam	9 years	(1991 – 1996 and 1998 – 2000)	2754	105
Kebumen	7 years	(1993 – 1995 and 1997 – 2000)	2514	18
Klirong	10 years	(1991 – 2000)	3021	9
Kuwarasan	9 years	(1991 – 1997 and 1999 – 2000)	2828	0
Petanahan	8 years	(1991 – 1995 and 1998 – 2000)	3242	9
Puring	9 years	(1991 – 1997 and 1999 – 2000)	3084	8
Rowokele	10 years	(1991 – 2000)	3019	50
Sadang	5 years	(1992, 1994, 1995, 1998, 1999)	3750	46
Sempor	8 years	(1992 – 1998 and 2000)	3946	62
Banjarnegara				
Banjarnegara	9 years	(1991 – 1999)	4137	286
Kaliwiro	10 years	(1991 – 2000)	3646	---
Mandiraja	6 years	(1991 – 1996)	3292	114
Purwonegara	4 years	(1992 – 1995)	2827	133
Wadas Lintang	8 years	(1993 – 2000)	3864	265

In Table 2-1 the average rainfall and elevation for each station are presented while the relationship between average rainfall and elevation is shown in Figure 2-2. From Figure 2-2 it can be seen that the relationship between average rainfall and elevation is not well defined. Since the R^2 for a linear correlation is low (0.37), it shows that the elevation is not the only factor that influences the rainfall.

Since Kaliwiro is located outside the extent of the DEM, this station is omitted from the record. From this point forward the number of rainfall stations used for this study is 17; 13 are located in Kebumen and 4 stations are in Banjarnegara.

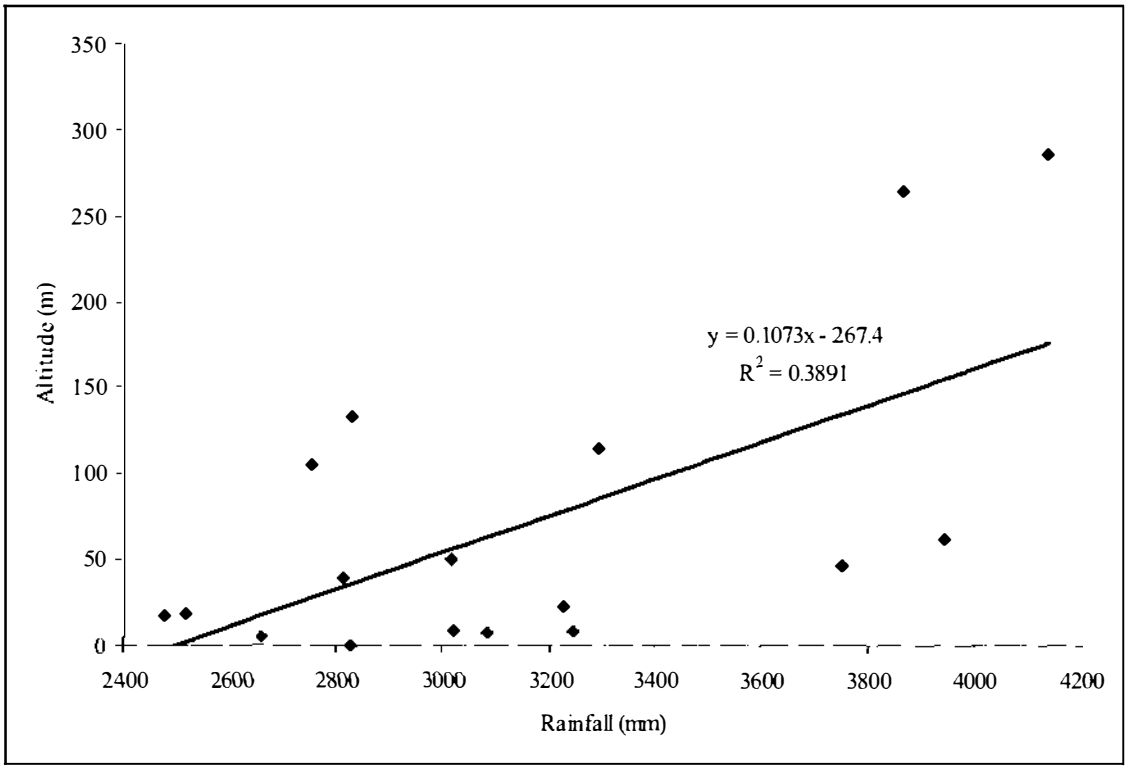

Figure 2-2 The correlation between rainfall and altitude for each rainfall station in the study area

To see the distribution of rainfall in the study area, the rainfall data were calculated monthly and averaged for all stations and all years (see Figure 2-3). The dry season occurs from May to September, while the wet season occurs from October to April. This pattern is influenced more by the monsoon climate than elevation. According to the climatic classification made by Schmidt & Ferguson (Waryono *et al.*, 1987), the

study area is classified as a moderately wet climate (C) with seven wet months (rainfall > 200 mm/month) and three dry months (rainfall < 100 mm/month).

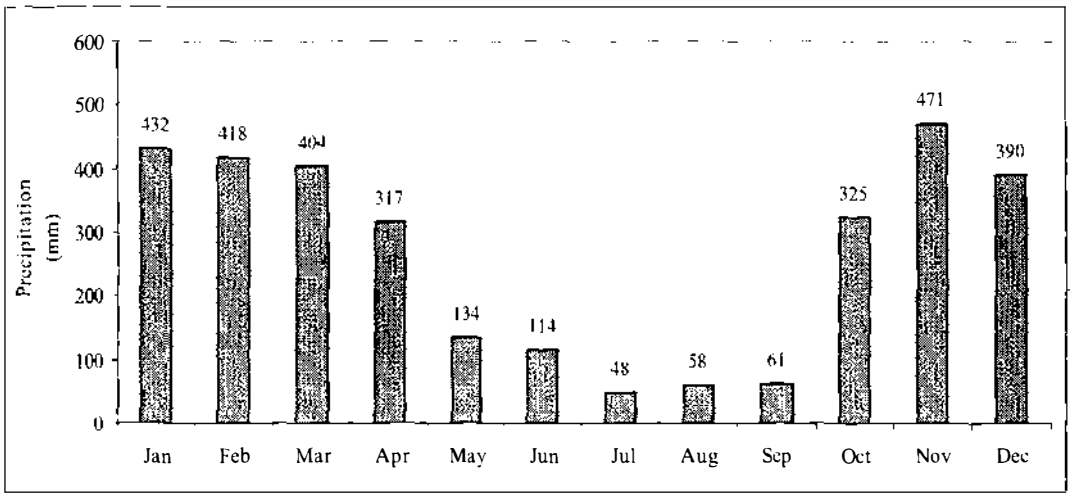

Figure 2-3 Rainfall pattern of the study area for the whole year

The rainfall pattern presented in Figure 2-3 is used as a source to make sure that during the wet months (from October to March the coming year) the ground is not bare and all soil conservation construction activities have to be done before the wet months are started.

2.4 Study Area Catchment

The study area covers the catchment of two main rivers: Luk Ulo and Telomoyo that both empty into the Indian Ocean. Managers use catchment units since erosion and runoff is often a watershed-based problem (El-Swaify, 1993). Another reason for using a catchment as a management unit is that any land cover changes will affect the characteristics of the watershed and consequently they will change the erosion rate as well (Cleaves, 2003). Since this study is dealing with erosion, the use of the catchment (watershed) as a management unit is an appropriate approach.

The delineation of the study area catchment was done manually by digitising boundaries according to the river networks and contours. The watershed boundary was also determined using the WATERSHED module in IDRISI. The main rivers and some of

their tributaries are presented in Figure 2-4, whilst in Figure 2-5 a comparison is made between two catchment delineations.

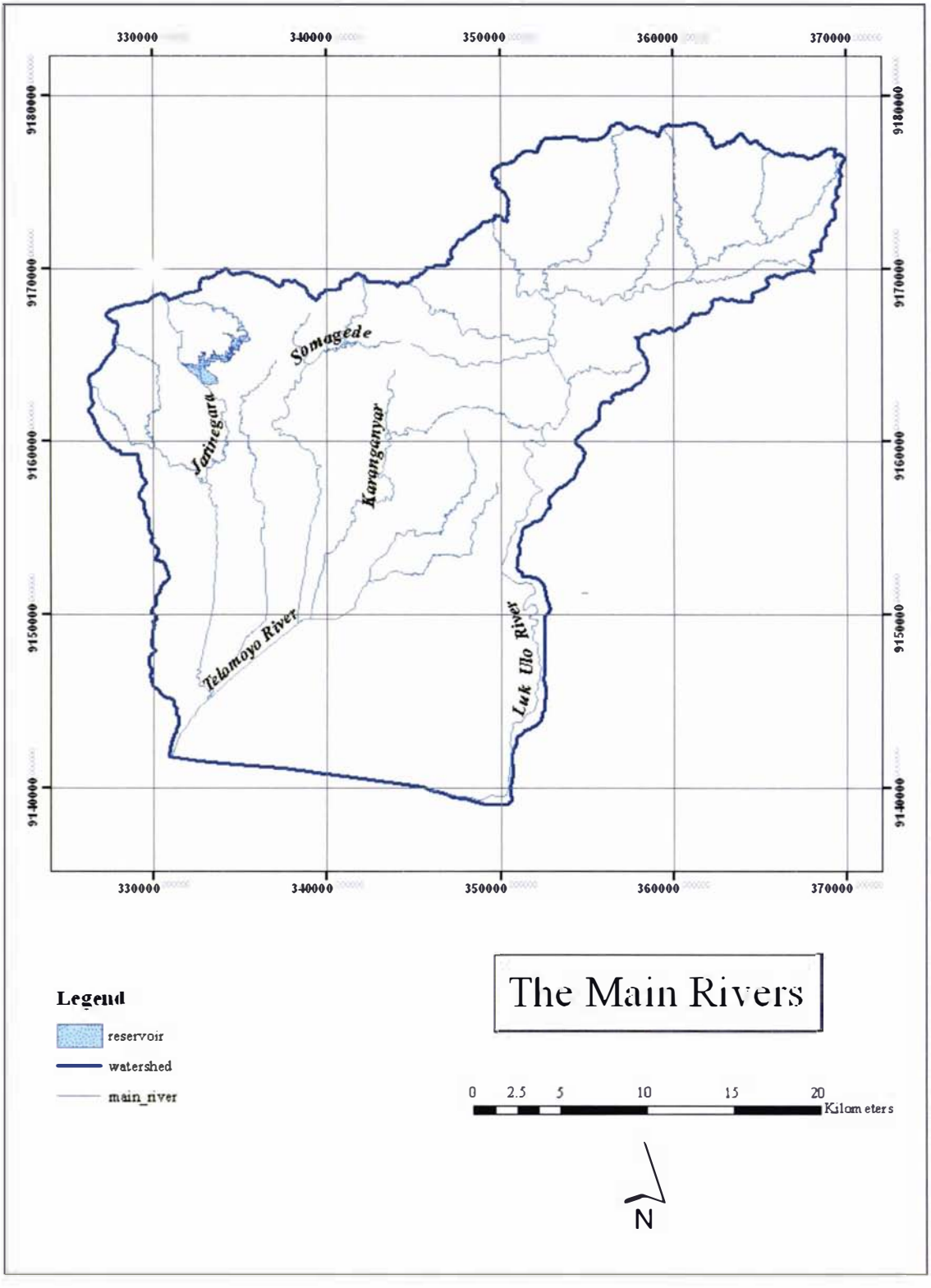

Figure 2-4 The main rivers of the study area are Telomoyo (left) and Luk Ulo (right)

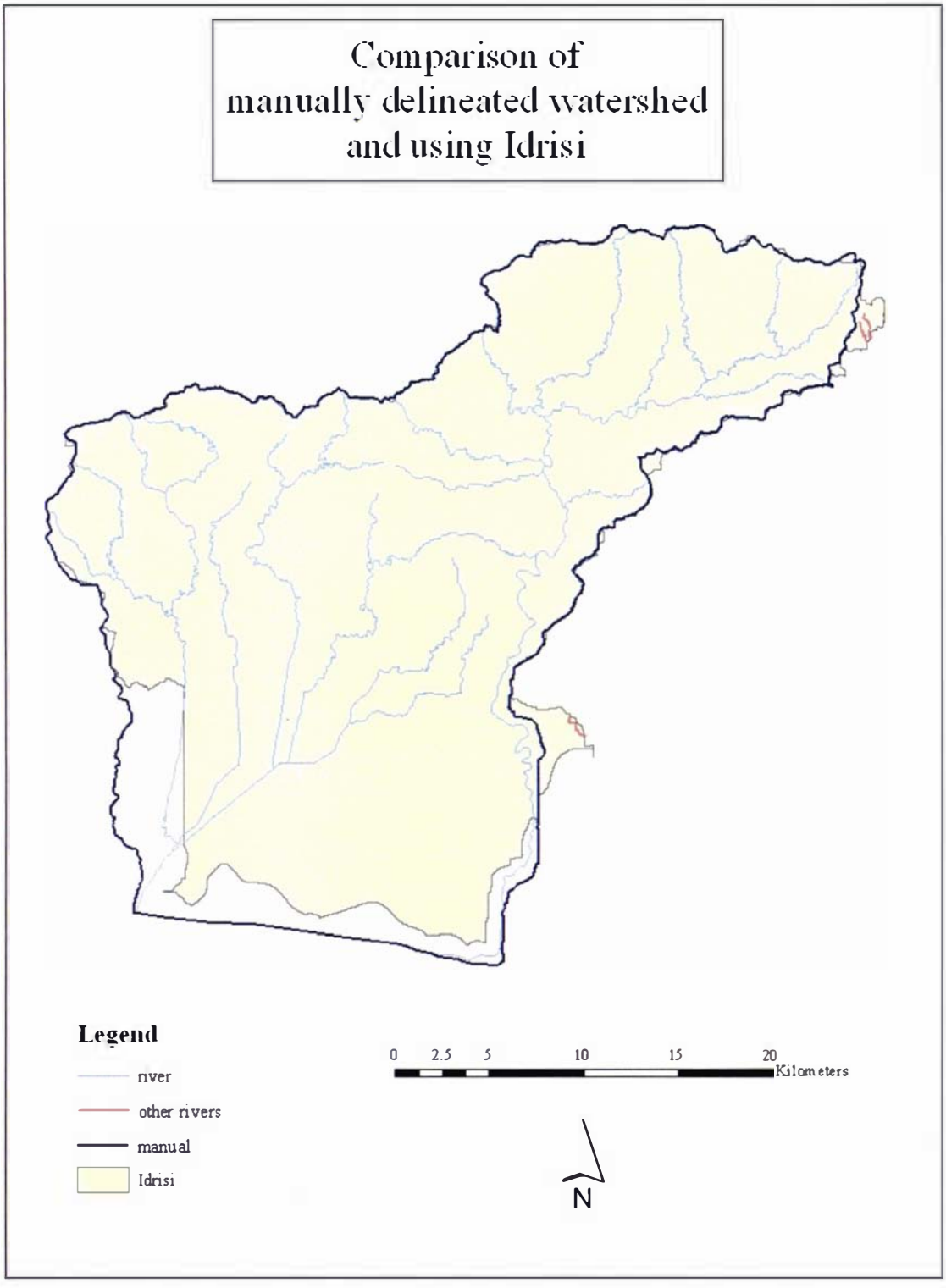

Figure 2-5 The comparison between manual and automatic watershed delineation

Using the WATERSHED module in IDRISI resulted in a different boundary in the southern part, it should, of course, be the coast line. Since the DEM was digitized from

50 metre contour lines, flat areas in the southern part of the watershed did not have enough information to draw a correct boundary line. To improve the watershed boundary automatically, more contour lines should be digitized up to the lowest altitude (12.5 metre) especially in the flat areas. However, in the future it is suggested that a computerised watershed boundary be created, and then adjusted manually using a topographic map with contour lines as a reference.

2.5 Land Use/Land Cover

The main agricultural crops in the Banjarnegara district are cassava (*Manihot esculenta*) and coconut (*Cocos nucifera*). Pine forest (*Pinus merkusii*), bamboo (*Bambusa vulgaris*), and some fruit trees (Pemerintah Kab. Banjarnegara, 2003) are also grown. In Kebumen the mixed forest consists of coconut, pine forest, teak (*Tectona grandis*), mahogany (*Swietenia macrophylla*), and acacia (*Acacia auriculiformis*). The crops on the lowland area are mainly rice (*Oryza sativa*), cassava, and peanuts (*Arachis hypogea*) (Pemerintah Kab. Kebumen, 2002).

In general, wetland rice is grown in the flat areas of the southern part of the watershed, while upland crops and forest plantations are found in the more mountainous, northern part of the watershed. Sometimes in the steeper areas the farmers still grow rice. Those fields are not irrigated, so rice is only grown during the wet season, while in the dry season these areas are left bare or planted with cassava which is more tolerant to the dry conditions (see Figures 2-6 and 2-7).

Figure 2-6 Wet season rice fields in the study area. In hilly areas, people make terraces to conserve the rain water

Figure 2-7 Cassava is a common crop in the study area during the dry season

Cassava is a very common crop in the study area because farmers prefer to grow it rather than maize, especially in dry fields. This is because the market for cassava starch is good in this area, and farmers receive additional income from processing the starch. The total cassava production from both districts is more than 500,000 tonne/year from 27,000 ha (Pemerintah Kab. Banjarnegara, 2003; Pemerintah Kab. Kebumen, 2002).

The mixed cover is usually on steeper slopes and higher elevation. It comprises fruit trees such as banana, avocado or coconut, and forest trees, such as acacia, pine trees, albisia (*Paraserianthes falcataria*), and mahogany. This land cover type is generally owned by the farmers and called '*hutan rakyat*' (literally, forest owned by people). In some places the farmers build their houses in these areas as well, especially if the *hutan rakyat* is close to the village. It is then called a homestead garden. Typical land cover of this type can be seen in Figures 2-8 and 2-9.

The monoculture forests belong to the government and are controlled by the State Forest Company (Perum Perhutani). The trees are pine, mahogany, acacia, and teak. The most common tree in the study area is pine (see Figures 2-10 to 2-12).

Figure 2-8 Typical *hutan rakyat* in the study area. Sometimes people build their houses in the middle of this land as well

Figure 2-9 Another example of mixed land use

Figure 2-10 Pine forest belonging to the State Forest Company (Perum Perhutani)

Figure 2-11 Mature pine trees showing scars from gum extraction

Figure 2-12 Young pine trees with and without perennial crops

An important forestry practice in Indonesia is the collecting of gum. Therefore, Perum Perhutani keeps pine trees until they are 40 years old. This arrangement allows the

farmers to collect gum but Perum Perhutani still harvest logs. In Kebumen, each year gum production nearly reaches 3,000 tonnes (Pemerintah Kab. Kebumen, 2002).

An additional benefit enjoyed by small-scale farmers is that they can utilize the forest area for two years after the logs are harvested. During this period, farmers plant perennial crops such as maize (*Zea mays*), while taking care of the young trees. After the second year, the farmers can no longer use the forest land.

The existence of perennial crops among the young pines can have two completely different impacts from the point of view of soil erosion. If the farmer uses the land and is cognisant of soil conservation principles, then that land will less erode. On the other hand, if the farmer leaves it without a perennial crop, or does not follow soil conservation practices, severe soil erosion can ensue. This is because Perum Perhutani uses clear cut methods to harvest logs irrespective of how steep the slope may be.

From the 2001 map produced by the South Java Flood Control Sector Project (SJFCSP, 2001), nine major land use types were identified in the study area. These land use types and the proportion of the study area they occupy are presented in Table 2-2 while the distribution of the land use can be seen in Figure 2-13.

There are also mixed land use practises in the study area. For example, bush (B) in the map may contain both bush and forest plantation, bush and other unspecified tree crops, bush and reforestation, bush and upland crops, and bush with regrowth following it's cultivation (SJFCSP, 2001).

Table 2-2 Major land uses in the study area (digitised data)

Land use	**Area**	
	(ha)	**(%)**
Agro Forestry (A)	730.1	1
Bush (B)	18223.1	21
Forest (H)	1130.5	1
Settlement (K)	15051.2	17
Tree crops/Estate/Plantation (P)	5394.6	6
Wetland Rice (S)	24903.1	28

Land use	Area	
	(ha)	(%)
Un-vegetated (T)	2243.3	3
Upland Crops and Forest Plantation (U)	20069.8	23
Water (W)	320.0	0
Unspecified	485.9	1
TOTAL	88551.6	100

2.6 Soils

The SJFCSP soil map (see Figure 2-14) shows that the dominant soils in the study area are Dystropepts (41%). These are defined as 'slightly weathered soils of hot climates with low subsoil base saturation values' (Fletcher & Gibb, 1990). Most areas with these soils are covered by forests. The second most abundant soils are Tropohemists (32%) - 'swampy, half decomposed, organic soils often of hot climates, with interbedded mineral layers' (Fletcher & Gibb, 1990). The principal land use on these soils is rice fields. The original map also contains soil depth data. It has effective soil depth, top soil and sub soil depth for each map unit.

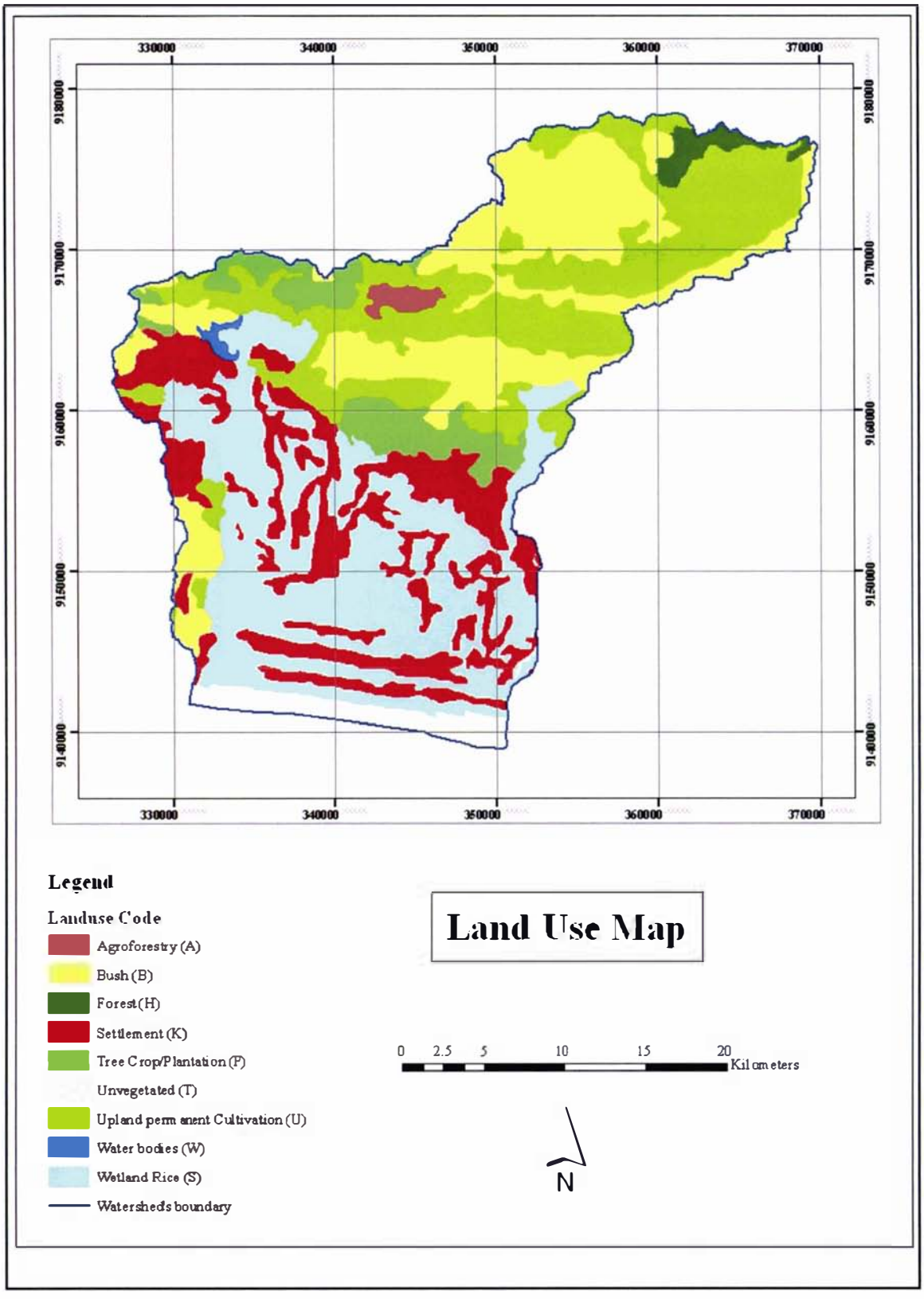

Figure 2-13 Land use map of the study area. Source: SJFCS Project.

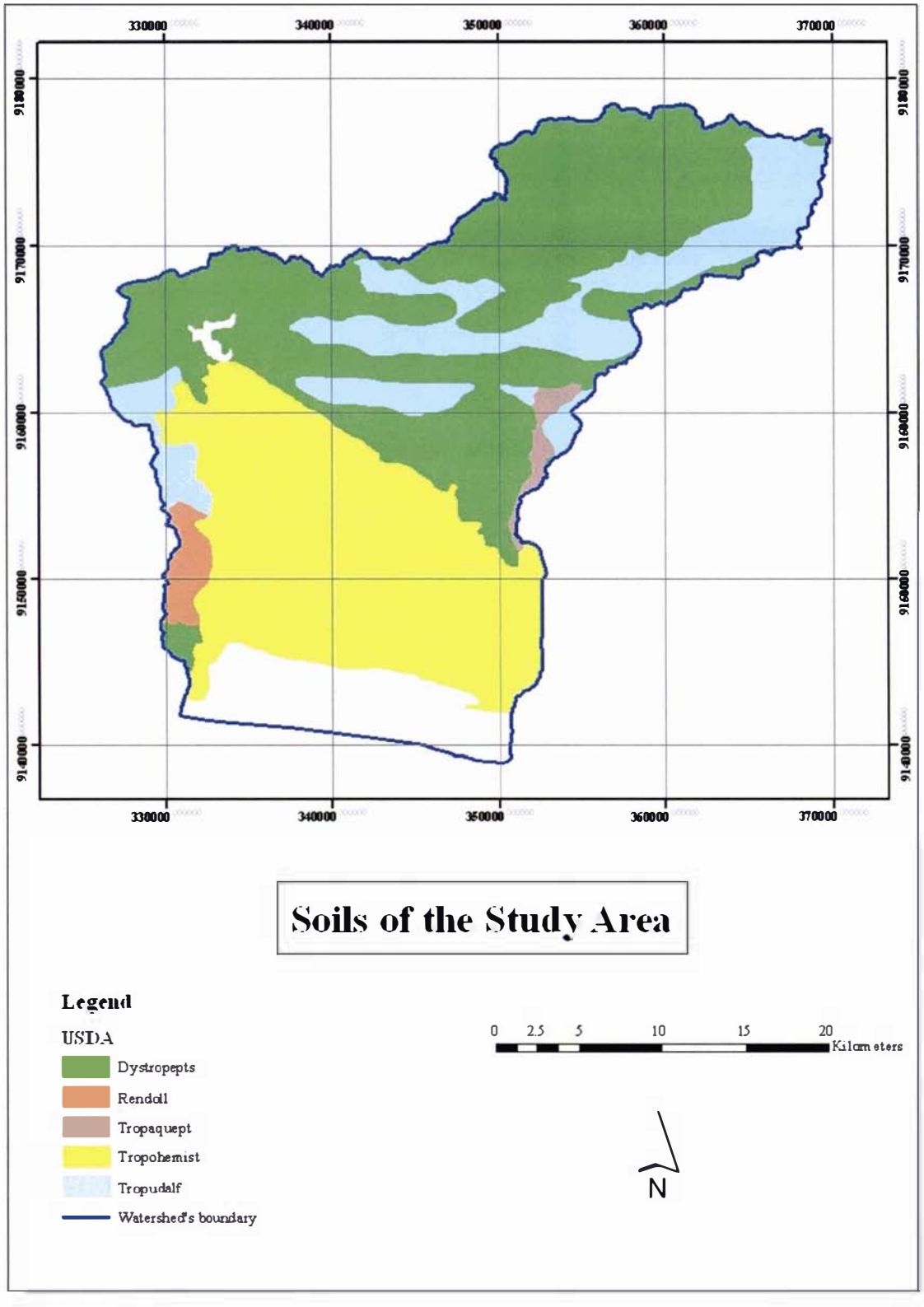

Figure 2-14 Soils of the study area. Source: SJFCS Project.

During the course of the project the land was classified and mapped according to its critical condition. An area of land is defined as in critical condition if its function as production land cannot be achieved. The failure mostly because of the incapability of the soil to let food crop grow (the soil is too thin or too infertile). Therefore this area is usually recommended to be forested. More than half of the total study-area is classified as potentially or actually critical (SJFCSP, 2001).

2.7 Soil Erosion

With high rainfall and erodible soils, soil erosion is common throughout the study area. This situation is exacerbated by poor management practices. Inside the forest, erosion also occurs although on a lesser scale. The photos in Figures 2-15 to 2-19 show some erosion sites in the study area.

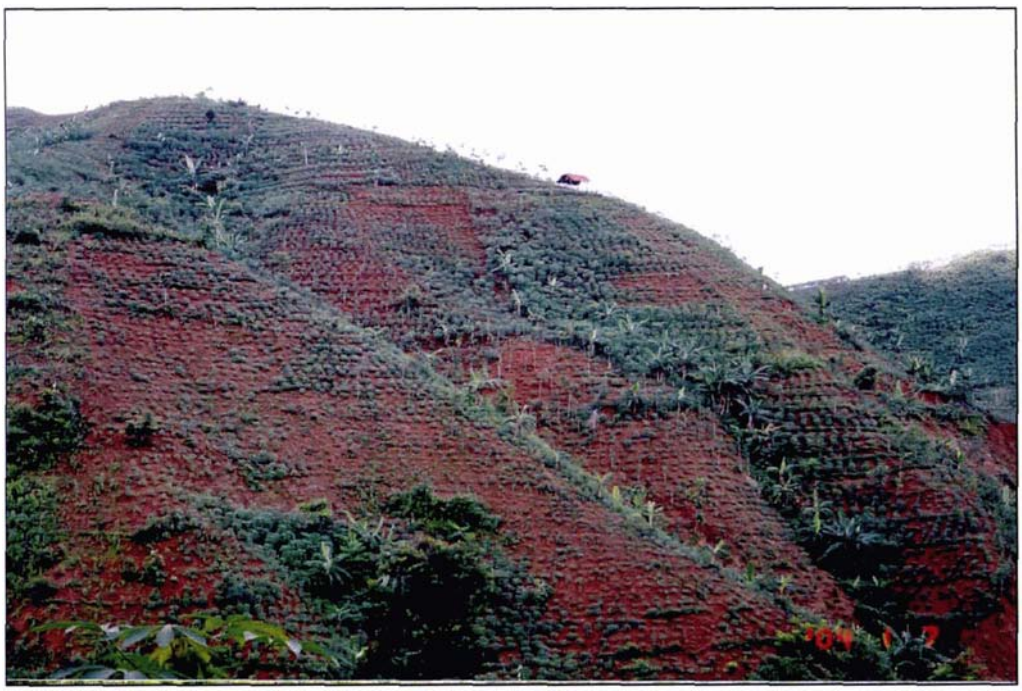

Figure 2-15 Cassava planted on a steep slope without terraces

Figure 2-16 Dry-land cultivation on steep slopes

Figure 2-17 Small land slide on the roadside

Figure 2-18 Erosion in the pine forest

Figure 2-19 Erosion on a dry, steep slope

DATA COLLECTION

In this study the data were derived mostly from existing maps and imagery. Three kinds of map were used: topographic maps, a soil map (already explained in Section 2.6) and a geological map. Since this study was not concerned with change detection, only one Landsat7 image was used. There were some aerial photos of the study area available; they came in two different scales: 1:20000 and 1:50000. For the detailed analysis two of the 1:20000 aerial photos were used. These aerial photos were also used by the State Forest Company (Perum Perhutani) for forest management planning.

3.1 Topographic Maps

The topographic maps used were 1:25000 scale maps with a Universal Transverse Mercator (UTM) projection produced by *Badan Koordinasi Survey dan Pemetaan Nasional/Bakosurtanal* (= the National Coordinating Agency for Surveys and Mapping) in 1999/2000 based on 1:50000 aerial photographs produced in 1993/1994. Each sheet contained information such as: transportation networks, river networks and other water bodies, village and city outlines, administrative boundaries, contour lines, spot heights, and mapping control points. These maps had also been colour-coded for different land covers (irrigated/non irrigated rice field, plantation, forest, scrub, open land, and swamp) and villages/built up areas.

The topographic maps were scanned at 300 dots per inch (DPI) therefore the resolution of the scanned map was 2.12 metres. The whole study area was covered by twelve map sheets. Each map sheet was registered according to the UTM projection and then combined into a mosaic. The mosaic of scanned topographic maps was used as the principal registered image and so all other maps and imagery used were registered using this mosaic. The resulting topographic map is shown in Figure 3-1.

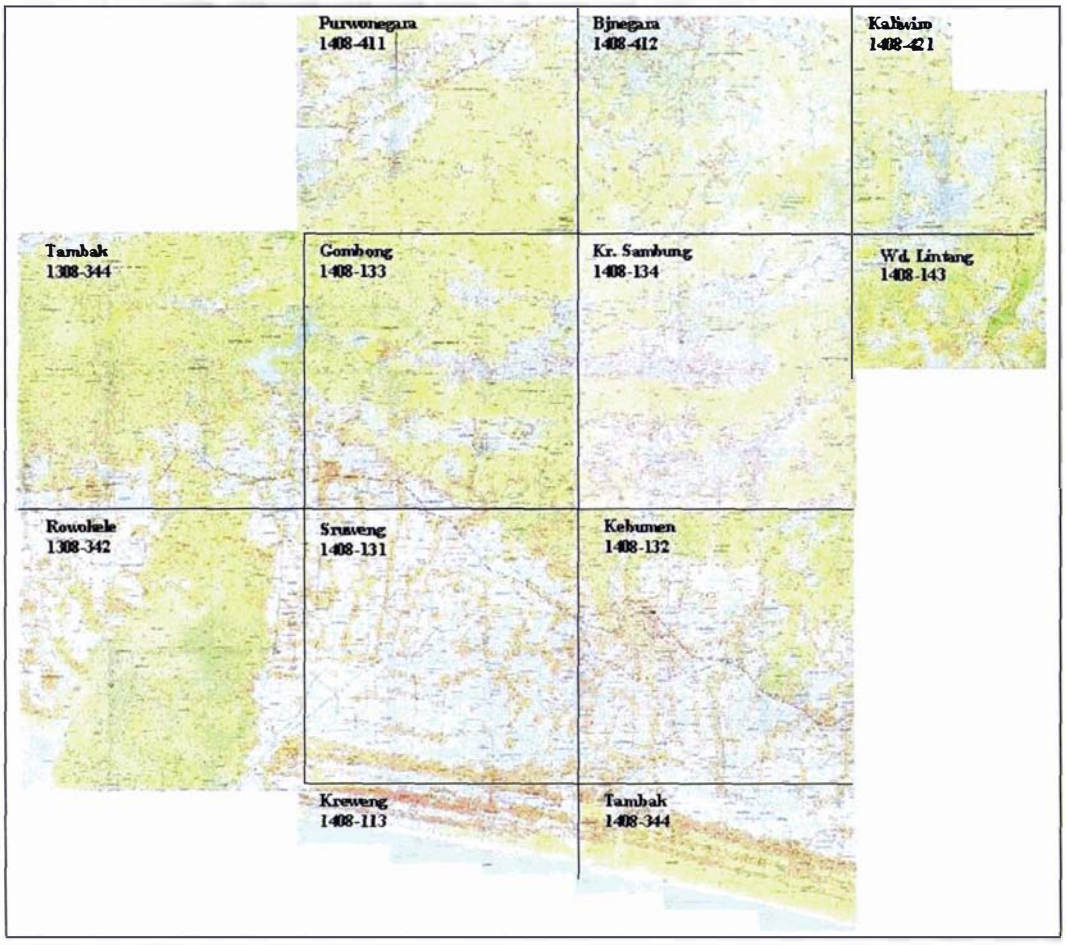

Figure 3-1 The topographic map mosaic used for this study. The name and number of each sheet is shown in the top-left corner

3.2 Geological Map

Two sources of geological data were used, a scanned 1:100000 scale geological map, and a geological 'map' interpreted from a supervised classification of the satellite image. The 1:100000 geological map was produced by the Geological Research and Development Centre under the Department of Mines and Energy in 1992 and 1996. Four map sheets were used and scanned at 100 DPI so that the resolution was 25.4 metres. Each map sheet was then registered to the topographical map and combined into a mosaic.

The geological units were digitised on screen using ARCView software; there were 25 geological units in the study area. The geological map is presented in Figure 3-2, with the legend explained briefly in Table 3-1. A detailed description of each unit is presented in Appendix A.

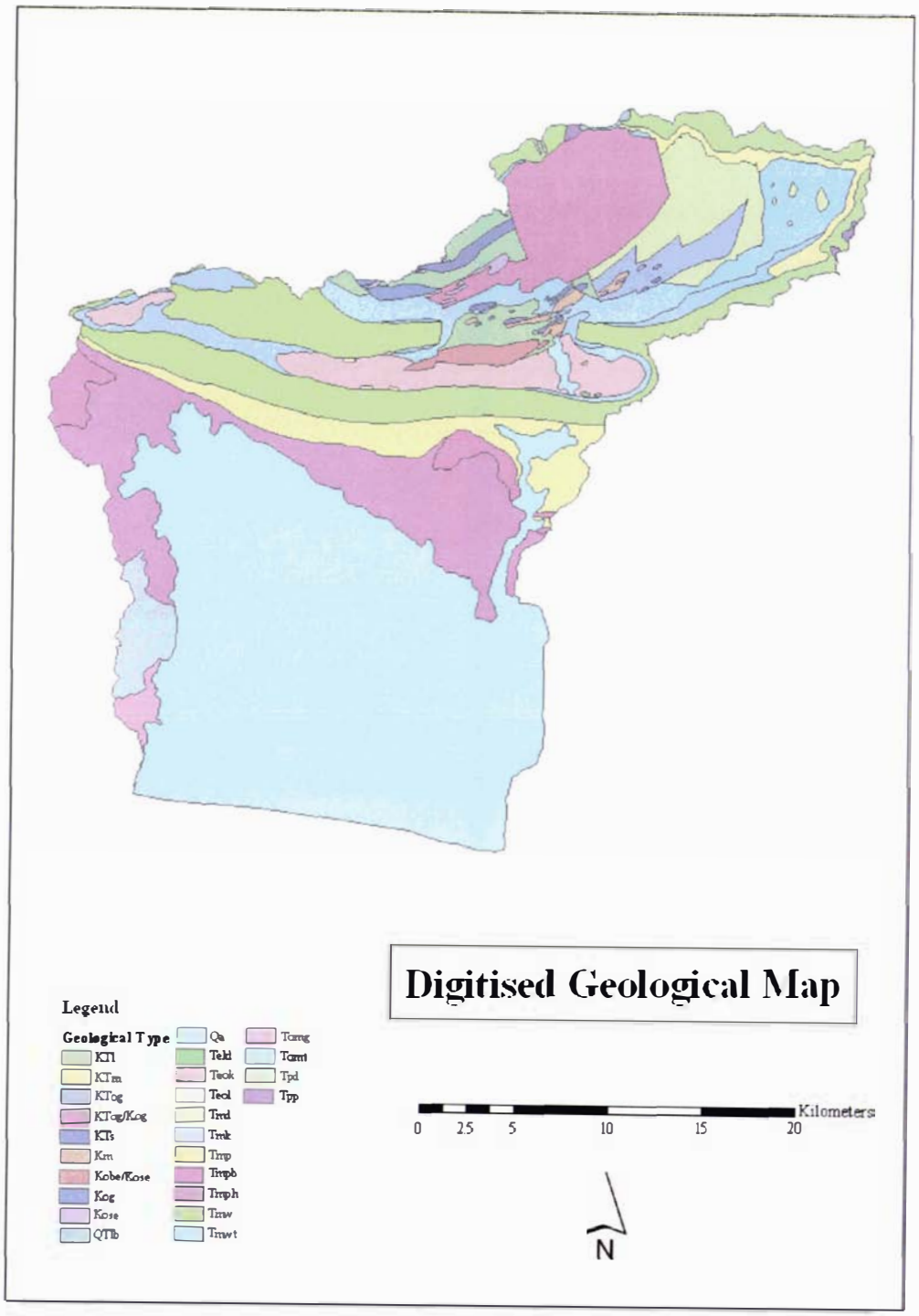

Figure 3-2 The geological map of the study area (digitised from a 1:100000 scale geological map)

A further geological map was created using the Landsat image and combining bands 5, 3 & 1 (Liu *et al.*, 2004). The training samples were selected using the digitised geological map as a guide. Twelve out of 25 units were identified from the geological

map and classified using a maximum likelihood classification. The result of the classification can be seen in Figure 3-3.

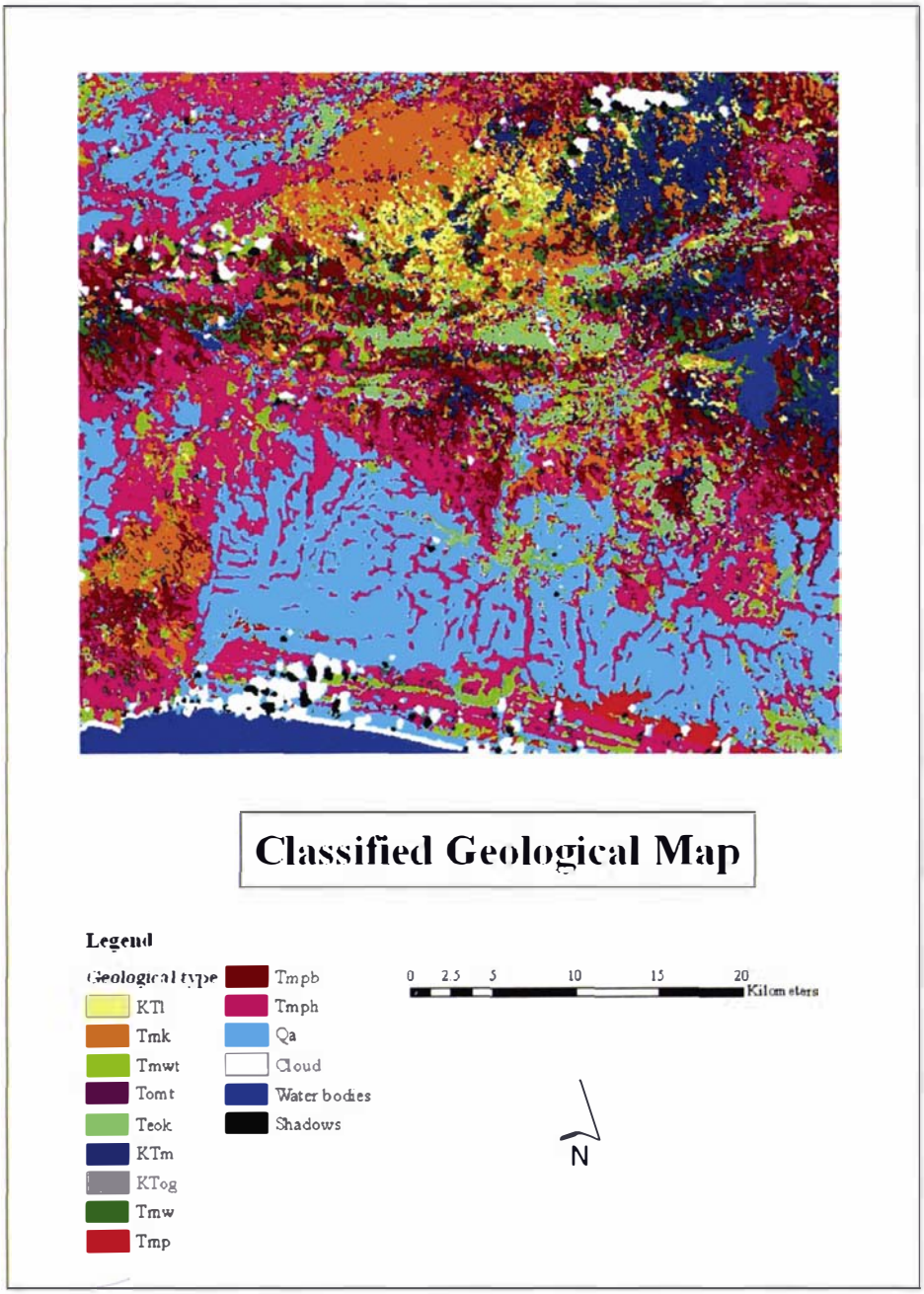

Figure 3-3 The geological map derived from classification of the Landsat7 image

Table 3-1 Short description of each geological unit found in the study area and its total area (in ha and %) (from the digitised Geological map)

Symbol	Description	Area	
		(ha)	(%)
KTl	Luk Ulo complex (melange of shale, siltstone, basalt, chert, mafics and ultramafics, schist, greywacke, granite, tuff and limestone)	1953.3	2
KTm	Brecciated rocks	3041.0	3
KTog	Mafics and ultramafics	1205.9	1
KTs	Greywacke	511.2	1
Km	Schist and phyllite	283.0	0
Kobe/Kose	Basalt and chert	551.7	1
Kose	Serpentinite	203.6	0
Kog	Gabbro	234.1	0
Ktog/Kog	Mafics and Gabbro	5521.2	6
QTlb	Breccia member of Ligung formation (andesitic volcanic breccia hornblende andesitic lava and tuff)	62.1	0
Qa	Alluvium (river and swamp deposits)	35329.7	40
Tekl	Reef limestone	13.9	0
Teok	Karang Sambung formation (clay, limestone, conglomerate, sandstone, claystone and basalt)	3290.7	4
Teol	Reefal limestone	6.4	0
Tmd	Diabase	45.0	0
Tmk	Kalipucung formation (limestone/shale)	1438.8	2
Tmp	Penosogan formation (conglomerate, sandstone, claystone, marl, tuff and rhyolite)	4875.4	6
Tmpb	Breccia member of Halang formation (andesite, basalt, limestone, and sandstone)	1400.6	2
Tmph	Halang formation (sandstone, conglomerate, marl, claystone and andesitic breccia)	9336.6	11
Tmw	Waturanda formation (sandstone, breccia, conglomerate, lahar and claystone)	11360.4	13
Tmwt	Tuff member of Halang formation (tuff, calcareous sandstone and tuffaceous marl)	2340.7	3
Tomg	Gabon formation (breccia with andesitic components)	501.3	1
Tomt	Totogan formation (breccia, claystone, marl, sandstone, conglomerate and tuff)	4921.1	6
Tpd	Damar formation (tuffaceous claystone, volcanic breccia, sandstone, tuff and conglomerate)	19.3	0
Tpp	Peniron formation (breccia with tuff intercalation)	104.2	0
TOTAL		88551.6	100

3.3 Satellite Image

The satellite image was acquired on 28th April 2001 by Landsat 7 using the ETM+ sensor. The whole image covers an area between -6.27^0 and -8.17^0 S and between 108.90^0 and 111.11^0 E. The World Reference System (WRS) path was 120, and the row was 65. The reference datum of this image was WGS84, and the map projection was UTM zone S49. The five multi-spectral bands have a 30 metre resolution; while the panchromatic band is 15 metres and the thermal bands are 60 metres.

The image was cropped to cover the study area between -7.41^0 and -7.79^0 S and 109.41^0 and 109.83^0 E (1531 columns and 1378 rows). Before cropping the image it was rectified to the topographic map. Rectification is a process of relating Ground Control Points (GCP) pixel coordinates into a map coordinate system (Jensen, 1986) which is the topographic map. Eight GCPs were selected and the average RMS Error was 0.054 pixel or 1.6 meters. Both the whole image and the cropped image are shown in Figure 3-4.

An advantage of Landsat TM and ETM+ compared with the previous Landsat series is its capability of handling vegetation information (Lillesand *et al.*, 2004) therefore, with the study area predominantly covered in vegetation, this image was suitable for land cover classification.

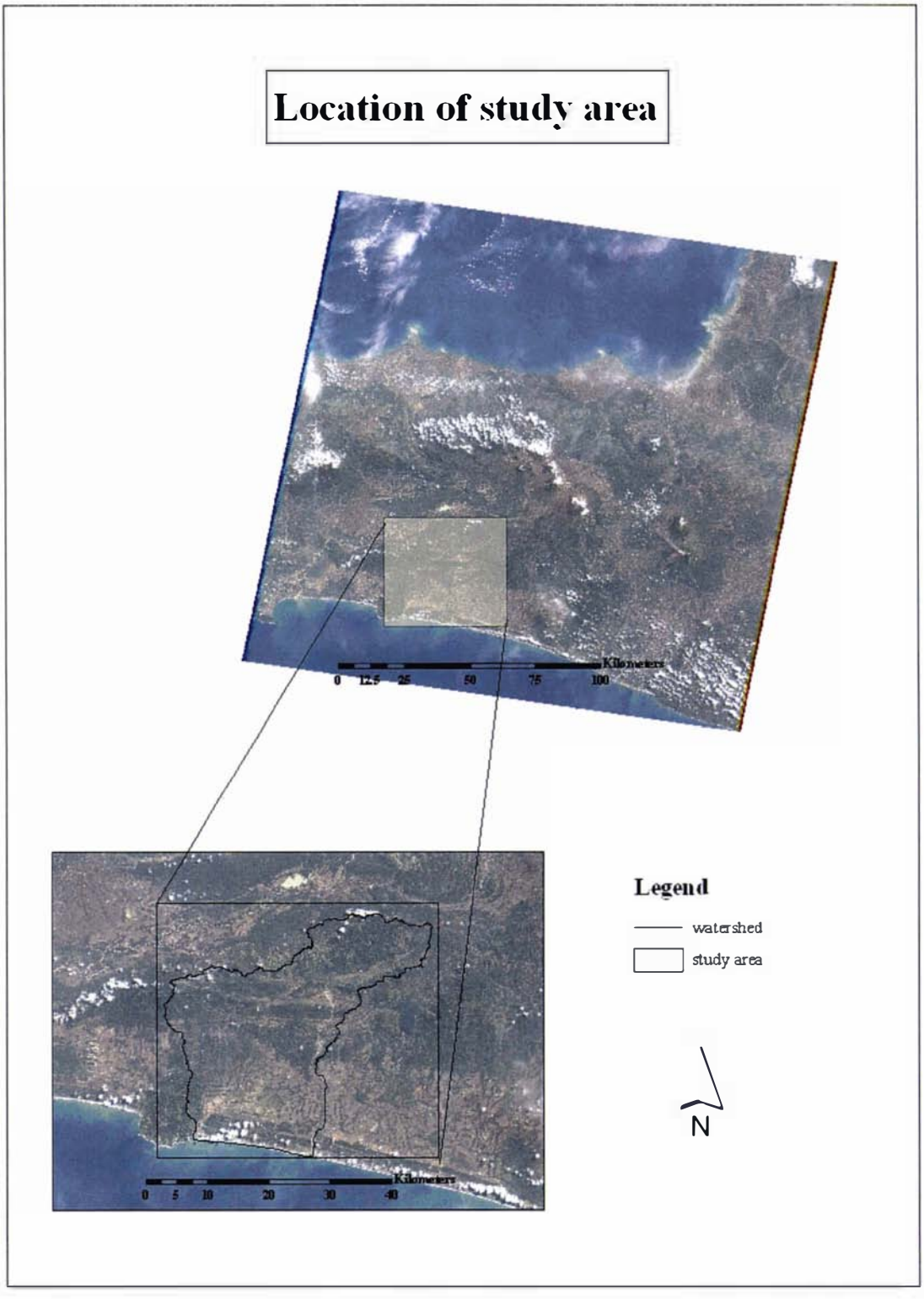

Figure 3-4 The location of the study area displayed in the Landsat7 imagery

3.4 Aerial Photographs

The aerial photos used in this study were acquired on 5th July 1993 and identified as Run 22N/29 and Run 23F/16. Each aerial photo covered one sub catchment: Kedung Tangkil and Binangun respectively. Since the photoscale was 1:20000 and they were scanned at 300 DPI the resolution of each pixel was 1.69 metres.

These two photos were registered to the topographic map. Four GCPs were selected for each photo and the average RMS Error was 3.2 pixels (5.4 metres) for Binangun and 1.9 pixels (3.2 metres) for Kedung Tangkil.

3.5 Digital Elevation Model

A Digital Elevation Model (DEM) is a database that contains information about the topography of a landscape (Bettinger & Wing, 2004). Each cell of the DEM contains a value representing elevation across the landscape. A DEM is not only used for topographic correction or slope and aspect calculation, but also to determine the accuracy of the watershed boundaries (Cheesman *et al.*, 2000).

Since an existing DEM for Luk Ulo – Telomoyo watershed was not available during the period of study; the DEM was created by digitizing contour lines from topographic maps. The contour interval in the maps was 12.5 metres but, to create the DEM, only the 50m contours were digitised for the whole study area. Actually to get a more accurate DEM, more contour lines should be digitised in the flat areas (see Section 2.4). Since this study was only interested in areas prone to erosion, flat areas were not the main concern.

The elevation ranged from sea level to over 1000 metres in the mountainous area. 1605 spot heights ranging from 1 metre elevation to 1038 metres were also used. Figures 3-5 and 3-6 show the contour lines and spot heights used in this study. Areas without contour lines were flatter areas with changes in elevation of less than 50 metres.

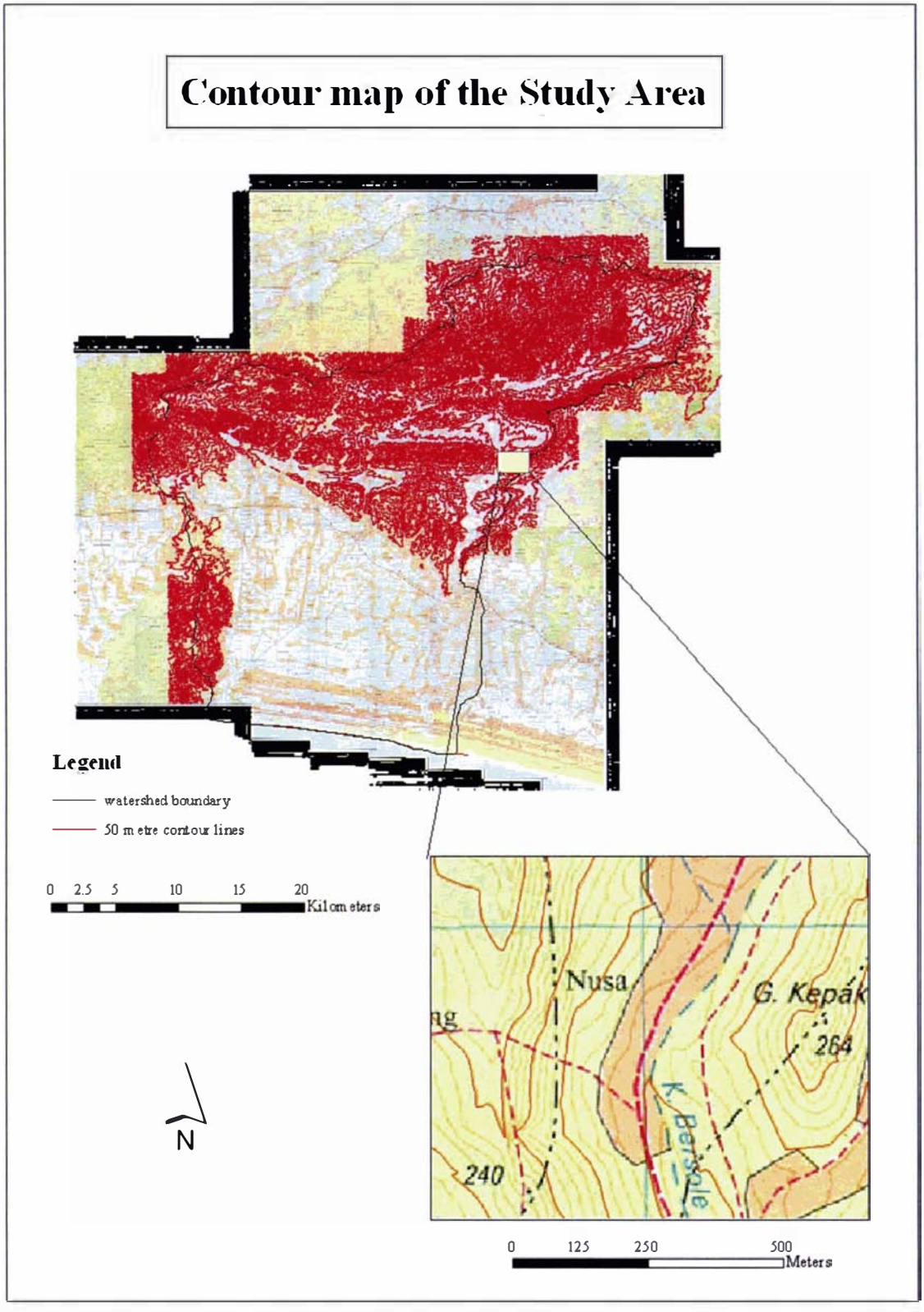

Figure 3-5 Contour lines used for building the DEM. The 50m contour interval is shown as darker lines in the inset

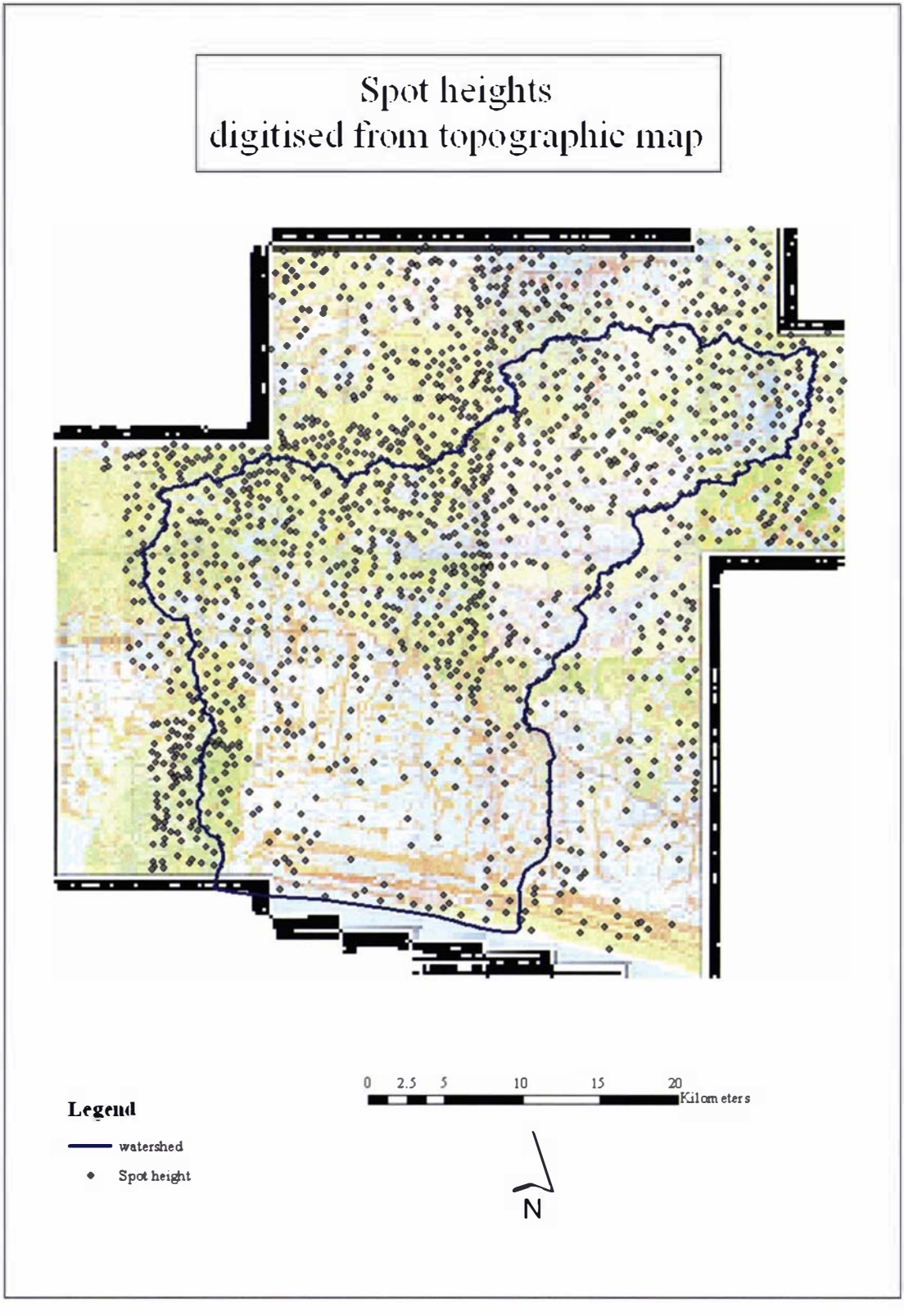

Figure 3-6 The spot heights used for building the DEM

The elevation contours and spot heights were converted into a grid format using the ARCInfo TOPOGRID command and a hydrologically correct grid of elevation from point, line, and polygon coverage was created (ESRI Support Centre, 2004). Other information used in creating the DEM included the river network and lake boundaries. The resolution was set to the same value as the Landsat image (30m).

After much trial and error using the TOPOGRID function, it was found that river network played an important role in constructing DEM. The correct shapes of the ridges and peaks depended on the flow of the river. The resulting DEM is presented in Figure 3-7.

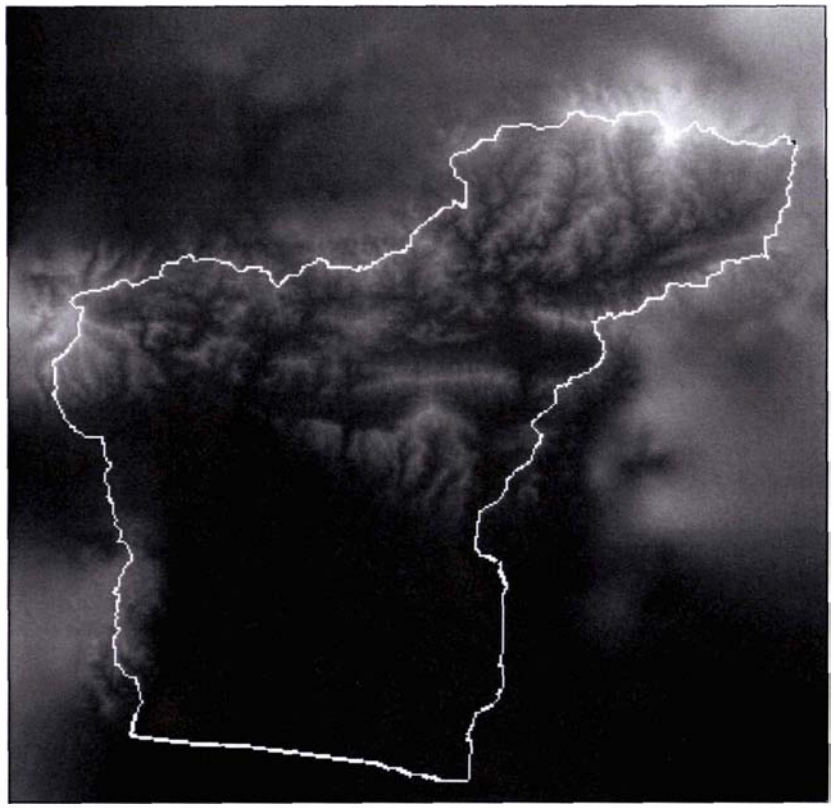

Figure 3-7 The 30 metre resolution DEM built from digitised contours and spot heights.

The advantage of using TOPOGRID when building a DEM compared with other software (such as GRIDDING in ERMapper) is that TOPOGRID acknowledges features that are not associated directly with elevation such as river networks, lake boundaries

and topographic depressions. By acknowledging these features the resultant DEM is more accurate.

3.6 Rainfall Map

3.6.1 Rainfall Data

The rainfall data for this study area was derived from 17 rainfall stations (one rainfall station was omitted because its location was outside the DEM extent (Section 2.3.1)). Each station had between four and 10 years of rainfall data (Table 2-1). The unavailability of the data for a certain year was because technical problems with the rain gauges.

The annual rainfall data were then ranked according to the wettest year for each station. The three wettest years experienced by the majority of the rainfall stations were used to create the rainfall surface. Those wettest years were 1992 (15 of 17 stations recorded 1992 as the wettest year), 1995 (10 of 17 stations) and 1998 (11 of 17 stations). A monthly rainfall map was then created for the study area based on the chosen years (see Table 3-2)

Table 3-2 Three wettest years chosen for each rainfall station followed by the number of months each station can contribute

Stations	1992	1995	1998	Number of months	Note
Adimulyo	**3386**	2990	**4028**	36	
Aliyan	**3381**	**4056**	*	35	1998 only has 11 months
Gombong	**4660**	4065	**4459**	36	
Karang Anyar	**3250**	2686	*	35	1998 only has 11 months
Karang Gayam	**3412**	3158	**4253**	36	
Kebumen	--	**2751**	**3802**	24	
Klirong	**4786**	3078	**4045**	36	
Kuwarasan	**4138**	**3674**	*	35	1998 only has 11 months
Petanahan	**5476**	2909	**3674**	36	

Stations	1992	1995	1998	Number of months	Note
Puring	**5880**	**3858**	*	34	1998 only has 10 months
Rowokele	**4924**	4066	**4071**	36	
Sadang	**4930**	**3658**	**4661**	36	
Sempor	**5003**	**4868**	**5350**	36	
Banjarnegara	**5486**	**5113**	**5290**	36	
Mandiraja	**4248**	**3913**	--	24	
Purwonegara	**4286**	**3750**	--	24	
Wadas Lintang	--	**4472**	**5260**	24	

bold = wettest year; -- = no data

3.6.2 Rainfall Interpolation Method

The existing rainfall data were used to predict the rainfall in un-gauged areas. This is difficult, as Sumner (1988) discovered, because precipitation varies according to differences in the type and scale of development of precipitation-producing processes. Furthermore, rainfall is also strongly influenced by topography and wind direction (Goovaerts, 2000; Guenni & Hutchinson, 1998; Hutchinson, 1998b; Sumner, 1988). The temporal analysis of precipitation is strongly site- or area-dependent and mapping it involves a degree of subjectivity (Sumner, 1988) especially when the rain gauges are far apart or in a different landscape. Rainfall interpolation is usually necessary since the number of rain gauges is often limited and there are areas where maintaining rain gauges is impossible due to site inaccessibility.

There are a number of methods for interpolating rainfall data and it is important to choose a method that matches the conditions. Choosing a simple method is generally preferred, as more sophisticated methods need more information, time and money to implement (Price *et al.*, 2000). The most common method used in Indonesia is assigning the un-sampled location based on Thiessen polygons or isohyets. Thiessen polygons use a triangular network with each gauge as the centre point, while isohyets portray precipitation in a spatially continuous manner (Sumner, 1988). These two methods do not count the effect of elevation or any other factors. Other methods include simple trend surface analysis (Hutchinson, 1995), Inverse Distance Weighted

(IDW), Delaunay Triangulations, and more advanced geostatistical methods. Two common geostatistical methods used are thin plate smoothing splines (Hutchinson, 1995, 1998a, 1998b; Hutchinson & Gessler, 1994) and kriging/co-kriging (Goovaerts, 1999, 2000). Both can include elevation as a factor in assigning rainfall at un-gauged sites such as suggested by Price *et al.* (2000).

Kriging is 'an interpolation technique to predict some value at an unmeasured location based on known points', while co-kriging allows a better estimate by adding a secondary variable which is sampled more intensely than the primary variable (ESRI Support Centre, 2004). If the primary variable is difficult or expensive to measure, then co-kriging can improve interpolation estimates without more intense sampling of the primary variable. Thin plate smoothing splines, which are part of the Radial Basis Function, work similarly to kriging or co-kriging, but less flexible and more automatic.

The difference between kriging/co-kriging and thin plate smoothing splines is that kriging/co-kriging requires more estimation, including estimating the auto-correlation for each variable and all cross-correlations (ESRI Support Centre, 2004), while thin plate splines do not (Hutchinson, 1995). In other words, kriging/co-kriging needs more data to estimate a surface while thin plate spline does it fully automated (Kesteven & Hutchinson, 1996) and this makes thin plate spline easier to use.

In kriging/co-kriging it is understood that observation close to each other tends to be more alike compared with observations farther apart (Goovaerts, 2000). This is the drawback of kriging/co-kriging - close observations may not always look alike since many factors affect them, such as position of the gauge relative to the mountains or ridges. On the other hand, Hutchinson (1998a) found that thin plate splines do not need prior calibration of spatial covariance structure, while kriging normally requires prior calibration of a variogram with nugget, sill and range.

Price *et al.* (2000) reported that the rainfall surface mapping software developed by M.F. Hutchinson of the Australian National University's Centre for Resource and Environmental Studies (ANUSPLIN) was a very robust prediction package. The software employs thin plate splines to create surface maps despite complex topography, low station density and potentially poor data quality. McKenney *et al.* (2001) found that thin plate smoothing splines are good for creating minimum and maximum

temperature maps for Canada, but they suggested more data were needed to improve the precipitation map. Furthermore, McKenney suggested that elevation is an important variable for the climate model. Overall ANUSPLIN (Hutchinson, 2004) was found to be the best rainfall mapping software for this study – especially when it was supported by a good digital elevation model (DEM).

The ANUSPLIN user guide (Hutchinson, 2004) records that the aim of the ANUSPLIN package is to provide a facility for transparent analysis and interpolation of noisy multi-variate data using thin plate smoothing splines. The package supports this aim by providing comprehensive statistical analyses, data diagnostics and spatially distributed standard errors. It also supports flexible data input and surface interrogation procedures.

The original thin plate (formerly Laplacian) smoothing spline surface fitting technique was described by Wahba (1979), with modifications for larger data sets due to Bates and Wahba (1982), Elden (1984), Hutchinson (1984) and Hutchinson and de Hoog (1985). The extension to partial splines is based on Bates et al. (1987). This allows for the incorporation of parametric linear sub-models (or covariates), in addition to the independent spline variables. This is a robust way of allowing for additional dependencies, provided a parametric form for these dependencies can be determined. In the limiting case of no independent spline variables (not currently permitted), the procedure would become simple multi-variate linear regression.

Thin plate smoothing splines can in fact be viewed as a generalisation of standard multi-variate linear regression, in which the parametric model is replaced by a suitably smooth non-parametric function. The degree of smoothness, or inversely the degree of complexity, of the fitted function is usually determined automatically from the data by minimising a measure of predictive error of the fitted surface given by the generalised cross validation (GCV). Theoretical justification of the GCV and demonstration of its performance on simulated data have been given by Craven and Wahba (1979).

A comprehensive introduction to the technique of thin plate smoothing splines, with various extensions, is given in Wahba (1990). A brief overview of the basic theory and applications to spatial interpolation of monthly mean climate is given in Hutchinson (1991a). More comprehensive discussion of the algorithms and associated statistical

analyses, and comparisons with kriging, are given in Hutchinson (1993) and Hutchinson Gessler (1994). Recent applications to annual and daily precipitation data have been described by Hutchinson (1995, 1998ab).

It is often convenient, particularly when processing climate data, to process several surfaces simultaneously. ANUSPLIN now allows for arbitrarily many such surfaces and introduces the concept of "surface independent variables", so that independent variables may change systematically from surface to surface. ANUSPLIN permits systematic interrogation of these surfaces, and their standard errors, in both point and grid form. ANUSPLIN also permits transformations of both independent and dependent variables.

The overall analysis proceeds from point data to output point and grid files suitable for storage and plotting by a geographic information system (GIS) and other plotting packages. The analyses by SPLINA and SPLINB provide up to six output files which provide statistical analyses, support detection of data errors, an important phase of the analysis, and facilitate determination of additional knots by ADDNOT for the SPLINB program. The output surface coefficients and error covariance matrices enable systematic interrogation of the fitted surfaces by LAPPNT and LAPGRD. The GCV files output by AVGCVA and AVGCVB can also assist detection of data errors and revision of the specifications of the spline model.

3.6.3 Rain Shadow Effect

Orographic and adiabatic factors combine to influence rainfall patterns and can create a rain shadow (Goovaerts, 2000). A rain shadow occurs when precipitation drops significantly on the leeward side of a mountain (Haugland, 1998) and this explains why Karang Gayam (105.24m) receives less rainfall than Sadang (46.18m) respectively (see Table 3-2). Karang Gayam is in the rain shadow of several mountains: (Watutumpang (313 m), Klabang (402 m) and Paduraksa (405 m). By contrast, Sadang is in an open and flat area and receives higher rainfall.

The rain shadow effect can be calculated by determining the position of each rainfall station according to its aspect and an aspect map can be generated from the DEM. A broad filter (101 x 101 median filter) was implemented to generalise the DEM and an

aspect map of the study area was created. The aspect was then smoothed using an 11 x 11 median filter. Due to the wind direction, which is mostly from Southeast (*The New International Atlas*, 1996), the windward side was taken to be facing a range between 45° and 225° and the leeward side faced 225 ° to 45°. The geolocation of each station along with its altitude and aspect can be seen in Table 3-3.

Table 3-3 The geographical position (EN), altitude (metres), aspect (°) and direction of each station in the study area

Stations	Easting	Northing	Altitude	Aspect	Direction
		(metres)		(°)	
Adimulyo	340541.75	9151999.45	5	244	SW
Aliyan	354794.31	9154364.66	39	118	SE
Gombong	336788.64	9160270.72	22	189	S
Karang Anyar	339779.20	9158729.89	17	217	SW
Karang Gayam	346816.40	9164339.32	105	28	NE
Kebumen	352296.07	9151786.80	18	160	S
Klirong	348778.44	9144044.51	9	252	W
Kuwarasan	335573.30	9152270.39	0	211	SW
Petanahan	344168.12	9143571.48	9	332	NW
Puring	337052.91	9144502.33	8	294	NW
Rowokele	328484.76	9159948.81	50	151	SE
Sadang	353603.89	9165286.10	46	188	S
Sempor	332761.83	9163327.05	62	113	SE
Banjarnegara	356054.43	9182146.39	286	329	NW
Mandiraja	337062.75	9175865.70	114	159	S
Purwonegara	341194.16	9177956.30	133	233	SW
Wadas Lintang	368986.32	9165099.16	265	234	SW

From Table 3-3 it can be seen that that there were eight stations in the leeward side which could experience rain shadow effect. However, these stations represented three different conditions: four stations in the low elevation, three stations in the high

elevation, and one station in moderate elevation. The four stations at low elevation are Adimulyo, Klirong, Petanahan and Puring. They will not experience the rain shadow effect because they sit in a flat plain. The high altitude stations are Banjarnegara, Purwanegara and Wadas Lintang. These stations, although outside the study area, were used because they were the highest elevation stations available for this study. Since there were not enough stations similar to these stations, there is no way to compare rain shadow effect for the high elevation stations.

The last rain shadow station, however, was surrounded by some non-rain shadow stations. This led ANUSPLIN to conclude that this station was an outlier. To acknowledge the rain shadow effect in Karang Gayam, additional stations affected by the same effect were added to the study area to give more weight for Karang Gayam in the calculation. By trial and error, seven simulated stations were added at similar altitude and aspect as Karang Gayam. This addition meant that the model was able to recognise the rain shadow effect of Karang Gayam.

One or two of these simulated stations could be recommended as sites for additional rainfall stations to those already installed as long as the location was accessible.

The rainfall data for these simulated stations was based on the rainfall data of Karang Gayam. The simulated rainfall was estimated:

$$R_S = R_{KG} + (10\% * R_{KG} * a)$$

where: R_S = rainfall of new stations
R_{KG} = rainfall of Karang Gayam
a = a random number ranging from -1 – +1

Using the above equation, the simulated stations have rainfall similar to rainfall in Karang Gayam ± 10%.

The locations of the simulated rainfall stations are presented in Table 3-4, all are on the leeward side of the mountains. Figure 3-8 shows the positions of all rainfall stations used in this study.

Table 3-4 The geographical position (EN), altitude (metres), aspect (°) and direction of the simulated stations in the study area

Stations/nearest village	Easting	Northing	Altitude	Aspect	Direction
		(metres)		(°)	
ST1/Karang Rejo	353177.90	9163335.81	98	24	NE
ST2/Kepudang	346821.42	9166127.96	128	39	NE
ST3/Mlakakerep	349127.18	9163698.50	137	7	N
ST6/Pucangan	355902.41	9167614.75	115	14	N
ST7/Lokidang	352069.79	9168575.56	68	40	NE
ST8/Kedunglo	351068.18	9168410.50	64	33	NE
ST4/Karang Pucung	349803.18	9164703.55	68	28	NE

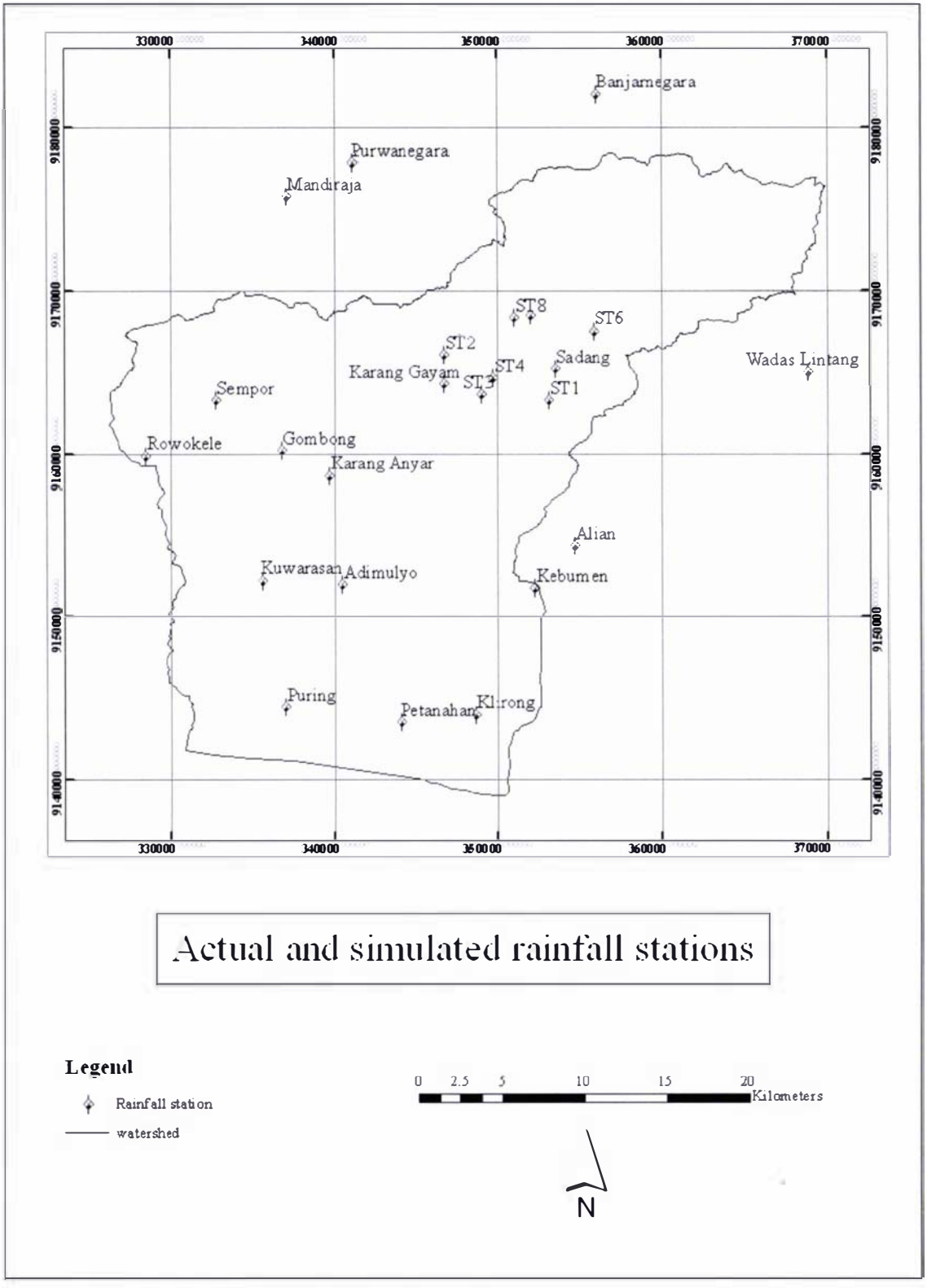

Figure 3-8 The location of rainfall stations used in this study. Location with names are actual stations, while those denoted 'ST' are simulated stations

3.6.4 Building the Rainfall Surface

Hutchinson (2004) also noted in the ANUSPLIN user guide that the surface fitting procedure was primarily developed for this task so that there are normally at least two independent spline variables, longitude and latitude, in this order and in units of decimal degrees. A third independent variable, elevation above sea-level, is often appropriate when fitting surfaces to temperature or precipitation. This is normally included as a third independent spline variable, in which case it should be scaled to be in units of kilometres. Minor improvements can sometimes be had by slightly altering this scaling of elevation. This scaling was originally determined by Hutchinson and Bischof (1983) and has been verified by Hutchinson (1995, 1998b).

Over restricted areas, superior performance can sometimes be achieved by including elevation not as an independent spline variable but as an independent covariate. Thus, in the case of fitting a temperature surface, the coefficient of an elevation covariate would be an empirically determined temperature lapse rate (Hutchinson, 1991a). Other factors which influence the climate variable may be included as additional covariates if appropriate parameterizations can be determined and the relevant data are available. These might include, for example, topographic effects other than elevation above sea-level. Other applications to climate interpolation have been described by Hutchinson *et al.* (1984ab, 1996a) and Hutchinson (1989a, 1991ab). Applications of fitted spline climate surfaces to global agroclimatic classifications and to the assessment of biodiversity are described by Hutchinson *et al.* (1992, 1996b).

To fit multi-variate climate surfaces, the values of the independent variables need only be known at the data points. Thus meteorological stations should be accurately located in position and elevation.

The surfaces were built using data from 24 rainfall stations (17 already available stations and 7 simulated) and information about the Easting, Northing, altitude and aspect of each station. The Easting and Northing were used as the independent variables, while DEM and aspect were assigned as the covariates. By using elevation as a covariate the performance of the rainfall creation was increased.

DEM and aspect surfaces were converted into floating point files so that they could be read by ANUSPLIN. The commands used were SPLINA (to build a relationship

between the rainfall data and the other factors) and LAPGRD (to create rainfall surfaces according to the above relationship). An example of the rainfall surface of the study area is presented in Figure 3-9, while Table 3-5 shows the result of SPLINA and LAPGRD for each month. All rainfall data, rainfall surfaces, printouts of SPLINA and LAPGRD outputs and the detail of the rainfall surfaces are presented in Appendices B – E.

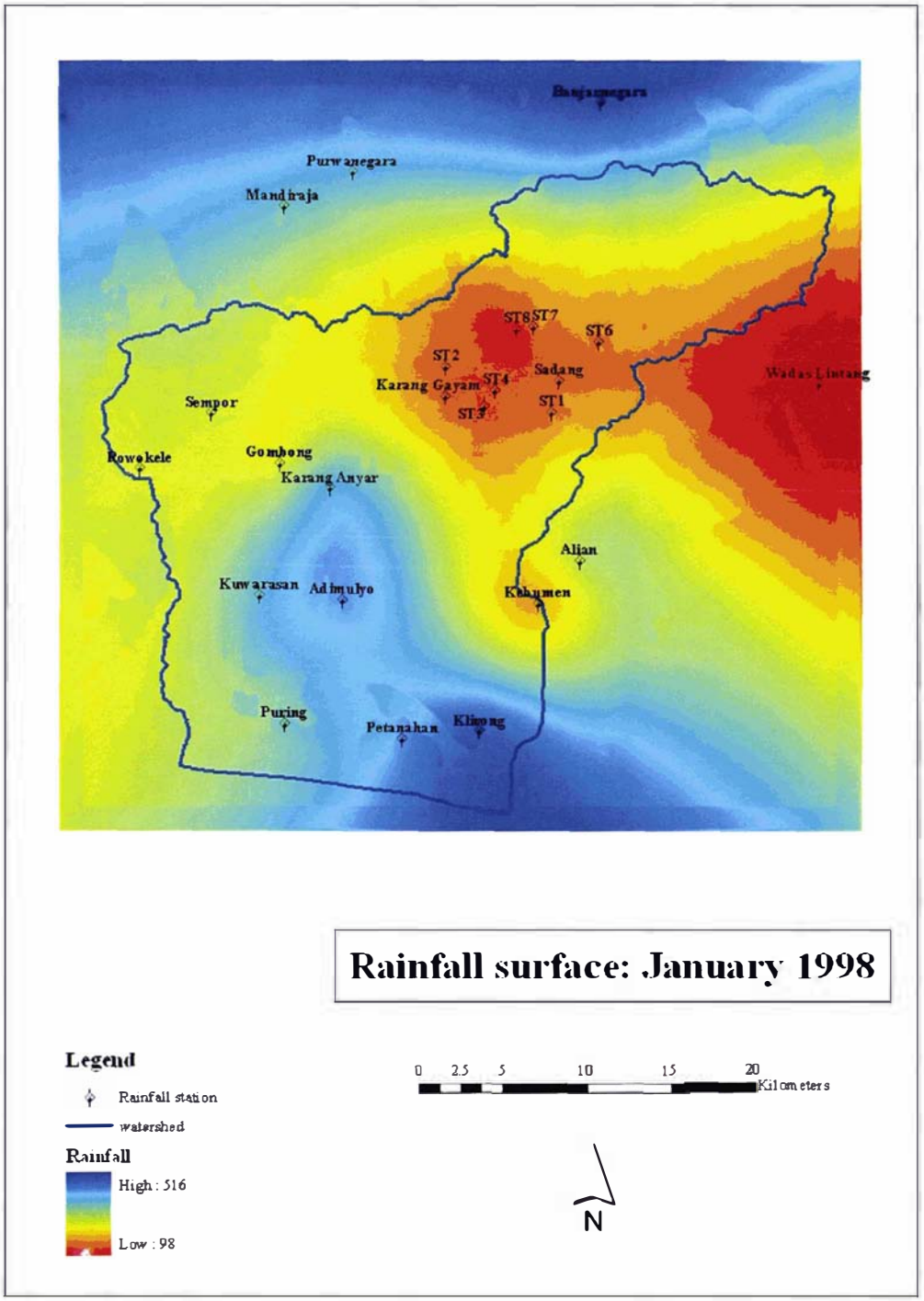

Figure 3-9 The January 1998 rainfall surface for the study area

Table 3-5 Monthly data output from SPLINA and LAPGRD

Month	Mean	Range*		RTGCV	RTMSE
1992					
January	308	-183 –	910	81.3	0.123E-01
February	386	147 –	692	28.8	0.434E-02
March	324	-492 –	1130	135.0	66.8
April	419	-199 –	987	89.2	0.134E-01
May	205	-245 –	782	67.6	0.102E-01
June	181	-132 –	616	36.8	0.575E-02
July	96	-124 –	398	26.5	0.574E-02
August	354	149 –	953	76.2	37.7
September	313	-341 –	1140	58.6	31.3
October	657	368 –	1320	50.7	22.0
November	595	300 –	1190	76.5	42.2
December	345	-213 –	1010	76.0	0.104E-01
1995					
January	409	-150 –	809	80.9	39.6
February	543	238 –	1140	57.7	0.939E-02
March	423	63 –	930	98.6	0.161E-01
April	232	-128 –	443	14.9	0.242E-02
May	117	-34 –	613	28.8	0.468E-02
June	294	78 –	641	60.8	27.3
July	74	-19 –	364	23.6	11.7
August	1	-3 –	6	2.5	1.06
September	2	-6 –	25	2.6	0.416E-03
October	401	24 –	1200	91.8	45.5
November	625	352 –	1710	99.4	47.1
December	437	144 –	590	117.0	51.6
1998					
January	258	98 –	516	43.9	3.42

Month	Mean	Range*		RTGCV	RTMSE
February	356	108 –	1070	47.9	0.753E-02
March	363	-315 –	871	58.8	0.129E-01
April	524	-243 –	1180	43.5	13.4
May	134	-35 –	434	29.4	0.459E-02
June	429	59 –	1360	97.8	41.0
July	290	59 –	761	73.3	25.1
August	99	18 –	255	12.5	0.197E-02
September	196	-292 –	514	44.9	9.58
October	551	27 –	908	107.0	44.1
November	615	-151 –	1020	68.6	0.108E-01
December	506	427 –	799	93.3	39.8

* The negative values reflect the estimation modelling used by the LAPGRD programme. In actual fact the range would start from zero rainfall.

The mean values from the 24 stations (Table 3-5) were inputted to the software. The range reflects the rainfall value predicted by the software for each pixel in the study area. RTGCV and RTMSE values are presented in Appendix E and show the amount of error for each map generated by ANUSPLIN. Square root of Generalised Cross Validation (RTGCV) is the predictive error which includes measurement error in the data (Hutchinson, 2004; Kesteven & Hutchinson, 1996) while the Root Mean Square Error (RTMSE) is an estimate of the true error of the fitted surface after the effects of measurement error have been removed (Kesteven & Hutchinson, 1996). Therefore RTMSE is always smaller than RTGCV.

The software generates an indicator of the level of confidence one can have in the monthly rainfall generated from the available data. When a signal is flagged it indicates that the system has failed to find an optimum smoothing parameter value (ρ) because of insufficient data. As the result, the model might underestimate or overestimate the predicted rainfall because the smoothing parameters are responsible for determining the balance between the real data and the smoothness of the spline (Kesteven & Hutchinson, 1996). For example, the January 1998 map (Figure 3-9) showed that the

high altitude area at the top of the map was less wet than the low flat area at the bottom. It overestimated the value of Petanahan and Klirong stations in the south and underestimated the rainfall in the north of the study area due to the lack of rainfall stations at higher altitude in the north. Unfortunately no simulated station could be placed in the northern part of the study area because rainfall information was unavailable during the study period.

In this study, 21 out of 36 signals were flagged (see Appendix E for the log file) to indicate that there were insufficient rainfall stations for the model to operate with the required level of confidence. No rain shadow effect was identified when the 17 rainfall stations were used in the model. To compensate for the limited number of stations, seven simulated stations were created and when these were included in the calculation the rain shadow effect was recognised.

Using a similar method as with the rain shadow area, the northern, high altitude sector of the study area could be simulated using other stations outside the study area but with the same altitude and aspect. Enlarging the size of the study area, for example by utilizing all the rainfall stations in Java, is another alternative to improve the result of the prediction, but this is beyond the scope of this study.

In a pilot study, two extreme months were chosen to compare the surface developed by ANUSPLIN and co-kriging. The months of September 1995 (with the smallest error = 0.416E-03) and March 1992 (with the largest error = 66.8) were chosen. Both models use the DEM and aspect as the covariates. After the surfaces were constructed, the value of rainfall for every station was determined (using IDRISI) and compared with actual rainfall. The comparisons are presented in Table 3-6 and Figure 3-10.

Table 3-6 A comparison between the actual rainfall and a prediction using ANUSPLIN and co-kriging (mm)

Rainfall station	Actual		Predicted			
			ANUSPLIN		Co-kriging	
	Sep'95	Mar'92	Sep'95	Mar'92	Sep'95	Mar'92
Adimulyo	0	182	0	241	3	332
Aliyan	0	380	0	356	-1	136
Gombong	9	328	9	321	3	249
Karang Anyar	0	230	0	314	3	292
Karang Gayam	0	177	0	108	-4	-8
Kebumen	0	--	0	325	0	195
Klirong	0	286	0	274	3	349
Kuwarasan	8	280	8	237	3	282
Petanahan	0	331	0	370	6	481
Puring	5	343	5	318	5	419
Rowokele	0	330	0	335	0	189
Sadang	0	839	0	656	1	257
Sempor	4	330	4	280	0	131
Banjarnegara	3	808	3	815	6	499
Mandiraja	21	464	21	457	3	211
Purwonegara	0	604	0	606	3	334
Wadas Lintang	8	--	8	813	4	323
ST1	0	168	0	235	-4	-6
ST2	0	186	0	232	-2	85
ST3	0	168	0	105	-4	-34
ST6	0	186	0	204	-4	-25
ST7	0	176	0	213	-3	40
ST8	0	163	0	243	-2	67
ST4	0	162	0	175	-3	-5

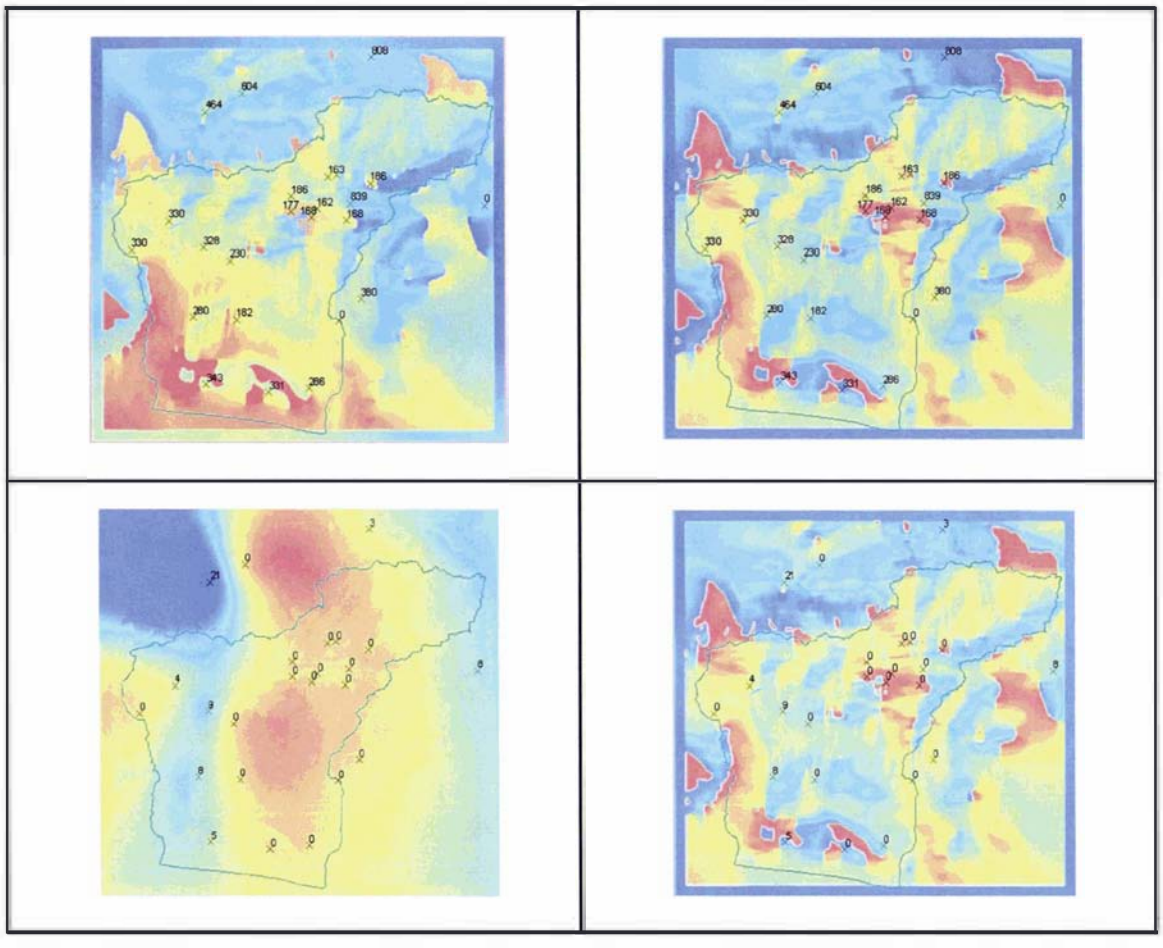

Figure 3-10 A comparison of the surfaces built using ANUSPLIN (left) and co-kriging (right) during March 1992 (upper) and September 1995 (lower). The red shaded area shows the lowest value and the shaded area blue indicates the highest value. The numbers show monthly rainfall.

From Table 3-6 it can be concluded that the co-kriging method failed to estimate the rain shadow effects. For Karang Gayam, it assigned September 1995 (0 mm) and March 1992 (177 mm) as -4 and -8 mm respectively while ANUSPLIN gave more reasonable values (0 and 108 mm respectively). This condition was repeated for the seven simulated rain shadow stations. Therefore, it may be concluded that, using the available data for this study, ANUSPLIN is a more reliable estimator of rain shadow effects than co-kriging.

The co-kriging method also failed to predict surfaces where there was too large a gap in the data. ANUSPLIN, on the other hand, once again was able to estimate rainfall despite the gaps. For example, the surfaces developed from co-kriging do not show differences for March 1992 (177mm rainfall) or September 1995 (0mm rainfall), while

in ANUSPLIN they show different patterns as well as values. It can be said that co-kriging predicts the same patterns but with different values. From the results of co-kriging and ANUSPLIN it seems more advisable to use ANUSPLIN to create rainfall surfaces for the study area.

Given that the location rainfall stations is critical to the success of the rainfall estimation programmes, it would make more sense to place rainfall stations at critical location points rather than administrative sites like district offices as they are right now. These critical locations should include:

- Higher altitude. More stations need to be located at higher altitudes since these areas generally experience more rain.
- Different aspect. Locate rainfall stations in different aspects in order to identify the rain shadow effect which has not been considered before.
- Specific land cover. Large expanses of specific land cover will influence the micro climate. When this type of land cover is not represented by a station, this will not be captured in the map.

Where the proposed locations are not easily accessible, a fully automatic rainfall recorder may be the solution.

3.7 Heavy Rain

Sometimes rainfall is exceptionally heavy and causes life-threatening landslides and flooding. Heavy rain is defined as 'precipitation that exceed 0.3 inch/hour (7.6 mm/hour)' while moderate rain has precipitation between 0.10 – 0.20 inch/hour (The Weather Channel, no date). Compared with the threshold value for rainfall that causes erosion (see Section 2.3.1) this value is smaller, but since landslide usually happens in steep slopes, landslide could happen before the erosion threshold is passed over

Over a 24-hour period this can be extrapolated to approximately 180 mm/day (designated as a major storm) and 70 mm/day (a moderate storm) respectively. During a ten-year period to 2000 in the study area, 20 major storms were recorded by nine of the 17 rainfall stations. The rainfall data for the major storms for each station is presented in Table 3-7 and Figure 3-11.

Table 3-7 Heavy rainfalls (> 180 mm/day) events, monthly and annual rainfall data within 10 years data of 17 rainfall stations

Station	No. of rain events	Heavy rain		Monthly rainfall		Annual rainfall	
		date	Rainfall (mm)	month	Rainfall (mm)	year	Rainfall (mm)
Adimulyo	1	7 Oct	215	Oct	839	2000	3482
Alian	--	--	--	--	--	--	--
Gombong	4	3 Oct	236	Oct	923	1996	3459
		18 Oct	257	Oct			
		13 Feb	222	Feb	516	1997	1222
		9 Nov	248	Nov	879	2000	4129
Karang Anyar	1	18 Oct	223	Oct	609	1996	2499
Karang Gayam	--	--	--	--	--	--	--
Kebumen	1	18 Oct	198	Oct	609	1996	--
Klirong	--	--	--	--	--	--	--
Kuwarasan	3	22 Mar	261	Mar	449	1996	3839
		28 Oct	247	Oct	899		
		19 Oct	190	Oct	725	1992	4138
Petanahan	--	--	--	--	--	--	--
Puring	--	--	--	--	--	--	--
Rowokele	6	31 Aug	348	Aug	672	1992	4924
		18 Oct	195	Oct	877		
		20 Jun	190	Jun	453	1995	4066
		11 Oct	216	Oct	698		
		22 Mar	200	Mar	583	1996	4236
		18 Oct	275	Oct	1074		
Sadang	--	--	--	--	--	--	--
Sempor	1	3 Nov	203	Nov	896	1998	5350
Banjar-negara	2	4 Apr	182	Apr	646	1992	5486

Station	No. of rain events	Heavy rain		Monthly rainfall		Annual rainfall	
		date	Rainfall (mm)	month	Rainfall (mm)	year	Rainfall (mm)
		29 Aug	225	Aug	497		
Mandiraja	--	--	--	--	--	--	--
Purwa-negara	--	--	--	--	--	--	--
Wadas Lintang	1	3 Feb	236	Feb	725	1995	4472

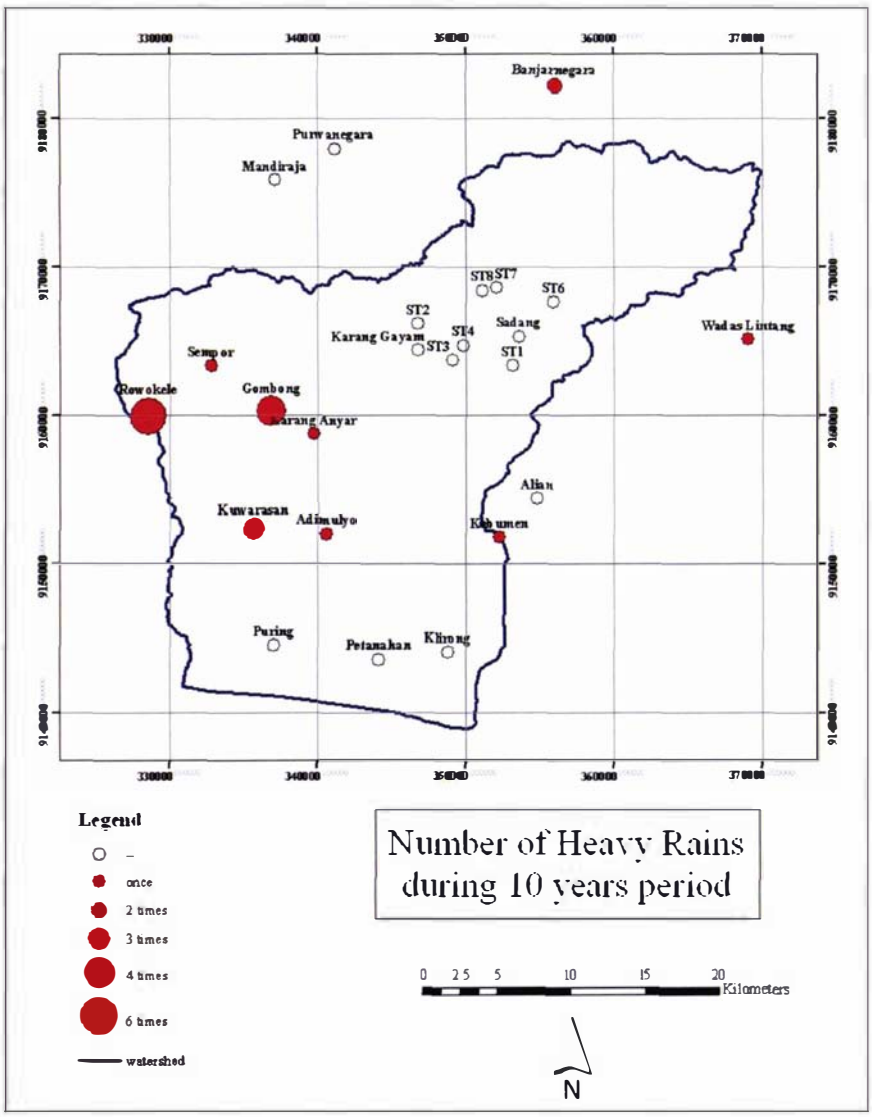

Figure 3-11 Stations that recorded heavy rains (> 180 mm/day) during 10 years data (1991 – 2000)

From Table 3-7 and Figure 3-11 it can be seen that rainfall patterns varied over the study area. The three stations closest to the beach (Puring, Petanahan, and Klirong) did not record any heavy rainfall during the whole 10-year period. Due to the higher altitude, the stations further north received heavier rainfall. However, Karang Gayam did not record heavy rainfall.

Sadang, on the other hand, is in the rain shadow and therefore receives less rain. Although not all stations experience heavy rain, most of the rainfall in the study area still exceeds 70 mm/day which is designated as moderate rainfall. The monthly rainfall data for all the rainfall stations during a 10-year period are presented in Appendix B.

Reliable rainfall recording stations and robust rainfall prediction models are essential if one wants to identify potential erosion sites in the study area. The combination of geological conditions, drainage characteristics, slope factors, vegetation, removal of underlying support and other conditions are all contributory factors to landslides and slips (California Department of Conservation, 1999). In the unconsolidated material, debris landslides are common and often occur during high intensity storms (California Department of Conservation, 1999).

Since high intensity storms or heavy rains can trigger debris slides, rainfall stations in areas that often experience heavy rain can provide the most useful information. By combining these data with other influencing factors, such as slope, geological type and soil factor, areas prone to debris slides can be predicted.

THE USE OF REMOTE SENSING AND GEOGRAPHIC INFORMATION SYSTEMS

4.1 Introduction

Satellite remote sensing is such an important source of data for studies of the Earth and environmental science, because of its ability to capture information of a large part of the Earth's surface and to acquire repeated measurements of the same area on a regular basis (Donoghue, 2002). These features make remote sensing an excellent tool for monitoring the environment, especially in remote areas. Interpretation of remotely sensed imagery can provide land cover information. The combination of this product with a GIS provides a powerful tool not only in monitoring but also in planning. GIS can be used as a decision-making tool based on geographically referenced information where the information is supplied by remote sensing. Landsat TM imagery for example, is often used in combination with GIS for forest management planning (Grossman & Forrester, 2001).

According to Lillesand *et al.*, (2004) remote sensing is defined as:

> '...the science and art of obtaining information about an object, area, or phenomenon through the analysis of data acquired by a device that is not in contact with the object, area, or phenomenon under investigation' (Lillesand *et al.*, 2004, p. 1),

while they describe GIS as:

> '...computer-based systems that can deal with virtually any type of information about features that can be referenced by geographical location. These systems are capable of handling both locational data and attribute data about such features' (Lillesand *et al.*, 2004, p. 45).

The next sections describe the use of remote sensing and GIS in more specific areas; forestry and soil conservation. Since this study focuses on Indonesia, the development of remote sensing and GIS in Indonesia is also discussed.

4.1.1 Remote Sensing and GIS in forestry

In the field of forestry, there is a need to have as much relevant information as possible on the conditions in the forest to prescribe treatments, to help formulate policy, and to provide insight and predictions on future forest condition and health (Franklin, 2001). Such information can be gathered using remote sensing; it is an auxiliary tool used to obtain data for a specific purpose (Smith, 1993), such as land cover classification, timber volume and forest biomass estimation (Nezry *et al.*, 2000), and forest productivity approximation (Franklin, 2001). With a series of images it can be used to detect changes accurately and to help explain more fully the implications of forest changes and activities (Franklin, 2001). It is also a useful tool for the assessment of environmental conditions, either in an existing forest or prior to planting a new one (Grossman & Forrester, 2001).

Traditionally, information about forests was obtained by manual sampling in selected small areas of the forest. The data then had to be extrapolated and applied to the entire forest. Using remote sensing, foresters can acquire more accurate and cost-effective information (such as forest age, species distribution or estimated timber volume) and can directly observe as large an area as necessary (Grossman & Forrester, 2001).

The preferred imagery sources from which land cover information is derived, especially forest cover, are Landsat, SPOT (*Satellite pour l'Observation de la Terre*), and Radar. Hyyppä *et al.* (2000) found that Landsat and SPOT gave more information for forest inventory compared with Radar, while Oliver (2000) found the reverse. Oliver found that Radar imagery gave better results for tropical rainforest and boreal forest because it did not require the areas to be cloud-free. Furthermore, Lillesand *et al.* (2004) noted that Landsat Thematic Mapper (TM) and Enhanced Thematic Mapper (ETM+) have an increased capability to handle vegetation information, and this kind of information is useful in determining cover management values for calculating the potential soil loss.

The aerial photograph is an example of a remotely sensed product, which has been used in forestry since 1945 (Hegg & Driscoll, 1982). To obtain information from an aerial photograph, a manual interpretation is made and usually supported by a ground survey (Skidmore, 1989). Although the qualitative interpretation of an aerial photograph by a skilled interpreter - in many cases – is more accurate and precise (Coppin *et al.*, 2001),

the disadvantage of this method is that it is labour intensive and very subjective. The subjectivity is introduced because of the different levels of individual interpreters' capabilities and can result in inconsistencies (Skidmore, 1989).

Another application of remote sensing in forestry is its use to examine carbon stocks and their response to human interference through deforestation and other forms of land use change (Donoghue, 2002; Wulder *et al.*, 2004). The use of NDVI (Normalised Difference Vegetation Index derived from multispectral satellite imagery) for calculating LAI (Leaf Area Index) is another application of remote sensing in forestry. LAI can be used to estimate evapotranspiration of a forest (Sellers *et al.*, 1997 in Xavier & Vettorazzi, 2004). While for sustainable forest management, the application of remote sensing commonly includes classification of forest cover-type, estimation of forest structure, forest change detection, and forest modelling (Franklin, 2001).

Since the goal is to help satisfy as many as possible of these multidimensional needs for information, remote sensing should be the type of technology which is cost-effective and easy to understand. This statement is supported by Grossman & Forrester (2001) who said that with the use of multiple sensors and varied data collection and interpretation techniques, remote sensing is a versatile tool that can provide data about the surface of the earth to suit almost any need.

Apart from these positive features, remote sensing is sensitive to the effect of cloud and rain, which is very common in tropical forests (Grossman & Forrester, 2001). Often an image needs additional processing to accommodate the masking caused by rain and clouds before it can be used for further analysis.

Another hindrance to using remote sensing is that as a relatively new technology, it still has some drawbacks when applied in complex situations. These drawbacks include inappropriate choice of methodology, inexperienced or new users, incorrect datasets, or inappropriate scales. Improvements can be expected once the users become more experienced. While such situations may be only temporary, management have to consider and anticipate them before incorporating remote sensing in the system management (Franklin, 2001).

4.1.2 RS and GIS in soil conservation and erosion

Remote sensing offers the most efficient means of determining land cover for a large area. However as Cheesman *et al.* (2000) point out, soil erosion can not be quantified using land cover or slope information derived from imagery alone, it needs detailed ground measurements as well; and a tool is needed to integrate them. GIS is an appropriate device with the ability to integrate both remote sensing and ground data. Bhuyan *et al.* (2002) discussed the use of remote sensing for soil conservation and soil erosion. According to them some factors such as land cover, conservation tillage practice, and crop residue could be gathered from remote sensing, while other factors, such as soil depth, still needed to be gathered from the field.

Erosion modelling is difficult because of the complexity of the interaction between four main factors, i.e.: soil, topography, land use and climate. All of these factors except climate can be interpreted from imagery. For instance, land use and land cover information, can be gathered from a classified Landsat Thematic Mapper image (Lee, 2004). Topographic factors, including slope length and steepness can be retrieved from a DEM (Lee, 2004). Other data might come from existing maps that have been compiled from ground-based measurements. GIS offers a means of integrating all the datasets as well as the opportunity to determine those areas that might be susceptible to erosion.

One particular type of erosion, land-sliding, can be detected easily using remote sensing. Lee (2004) found that by using aerial photo interpretation he could identify recent landslides from breaks in the forest canopy, bare soil, or other scars. After combining this information with other ground features that had already been mapped, the task of soil conservation planning was simplified.

GIS can be used to isolate and query the individual variables to see the contribution of each variable on the predicted erosion potential (Lee, 2004), and this information can be used to design conservation planning.

Metternicht and Zinck (1998) found that combining the thermal band with other Landsat TM bands gave information about surface rock fragments, since rocky soil heats more rapidly than rock-free soil. The result was that rock-free soil provided lower reflectance compared to rocky soils. This too was useful information for conservation planning.

4.1.3 Remote Sensing and GIS in Indonesia

Remote sensing and GIS are used not only in the forestry area; the Indonesian government has found the technology useful in many areas. On the website of SEAMEO Regional Centre for Tropical Biology (BIOTROP) (BIOTROP, 2003), they offer several GIS and remote sensing applications for managing the natural resources and environment, such as oil and gas, mineral exploration, coastal and shallow marine habitat, oil palm plantation, and fishing planning. Furthermore, research on the use of remotely sensed data from Landsat-TM to support sustainable forest management in East Kalimantan were made by Aguma & Hussin (2002). They used Landsat to verify some ecological criteria and indicators for tropical timber certification. Triparthi & Radiarta (2003) used bands 1 and 2 of Landsat 7 ETM+ to map coral reef habitat along the Riau archipelagos. Lepoutre *et al.* (1998) on the other hand, used a high-resolution panchromatic SPOT (PAN and XS) to improve the management of irrigation schemes in West Tarum (West Java).

Remote sensing has been used for post-disaster planning as well. After the tsunami hit Indonesia on 26th of December 2004, the remote sensing and GIS community in Indonesia prepared images of Nanggroe Aceh Darussalam Province, which was hit by the tsunami (RSGISForum, 2005). The images were used to help the government to re-establish the area by locating relatively safe areas to build temporary houses for refugees, relocating power lines, roads and other infrastructural works which need current spatial information. In the future, the coastline of the north and west part of Nanggroe Aceh Darussalam's map will be redrawn using the latest imagery.

4.2 Atmospheric and Topographic Correction

4.2.1 Atmospheric Correction

Atmospheric correction refers to the way the effects of aerosols, thin clouds and cloud shadows are removed from an image to improve its quality. Liang (2001) found that atmospheric effects such as molecular scattering and absorption by ozone and oxygen were relatively easy to remove, while the aerosol effect was quite difficult to eliminate.

Liang (2001) compiled some of the common methods used in correcting atmospheric effects, such as: invariant-object, histogram matching, dark object and contrast reduction. Some of the methods, especially those used to remove the effects caused by scattering and absorption, require *in-situ* field measurement (Chavez, 1996). Such methods are difficult to apply since the *in-situ* data on the day the image was taken are difficult to obtain. The optimum atmospheric correction procedure according to Chavez (1996) is better to be based on the digital image and does not require *in-situ* field measurements.

The invariant-object method is simple and straightforward, but it is essentially a statistical method and performs only a relative correction. This model also has difficulty in correcting heterogeneous scattering (Liang *et al.*, 2001).

Liang (2001) also found that the histogram matching method does not work well if the spatial distribution of aerosol loadings varies dramatically. This method assumes that the surface reflectance histograms of clear and hazy regions are the same.

Dark Object Subtraction (DOS) is probably the most popular atmospheric correction method, especially for dense vegetation. The method does not work well if the dense vegetation is not widely distributed over the hazy regions (Liang *et al.*, 2001). DOS is simple to apply, because it is strictly an image-based procedure and does not require *in-situ* field measurement (Chavez, 1996). In spite of this, for reflectance values greater than 15 percent, the accuracy of this correction is often not reliable.

The contrast reduction method is good for desert dust monitoring (Liang *et al.*, 2001), but not for all applications since its assumption of invariant surface reflectance does not always happen in reality.

The apparent reflectance model converts at-satellite radiances to reflectance (Chavez, 1996). This model is simple, easy to apply and it does not require *in-situ* field measurement. However, the accuracy is not acceptable in some applications, especially using TM bands 1 and 4 (Moran *et al.* as cited in Chavez, 1996).

4.2.2 Topographic Correction

In many instances, particularly in mountainous regions, there exist variations in surface illumination, resulting in areas that receive direct sunlight, areas in complete shade, and variations between these extremes. This is due to topographic slope and aspect relative to the position of the sun. These effects affect the brightness values of the pixel, and should be corrected before any classification is made (Civco, 1989; Fahsi *et al.*, 2000).

Topographic correction refers to compensation for different solar illumination due to irregular shape of the terrain (Riaño *et al.*, 2003). When this correction is properly applied to an image, the topographic effect is lessened, and objects having the same reflectance properties show the same pixel value despite their different orientation to the sun's position (Botanical Institute, 2002). However, the main difficulty in applying topographic correction is related to the lack of standard and generally accepted models (Riaño *et al.*, 2003).

In general the topographical effect can be corrected with or without the use of DEM (Riaño *et al.*, 2003). The accuracy of image classification in a heterogeneous forest with rugged terrain is improved by using a DEM as additional band (Dorren *et al.*, 2003). This is because the error in classification could be resolved through the use of auxillary data, especially topography (Foody & Hill, 1996). Without a DEM, the correction is much simpler, since it is based only on band ratioing. The consequence is that the image loses its spectral resolution, which is a drawback for multispectral analysis (Colby & Keating, 1998; Riaño *et al.*, 2003).

When using a DEM, it is important to ensure that the resolution of the DEM is the same as the uncorrected image (Civco, 1989; Ekstrand, 1996). Two different types of approach are commonly used to correct the topographic effect; one based on a terrain calculation, and the other based on vegetation information.

The terrain approach is called the Sun-Terrain-Sensor (STS) method, it flattens the terrain by changing the sun-geometry crown, which is actually independent of terrain (Gu & Gillespie, 1998). Models that use this approach are: Cosine, Minnaert, and C-correction (Civco, 1989; Gu & Gillespie, 1998). These models are good for less structured surfaces (Gu & Gillespie, 1998) but sometimes under- or over-correct the image (Civco, 1989).

The method based on vegetation knowledge is encouraged by Riaño *et al.* (2003) and Gu & Gillespie (1998). According to Gu & Gillespie (1998), topographic effects in forest images are related to the forest canopy which should be normalized. They proposed the Sun-Canopy-Sensor (SCS) method to correct the topographic effect in forested areas. The main difference between this method and STS is the use of terrain slope as an addition to the incidence angle ($\cos(i)$).

Another method based on vegetation knowledge has been developed by Dymond & Shepherd (1999). They suggested that the effect of solar radiation and reflectance on vegetation in sloped areas should be corrected before doing any classification. This method considers both the incidence (i) and exitance (e) angles (Dymond & Shepherd, 1999; Dymond & Shepherd, 2004; Dymond *et al.*, 2001). The main difference between this method and the previous method proposed by Gu & Gillespie (1998) is that this method calculates the irradiance and reflectance of the image. For the irradiance, it needs quite a large volume of information, such as climatological mean profile of pressure, temperature, water vapour, and ozone, while the reflectance is calculated by comparing the incidence and exitance angles of the sloped and horizontal surfaces (Shepherd & Dymond, 2003). This method would be difficult to apply in this study because not all of this information was commonly available in Indonesia.

Incidence angle is defined as 'the angle between the normal to the ground and the sun rays' (Dymond *et al.*, 2001; Riaño *et al.*, 2003). The incidence angle is calculated as follows:

$$\cos(i) = \cos(sz)\cos(\beta) + \sin(sz)\sin(\beta)\cos(az - aspect)$$

where:
β = slope angle (^{0})
sz = solar zenith angle (^{0})
i = incidence angle (^{0})
az = solar azimuth angle (^{0})
$aspect$ = direction of the slope (^{0})

The slope and aspect angles are derived from the DEM, while the solar zenith and azimuth angles are obtained from the image header.

The formulae of the methods described above are presented as follows:

- Cosine correction $$L_H = L_T \frac{\cos(sz)}{\cos(i)}$$

- Minnaert correction $$L_H = L_T \left[\frac{\cos(sz)}{\cos(i)} \right]^k$$

- C-correction $$L_H = L_T \left[\frac{\cos(sz) + c}{\cos(i) + c} \right]$$

- SCS correction $$L_H = L_T \frac{\cos(\beta)\cos(sz)}{\cos(i)}$$

where: L_H = radiance observed for a horizontal surface

L_T = radiance observed for sloped terrain

$\cos(sz)$ = cosine of sun's zenith angle

$\cos(i)$ = cosine of sun's incidence angle

c $= b/m$; b = intercept of the regression

m = gradient of the regression

k = Minneart constant; a value which represent how close a surface is to an ideal diffuse reflector (1 – 0)

Cosine correction is the most widely used method for correcting the topographical effect (Riaño *et al.*, 2003), but it has been found that this method tends to over-correct the image. The SCS geometry was developed for topographic correction of forest images based on the sun-canopy-sensor model (Gu *et al.*, 1999).

4.3 Supervised and Unsupervised Classification

The objective of image classification is to replace visual analysis of the image data with quantitative techniques for automating the identification of features in a scene (Lillesand *et al.*, 2004). According to Franklin (2001) the objective of forest classification is to generate spatially explicit generalizations that show individual classes selected to represent different scales of forest organizations. This normally involves the analysis of multi-spectral image data and the application of statistically

based decision rules for determining the land cover identity of each pixel in an image, although most statistical procedures are based on the reflectance and ignore shape, size, position and association such as is used in an aerial photo interpretation (King, 2002).

Some basic steps for classifying an image are (Franklin, 2001):

- Development of a classification system comprised of individual and hierarchical classes across the landscape
- Derivation and implementation of methods and algorithms that can be applied with understandable error patterns and identifiable uncertainty in decision making
- Application of a statistically sound accuracy assessment and validation of mapping products

Regardless of the types of classes selected, experience has shown that the classification scheme must be developed with full involvement of at least two collaborative interests:

- Those generating the classification products
- Those using the classification products

Occasionally these two groups are one and the same; but too frequently, the users are not directly involved in the classification process. Acquiring user input into the classification scheme at the beginning of the process will almost certainly help generate more usable classification products from remote sensing imagery, while asking for user input only to evaluate the finished product is not a wise option (Franklin, 2001).

A ground cover thematic map derived from a computerised classification should be based on some ground truth data gathered by the user from selected training areas. This is applied whether employing unsupervised or supervised classification (Thomas *et al.*, 1987). The accuracy of the thematic map depends on the user's ability to extrapolate successfully from the training areas to the whole mapped area. A Confidence Level (CL) is the probability of at least a number of pixels being correctly classified when a random sample of pixels is selected, and it is expressed in percentage (Thomas *et al.*, 1987).

Two different techniques are used when classifying an image; supervised and unsupervised classification.

4.3.1 Supervised Classification

Supervised classification requires the analyst to determine each class by specifying the computer algorithm and numerical descriptors (training areas) of the various land cover types present in a scene (Lillesand *et al.*, 2004). Each pixel in the image data set is categorised into the land cover class it resembles most closely. If the pixel does not match the training area, it may then be labelled as "unknown". The result from such a classification could be used as an input for the GIS analysis (Lillesand *et al.*, 2004).

Campbell (2002) listed the advantages and disadvantages of supervised classification as follows. In the supervised classification the analyst can control the information categories; there is no difficulty in matching the information categories with the classified image; it is easy to detect errors in classification and the classification is connected to a known identity. The limitations are: the classes requested by the analyst may not exist; the training areas may be designed poorly or selected wrongly; determining the training area can be difficult and time consuming; and sometimes the analyst may have missed a unique category because it is too small to be distinguished or the analyst does not have knowledge of it.

Different algorithms may be use in supervised classification to group the pixels, such as: minimum-distance-to-means classifier, parallelepiped classifier, and Gaussian maximum likelihood classifier.

The minimum-distance-to-means method is mathematically simple and computationally efficient, but it is insensitive to different degrees of variance in the spectral response data (Lillesand *et al.*, 2004). This problem makes it not widely used in applications where spectral classes are close to one another in the measurement space and have high variance.

The parallelepiped classifier uses a rectangular area from a two-channel scatter diagram, or a cube if working in three dimensions, and so on (Lillesand *et al.*, 2004). An unknown pixel will be classified according to the region it lies within; or unknown if it

lies outside all regions. Like the minimum-distance-to-means classifier, this method computes very quickly and efficiently.

The Gaussian maximum likelihood classifier assumes that the distribution of the pixel values is normal, therefore the pattern can be described by the mean vector and the co-variance matrix (Lillesand *et al.*, 2004). An unknown pixel will be assigned according to the highest probability value or unknown if the probability values are less than a threshold value set by the analyst. Although this method is popular, it computes at a much slower rate than the previous methods.

4.3.2 Unsupervised Classification

Unsupervised classification aggregates image pixels into natural spectral groupings or clusters present in the image values (Lillesand *et al.*, 2004). It is assumed that the same class will have values that are close together in the measurement space, whereas data in different classes should be comparatively well separated (Lillesand *et al.*, 2004). Since the classes are formed from similar spectral values, the identity of the classes is not known unless the analyst understands the condition of the location very well.

The advantages and disadvantages of unsupervised classification according to Campbell (2002) are listed as follows. In unsupervised classification human error is minimised, knowledge of the study area is not needed and unique categories are easily recognised. The disadvantages are: difficult to match the classes derived from the classification to the available categories, the spectral properties that change over time make the informational categories change too, and the analyst has a limited control over the classes.

King (2002) stated that unsupervised classification should not be carried out on an image containing clouds, significant relief, shadows and other unfamiliar spectra because it could result in a mixed-up classification. Therefore, it is suggested that one performs atmospheric and topographic correction first before conducting the classification.

ISODATA (Iterative Self-Organizing Data Analysis) is a method used to classify the pixel by permitting the pixels to change cluster from one iteration to the next, by merging, splitting, and deleting clusters (Lillesand *et al.*, 2004). The iteration will stop

when there are no more clusters changing or the maximum number of iterations is reached.

Hybrid classification uses both supervised and unsupervised techniques to improve the accuracy and efficiency of the classification process. For example, the training areas for the supervised classification might be gathered from the unsupervised classification.

Artificial neutral networks, another new method to classify more heterogeneous areas, can be used to do either traditional classification or more complex types such as spectral mixture analysis (Lillesand *et al.*, 2004). This method does not need training classes with normal distributions, therefore a wider range of input data can be used. This capability eanbles neutral network classification to perform relatively rapidly (Lillesand *et al.*, 2004) and more effectively in forest environments (Dwivedi *et al.*, 2004; Woodcock *et al.*, 2001).

4.4 Land Cover

Land cover is the visible evidence of land use that includes both vegetative and non-vegetative features (Campbell, 2002). Different to the land use that puts emphasis on the economic role of the land, which makes land use an abstract feature, land cover is more concrete and this makes it subject to direct observation. A land cover map is usually the result of image classification; it is considered an essential element for modelling and understanding the earth as a system (Lillesand *et al.*, 2004).

USGS (US Geological Survey) classifies the land cover through different levels, in which each level has its own level of detail, depending on the sensor system and image resolution. Levels I and II are for users who are interested in wider areas, such as nationwide, provincial or state wide, while levels III and IV, which contain more detailed information, are more appropriate for local planning and management activities (Lillesand *et al.*, 2004).

Interpreting the land cover in tropical areas only from its reflectance is not enough, tropical forest has such an intermix of species that it makes it difficult to distinguish between them (Bhandari & Hussin, 2003; King, 2002). Therefore, it is suggested that

other interpretation elements such as position and size be used in conjunction with reflectance to make the classification easier.

Classifying land cover from an image often requires combining or ratioing some channels to obtain a clearer signature of an object from the image since each channel has its own primary usage. Table 4-1 shows each channel and usage of Landsat ETM+.

Table 4-1 Landsat ETM+ spectral bands (Lillesand et al., 2004)

Band	Wavelength (μm)	Channel	Resolution (metre)	Principal applications
1	0.450 – 0.515	Blue	30	Designed for determining water body and coastal water mapping, soil/ vegetation discrimination, forest type mapping, and cultural feature identification
2	0.525 – 0.605	Green	30	Designed to measure green reflectance of vegetation and cultural feature identification
3	0.630 – 0.690	Red	30	Designed to sense in a chlorophyll absorption, plant species differentiation and cultural feature identification
4	0.750 – 0.900	Near Infra Red (IR)	30	Designed for determining vegetation type, vigor, biomass content. Delineating water bodies and soil moisture
5	1.55 – 1.75	Mid IR	30	Indicative of vegetation moisture content, soil moisture, and for differentiate snow from clouds
6	10.40 – 12.50	Thermal IR	60	Useful for vegetation stress analysis, soil moisture discrimination, and thermal mapping

Band	Wavelength (μm)	Channel	Resolution (metre)	Principal applications
7	2.09 – 2.35	Mid IR	30	Useful for discrimination of mineral and rock type, and sensitive to vegetation moisture content
8	0.520 – 0.900	Panchromatic	15	Higher spatial resolution can reveal more details of all earth surface features

Various band combinations can be used to aid image interpretation: using just the red, green and blue channels (RGB-321) results in true colour, while the combination of green, red and near-infra red channels (RGB-234) provides a false colour image that might distinguish vegetation better. The combination of the mid-infra red, red, and blue channels (RGB-531) is sometimes used to classify rock types (Liu *et al.*, 2004). On the other hand, Achard *et al.* (2001) found that the use of inappropriate spectral bands or indices, choice of training sites and choice of number of classes may result in very different resulting classes.

NDVI is an example of ratioing two channels to get a clearer signature. It is often used to differentiate kinds of vegetation. It not only combines the channels but normalises the relationship between the near-infra red and the red channels as follows:

$$NDVI = \frac{(NIR - R)}{(NIR + R)}$$

where: NIR = near-infra red channel (Band 4)
R = red channel (Band 3)

NDVI values range between -1 and +1 with expectation that high NDVI value would be found in areas of high leaf (Bhuyan *et al.*, 2002; Franklin, 2001). By understanding the spectral definition of each band, the right band combination will result in an accurate classification.

Another area of considerable recent interest in land cover classification is in the development of multiple classifiers, the process of combining independent classification algorithms to increase the accuracy with which land cover maps are produced (Aplin,

2004). Aplin (2004) and Petit & Lambin (2001) also noted that there is new approach in classifying land cover by combining different data sources. This is useful since certain sources of data are particularly suitable for discriminating specific land cover features. Examples for this include using hyperspectral imagery to distinguish subtle differences in vegetation growth, or incorporating elevation and temperature in the classification (Aplin, 2004) or combining panchromatic aerial photographs with SPOT (*Satellite pour l'Observation de la Terre*) multi-spectral (Petit & Lambin, 2001). Combining the 15 metre panchromatic band of Landsat ETM+ to the other 30 metre bands was also increase the capability to detect small patches of forest missed by the coarser resolution (Masek *et al.*, 2001).

4.5 Accuracy Assessment

Usually the accuracy of a thematic map is determined empirically by comparing the map with the corresponding reference or ground data. The results are tabulated in the form of a square matrix called the matrix of confusion. The elements of the principal diagonal of the matrix represent the correct matches and the remaining elements are the mismatched (Gopal & Woodcock, 1994).

Carmel *et al.* (2001) described the error that resulted from comparing a classified image and the ground reality as classification error. This error is measured by counting the classes where actual and observed classes differ and it is summarised in an accuracy matrix. This method is similar to the method used by Gopal & Woodcock.

In that matrix rows give a measure of producer's accuracy, and columns show user's accuracy. Producer's accuracy indicates the probability of a test or reference location known to belong to a certain category is accurately labelled at that category, while user's accuracy indicates the probability that a test of reference location labelled as a certain category belongs to that category (Gopal & Woodcock, 1994; Zhuang *et al.*, 1995). The user's accuracy or producer's accuracy is not the accuracy for a given classification category (Zhuang *et al.*, 1995) since most of the accuracies do not give the same value. The mapping accuracy for each class is the percentage of the correct matches compared to all samples in the same row and column of that particular class.

The user's accuracy details the error of commission (NOAA Coastal Service Center, 2005) which measures the ability to discriminate within a class but the classifier incorrectly put into other classes (Short, 2004). The producer's accuracy, on the other hand, details the error of omission (NOAA Coastal Service Center, 2005). Errors of omission occur when one class on the ground is misidentified as other class(es) (Short, 2004).

4.6 Methodology

This section describes the processing of the Landsat image: atmospheric and topographic correction, land cover classification and accuracy assessment. The full procedure that was followed is illustrated in the flow diagram shown in Figure 4-1.

4.6.1 Atmospheric and Topographic Correction

The method adopted for atmospheric correction was Dark Object Subtraction (DOS), while for the topographic correction, three methods were tested: cosine, C and SCS correction (Section 4.2.2).

4.6.2 Supervised and Unsupervised Classification

A stratified method of two and three bands combinations was used for supervised classification and a single combination of three bands was applied for the unsupervised classification. The band combinations were chosen by considering the application of each band in Table 4-1 and as well as trial and error. The supervised classification used RGB-754, RGB-532 and NDVI, while RGB-721 was used for the unsupervised classification. Figures 4-2 and 4-3 show the procedure followed to produce a land cover classification using a series of different band combinations. The results of each classification can be seen in Figures 4-8 to 4-11.

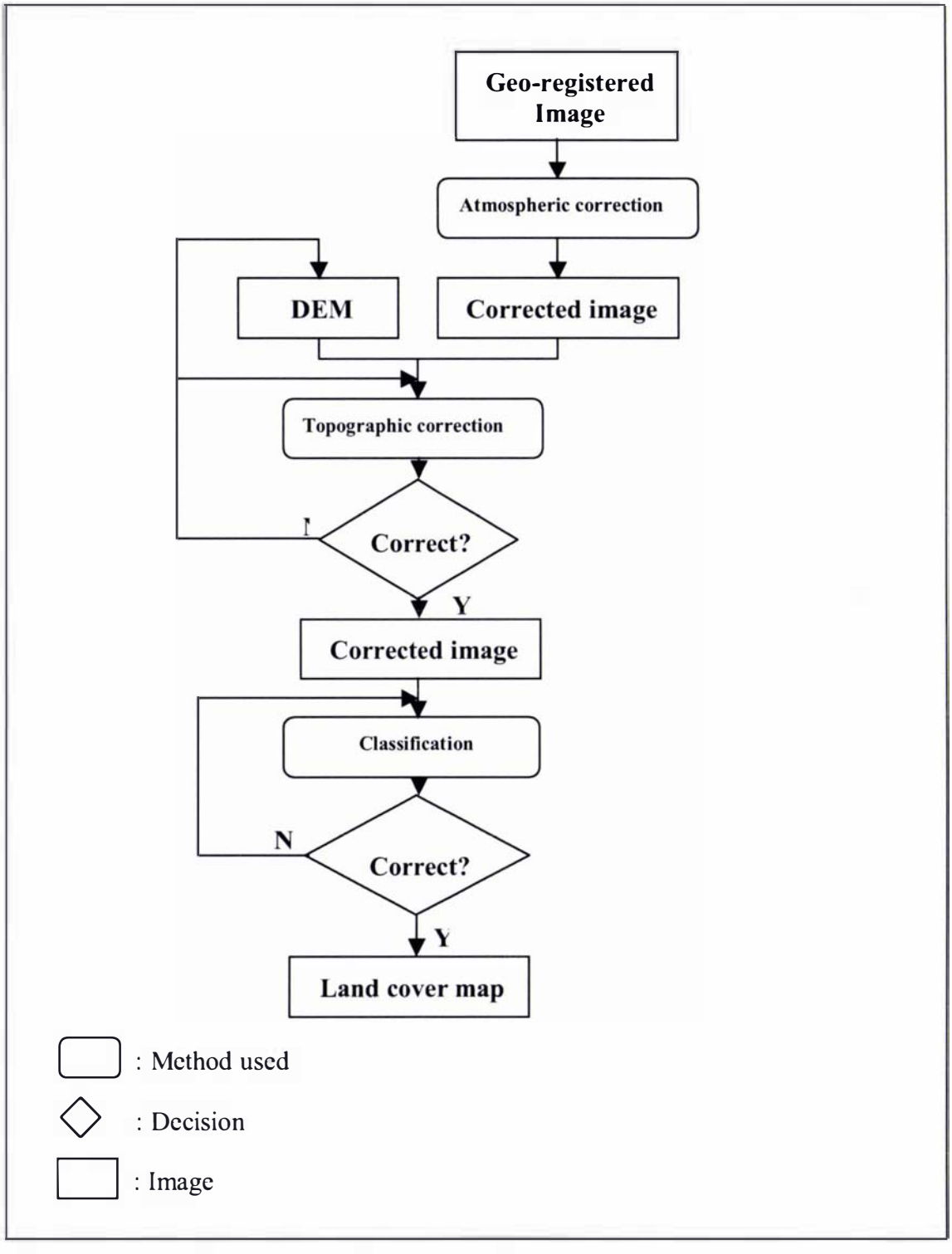

Figure 4-1 Flow diagram of land cover classification

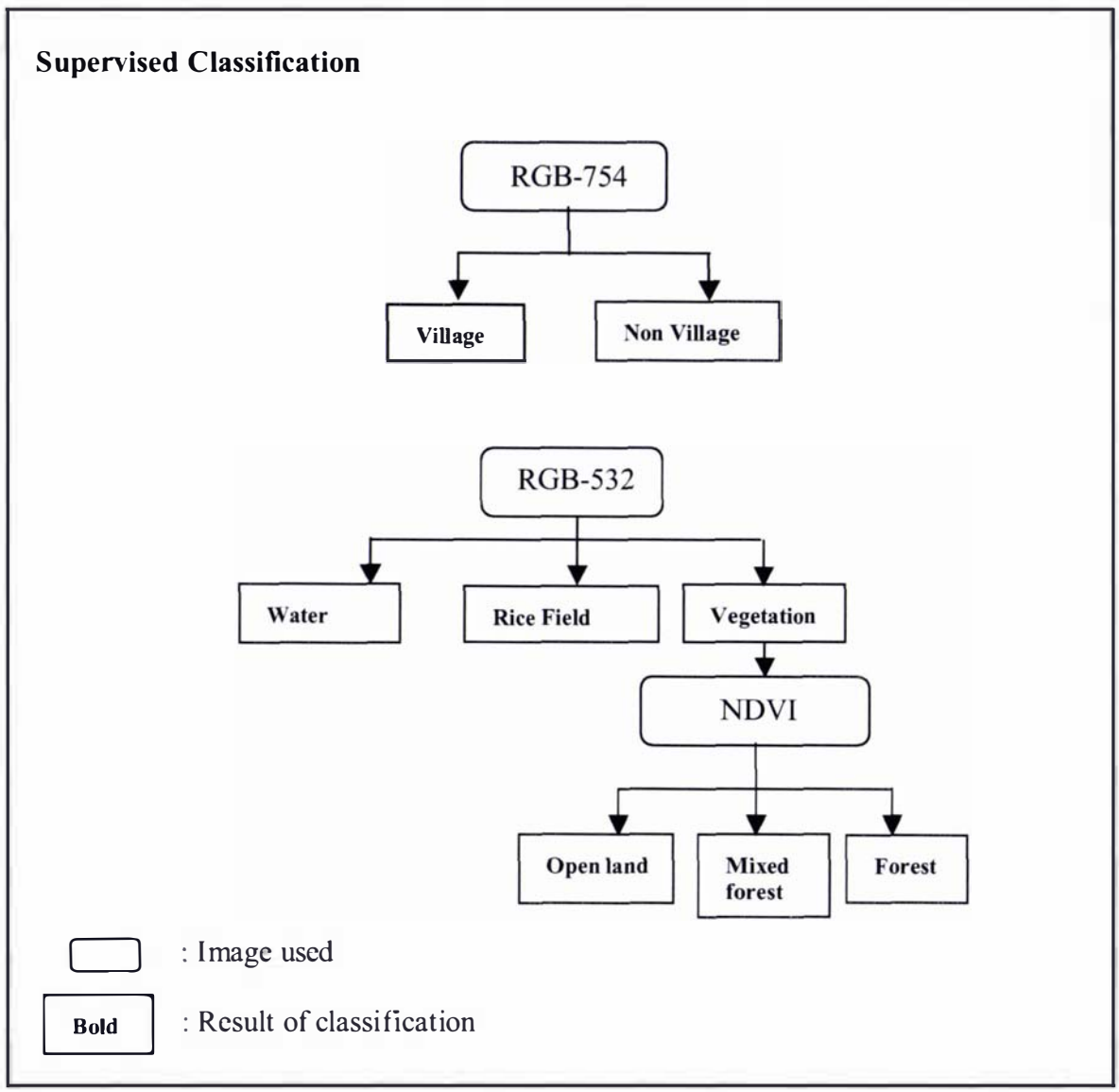

Figure 4-2 Flow diagram of detailed land cover classification using supervised classification.

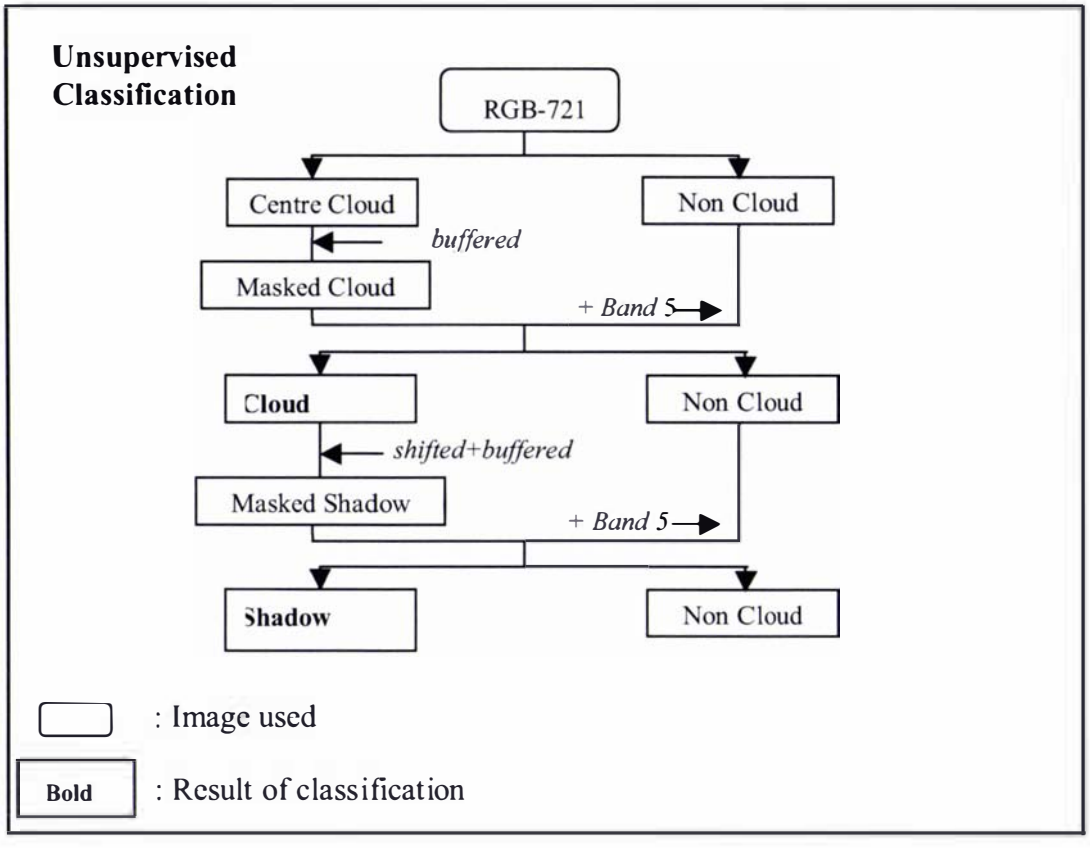

Figure 4-3 Flow diagram of unsupervised classification to capture cloud and shadow from the image

4.6.3 Compilation of the Supervised and Unsupervised Classification

Since the classification was a stratified classification, the entire individual results had to combine. The sequence was important as it determined which land cover was to be preserved or overridden.

The sequence used was as follows:

- 1 RGB-532 was classified first to determine rice fields, water bodies and vegetation
- 2 RGB-754 was classified to identify villages which would replace rice fields if the pixel had been assigned to this class previously
- 3 NDVI was then used to classify open land, mixed and monotype forest

– 4 clouds and their shadows were identified using the RGB-721 combination.

4.6.4 Accuracy Assessment

The accuracy assessment was effected using two techniques; one involved comparing the classified image with the land cover classes shown on the topographic map, and the other used ground truthing in places where photographs had been taken during field visits. For the first comparison, a thousand points were distributed randomly across the classified image and topographic map. The land cover class that had been assigned to each point was assessed for both image and map and the results put into matrix of confusion to determine the accuracy.

The data from the topographic map were assessed manually. The land cover classes on the topographic map were: villages, irrigated rice field, rainfed rice field, plantation (consisting of coconut plantation, teak, albisia, and pine forest), forest, shrubs, open land, and bare land. To match these classes with those in the classified Landsat image, some of the classes on the topographic map were combined. The rainfed and irrigated rice fields were grouped as rice fields; shrubs, open land and bare land were combined into a single open land class. Table 4-2 shows the various combinations and compares the land cover classes from both sources.

Table 4-2 Comparison between land cover classes from the classified Landsat image and the topographic map

Classified imagery	**Topographic map**
Water bodies	Rivers and other water bodies
Villages	Villages
Rice field	Irrigated and rainfed rice field
Open land	Shrubs, open land, and bare land
Mixed forest	Forest
Forest/monotype forest	Plantation (coconut, teak, albisia, and pine)

Where photographs had been taken on the ground, the features that could be identified in the photographs were compared visually with the classes that had been assigned in

the classified Landsat image. Seven locations were used; the photographs of these sites captured a range of land covers and provided a good check on the accuracy of the classification. The locations of the photo sites are presented in Figure 4-4.

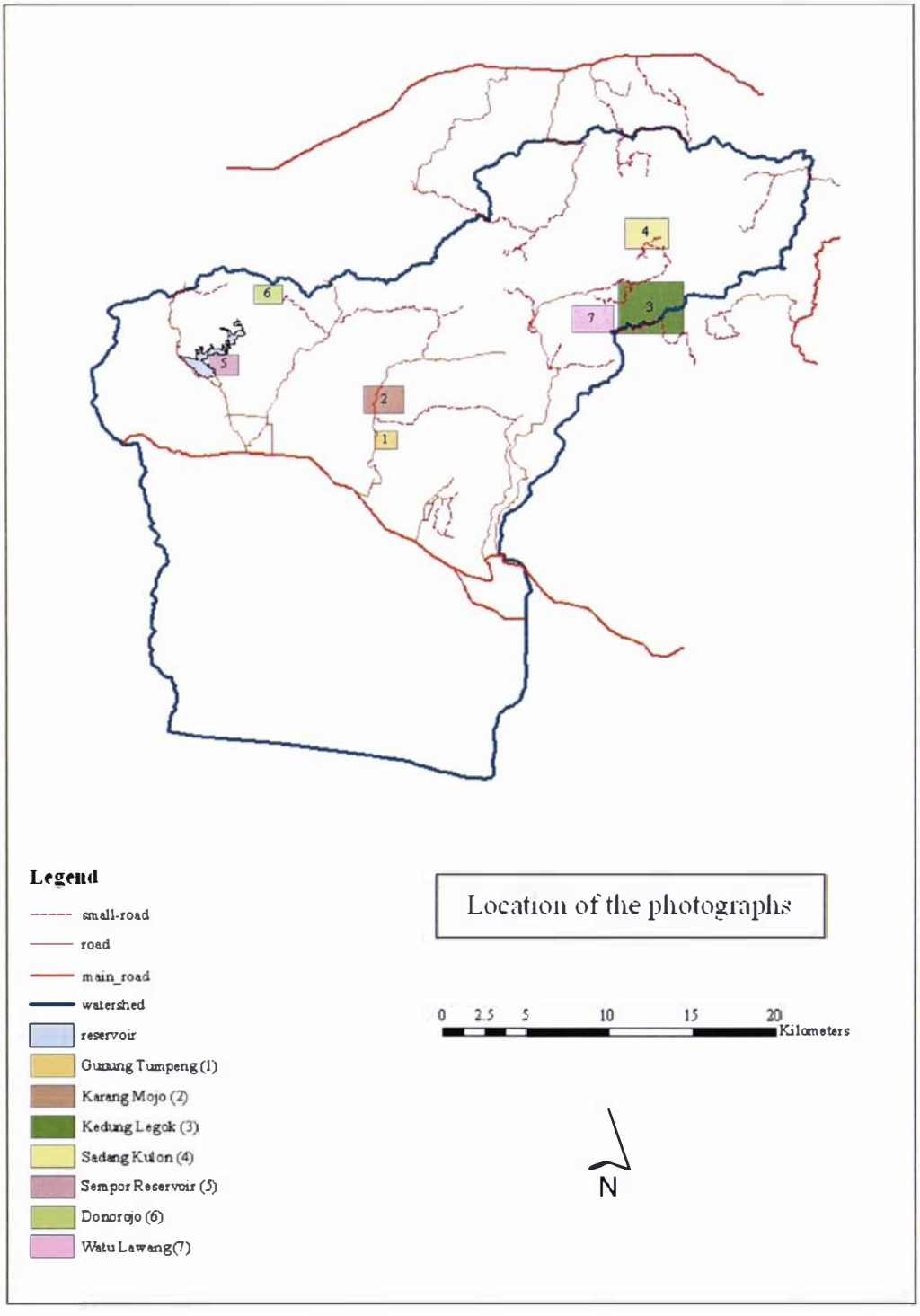

Figure 4-4 Locations of the photos used to test the accuracy of the classified image

4.7 Results and Discussion

4.7.1 Atmospheric and Topographic Correction

Before the atmospheric and topographic corrections were carried out, the Digital Number (DN) values of the pixels were converted into radiance values. From the image metadata, the minimum and maximum radiance and DN range of each band were noted (Table 4-3). The radiance value for each pixel in each band was calculated using the following equation:

$$Radiance = \frac{(L\max - L\min)}{(Qcal\max - Qcal\min)} * (Qcal - Qcal\min) + L\min$$

Where: L max = radiance maximum value
L min = radiance minimum value
$Qcal$ max = pixel value maximum = 255
$Qcal$ min = pixel value minimum = 0
$Qcal$ = digital number of each pixel

Table 4-3 The minimum and maximum radiances for each Landsat band

Band	Radiance value (μW/cm²/st/nm)	
	Minimum	Maximum
Band 1	-6.20	191.60
Band 2	-6.40	196.50
Band 3	-5.00	152.90
Band 4	-5.10	241.10
Band 5	-1.00	31.06
Band 61	0.00	17.04
Band 62	3.20	12.65
Band 7	-0.35	10.80
Band 8	-4.70	243.10

By applying this equation to the values in Table 4-3, the radiance for each pixel for bands 1, 2, 3, 4, 5, and 7 can be calculated. This calculation was applied to the whole image.

The atmospheric correction method used in this study was DOS. This method was chosen due to its simplicity and ease of use. DOS does not require *in-situ* or other climatic data and recognises, that within an image some pixels are in complete shadow which makes their surface black (Chavez, 1996) and it is therefore necessary to exclude these pixels from any future processing. The histogram transformation (Figure 4-5a) shows the input limit value of the imagery. For example, the radiance value of Band 1 is -6.9 to 179.2 (shown in the bottom part of Figure 4-5a). The negative values belong to the pixels in areas outside the image (see Figure 4-5b) and are shown as a black vertical line in the left-hand side of the histogram.

The zero value of each band is displayed when the cursor is placed on histogram and the pixel value is then displayed (Figure 4-5a). The correction is made by shifting the zero digital number from the spectral value until the digital number is greater than zero.

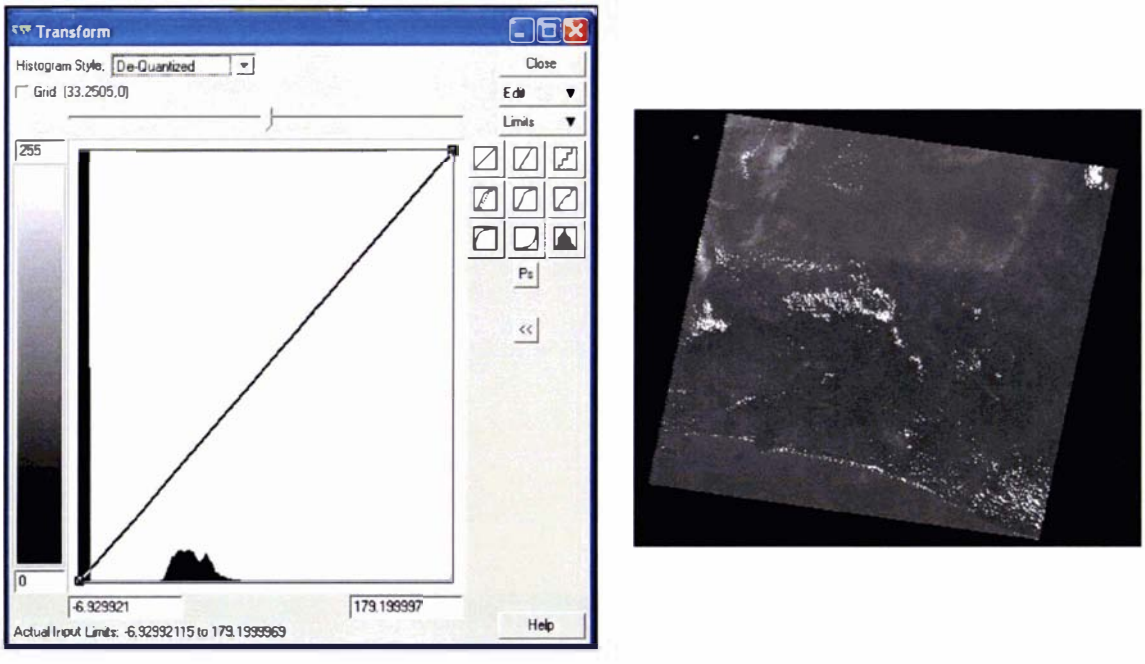

a b

Figure 4-5 The histogram of Band 1 shows the zero value that shifted in the spectral value

Band 1 required the greatest correction, while bands 5 and 7 required none. This was because aerosol and haze more often affect bands 1, 2 and 3 rather than bands 4, 5 and 7 (Liang *et al.*, 2002). After applying the atmospheric correction, all bands were clipped, saved and then corrected for topography. The radiance values and the dark object value for each band are presented in Table 4-4.

Table 4-4 The range of radiances and dark object values for each band

Bands	**Radiance values**	**Dark object value**
Band 1	0 – 179	33
Band 2	0 – 184	20
Band 3	0 – 143	8
Band 4	0 – 231	2
Band 5	0 – 29	0
Band 7	0 – 10	0

Note: Band 6 was not used in this study

The most important ingredient for performing a good topographic correction is an accurate DEM (Fahsi *et al.*, 2000). Furthermore, Fahsi *et al.* noted that removal of the topographic effect is considered successful if the spectral variability over areas of varying terrain is substantially reduced.

From the topographic correction methods described in Section 4.2.2, three methods were tested for this study:

- Cosine correction
- C correction
- SCS correction

Figure 4-6a through to d show a colour composite using the original pixel values and the three images that resulted after applying the different topographic correction methods.

From the image metadata, the information required for topographic correction was:

- The image was taken on 28th April 2001 around 9.30 am
- The sun azimuth = 54.2080085 degrees
- The sun elevation = 53.4585842 degrees
- The calculated solar zenith angle was 36.5414158 degrees

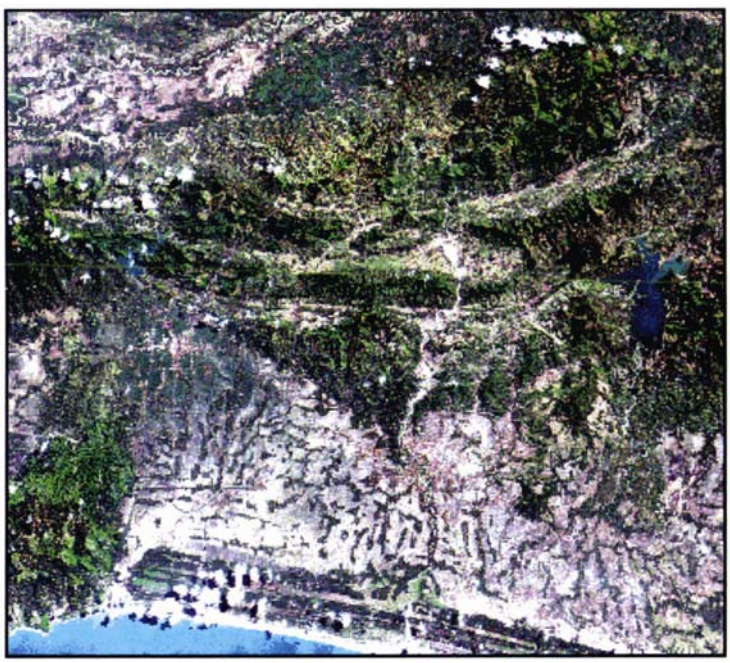

a. The original image, as an RGB-321 composite.

b. The image after C correction.

c. The image after the Cosine correction

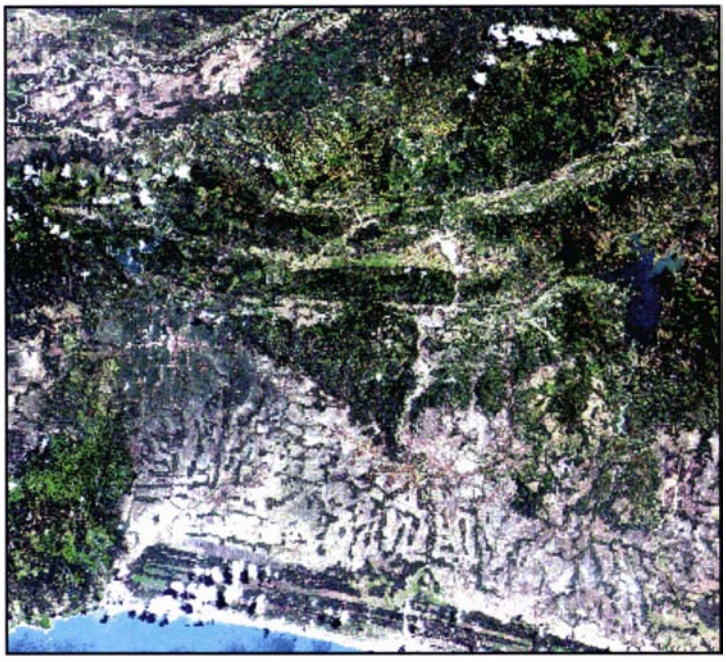

d. The image after the SCS correction

Figure 4-6 Colour composites created from the original pixel values and after applying the three topographic correction methods.

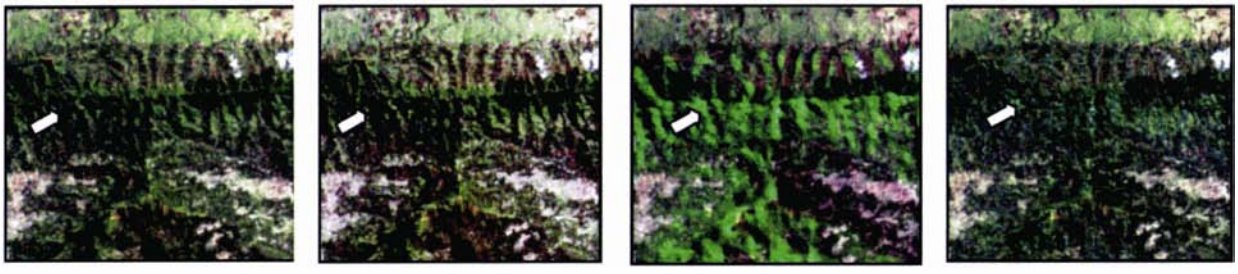

a. Original b. C – correction c. Cosine d. SCS

Figure 4-7 A comparison of the topographic correction methods used, specifically in a hilly area. The arrow highlights where the different methods appear to have the most effect.

The results of the topographic corrections shown in Figures 4-6 and 4-7 highlight the fact that the corrected images varied depending on the method applied. Correcting the image using the C method did not affect enough alteration to the original image and the corrected image still showed a topographical effect (under-correction). The values of C (which is the linear correlation between the uncorrected image and cos (i)) were large

for all bands (398 – 3222 in this study area); and as Gu & Gillespie (1998) found, although the C value was large, it still did not result in much improvement.

The cosine method, on the other hand, resulted in negative topography (over-correction). Some hills in the original image looked like valleys in the corrected image. Gu & Gillespie (1998) acknowledged this problem as well. They noted that this over-correction was because of underestimating the reflectance of sun-facing slopes and overestimating the reflectance of slopes facing away from the sun. This incorrect estimation results in the negative topography or the 'valley-look' in the corrected image. These two models showed that sun-terrain-sensor normalization was not the most suitable technique: it did not adequately remove the topographic effects of the highly structured forest canopies (Gu & Gillespie, 1998).

The SCS method, on the other hand yielded the best result because it normalised the sunlit area by projecting the sloped surface in the sun direction to horizontal (Gu & Gillespie, 1998). Thus this method used slope angle in addition to the incidence angles. In the areas around the arrow in Figure 4-7d, the tone and colour of forest were uniform over the whole area. This was the method used for correcting all of the images throughout this study.

4.7.2 Supervised and Unsupervised Classification

The land cover types in the study area include forest (monotype and mixed), open land, rice fields, villages, and water bodies. To extract these land cover classes, the classification was carried out according to the flow charts shown in Figures 4-2 and 4-3. For the supervised classification a Gaussian maximum likelihood classifier was used. Each classified image was also filtered using a Ranking-Majority 3 x 3 kernel; this removed isolated pixels that differed in class to those around them and gave the image a smoother appearance. It replaced the central pixel with the majority class of nine neighbouring cells but did not change the essential features of the classification.

As part of the supervised classification process, training classes were chosen from each band combination (RGB-754 and RGB-532) through visual interpretation, and then cross checked with the topographic map, since the topographic map also showed the major land cover types (the detail of the topographic map is presented in Section 3.1).

If a training area's boundary did not match that of the topographic map, then the boundary was adjusted until it did match. No training areas were delineated in portions of the image where the land cover determined visually did not match that on the topographic map. In the final analysis, all training areas were within the land cover's boundary and matched to the topographic map.

The optimum size of a training area varies depending on the heterogeneity of the landscape and land cover. In general the total size of several training areas for each category should be at least 100 pixels (Campbell, 2002) or 9 ha in this study area.

The RGB-754 composite was used to differentiate areas occupied by the villages from the rest of the study area. So for this image only training areas for the villages were required. From Table 4-1, bands 4, 5 and 7 should be better for detecting vegetation types and soil moisture, while bands that are better for identifying cultural features should be bands 1, 2 and 3. In this instance, village classification using RGB-754 was better than RGB-321, especially when the villages were surrounded by trees. It could be that since the soil around the houses was drier (because usually it was plastered) RGB-754 picked out villages more successfully. The training areas for villages were spread throughout the study area; they occupied 94.7 ha (1052 pixels) or 0.05% of the total study area.

In some areas the rice fields and villages had similar reflectance. This was because the farmers often plant trees around the edges of their property as well as their houses. If the rice field was dry, then the reflectance was similar to the homestead garden or open land. Therefore, rice fields, open land and villages had to be classified using different band combinations. Villages were classified using RGB-754; rice fields using RGB-532 and open land was distinguished using NDVI (see Figure 4-2).

The RGB-754 composite could be used to differentiate villages from rice fields because bands 5 (mid infrared) and 4 (near infrared) are able to detect soil moisture and water bodies. Since the soil moisture content of rice fields was higher than villages, the reflectance of rice fields and villages in these bands was different. All of the villages classified using this band combination were found to be correct, especially when the training classes for the village were cross-checked with the topographic map. Figure 4-8 shows the classified villages after being filtered using majority 3 x 3 kernels.

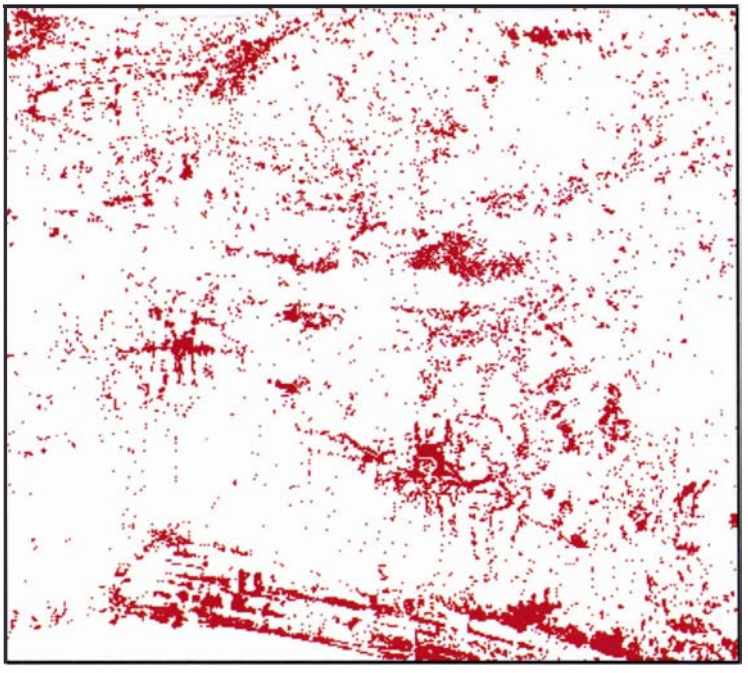

Figure 4-8 Classified image of village (red) and non village (white) area filtered using majority (3x3)

The RGB-532 composite was used to distinguish vegetations, rice fields and water bodies. The sizes of the training areas for these features were 1002.24 ha (11136 pixels), 782.55 ha (8695 pixels), and 427.32 ha (4748 pixels) respectively. Bands 3 and 2 were designed to pick up chlorophyll and vegetation, while band 5 can be used to identify water bodies. Thus, this band combination could easily identify water bodies and vegetations, and rice fields were found to occupy much of the rest of the image. The result of this classification after also being filtered is presented in Figure 4-9.

Since vegetations in the above classification consist of mixed forest, monotype forest and open land, they needed further separation. The NDVI image was used for this purpose after the other land cover types (already identified) were masked out.

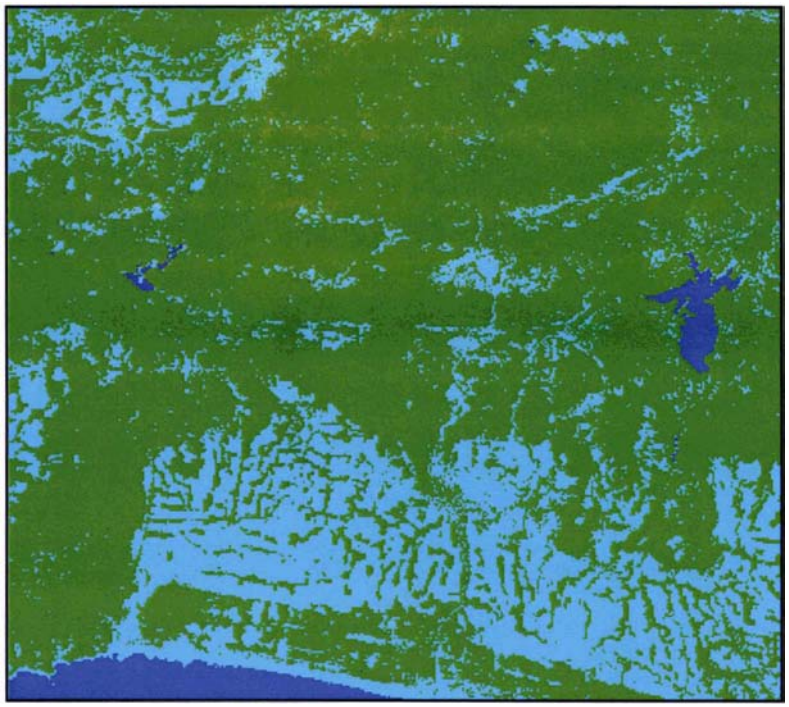

Figure 4-9 A supervised classification of the RGB-532 composite showing trees (green), rice fields (cyan) and water bodies (blue) after filtering using majority (3x3) kernel.

The NDVI values ranged from -0.882 up to 1. A low NDVI value indicates areas with low vegetative cover, while the higher value means denser vegetative cover (Bhuyan *et al.*, 2002; Bureau of Meteorology, 2004). Since the negative values of NDVI are often associated with water bodies (Bureau of Meteorology, 2004), all NDVI values less than 0 were assigned as water bodies and then masked out as well. By trial and error, the thresholds for mixed and monotype forests, and open land were determined. They were:

- > 0.80 monotype forest
- 0.65 – 0.80 mixed forest
- 0.15 – 0.45 open land

Areas with smooth texture and similar tone were vegetation with homogeneous height and age (Vieira *et al.*, 2003), and in this study area they were pine production forest managed by Perum Perhutani.

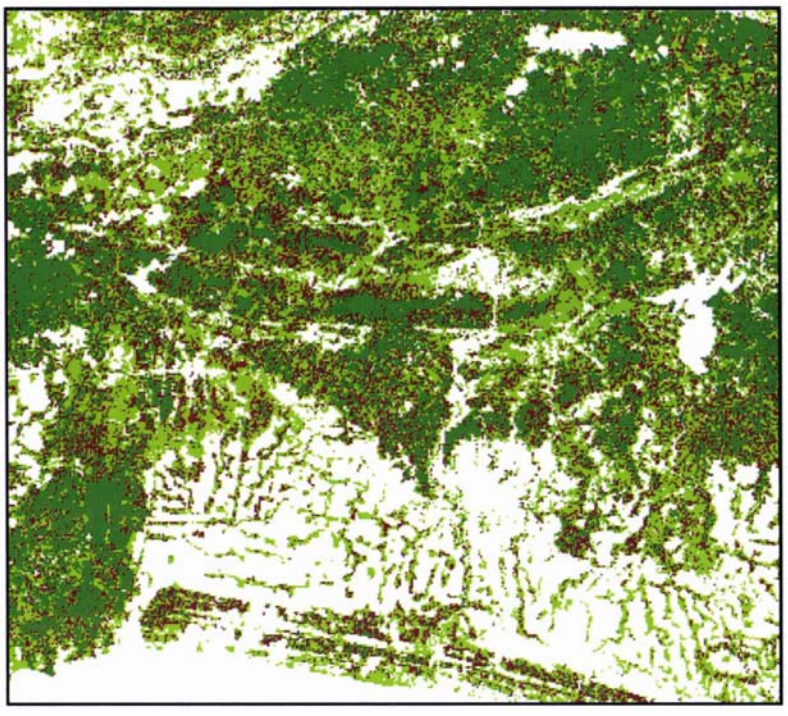

Figure 4-10 The result of NDVI classification: open land (brown), mixed forest (light green), and forest (dark green). The rest of the area (white) was masked (rice field, village, and water bodies)

Unsupervised classification of the RGB-721 composite image was used to differentiate cloud in the image and the steps followed were illustrated in Figure 4-3. The cloud and cloud shadows needed to be masked out because the features under them can not be identified. By trial and error it was found that using the isoclustering algorithm and producing only three classes, the clouds were differentiated from the other land covers. Classes 2 and 3 were clouds and class 1 was the rest. To make sure that all clouds were selected (especially the small isolated ones); a 100-metre buffer was generated around the clouds. This process was carried out in ARCMap after first converting the classified ERMapper-raster file into polygons. Next, a check was made to ensure that all the clouds were included and then after buffering, the resulting polygon file was converted back into an ERMapper raster file.

In addition to the unsupervised classification, it was found that more clouds could be identified simply by specifying a threshold value in Band 5. By trial and error the threshold was found to be 15. By selecting every pixel in band 5 greater than 15 and combining these with those identified in the buffered-cloud image all the clouds were

delineated. This technique was found to include the small isolated clouds so long as those clouds were covered by the buffered-cloud. Band 5 was chosen because it can display the cloud clearly and it was designed to detect cloud (Table 4-1). The equation used was as follows:

If band 5 > 15 and buffered-cloud image = 1 then 1 else null

Shadows may cause pixels to have similar reflectance values too, and thus be confused with surfaces that belong to different logical classes (Giles, 2001). From the unsupervised classification, clouds were easily separated from the image, but the shadows of the clouds were more difficult because they had similar reflectance values to the water bodies and wet rice fields. To pick up the shadow, the procedure used was similar to the procedure for determining the cloud class. Since the shape of the clouds and their shadows were similar, the cloud image was used to pick the shadow up. The image was copied, assigned to 8 (the value for shadows) and converted into ARC Map polygon coverage. Using the MOVE command in ARC Map, the polygons were then shifted to the lower left direction. These polygons were buffered for 100 m, to make sure that they covered all cloud shadows. By a similar technique to that used for the cloud, the shadow was determined. The only difference was that cloud shadows could not override the cloud.

Like finding the threshold for the cloud, the threshold for the shadows was done by trial and error. Using band 5, the reflectance value of shadows ranged from 1 to 5. Combining the three images (band 5, classified cloud and buffered shadow) resulted in identifying those pixels that should occupy the cloud shadow class. Thus, the shadows were anywhere under the buffered shadow as long as those pixels were not already classed as cloud. The equation used is presented below, while the classification of clouds and their shadows is presented in Figure 4-11.

If band 5 >= 1 and band 5 < 5 and classified cloud <> 1 and buffered-shadow = 8 then 8 else null

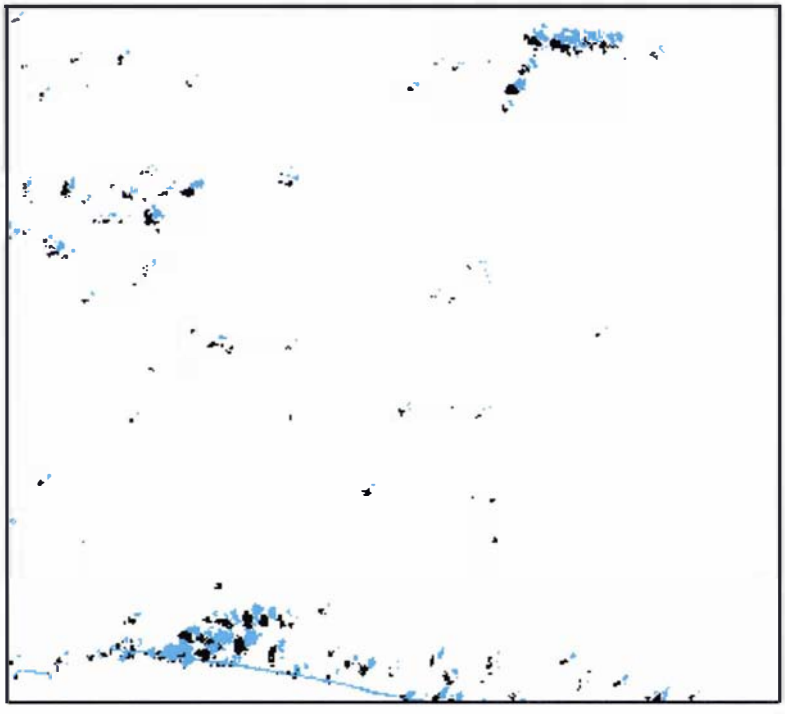

Figure 4-11 Result of the unsupervised classifications for the clouds (cyan) and shadows (black)

4.7.3 Compilation of the Supervised and Unsupervised Classification

The classifications resulted in four images which were combined into a final land cover map. The individual classifications were village cover from RGB-754 (Figure 4-8), water bodies and rice fields from RGB-532 (Figure 4-9), open land, mixed forest, and forest from NDVI (Figure 4-10) and clouds and shadows from RGB-721 and band 5 (Figure 4-11).

Since the pixels were often assigned into different land cover classes when applying different classification methods (such as village in RGB-754 might be assigned as rice field in RGB-532), it was important to organize the classified images in a certain sequence.

From the sequence mentioned in Section 4.6.3, the compilation was done in ERmapper following the equation below:

If RGB-532	=	4 then 4 else	- 4	=	rice field
If RGB-532	=	2 then 2 else	- 2	=	water bodies
If RGB-754	=	3 then 3 else	- 3	=	villages

If NDVI	=	5 then 5 else	- 5	=	open land
If NDVI	=	6 then 6 else	- 6	=	mixed forest
If NDVI	=	7 then 7 else	- 7	=	forest
If RGB-721	=	1 then 1	- 1	=	cloud
		else 8	- 8	=	shadow

The result of applying this equation can be seen in Figure 4-12.

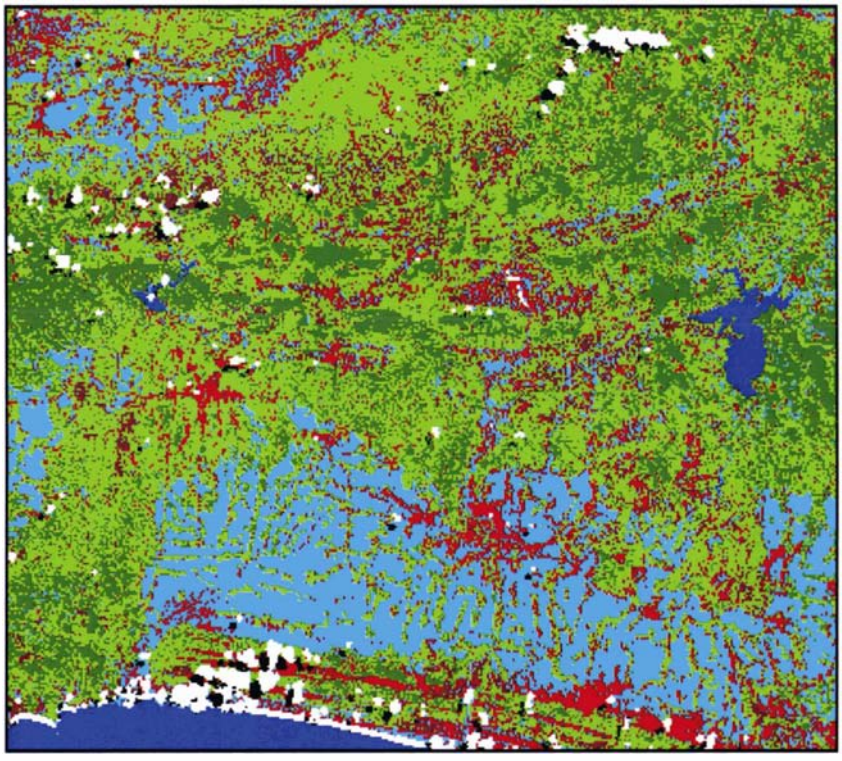

Figure 4-12 Final classified image after overlaying four preliminary classification images: 1= cloud (white), 2= water (blue), 3= village (red), 4= rice field (cyan), 5= open land (brown), 6= mixed forest (light green), 7= forest (dark green), 8= shadow of clouds (black)

4.7.4 Accuracy Assessment

Unfortunately it was not possible to do the ground truthing after the classification was finished. Such subsequent ground truthing could be used to refine the training classes which at the end will improve the accuracy of the classification (Gao *et al.*, 2004). Due

to the absence of ground truthing, the accuracy assessment was done in two ways; by comparing the classification at a large sample of random locations to the land cover class assigned on the topographic map, and by comparing the classified image to some areas that could be identified from photographs taken while in the field. In the former method, which produced a matrix of confusion, not all the sample points that were distributed on the topographic map were used because the topographic map had a smaller extent than the Landsat image. Other sample points which were located in the cloud and cloud shadows were not considered because those classes did not exist in the topographical map. For these reasons, the sample points used totalled 770 out of 1000 points originally generated.

The matrix of confusion resulting from the comparison of the topographic map and the final classified image is shown in Table 4-5.

Table 4-5 The matrix of confusion of topographic map and the classified image

	Topographic map classes							**User's accuracy (%)**	**Comm. error (%)**
Image classes	**2**	**3**	**4**	**5**	**6**	**7**	**sum**		
2. water	3						3	100.0	0.0
3. village		40	24	10		4	78	51.3	48.7
4. rice fields	2	1	118	3			124	95.2	4.8
5. open land		3	18	24	1	13	59	40.7	59.3
6. mixed f.	2	65	36	74	2	117	296	0.7	99.3
7. forest		21	12	24		153	210	72.9	27.1
Total column	7	130	208	135	3	290	770		
Producer's accuracy (%)	42.9	30.8	56.7	17.8	66.7	53.3		44.2	
Omission error (%)	57.1	69.2	43.3	82.2	33.3	46.7			

Table 4-5 shows that the accuracy of the classification is only 44%. The low accuracy was mainly because the forest and mixed forest classes identified in the Landsat image were defined differently in the topographic map. The plantation in the topographic map is a mixture of forest and mixed forest in the image. This is because pine forest is classified as forest in the image, while coconut or albisia trees are classified as mixed forest. That is why nearly half of the mixed forest in the Landsat image is represented as plantation on the topographic map.

Rice fields have the highest classification accuracy, 95% of rice fields in the classified image was also rice fields in the map. However some rice fields in the map were classified as other land covers, such as mixed forest, villages or open land. This happened because of the appearance of the rice field; in the dry season rainfed rice fields can look like open land.

Mixed forest had the poorest classification. The mixed forests in the image were mapped as plantation (nearly 40%), open area (25%) or villages (22%). This classification may be improved if the threshold value for NDVI used to separate mixed forest from plantation forests and open land was adjusted.

With regard to the second method used to test the accuracy of the classification, three photos show areas where the classification was mostly correct, while four other photos highlight the difficulties experienced when classifying the image. The three photos of areas that were classified most accurately together with a description of the areas are presented in Figures 4-13 to 4-15. The other four photos (Figures 4-16 to 4-19) are presented in the proceeding sections according to the perceived cause of error in the classification.

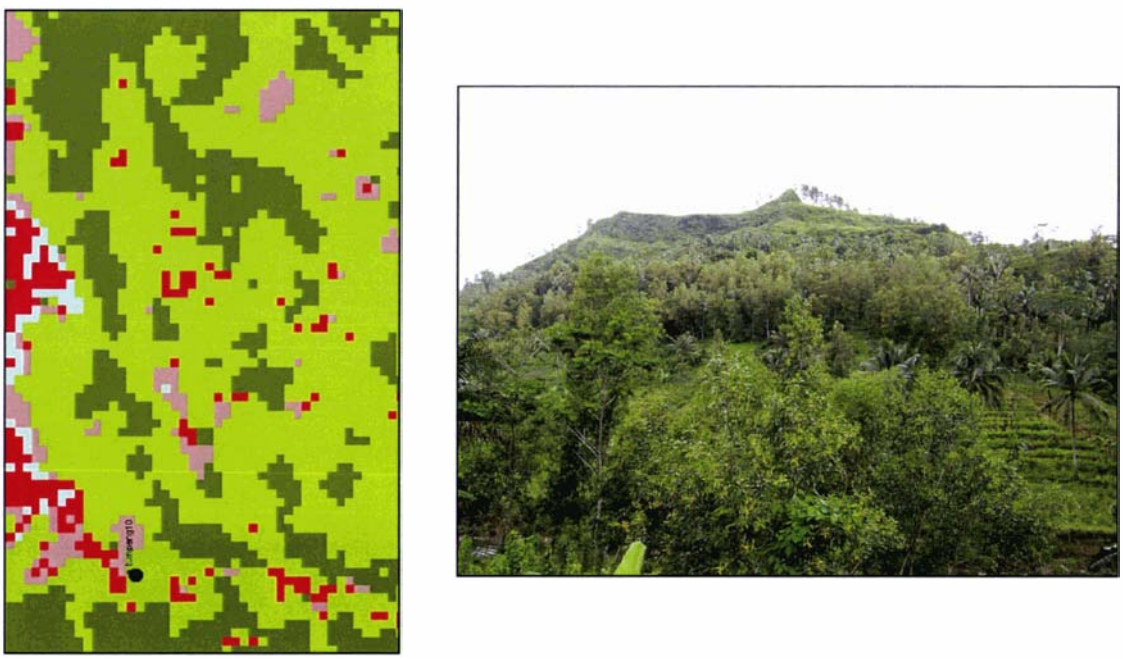

Figure 4-13 A comparison between classified image of mixed forest (light green) with some patches of open land (brown) and forest (green) with a photograph of the same location. The photo was taken from a coordinate of 343347.30 mE, 9159587.74 mN

Figure 4-13 displays a hilly area called Gunung Tumpeng (238 m asl). This forest area was owned by Perum Perhutani, but now is planted with different kinds of forest trees (mostly acacia) and food crops (lower right corner of the photo). In the classified image the area was classed as mixed forest with some (plantation) forest in between. The top of the hill is still under pine forest, which is displayed as forest in the centre of the image. The villages in the left side of the classified image are not covered in the photograph.

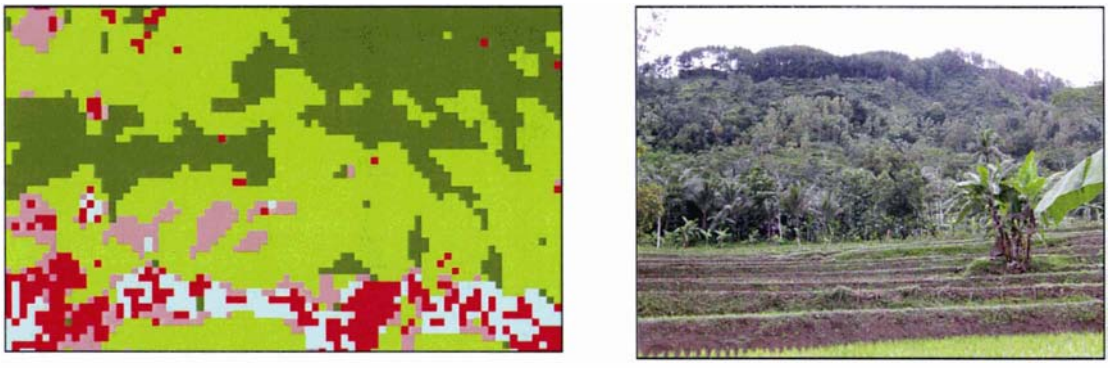

Figure 4-14 The image shows mixed forest (light green) with a row of rice field (cyan), open land (brown) and villages (red). The photo was taken from a coordinate of 343346.34 mE, 9161201.61 mN (Karang Mojo)

Figure 4-14 displays a moderately accurate classification with rice fields in the lower side matching the photograph well. The open land, located below the mixed forest also agrees well with what can be seen in the photo; it is the area in front of the coconut trees in the photograph. Pine trees in the background of the photo are classed as forest in the centre of the image, while the forest in the right-hand corner of the classified image is located on the other side of the hill. Rice fields in the foreground of the photo are shown as a mixture of rice field, village and open land in the classified image. The actual village is not shown in the photo but it is located just out of shot on the left side.

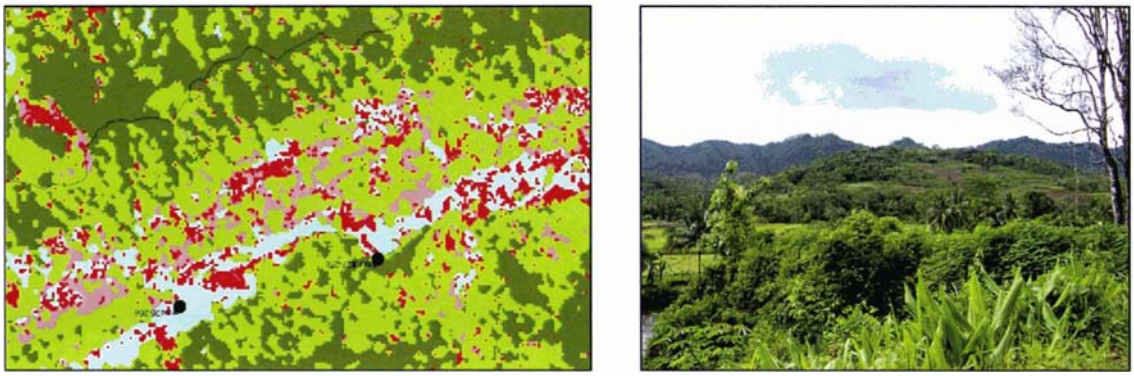

Figure 4-15 The image shows the mixed forest (light green) with forest (green) in the upper part and a mixture of rice field (cyan), villages (red) and open land (brown) in the middle. The photo was taken from a coordinate of 358510.24 mE, 9169182.02 mN (Kedung Legok)

Figure 4-15 shows a relatively broad area, from hills in the background of the photo which is the watershed boundary of the study area (a line shown in the classified image), up to the open land in the middle of the classified image. The forest in the hills shows some slips and bare land. These slips and bare land were correctly assigned as open land, and the villages were spread among the forest and mixed forest. The open land and some rice fields within the mixed forest in the centre of the classified image are displayed in the middle part of the photo mixed with scrub in the foreground.

Factors that influenced the accuracy of the classification were: the complexity of the study area, band combination selection and date of image acquisition.

4.7.4.1 The Complexity of the Study Area

This study looked mostly at rural areas where the average land ownership is 0.4 ha, except Perum Perhutani's forest. In the open land, for example, farmers plant different crops such as cassava, maize or trees. Where food crops dominated the land, it was called open land, but it was called mixed forest (or *hutan rakyat* = forest owned by people) when trees dominated the areas. These land uses, when sited next to each other, gave different reflectances compared to areas that had the same land cover but surrounding areas were more uniform in land use. This is typical of the mixed pixel problem where values are assigned according to the dominant land cover in the vicinity.

Furthermore, for a smoother appearance, the classified image was filtered using Majority 3x3 kernels, which meant that the size of the smallest distinguishable classified land cover became 900 x 900 square metres (=0.8 ha). This also meant that the classified land cover might be a combination of two or more land ownerships, or two or more land uses.

An example of this error is demonstrated where open land in the topographic map (shrubs, bare land, and open land) became mixed or monotype forest in the classified image (Table 4-5). The small patches of shrubs or bare land around mixed or monotype forest (usually because of reforestation failure) were assigned as mixed or monotype forest. This resulted in a high omission error of open land (more than 80%). It also meant that less than 20% of classified open land was shown as open land in the topographic map (Figure 4-16).

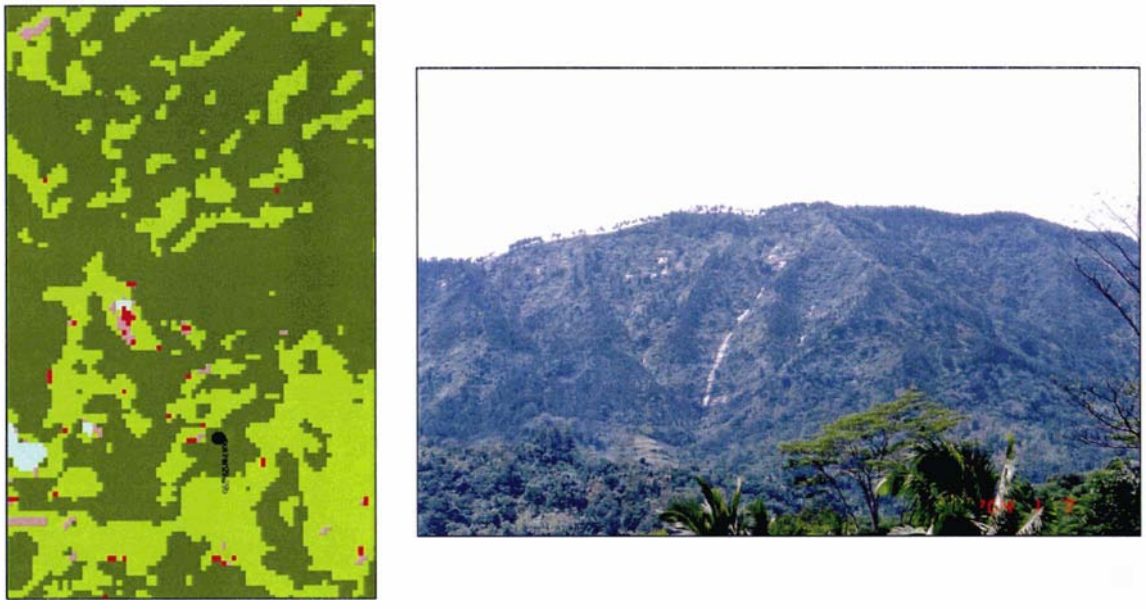

Figure 4-16 A comparison between classified image of mixed forest (light green) and forest (green) with a photograph of the same location. The photo was taken from a coordinate of 360867.86 mE, 9172090.21 mN

Sadang Kulon, shown in Figure 4-16, is a high altitude location (around 400 m asl.). The photograph shows some slips and bare land (the whitish patches and slashes in the centre of the photo) which can be picked up on the classified image; they were assigned as a mixture of village and open land (small red and brown dots in the centre of the image). This conformed to the land use classification on the topographic map, since

bare land was grouped with open land. The mixed forest surrounding the bare land (light green in the image) was actually shrubs, a result of the failed reforestation attempt in this area. From this example, one can see how difficult it is to classify shrubs and bare land. The forest and mixed forest in the upper part of the image is on the other side of the hill.

4.7.4.2 Band Combination Selection

The principal applications of each Landsat band are presented in Table 4-1. By using different combinations of these bands one might expect to be able to clearly distinguish between various land covers (Aplin, 2004). Unfortunately, not all band combinations proved successful, especially when two different land covers gave similar reflectance. For example, RGB-754 was used to classify villages more accurately than RGB-321. However, since bands 4, 5 and 7 were designed to capture vegetation; many pixels classed as villages were confused with open land and mixed forest. On the other hand, RGB-532 which used to differentiate soil according to its moisture content (water bodies, rice fields, and trees); often classed villages as rice fields. Table 4-5 shows that, of the 130 village test samples from the topographic map, only 30% were correctly classified as villages in the Landsat image; while nearly 50% were classified as mixed forest. Villages in the classified image were actually rice fields (30%) and open land (20%) on the topographic map. This showed the poor classification of the villages, especially those associated with bare land, open land, and some of the mixed forest. The problem of distinguishing between villages, open land and mixed forest arises because all these land cover types contain trees. Villages in the study area are usually surrounded by trees such as coconut, banana, acacia, or albisia. Unfortunately, mixed forests consist of this combination too, especially acacia and albisia. The only thing that could differentiate villages from mixed forest or villages from open land was the percentage of vegetation cover, where mixed forest has the highest percentage and open land has the lowest.

On the other hand, open land too sometimes has trees, especially along the property boundary. As stated by Suprapto (2002), open land is an area commonly used for such purposes as household yards, rainfed agriculture, upland/plantation, open grassland or neglected as dormant land. Because of its nature, it is difficult to differentiate open land

from other land covers based solely on its reflectance. Examples of this situation are presented in Figures 4-17, 4-18 and 4-19.

Figure 4-17 shows a location near Sempor Reservoir. The classified image on the left side shows the water body, which is classified correctly (the photo clearly shows the lake and the shore). The mixture of village and dry land is the lake-shore and road (according to the photo). Most of the area in the left image is dominated by forest, which again is correct according to the photograph. It is pine production forest owned by Perum Perhutani. Patches of mixed forest in the classified image may be other types of trees such as acacia, albisia or banana (*Musa spp.*). One or two village/dry land pixels in the forest could be houses owned by Perum Perhutani's workers or bare land due to erosion or land degradation.

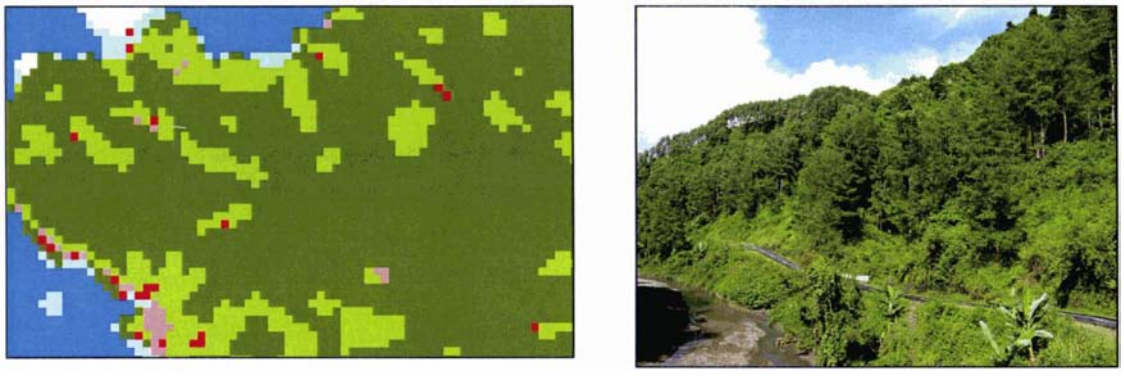

Figure 4-17 A comparison between classified image and a photograph of forestry dominated area. The photo was taken from a coordinate of 332901.63 mE, 9163141.40 mN

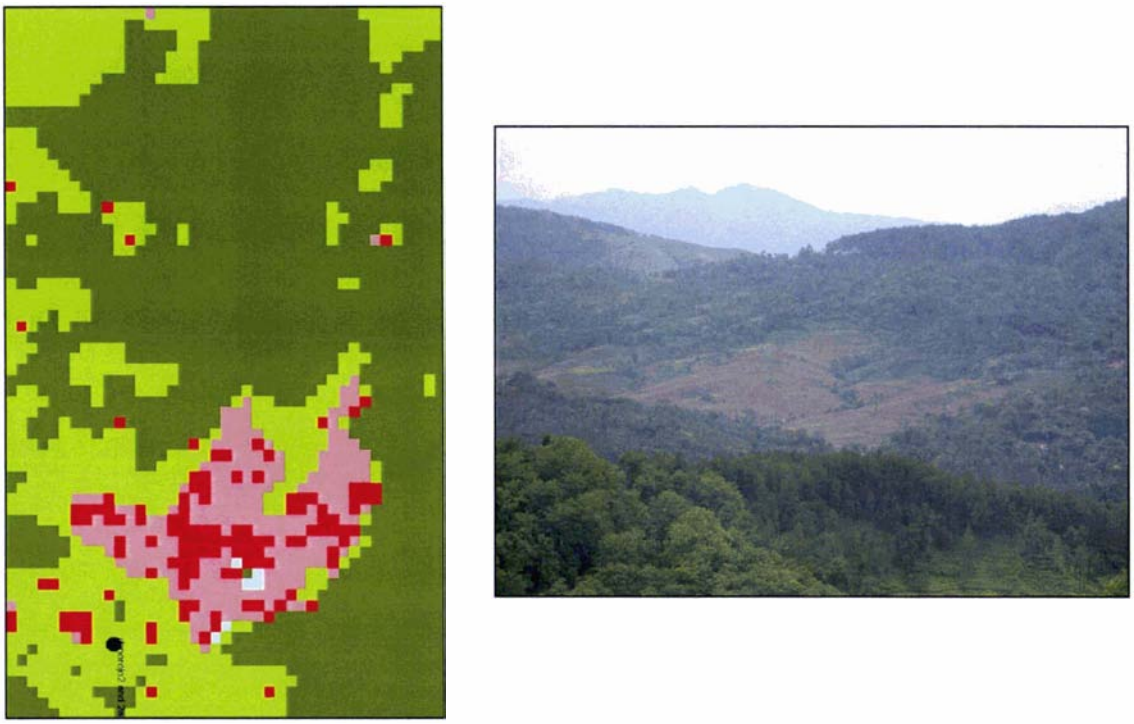

Figure 4-18 The classified image shows a mixture of villages and open land (red and brown) surrounded by forest and mixed forest (green and light green). The photo was taken from a coordinate of 337945.74 mE, 9168018.68 mN

Figure 4-18 is an area called Donorojo. The bare land in the middle of the photo shows a logged area which was then leased to the nearby farmers to grow food crops such as maize or cassava for 1 – 2 years and to maintain the young pine trees. This location is owned by Perum Perhutani for pine forest production. Like the situation in Figure 4-17, the villages and open land are mixed together.

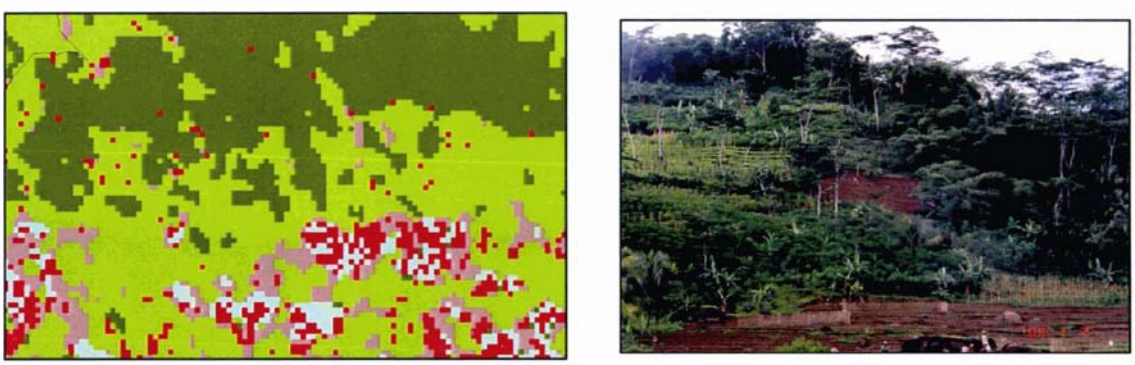

Figure 4-19 The image shows forest area (green) in the upper part of the image with mixed forest (light green) and a mixture of open land (brown) and villages (red).The photo was taken from a coordinate of 355032.17 mE, 9168201.40 mN

Watu Lawang is the location presented in Figure 4-19. The open and bare land mixed with rice field in the foreground are classified as a mixture of open land, villages and rice fields displayed in the middle of the classified image. A mis-classification is the village which should be open land. The forest and mixed forest are correctly classified.

The incorrect classification was due primarily to a less than ideal band combination, especially to classify villages. More investigation is needed before a more accurate separation of villages from other land covers can be achieved. Another possible reason for the misclassification was a limited range of radiance values in some bands. For example, band 5 had radiance values of 0 – 29 (Table 4-3). The classifier used 0 – 5 for cloud shadows and water bodies, and greater than 15 for clouds themselves (Section 4.7.2). This resulted with radiance values of 5 – 15 for other surface features such as soils and vegetation. A limited range of radiance values also limited the usefulness of band 7. It may be possible to produce better results by combining bands 5 and 7 with bands that have a greater range of radiance.

4.7.4.3 Date of image acquisition

The environmental conditions when the Landsat image was captured may have affected the accuracy as well. The image was captured on 28 April 2001, prior to its interpretation and classification that eventually produced the land cover map.

Typically at this time of the year the dry season begins and the rainfed/un-irrigated rice fields start to dry out. This situation can make the rainfed rice fields look like, and be classified as, open land in the image. From Table 4-5 the rice fields that were classified as open land accounted for 18 samples or 8.65% of the total rice field samples. Apart from the misidentification of open land and rice field, in general the accuracy of rice field class was much better than it was for the other land covers.

Time differences may have also contributed to the errors in classification. As already mentioned, the open land in the topographic map consisted of shrubs, bare land and open land. Thirteen out of 59 open land samples (22%) were forests in the topographic map. It is possible that the wrong classification was because of the appearance of forest when the aerial photo was taken (1993/1994) in comparison to the time when the survey (for making the topographic map) was done (1998). Also, when the Landsat image was captured three years later (2001), some forests had been logged and within three years

the land became covered in shrubs or remained open land, while in the topographic map it was still labelled as forest.

Separating open land from rice fields was difficult too, particularly when the photo was taken during the wet season (October – February). Rainfed rice field could become an open land in the dry season, or open land could become a rice field in the wet season. Figure 4-20 shows the condition of a rice field in the wet season.

Figure 4-20 Rice fields which could be classed as open land during the dry season. Photo was taken on January 4th , 2004

4.8 Conclusion

The classification of a Landsat image to produce a land cover map is relatively quick, simple and cost-effective. While the accuracy achieved in this instance was variable, improvements to the poorly classified areas could be achieved especially from using images acquired at different times of the year.

Atmospheric and topographic corrections are required before the image can be classified. The use of Dark Object Subtraction to reduce the haze in this image gave a good result, while the Sun-Canopy-Sensor method reduced the topographic effect significantly.

To effect a good topographic correction requires an accurate DEM. In this study the DEM was interpolated from contours digitised from a scanned topographic map. The use of the TOPOGRID module in ARCInfo was found to be suitable for this work, since it not only uses the spot heights and the contours in the calculations, but it acknowledges the river network and the reservoirs as well.

When classifying land cover in a very diverse region such as in the study area, one cannot expect a good result from a single band combination. Classifying land cover using a stratified method resulted in the identification of most of the different land covers in the study area.

Separating villages from other land cover types was the most difficult task. By combining bands which have the capability to detect moisture in both soil and vegetation with bands that capture cultural features, a reasonable solution was found. Ratioing the bands was another technique used; this involved trial and error to determine the threshold of NDVI values to separate open land, villages, mixed forest and monotype forest.

SOIL EROSION PREDICTION

5.1 Introduction

Soil erosion is a common problem throughout the world, with differing degrees of severity for each country. Developing countries find that erosion is a substantial problem but they do not always have suitable means to reduce it. The cost of soil erosion is significant, sometimes up to 15% of the Gross National Product (Barbier & Bishop, 1995). Developed countries usually have the technology to combat erosion because they have done enough research. However, most of the research done in developed countries cannot be applied straightaway in developing countries as it needs adjustment for the local conditions. Different conditions (Boggs *et al.*, 2001) such as climate, topography, soil type and land cover as well as the social and economic situations in the developed countries have resulted in different kinds of data being available, and this is another obstacle to the implementation of an erosion model in developing countries. Researchers need to collect their own data before they can be confident in a particular erosion model. To do this they should understand how that model works, as well as understanding the processes of erosion.

Sedimentation is a consequence of erosion further up a watershed. In general terms, soil erosion is:

> '...the physical removal of topsoil by various agents, including falling raindrops, water flowing over and through the soil profile, wind velocity, and gravitational pull' (Lal, 1990a, p.3),

while sedimentation is:

> '...the process or action of depositing solid material that is detached from the soil mass by erosion agents. The process begins with sediment detachment from uplands and ends with an eventual transport to the ocean, which may take up to a million years to be completed' (Lal, 1990a, p. 4).

Lal (2001) found that erosion is a natural process; if the rate of soil loss and soil development is balanced, it also produces fertile alluvial and loess soils. However, when the rate of soil loss is faster than soil development, there is not enough time for

the eroded soil to recover; therefore the soil quality will degrade. When this condition is ignored, there will be a severe impact on the environment.

Since wind erosion is not a common problem in the study area, the erosion referred to in this study is mostly caused by water and/or gravity. The best way to examine, plan for and predict erosion is through a watershed delineated area (Toy *et al.*, 2002). A watershed is an area, topographically delineated, that captures water in any form, such as rain, snow or dew, and drains it into a common water body (de Barry, 2004; Dixon & Easter, 1986).

The watershed approach is holistic; it enables planners and managers to consider many facets of resource development. Land-use activities and upland disturbances often result in a chain of environmental impacts that can be readily examined within the watershed context (Dixon & Easter, 1986). The size of a watershed varies, depending on the type of erosion to be studied. Soil conservation practices such as terracing, contouring or strip-cropping can be identified using a small first-order watersheds (1 – 2 ha in size), while studies of ephemeral gully erosion and its control require larger watersheds of about 2 – 40 ha in size (Toy *et al.*, 2002).

Hamilton & Pearce (1986) found that a watershed is a good planning unit to identify areas prone to mass movements and to design measures to prevent those movements. Restoration of forests in critical areas, if they have been cleared, needs careful consideration of watershed management.

According to Lal (2001) factors influencing soil erosion include: soil erodibility (influenced by management); erosivity (influenced by climate, including drop-size distribution and intensity of rain, amount and frequency of rain and runoff); chemical reactions such as weathering; terrain characteristics and land- and ground-cover. Social, economic and political factors can also influence the rate of erosion. There are two ways to control it: by reducing erosivity, or by reducing the susceptibility of the soil to erosion and increasing the capability of the soil to resist the forces applied by the erosive agents (Toy *et al.*, 2002).

The objectives of this chapter are to discuss the importance of erosion impact in forested areas, to predict potential erosion, to find areas at risk from erosion in the study area, and to recommend sustainable forest management.

5.2 Erosion in Forest Areas

The rationale for understanding erosion in forested areas is different from that in agricultural land. In agricultural land nutrient losses and land degradation are important, while in forests the focus is more on the degradation of streams and waterways because of the eroded material (Ziemer, 1986). Since the emphasis is different, the factors collected and studied will be different, too. Unfortunately there have been attempts to apply erosion models from agricultural land to forested watersheds. This effort generally fails because of inappropriate basic assumptions (Ziemer, 1986).

Compared with erosion studies in agricultural areas, erosion research on forested areas is not so common. Some possible reasons are: (i) since no erosion occurs while the forest still exists (Bruijnzeel, 1990 cited by Hartanto *et al.*, 2003), it is thought that it is not a crucial problem; (ii) the locations of forested watersheds are often difficult to reach, so it is not easy to collect the data (Sun & McNulty, 1999); and (iii) research in forests takes more time than on agricultural land (Ziemer *et al.*, 1991).

Even though erosion research on forested areas is not as popular as research on agricultural land, there has been, however, some research about erosion measurement in Indonesian forests. Kusumandari & Mitchell (1997) found that the erosion rate under forest and agro-forestry in West Java was 95 to 100 tonnes.ha^{-1}.year^{-1}. In Java, Lal (1990b) measured erosion under some plantation forest, namely *Albizzia falcataria*, mahogany, and teak. The erosion rates were 0.8 to 1.1 tonnes.ha^{-1}.year^{-1} but when the trees were cut, the erosion increased drastically. In a pine logging area in Central Java, Priyono & Savitri (1998) calculated erosion during the logging period (4 to 6 months). The soil loss was 50 tonnes/ha in the felling area alone.

In the above studies, there was no research about where the potential erosion might occur. Such study is important because, as stated by Ziemer (1986), the key to successfully managing erosion and sedimentation is to increase the ability to:

- identify potentially erodible sites
- assess appropriate activities on those sites correctly
- have a better political or regulatory system that promotes appropriate actions.

By knowing the potentially erodible areas, forest managers and decision makers can plan soil conservation activities at the same time as their logging activities, thereby minimising erosion during logging.

During erosion studies in forested areas, Lal (1990b) found that the predominant erosion processes under undisturbed natural forest cover are splash, creep and sheet flow, which are sometimes reduced by thick layers of litter or dense undergrowth. Dense ground cover is the main factor which could minimize the erosion rate in the forest (Kusumandari & Mitchell, 1997). Rill and gully erosion occurred as a result of disturbance by land-management activities (Lal, 1990b) such as logging, road construction, and burning in addition to the amount of rainfall (Elliot *et al.*, 2000; Ziemer, 1986). These logging activities usually result in temporary gaps in the forest canopy (Cheesman *et al.*, 2000) and in these temporary gaps, increased erosion usually takes place for one to three years before it returns to its condition before the disturbance (Elliot *et al.*, 2000; Priyono & Savitri, 1998). Although this situation is only temporary, it is not suggested that erosion should be tolerated in logging areas. Since soil erosion is one of the aspects that can be controlled in Sustainable Forest Management (SFM) (Higman *et al.*, 1999), action should be taken to minimize it.

Often forest managers are not aware of soil erosion because they are not adequately informed about the consequences of logging operations as they relate to sustainable forest production (Hartanto *et al.*, 2003). This may be due to a poor logging management systems, where the planning – implementation – monitoring loop of the logging operations is not closed. In particular this feedback or monitoring following logging is mostly not considered part of logging management. The result is that logging operations fail to achieve the criteria of SFM and could be described as being out of control. Therefore, this study is one of several ways to improve this situation.

Since logging is part of timber production, it cannot be avoided in production forest even if it is likely to cause many environmental problems. As long as the problems are addressed properly, the negative impacts can be minimized. Some impacts of logging are:

- Soil fertility reduction (Hartanto *et al.*, 2003). When rainfall hits bare ground, it dislodges soil particles and then runoff transports the sediment and associated

nutrients off the watershed. Every effort needs to be made to minimize the length of time when the ground is bare.

- Hydrological cycle change (Cleaves, 2003). Any land-cover changes from forest into agriculture or villages within a watershed will affect the hydrological cycle. The removal of trees and vegetation due to logging reduces the transpiration of groundwater, especially where the groundwater is near the surface. Since the transpiration is reduced, the groundwater level will increase. Logging also reduces infiltration due to soil compaction during logging activities. This will increase runoff in the rainfall event, and can lead to flooding.
- Erosion increase (Cleaves, 2003). In a small watershed, erosion rates will change when land-use changes. From the forested watershed, logging will increase the erosion rate, and it will become higher when the land-use is converted into agriculture or buildings. Ziemer (1986) suggested that if a small block of forest is logged, the rest of the forest will buffer the effect downstream, but this still needs more study. The proportion of watershed that could be logged without degradation is still a speculation and is based on the assumption that erosion is uniformly distributed (Ziemer, 1986). In Indonesia, the minimum percentage of forest that has to be left standing in the whole watershed is 30% (Section 18:2 "UU No. 41 tentang Kehutanan [*The Law Number* 41 *on Forestry*]," 1999).
- Stream quality degradation (Ziemer, 1986). Logging activities usually pollute watercourses and streams. To minimize sediment entering streams, roads should be built at least 50 metres from the stream (Elliot *et al.*, 2000), depending on the soil parent materials. Building buffer zones along streams can help as well. In Indonesia this regulation is written in Section 50:3 of the Law Number 41 on Forestry, which says that logging is prohibited within 500 metres from lakes or reservoirs, 100 metres from rivers and 50 metres from streams.

An understanding of logging systems is important. The logging method which minimizes disturbance to the soil surface is a good option especially for soils that are prone to erosion. Regarding this condition for tropical soils, more consideration should be given to adopting logging systems from non-tropical-forest regions (Reynolds, 1990). A skidder, for example, will cause the greatest erosion compared with other logging systems such as cabling, because skidders can reduce soil infiltration by

disturbing litter cover and compacting the soil (Elliot *et al.*, 2000). Other impacts of forest harvesting, such as scraping of the surface soil, will also result in crop yield reductions, soil compaction and soil variability increases (Reynolds, 1990).

5.3 Predicting the Potential Erosion and Erosion Risk

There are two ways to predict soil erosion, qualitative and quantitative. Predicting erosion qualitatively will result in areas which have high to low potential erosion risk in a relative sense. This information is important for planning soil conservation measures according to risk level (Bartsch *et al.*, 2002) or developing appropriate strategies on erosion hazard assessment (Gournellos *et al.*, 2004). Furthermore, land managers and policy makers are more interested in the spatial distribution of soil erosion risk than in absolute values of soil erosion loss (Lu *et al.*, 2004).

Quantitative erosion prediction, on the other hand, attempts to predict the amount of soil eroded from a certain area. Soil loss information is collected for calibrating a tool or designing erosion model. The tool or model will be used for a certain area if the predicted and measured erosion match each other. Another use of quantitative erosion measurement is for monitoring the effectiveness of a soil conservation plan within a certain area.

Vrieling *et al.* (2002) developed erosion risk mapping based on the combination of geology, soil, relief, climate and vegetation, while Cohen *et al.* (2005) and Lu *et al.* (2004) used K (soil erodibility), LS (slope), and C (vegetation) factors both for USLE (Universal Soil Loss Equation) and RUSLE (Revised Universal Soil Loss Equation), or just for assigning risk classes for slope, soil texture, and land cover (Brown & Richardson, 1998). Darmawan *et al.* (2001) proposed vegetation type, slope gradient and percentage of bare soil maps to be used to predict soil erosion hazards in East Kalimantan, Indonesia.

Potential erosion itself is inherent in the land irrespective of current land-use or vegetation cover, while actual erosion relates to the current land-use and management conditions (Vrieling *et al.*, 2002). Therefore, understanding potential erosion is important, especially for areas susceptible to erosion. Vrieling *et al.* also found that

information about potential erosion in a certain area may be used as guidance in proposing land-use and soil conservation measures.

In most areas where erosion has yet to occur, quantitative prediction models are not reliable. Therefore, it is suggested that the qualitative approach is better for indicating the spatial distribution of any potential erosion risk (Vrieling *et al.*, 2002). In general, factors used to predict potential erosion are climatic characteristics, soil properties, topography, and land management (Cheesman *et al.*, 2000; Elliot *et al.*, 2001; Vrieling *et al.*, 2002). While the factors are interrelated, each factor brings its own errors as well. Those errors will easily accumulate throughout the process and they will affect the result of any prediction. Consequently each factor should be handled carefully to minimize the accumulative error.

Qualitative erosion assessment usually uses secondary data such as maps, aerial photos or images (Wang *et al.*, 2003), especially when it involves a large area. These auxiliary data increase the efficiency and accuracy of the analysis. Although secondary data fulfil the analysis requirements, ground checking is important for checking the accuracy of the analysis.

Despite the fact that actual erosion under forest land uses is negligible to low, it does not mean that the potential erosion is also small. Therefore, there is still much research to be done in the forested areas of Indonesia. The common topics are mostly related to erosion recovery conditions such as post-forest fire (Darmawan *et al.*, 2001) or to erosion monitoring (Hartanto *et al.*, 2003; Kusumandari & Mitchell, 1997; Priyono & Savitri, 1998). However, estimation of potential erosion, which can then be used for soil conservation planning to prevent erosion, is not a common topic for research in Indonesia. Few researchers have worked on the identification of potential erosion, especially in forested areas. They use actual soil erosion values to design soil conservation measures to reduce present erosion.

When the rate of soil loss is very high, areas prone to erosion have to be identified using spatial modelling and prediction tools, so appropriate conservation measures can be implemented (Metternicht & Gonzalez, 2005; Priyono & Savitri, 1998) and the loss due to soil erosion can be minimized. Metternicht & Gonzalez used a fuzzy logic-based approach in locating and differentiating erosion hazard areas; inputs included vegetation

cover percentage, rock fragments density, abundance of whitish topsoil, landscape position and slope gradient. Although they used minimal input data, this model still required considerable expert knowledge about erosion causes as well as a good understanding of erosional processes.

Climate, topography, soil characteristics and land usage are the main contributors to soil erosion (Chang *et al.*, 2003; Toy *et al.*, 2002). Each factor works both independently and interactively, and each factor can contribute differently.

5.3.1 Climate

Precipitation is the most important climate factor that causes water erosion (Gournellos *et al.*, 2004). Raindrops can detach soil, and runoff can entrain, transport, and deposit soil particles to other places (Toy *et al.*, 2002). Since erosion means soil detachment, transport and deposition from one place to another, it is evident that precipitation affects the whole erosion process. It can also be said that soil erosion is less likely to happen if it is not raining.

There are two occasions when precipitation does not necessarily produce erosion. They are: when rain falls into freshly tilled dry soil (Wischmeier, 1976), and when rainfall intensity is not high enough to produce runoff (Xie *et al.*, 2002). When rain falls on relatively dry soil, all of the water will infiltrate and no runoff occurs. However, when rain falls on a pre-saturated soil, runoff begins quickly and most of the rain becomes runoff (Wischmeier, 1976). In a low rainfall year, most or all rains may fall on dry, receptive soil. In an extremely wet year, the probability of erosive rainstorms striking on pre-saturated soil is much greater (Wischmeier, 1976). In addition, erosion is greatest when the peak period of precipitation corresponds to the period when the soil is most exposed to raindrop impact and surface runoff. Significant reduction in erosivity can be achieved by ensuring that these two peaks do not correspond (Toy *et al.*, 2002). One of the soil conservation objectives is to prevent these two periods happening at the same time.

Since not all rainfall events cause soil erosion, a threshold needs to be set to separate the erosive rainfall from other rainfall events. In their paper, Xie *et al.* (2002) reported different threshold values for erosive rainfall. Wischmeier and Smith (1978) and

Hudson (1995 as cited by Xie *et al.*, 2002) proposed values of 12.7 mm/hour and 25 mm/hour respectively, while Xie *et al.* (2002) suggested 12 mm/hour as a threshold value (see Section 3.7). Wischmeier & Smith (1978) found that 0.25 inches (6.4 mm) of rain will be erosive if it pours within 15 minutes. In reality it is difficult to separate erosive and non-erosive rainfalls completely based on only one or two threshold values because of the complexity of rainfall characteristics and the variation of responses to runoff and soil loss (Xie *et al.*, 2002). Unfortunately, the choice of this separation may over- or under-estimate the predicted erosion which in turn will influence the soil conservation measure chosen to lessen the erosion. Since erosion is a non-reversible process, it is better to manage the land conservatively rather than sacrifice the soil to erosion; this means that it is preferable if the predicted erosion is over-estimated, than under-estimated.

Xie *et al.* (2002) also found that, compared to the whole watershed, plots gave a different response to the same rainfall, which makes the threshold value decision more complicated. It means that the threshold value depends on the rainfall characteristics, the soil condition, and the measurement method (hillslope vs. watershed).

5.3.2 Topography

The most important topographic factor affecting erosion is slope, in particular, slope length and slope steepness. Slope steepness is more dominant in inducing erosion than is slope length (Wang *et al.*, 2003). It is agreed by Chang, *et al.* (2003) that the steeper the slope, the faster the water runs off and the soil loss increases with any increase of water runoff. Lal (2001) also mentioned the same thing, he found that the slope factor is more significant in causing erosion than land cover, while Gournellos *et al.* (2004) suggested that slope forms and inclination are the second most important factors after rainfall.

A complex watershed which has irregular slope steepness and length will provide an opportunity for the sediment to be deposited along the slope. Therefore, averaging the slope will not give a correct result because it estimates a generalized sediment deposition. A complex watershed, according to Wischmeier (1976), must be subdivided into sufficiently uniform areas for which representative values can be defined.

5.3.3 Soil Characteristics

The erodibility of soils varies greatly; some soils are more erodible than others. Soil with high clay content, for example, will be more resistant to detachment. Sandy soil, although it is easily detached, does not easily trigger runoff even if in high precipitation (Toy *et al.*, 2002). Silt, on the other hand, is most erodible (Wischmeier & Smith, 1978).

Chang *et al.* (2003) found that organic matter increases soil permeability which also increases the ability of soil to absorb water in the rain event. If soil is able to absorb more water, the possibility of runoff will decrease. This situation also leads to better conditions for vegetation to grow and the development of a better soil structure to resist erosion. Soil erodibility, varies during the year, depending on the soil moisture content (Toy *et al.*, 2002). When the moisture content of soil is high, such as during a wet period, runoff is more easily generated and subsequently erosion increased.

Rock type is another factor to determine areas prone to erosion. Liu *et al.* (2004) found that poorly consolidated or soft rock types such as turbidites and mudstone are easily eroded, while gypsum, limestone and conglomerate are more stable. Schist and brecciated rocks are other rock types that are easily eroded as well (Sutikno, 2005).

5.3.4 Land Use

Toy *et al.* (2002) found that erosion actually occurs in exactly the same way on all land regardless of use, however, the type of land cover can have an influence. Undisturbed land use, such as forested areas, will be less erodible than disturbed land, such as logging sites, cultivated fields, or grazing areas. Vegetation reduces erosion by developing a canopy to intercept raindrops, and increasing ground roughness to reduce runoff velocity. It also aggregates the soil to increase soil porosity and this too reduces runoff (Chang *et al.*, 2003).

Canopy cover is really important factor in reducing erosion. A good plant cover can generally prevent surface erosion, and a well-developed tree cover may also reduce shallow landsliding (Bruijnzeel, 2004). Therefore canopy cover is different to land use because the same land use might result in different canopy protection depending on the condition of the canopy. In contrast to Section 18:2 ("UU No. 41 tentang Kehutanan

[*The Law Number* 41 *on Forestry*]," 1999), Bruijnzeel mentions that the removal of more than 33% of forest cover results in significant increases in annual streamflow during the first three years, and this is probably a consequence of increased runoff. After that period, it decreases again. Maximum erosion control is gained by choosing plants and managing them so that they have their maximum canopy during the periods of maximum erosivity.

Graham (1973, cited by Stott, 2005) noted that trees can reduce erosion through mechanical strengthening and binding of the soil by the roots. Trees protect the soil surface from rainsplash (and bushes protect it from throughfall drip below a forest canopy) while roots and rhizomes help to bind the soil.

5.3.5 Erosion Risk

Usually erosion risk is associated with soil loss, which is estimated by evaluating the physical factors contributing to erosion: slope, soil texture and structure, land and ground cover, and rainfall (Bartsch *et al.*, 2002; Boggs *et al.*, 2001; Brown & Richardson, 1998; Cheesman *et al.*, 2000; Cohen *et al.*, 2005; Lu *et al.*, 2004). The results are then ranked and grouped into several erosion risk classes.

Using the same approach as used by MacEwan *et al.* (2004a) for land use modelling, the proposed method in this study adopted a risk analysis which considers the environmental value of the land cover when predicting erosion risk.

Information about risk is important, especially for decision makers when they are producing targeted policy and action plans for a range of natural resource management issues (MacEwan *et al.*, 2004a). Rao (2001) also suggested that risk analysis is an important pre-cursor to sustainable development.

According to MacEwan *et al.* risk is 'a product of the likelihood that something will happen and the consequence suffered if it happens'. Risk is obtained from a combination of likelihood and consequence as shown in Figure 5-1.

In the soil erosion risk analysis the susceptibility to erosion is dependent on slope, geology and land cover. The management is the ability to control the amount of ground cover and its timing from the effect of rainfall pressure. The pattern and amount of

rainfall indicate how hard to manage the ground to avoid the destructive effect of rainfall. Therefore rainfall is used as a measure of management pressure. The likelihood of erosion associated with a logging event is dependent on the probability of a damaging rainfall event in areas susceptible to erosion, such as when the soil is bare after logging.

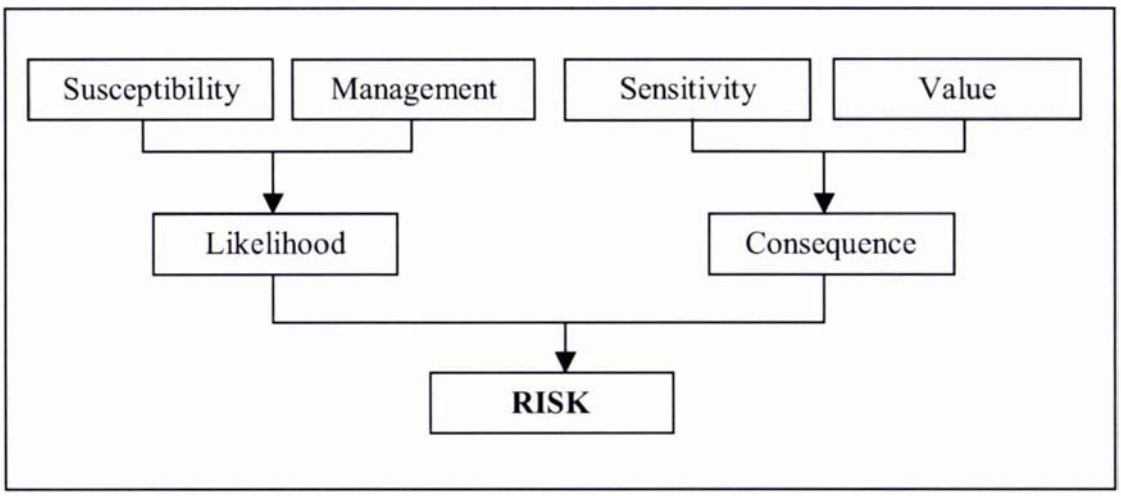

Figure 5-1 Schematic representation of components of risk (MacEwan *et al.*, 2004b)

Sensitivity is the level of response of an environmental asset to a threatening condition, while the value of the environmental asset is based on environmental, social and economic services provided by the asset.

According to MacEwan *et al.* the consequence of degradation of an asset in response to a particular threatening process depends on how incapacitated or dysfunctional the asset becomes, should that particular form of degradation occur, and on the functional, aesthetic or rarity value of the remnant. So in this analysis, the threatening process is erosion and the asset being eroded is the soil and those land cover elements that are dependent on the soil. The soil will be considered in terms of the type and depth of its horizons. The land cover elements will be considered from two perspectives. Non forest areas will be masked from the analysis because they will not be logged. Both forested and cleared areas within forests will be assessed according to their contribution to future biodiversity and the inherent short and long-term future productive potential of the soil.

5.4 Methodology

Land cover dynamics in the study area are quite prominent, because farmers sometimes change their open land into mixed forest or vice versa. Those areas that are unlikely to be converted to forest (rice field and villages) are excluded from analysis. But all other land cover is included because it could be forested in the next rotation.

There are two steps in assessing the erosion risk in an area: (1) determining the likelihood of erosion and (2) evaluating the consequence. The erosion likelihood is assessed using the flowchart shown in Figure 5-2 while the steps followed in assessing the consequence and risk are presented in Figure 5-3 (these Figures were adopted from MacEwan *et al.* (2004b)).

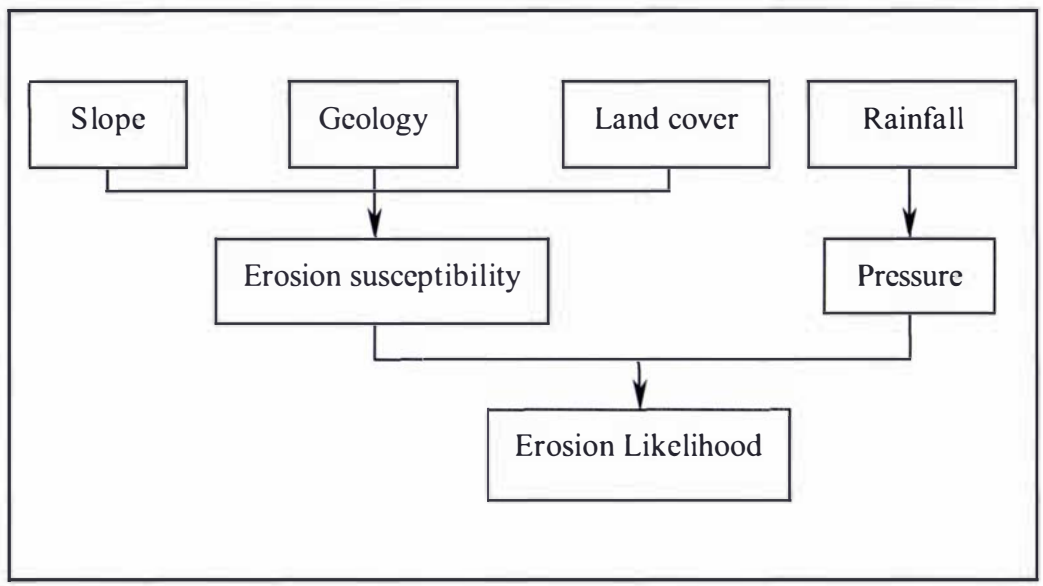

Figure 5-2 Flow diagram of erosion likelihood assessment

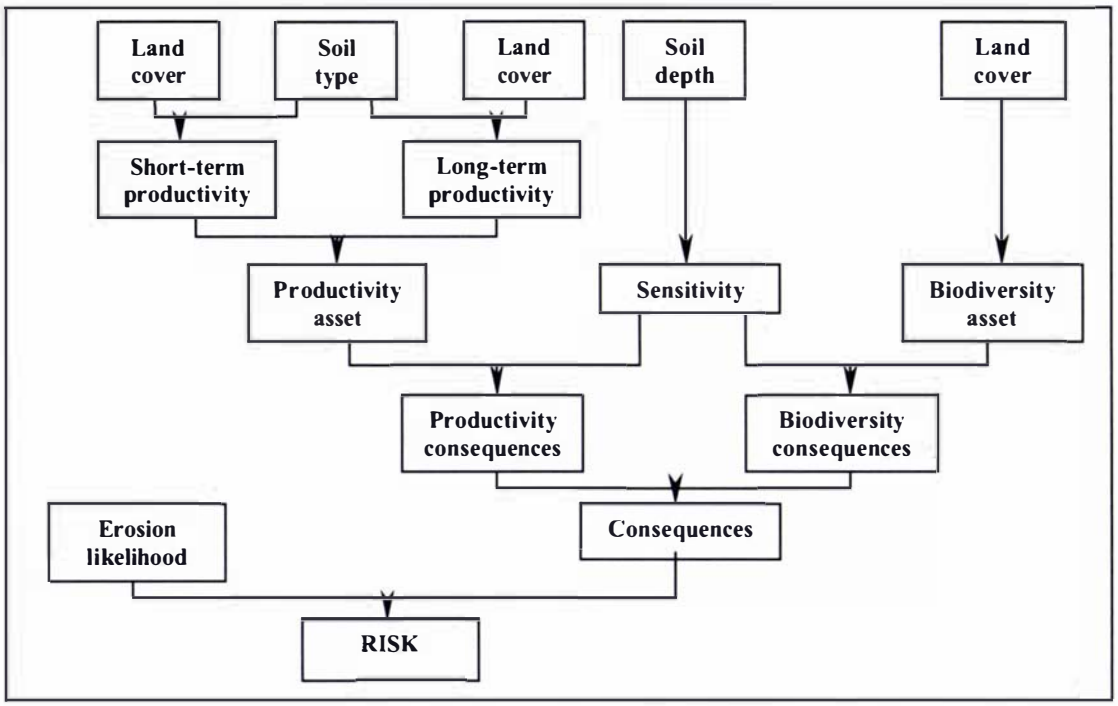

Figure 5-3 Flow diagram of erosion risk assessment

The flow diagrams in Figures 5-2 and 5-3 show that most of the combinations require 2-dimensional (2-D) relationships except for the 'slope-geology-land cover' combination in Figure 5-2 which needs a 3-dimentional (3-D) relationship. The 2-D relationship as suggested by Standards Australia & Standards New Zealand (2004) for risk is presented in Figure 5-4. This is used as the basis for the 2-D and 3-D relationships in this study.

Likelihood	Consequences				
	I	II	III	IV	V
A	medium	high	high	very high	very high
B	medium	medium	high	high	very high
C	low	medium	high	high	high
D	low	low	medium	medium	high
E	low	low	medium	medium	high

Figure 5-4 The 2-D relationship used to determine level of risk

The relationship between likelihood and consequences for every application will be different. It is reflected in the level of risk for each cell.

For this study, each factor is graded into three classes using an ordinal scale (Standard Australia & Standard New Zealand, 2004): low (1), moderate (3), and high (5). When two factors are processed they result in five classes: low (1), moderately low (2), moderate (3), moderately high (4), and high (5). Based on a relationship made by Standard Australia & Standard New Zealand (2004) (see Figure 5-4), the relationship of the five new classes to the original classes is presented in Figure 5-5. For the three classes a simplification of Figure 5-5 is presented in Figure 5-6.

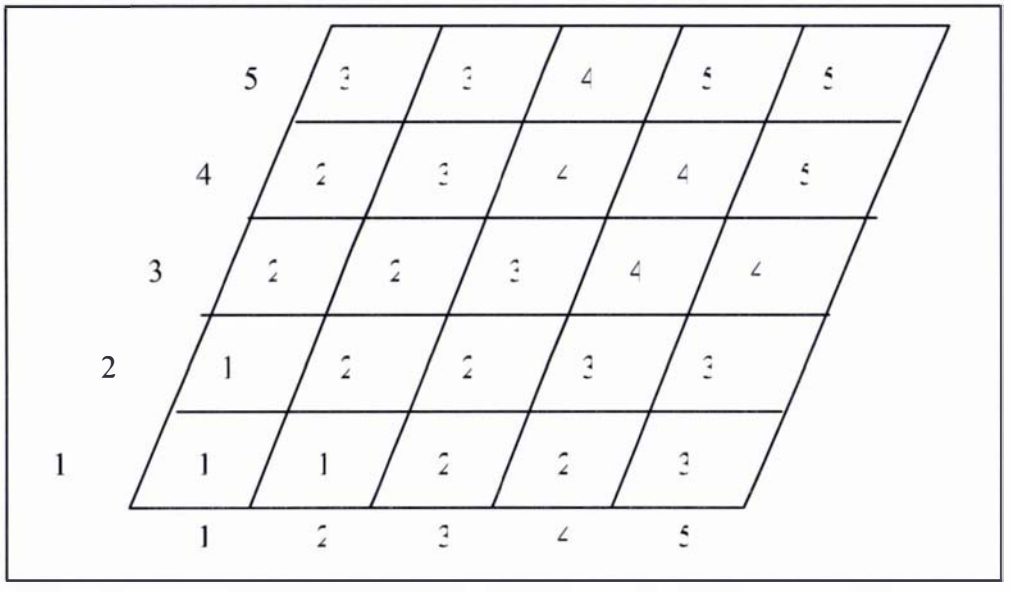

Figure 5-5 The 2-D relationship of factors with five classes. 1 = low, 2 = moderately low, 3 = moderate, 4 = moderately high, and 5 = high.

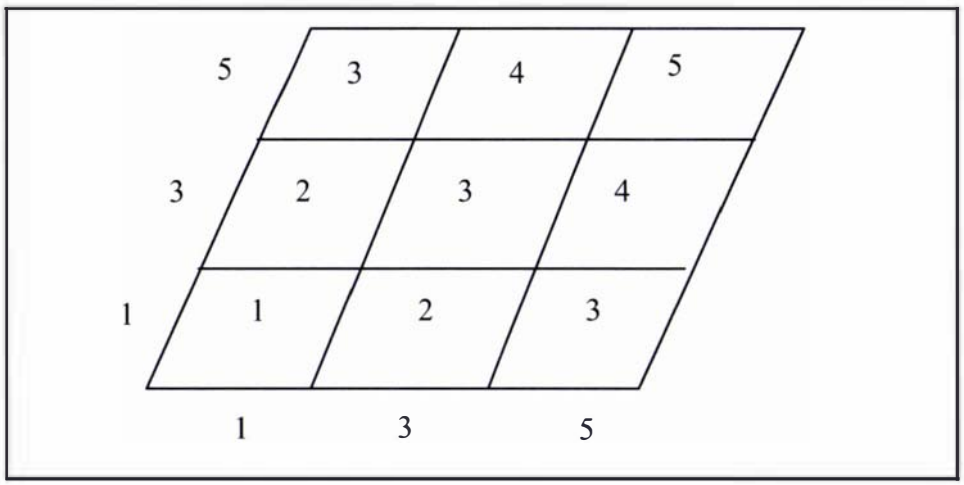

Figure 5-6 The 2-D relationship of factors with three classes. 1 = low, 2 = moderately low, 3 = moderate, 4 = moderately high, and 5 = high.

Both the five and three class grading have equal weights. Each class in the horizontal position is identical to the class in the vertical position. In other words, the combination of, for example, low class in factor 1 and high class in factor 2 is the same as high in factor 1 and low in factor 2. By using this approach, the correlation of both factors is distributed normally as well.

For the 3D relationship, however, each factor is weighted unequally. The dominant factor is slope, followed by geology, while land cover is the least dominant factor (Bruijnzeel, 2004; Gourmellos *et al.*, 2004). The assumptions made in correlating these factors were:

- If the slope is classed as 'high (5)' then the result of any relationship is 'high (5)'
- If the geology is 'high (5)', the result might be less than 'high (5)'
- If the land cover is 'high (5)' and no other factor is 'high (5)' then the result is less than 'high (5)'

The complete correlation among these three factors is presented in Figure 5-7.

The risk of erosion increases dramatically after forest is logged. It is important to know the position and level of risk after logging, so that suitable conservation measures are able to be planned. Land cover and soil type and depth are the main factors that determine the risk level of a logged area.

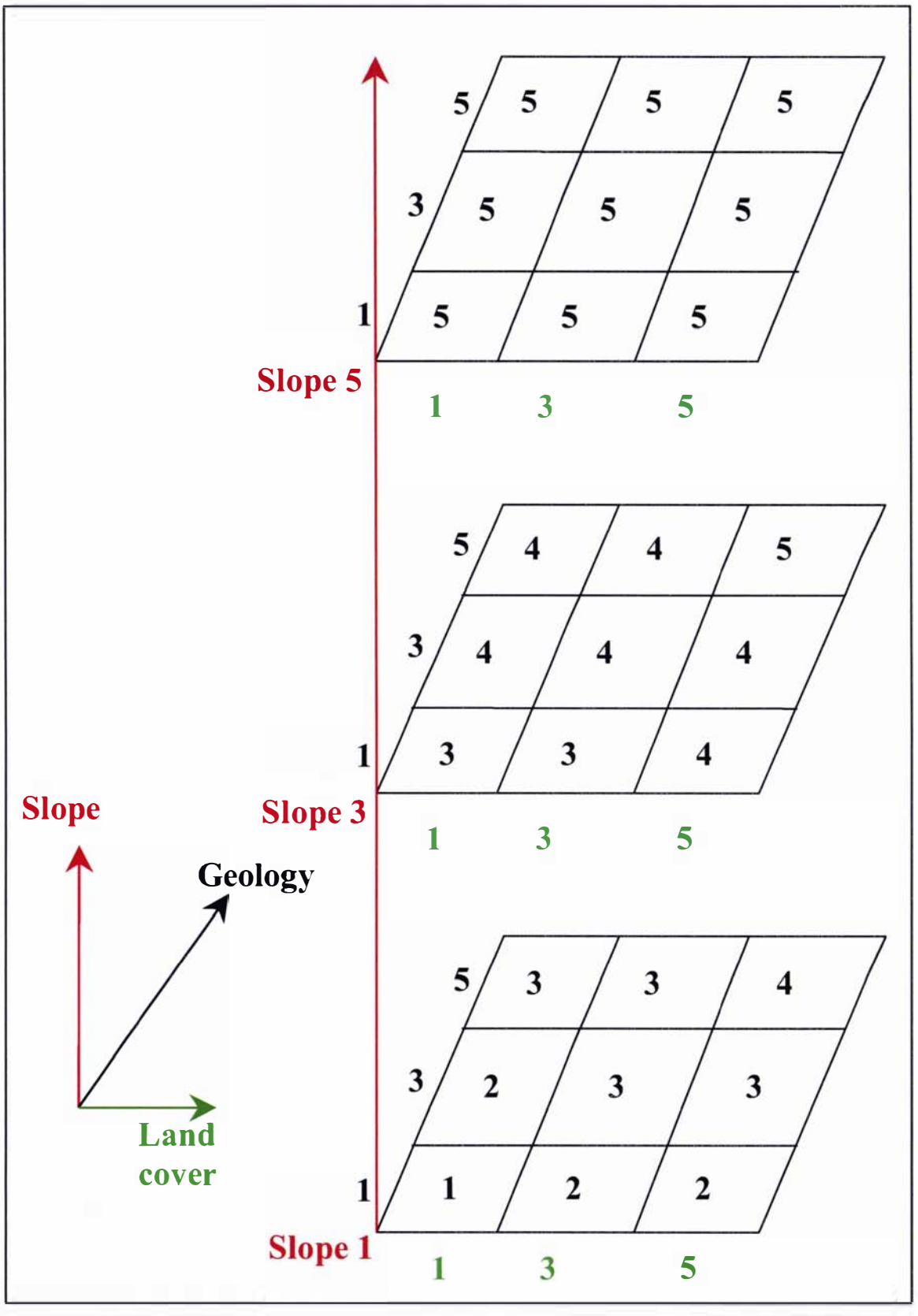

Figure 5-7 The 3-D relationship between slope (red), geology (blue) and land cover (green) leading to erosion susceptibility classes. 1 = low, 2 = moderately low, 3 = moderate, 4 = moderately high, and 5 = high.

Soil type, combined with land cover is used to determine productivity asset value, while land cover alone is used to determine biodiversity asset value. Since the threatening factor is erosion, one of the main soil characteristic that is affected is soil depth. Therefore, soil depth is used to assess the sensitivity to erosion (see Figure 5-3). More detailed explanation about soil sensitivity is presented in Section 5.4.5.2.

5.4.1 Rainfall factor

The rainfall map was created using the ANUSPLIN software distributed by the Centre for Resource and Environmental Studies (CRES), the Australian National University, Canberra, Australia. Detail of this process is presented in Section 3.6.4. The rainfall map was then grouped into classes (from low to high) for the analysis.

Since Indonesia set a risky limit for removing forest in a watershed (Section 5.2 compared to Section 5.3.4), the threshold value for rainfall has to be made low enough to balance it. The threshold used to group the rainfall data was the ratio between the number of dry months to wet months in a year (Q). A dry month is when the total rainfall in a month is less than 100 mm, while a wet month is when total rainfall in a month exceeds 200 mm (Schmidt & Ferguson, as cited in Waryono *et al.*, 1987).

The wet and dry month classification is commonly used in Indonesia to determine climate for an area and land use suitability. The threshold is based on the soil's condition for food crops, during a wet month the soil is considered wet enough to grow food crops. Therefore it can be assumed that in a wet month rainfall is frequently enough to cause erosion.

Another reason for using the dry month/wet month ratio with confidence is the characteristic of Indonesia's climate. Wet months occur in the rainy season when it rains almost every day. This situation does not give the soil a chance to dry before the next rain comes, and erosion is more likely to happen in this situation.

Threshold values for single rainfall events have been proposed by The Weather Channel (no date) or Xie *et al.* (2002) (7.6 mm/hour for heavy rain and 12.7 mm/hour for erosive rainfall respectively). However, because most of the rain gauges in Indonesia are not automatic, they cannot record the rainfall intensity. Therefore the thresholds

proposed by The Weather Channel and Xie *et al.* are not able to be applied in Indonesia at this time.

The ratio of dry months to wet months (Q) is also used to delineate climate regions in Indonesia. It identifies eight regions ranging from extremely dry to extremely wet. The equation to calculate the ratio of dry months to wet months (Q) is as follows:

$$Q = \frac{dry}{wet}$$

where: Q = ratio between the dry months and wet months
dry = number of dry months
wet = number of wet months

If the ratio is low, it means that the number of dry months is low and the number of wet months is high; so the probability of a damaging rainfall event is high. If the ratio is high, it means that the number of dry months is high, there are fewer wet months and the probability of a damaging rainfall event is low. The rainfall ratios corresponding to different rainfall probability classes were derived from rainfall ratio classes created by Schmidt & Ferguson (Waryono *et al.*, 1987). From eight available classes they were downsized into five classes (see Table 5-1).

Table 5-1 Erosion pressure class assessed in terms of probability of erosion causing by rainfall event

Probability of a damaging rainfall event	**Rainfall ratio (Q)**	**No. of wet months**	**No. of dry months**
High (5)	0 – 0.14	7 – 12	<= 1
High-moderate (4)	0.14 – 0.60	2 – 9	1 – 4
Moderate (3)	0.60 – 1.00	1 – 7	1 – 7
Moderate-low (2)	1.00 – 1.67	1 – 5	1 – 7
Low (1)	> 1.67	0 – 4	1 – 12

5.4.2 Slope factor

The slope map was generated from a DEM using the ERmapper software. The slope ranged from 0° in the southern part of the study area to 48.63° in the hilly part. This factor was divided into three erosion risk classes, high, moderate, and low. The classes reflected the effect of slope steepness on erosion; the steeper the slope the more prone the area to erosion. This classification was based on slope classification made by Fletcher & Gibb (1990) which divided slope into 9 classes. From that classification, flat to moderate sloping (3 classes) were classified as contributing to little erosion susceptibility, strongly sloping (1 class) was adjudged to make a moderate contribution, and moderately steep up to precipitous (5 classes) were classified as making a high contribution to erosion susceptibility.

Table 5-2 Slope contribution to erosion susceptibility

Slope contribution to erosion susceptibility	Slope steepness
High (5)	> 25°
Moderate (3)	15 – 25°
Low (1)	< 15°

5.4.3 Geological factor

The geological factor used in this analysis was derived from a classified RGB-531 image (Section 3.2). There were 12 geological types in the study area:

- KTl (Luk Ulo complex)
- KTm (Brecciated rocks)
- KTog (Mafics and ultramafics)
- Qa (Alluvium)
- Teok (Karang Sambung formation)
- Tmk (Kali Pucung formation)
- Tmp (Penosogan formation)

- Tmph (Halang formation)
- Tmpb (Breccia member of Halang formation)
- Tmw (Waturanda formation)
- Tmwt (Tuff member of Waturanda formation)
- Tomt (Totogan formation)

As was done with slope factor, the geological types in this study area were grouped into three classes depending on the rock type's susceptibility to erosion. The easily eroded types were classified as high, while the least erodible rock types were classified as low. The types of each class are presented in Table 5-3, while detailed description of each type is presented in Appendix A.

Table 5-3 Geological contribution to erosion susceptibility

Geological contribution to erosion susceptibility	**Geological type**
High (5)	KTl, KTm, Tmpb, Tmph, Tmw, Tomt
Moderate (3)	KTog, Teok, Tmk, Tmp
Low (1)	Qa, Tmwt
Others	Water bodies, clouds

5.4.4 Land cover factor

The land cover type was created by analysing the Landsat7 image. Using the image classification (described in Chapter 4) the land covers in the study area were:

- Water bodies (reservoir)
- Village
- Rice field
- Open land
- Mixed forest
- Monotype forest

As is explained earlier, there were three land cover types that were assessed for erosion risk. They were open land, mixed forest, and monotype forest. Monotype forests in this study area are mostly pine trees (*Pinus merkusii*), while mixed forests are combinations of small blocks of acacia, teak, or mahogany. In this study, monotype forest is also referred to simply as forest.

Land cover was assessed for its contribution to erosion susceptibility and the asset value. For the contribution to erosion susceptibility, land covers were grouped into three classes. If the land cover was easily eroded then the level was high, while land cover which was able to prevent erosion was grouped into low contribution to erosion. The mixed forest has more open space compared to monotype forest, because in the mixed forest the distances between trees are irregular. The classes are presented in Table 5-4 as follows:

Table 5-4 Land cover contribution to erosion susceptibility

Land cover contribution to erosion susceptibility	**Land cover**
High (5)	Open land
Moderate (3)	Mixed forest
Low (1)	Monotype forest
No contribution to erosion susceptibility (0)	Village, water bodies, rice field, clouds

5.4.5 Environmental factors

Three environmental factors were used in this study to assess the environmental consequences of an area being logged. These factors were land cover, soil type and soil depth. The environmental consequences were assessed in terms of the asset value and sensitivity of the asset value to erosion. The asset value was derived from land cover and soil type, while the sensitivity was assessed from soil depth.

5.4.5.1 Environmental asset value

The asset values assessed were potential productivity and biodiversity (see Figure 5-3). As one of the factors in determining the asset values, land cover combined with soil type were used to predict the potential productivity of cleared land (Richardson *et al.*,

1999). The productivity itself, which is represented as income, was differentiated into short- and long-term productivity. Short-term productivity is determined for the two to three years after the land is cleared. This is the period when Perum Perhutani allows farmers to grow and harvest food crops while they take care of the forest trees. Long-term productivity is determined for the period that follows while the trees are growing until the next logging and food crops are not allowed to be planted.

For short-term productivity, an area which formerly was forest or mixed forest is assumed to give higher income than formerly open land. In the long-term productivity, however, forest will give potentially higher income than mixed forest. This is because people are able to tap the gum from pine trees in the forest, while in the mixed forest the income only starts when the trees are ready to be logged. In each case it is assumed that the new forest following logging will be of the same type as the logged forest.

For formerly open land, it is assumed that open land only received income from food crops and the soil was in lower fertility condition compared to forest and mixed forest. Therefore open land was assigned a moderate to low productivity. The class of productivity of each land cover is presented in Table 5-5. In a fully/detailed implementation, it is hoped that site specific information would be available to replace these assumptions.

Table 5-5 Predicted productivity class (in terms of income) for each land cover

Formerly land cover	**Short-term productivity**	**Long-term productivity**
Open land	Moderate (3)	Low (1)
Mixed forest	High (5)	Moderate (3)
Forest	High (5)	High (5)

Productivity is also dependent on soil type, whether the soil is inherently fertile or not. The soil types in this study area are: Dystropepts, Rendolls, Tropaquepts, Tropohemists, and Tropudalfs (see Section 2.6). The more fertile soil has higher potential productivity. Dystropepts and Rendolls soils are slightly and moderately weathered respectively. Tropohemists and Tropaquepts soils have a slow drainage, and Tropudalf

is well weathered soil (Fletcher & Gibb, 1990). The soil productivity asset class is presented in Table 5-6.

Table 5-6 Predicted soil productivity class for each soil type

Soil productivity asset class	Soil type
Moderately high (4)	Dystropepts, Rendolls
Moderate (3)	Tropohemists, Tropaquepts
Moderately low (2)	Tropudalf

Biodiversity asset class is determined from the former land cover. Mixed forest was assigned a high biodiversity asset class; since it had more than one type of trees then it is assumed that it had more varied organisms than forest which had monotype trees. However, open land had the lowest biodiversity asset value compared to the other two land covers. The biodiversity asset class is presented in Table 5-7.

Table 5-7 Biodiversity asset class of each land cover

Biodiversity asset class	Land cover
High (5)	Mixed forest
Moderate (3)	Forest
Low (1)	Open land

5.4.5.2 Environmental sensitivity

The sensitivity of the productivity and biodiversity asset values to erosion for a logged area is dependent on soil depth; the shallower the soil is the more sensitive its asset value is to erosion. The soil depth class used in this study was modified from the classification made by The Ministry of Forestry of Indonesia (Fletcher & Gibb, 1990).

The soil depth data available in this study area has two parts: effective top soil (0 to >30 cm) and overall soil depth (0 to 175 cm), this information is combined beforehand to produce soil erosion sensitivity class. The classification of these two different soil depths is presented in Table 5-8.

Table 5-8 Soil erosion sensitivity class derivation from soil depth:

Effective top soil (cm)	Overall soil (cm)	Soil erosion sensitivity class
< 10	< 30	High (5)
10 - 20	30 – 90	Moderate (3)
> 20	> 90	Low (1)

5.4.5.3 Environmental Consequence

The environmental consequence is a combination of both productivity consequence and biodiversity consequence. The productivity and biodiversity consequences were derived from correlating the productivity and biodiversity assets with environmental sensitivity using the 2-D relationship presented in Figure 5-5. The final environmental consequence is assigned as the worst scenario from the productivity and biodiversity consequences. Therefore, the highest class between those two consequences is chosen.

5.5 Results and Discussion

From this point on the analysis was done only inside the watershed boundary of the study area instead of using the whole image. The size of the study area is 88,551.6 ha, which is within the Luk Ulo and Telomoyo watersheds (more detail about the watersheds is described in Section 2.4).

5.5.1 Rainfall Surface

The rainfall surfaces were constructed by choosing three wettest years out of 10 years of rainfall data. Those three years were 1992, 1995 and 1998. The average of 10 years rainfall in this area was 3172 mm/year, but the average of these three wettest years was 4230 mm/year. The detail of the rainfall surface is described in Section 3.5 and all the rainfall data are presented in Appendix B.

ANUSPLIN created 36 monthly rainfall surfaces from 1992, 1995 and 1998. The characteristic of each surface has already been presented in Table 3-5. Some months got negative rainfall values which reflect the estimation modelling used by the LAPGRD programme. In actual fact the range would start from zero rainfall.

The rainfall value in each surface was then converted into a wet or dry month using the criteria given in Section 5.4.1. The total number of wet and dry months for each pixel and for each year was calculated by adding up 12 monthly surfaces. The number of wet and dry months for each year was then averaged for each pixel and was then used for the analysis. The result is presented in Table 5-9 while the distributions of the averaged wet and dry months are presented in Figures 5-7 and 5-8 respectively.

In Table 5-9 the average yearly rainfall calculated for each pixel in the study area ranged from 5 wet months and 4 dry months up to 10 wet months with no dry month, while the rest were moderate months, where precipitation was between 100 – 200 mm/month.

The maps in Figure 5-8 and 5-9 show that the study area is a relatively wet area: most of the area had nine wet months (46% of the study area - shown in orange in Figure 5-8 - experienced nine wet months) and a small area had only five wet months (less than 1%, which is shown in dark green in Figure 5-8). More than 58% of the study area experienced only one dry month, although there were areas with as many as four dry months (2%). These numbers show that during the chosen years (1992, 1995 and 1998), half of the study area experienced only one dry month and nine wet months, while the last two months were moderate.

Table 5-9 The number of wet and dry months calculated for each pixel in 1992, 1995 and 1998, and their averages

Year	**The range of number of**	
	Wet months	**Dry months**
1992	5 – 12	0 – 6
1995	5 – 10	2 – 6
1998	4 – 11	0 – 6
Averaged year	5 – 10	0 – 4

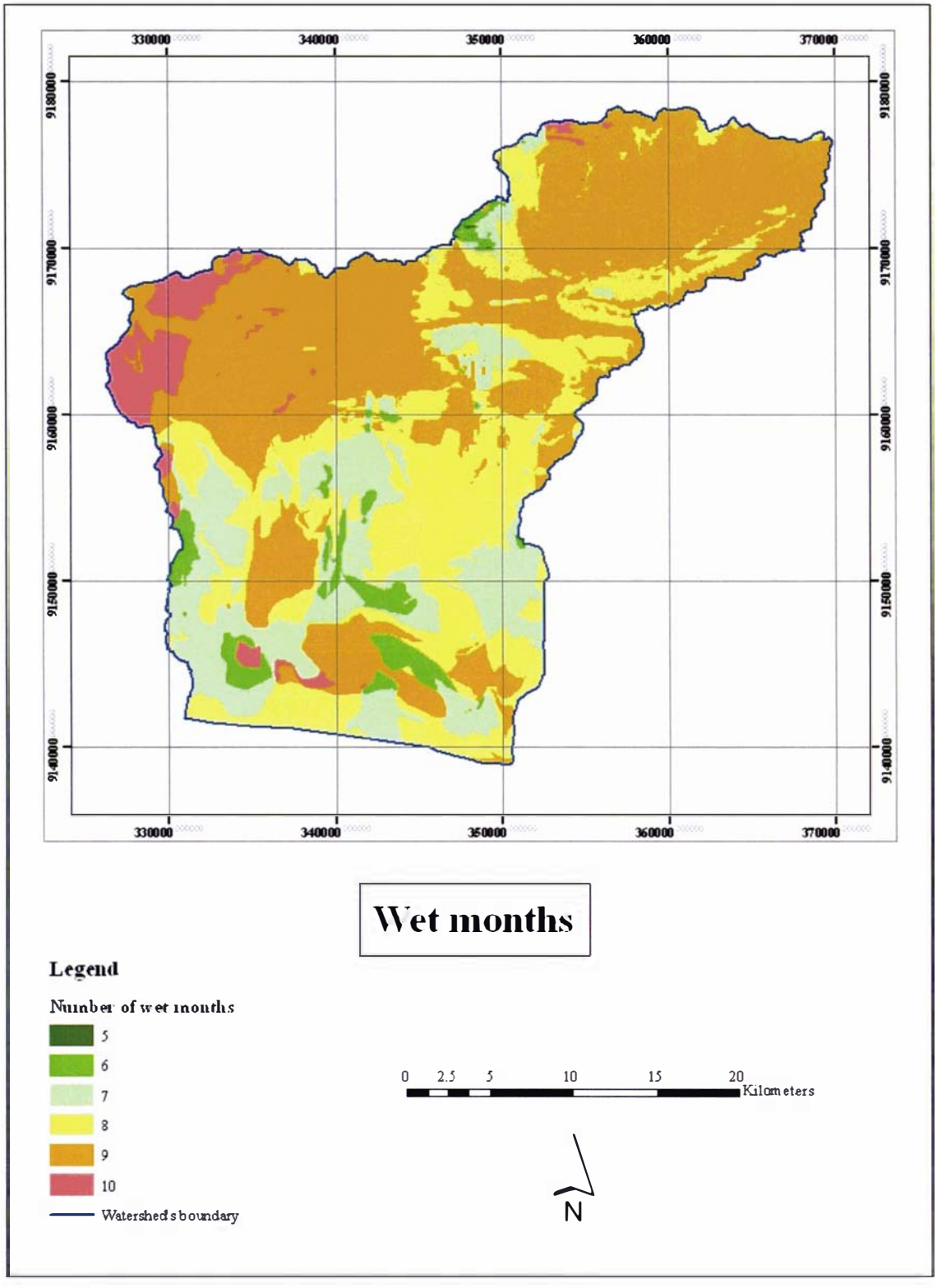

Figure 5-8 The number of wet months in the study area, averaged from three years (1992, 1995, and 1998). Dark green is the driest location, and red is the wettest.

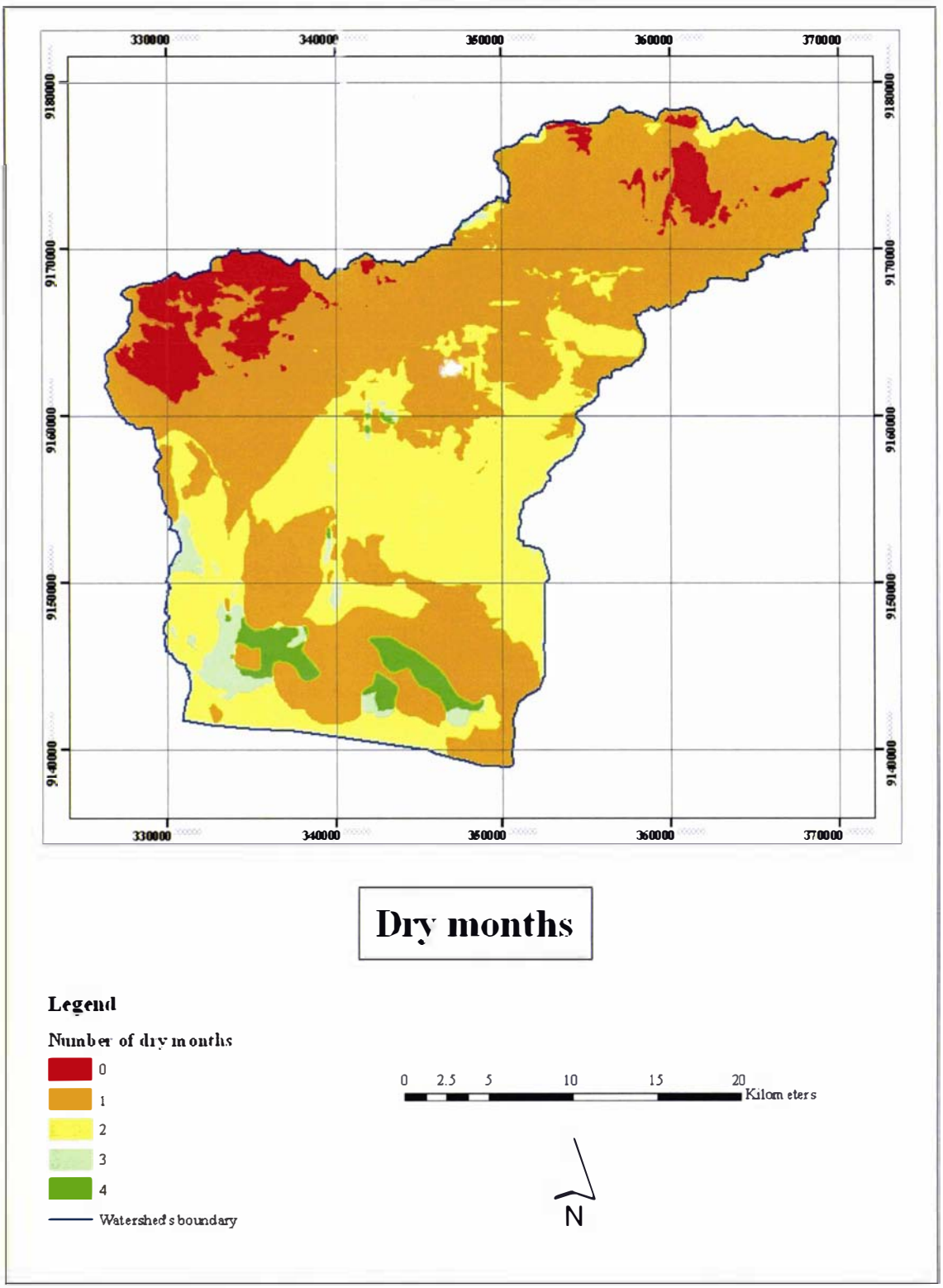

Figure 5-9 The number of dry months in the study area, averaged from three years (1992, 1995, and 1998). Green is the driest location, and red is the wettest.

The next step was calculating the Q value for each pixel in the study area. Using RATIO (ratio between the number of dry months and the wet months) in ERmapper's formula, the Q value was determined. It ranged from 0.07 to 0.82. Using criteria presented in Table 5-1, the distribution of rainfall pressure can be calculated and is shown in Figure 5-10.

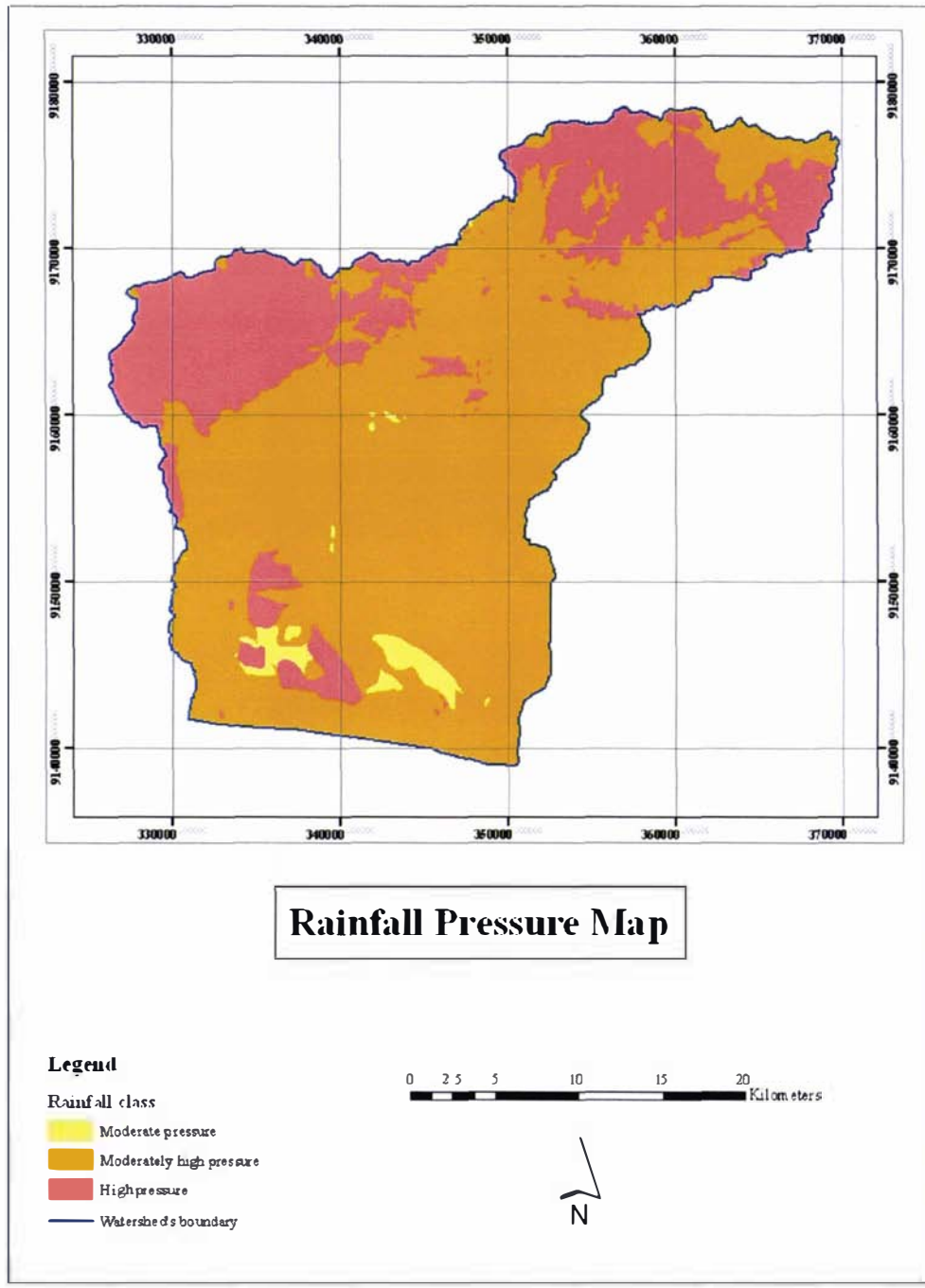

Figure 5-10 The distribution of the rainfall pressure classes.

In Figure 5-10 moderately high pressure occupied 70% of the study area, with 2% moderate and 28% high pressure. This situation illustrates that the pressure of erosion in this area is predominantly high.

5.5.2 Erosion Susceptibility

The erosion susceptibility data layer was generated by overlaying three erosion factors: slope, geology and land cover. The distribution of each class for each map is presented in Figures 5-11 up to 5-13, while in Tables 5-10 to 5-12 the area (ha) and percentage of each factor are shown.

5.5.2.1 Slope

The slope class data layer was derived from the DEM. Using the criteria presented in Table 5-2 a map was produced showing the distribution of slope classes that contribute to erosion susceptibility. The area of each slope class is presented in Table 5-10. A large proportion (61%) of the area (Figure 5-11) has low/gentle slopes which do not contribute too much to the erosion susceptibility, unless the geological contribution to erosion susceptibility is also high. Areas where the slope is steep (24%) have a high erosion susceptibility (see Figure 5-7).

Table 5-10 Area (ha) and percentage of each slope class (derived from DEM) according to the slope contribution to erosion susceptibility

Slope class	**Area**	
	(ha)	**(%)**
Low contribution to erosion susceptibility (slope < 15°)	53949.7	61
Moderate contribution to erosion susceptibility (slope 15 – 25°)	13181.4	15
High contribution to erosion susceptibility (slope > 25°)	21420.5	24
TOTAL	88551.6	100

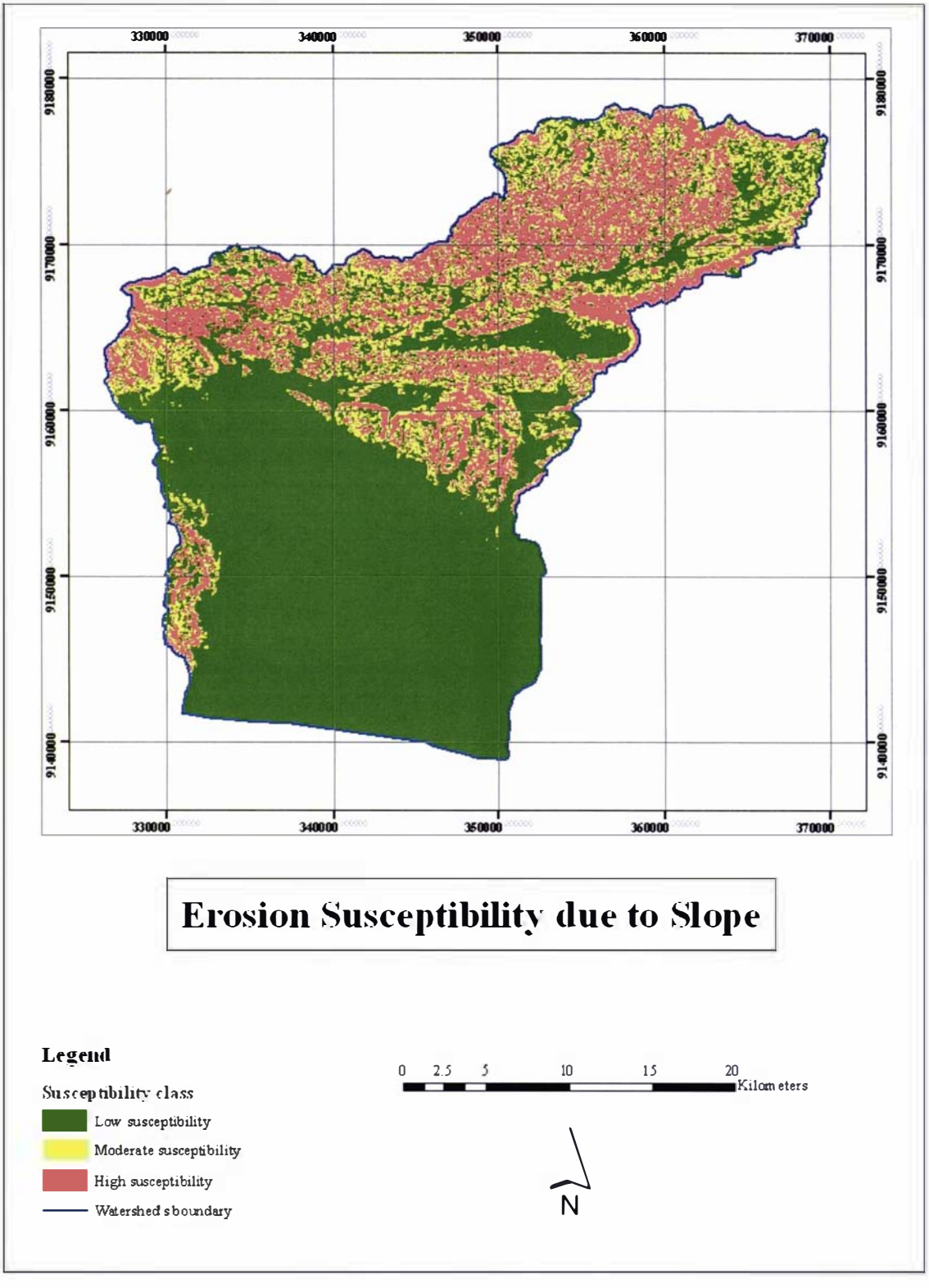

Figure 5-11 Distribution of the slope contribution to erosion susceptibility

5.5.2.2 Geology

The geological data layer was classified using criteria presented in Table 5-3 to determine the distribution of geological contribution to erosion susceptibility class in this study. The classification is shown in Table 5-11 and Figure 5-12. The low geological types of erosion susceptibility coincided with areas of low erosion susceptibility as determined from the slope map. These were mostly Alluvium (Qa) which occupied flat areas. Geological types with high erosion susceptibility, on the other hand, occupied more than 50% of the study area, and these types spread over the steep slopes. The full description of each geological type is presented in Appendix A, while in Table 5-11 the area (ha) and percentage of each susceptibility class are shown.

Table 5-11 Area (ha) and percentage of each class and each geological type in the study area (derived from classified image) according to the geological contribution to erosion susceptibility

Geological type	**Area**	
	(ha)	**(%)**
Low contribution to erosion susceptibility :		
- Qa (alluvium)	18497.3	
- Tmwt (Tuff member of Waturanda formation)	4322.3	
Total of low contribution to erosion susceptibility	22819.6	26
Moderate contribution to erosion susceptibility:		
- KTog (Mafics and ultramafics)	157.9	
- Teok (Karang sambung formation)	5092.6	
- Tmk (Kalipucung formation)	9239.7	
- Tmp (Penosogan formation)	1273.2	
Total of moderate contribution to erosion susceptibility	15763.4	18
High contribution to erosion susceptibility:		
- KTl (Luk Ulo Complex)	1997.5	
- KTm (Brecciated rocks)	8430.0	
- Tmpb (Breccia member of Halang formation)	10354.5	

Geological type	Area	
	(ha)	(%)
- Tmph (Halang formation)	19691.9	
- Tmw (Waturanda formation)	3527.6	
- Tomt (Totogan formation)	2245.8	
Total of high contribution to erosion susceptibility	46247.2	52
Others:		
- Water bodies and clouds	3721.4	4
TOTAL	88551.6	100

5.5.2.3 Land Cover

As already mentioned in Section 5.4, the land cover types used in this analysis were open land, mixed forest and monotype forest. Other land cover types such as rice fields and villages were masked out from the analysis along with water bodies, cloud and cloud shadows.

The land cover contribution to erosion susceptibility is the reaction of each land cover to erosion. If the soil under a certain land cover is easily eroded, it means that it has a high susceptibility to erosion, while the more stable soil has a low susceptibility to erosion. Using the classification in Table 5-4, a land cover contribution to erosion susceptibility map was produced. From the map (Figure 5-13), the low class belongs to monoculture forest which was the least erodible land cover (shown in green) while open land (shown in red) was the most erosion-prone land cover within this study area. Most of the region had a moderate susceptibility to erosion (43%) and consisted of mixed forest (Table 5-12).

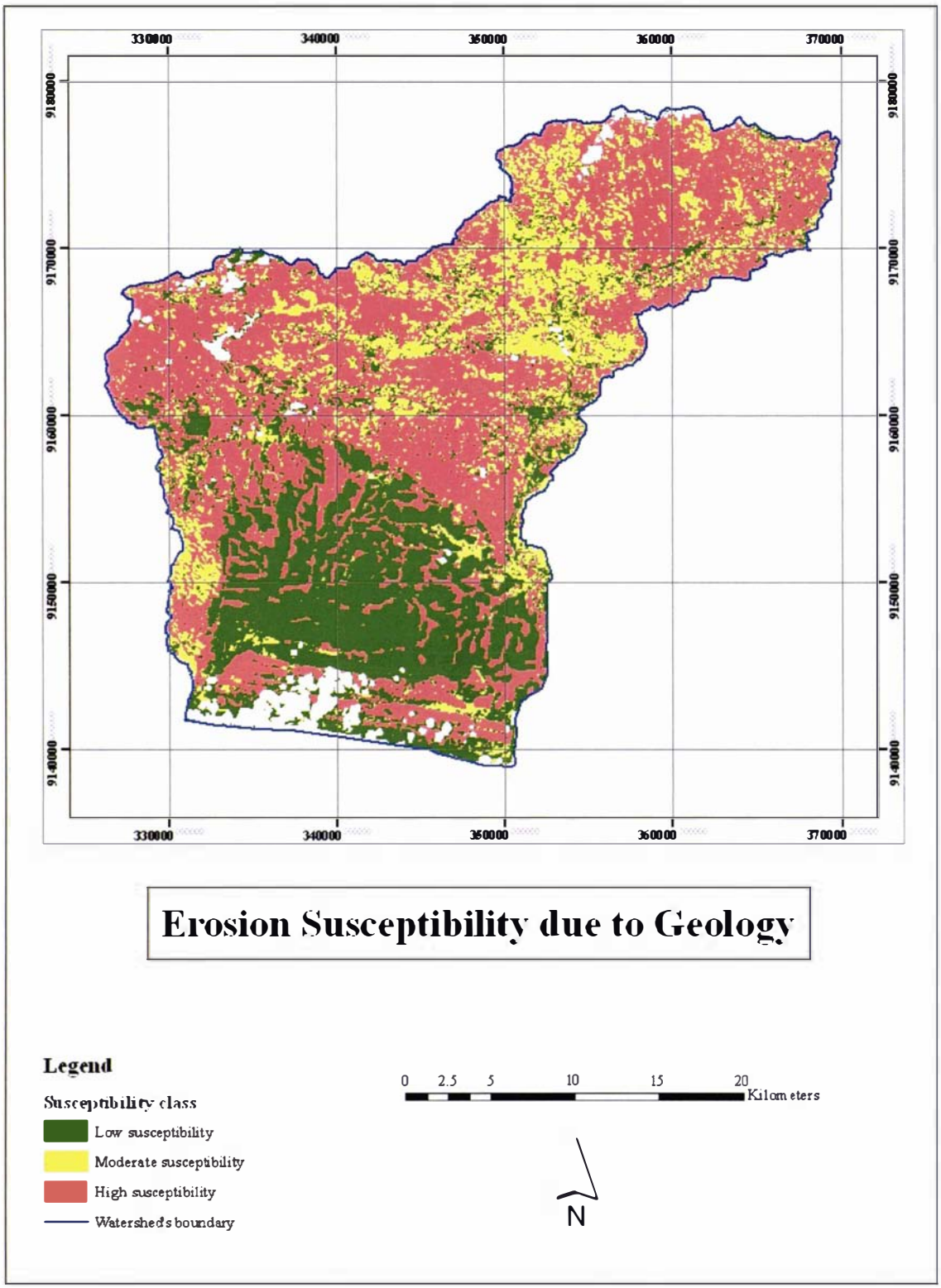

Figure 5-12 The distribution of the geological contribution to erosion susceptibility

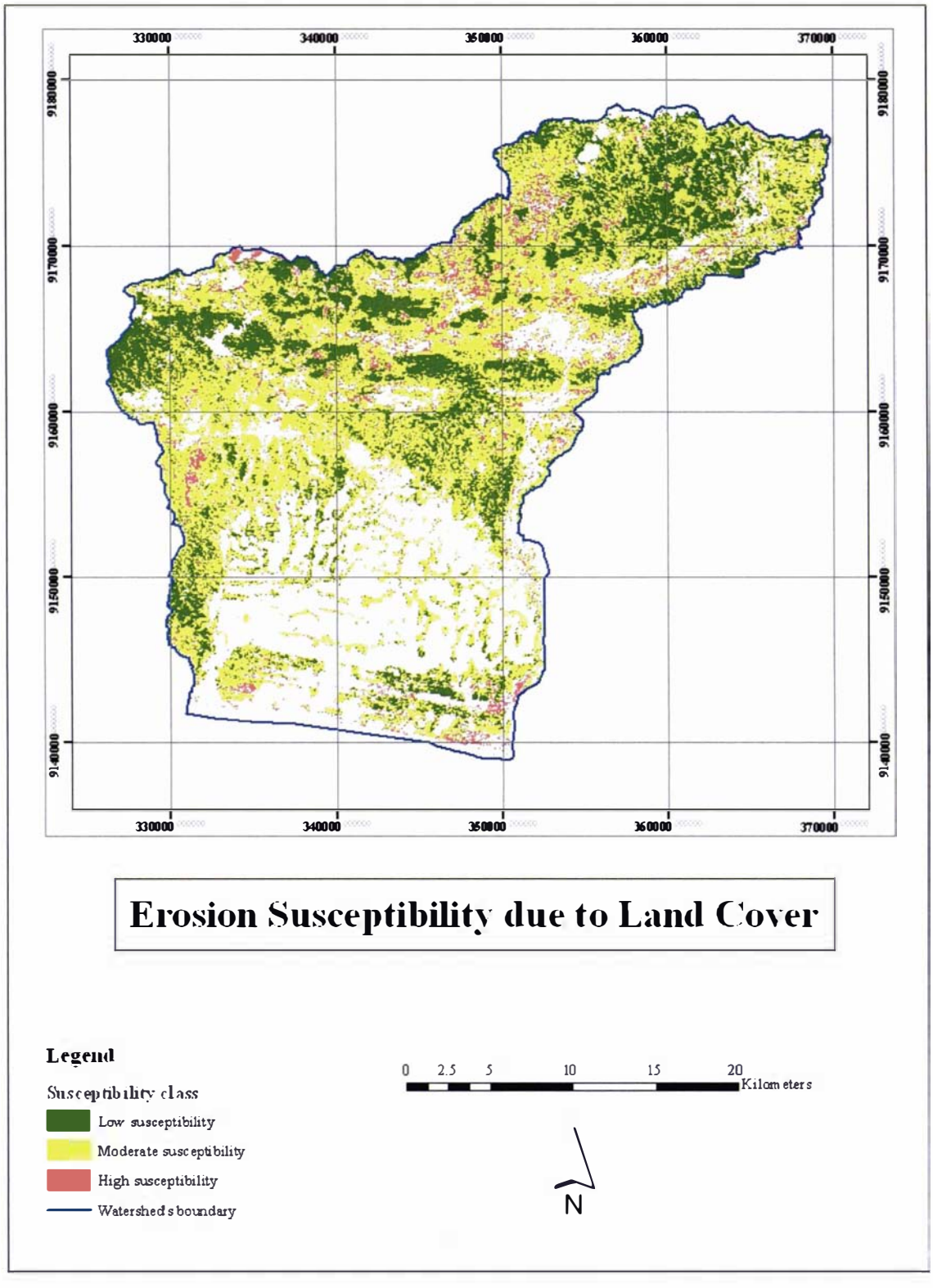

Figure 5-13 The distribution of land cover contribution to erosion susceptibility

Table 5-12 Area (ha) and percentage of each land cover type in the study area (derived from classified image) according to land cover contribution to erosion susceptibility

Land cover type	**Area**	
	(ha)	**(%)**
Low contribution to erosion susceptibility: forest	18261.4	20
Moderate contribution to erosion susceptibility: mixed forest	37679.3	43
High contribution to erosion susceptibility: open area	5969.9	7
Others (no contribution to erosion):		
- Rice field	16315.7	
- Villages	6603.9	
- Water bodies	202.1	
- Cloud and cloud's shadows	3519.3	
Total of no contribution to erosion	26641.0	30
TOTAL	88551.6	100

5.5.2.4 Erosion Susceptibility

The erosion susceptibility contributions (slope, geology, and land cover) were combined using the 3D relationship presented in Figure 5-7. This relationship was then translated into ERmapper's formula using 'if – then' statements. The equation was as follows:

if slope = 1 and geology = 1 and land cover = 1 then 1 else
if slope = 1 and geology = 1 and land cover = 3 then 2 else
if slope = 1 and geology = 1 and land cover = 5 then 2 else
if slope = 1 and geology = 3 and land cover = 1 then 2 else
if slope = 1 and geology = 3 and land cover = 3 then 3 else
if slope = 1 and geology = 3 and land cover = 5 then 3 else
if slope = 1 and geology = 5 and land cover = 1 then 3 else
if slope = 1 and geology = 5 and land cover = 3 then 3 else
if slope = 1 and geology = 5 and land cover = 5 then 4 else
if slope = 3 and geology = 1 and land cover = 1 then 3 else
if slope = 3 and geology = 1 and land cover = 3 then 3 else
if slope = 3 and geology = 1 and land cover = 5 then 4 else
if slope = 3 and geology = 3 and land cover = 1 then 4 else
if slope = 3 and geology = 3 and land cover = 3 then 4 else
if slope = 3 and geology = 3 and land cover = 5 then 4 else
if slope = 3 and geology = 5 and land cover = 1 then 4 else

if slope = 3 and geology = 5 and land cover = 3 then 5 else
if slope = 3 and geology = 5 and land cover = 5 then 5 else
if slope = 5 then 5 else 0

The result of combining three factors (slope, geology, and land cover) is presented in Figure 5-14, while the area (ha) and percentage of each susceptibility class are given in Table 5-13.

Table 5-13 Area (ha) and percentage of each erosion susceptibility class (resulting from overlaying slope, geology, and land cover data layers)

Erosion susceptibility class	**Area**	
	(ha)	**(%)**
Low susceptibility to erosion	528	<1
Moderately low susceptibility to erosion	4601.9	5
Moderate susceptibility to erosion	23531.7	27
Moderately high susceptibility to erosion	7897.2	9
High susceptibility to erosion	25351.7	29
No susceptibility to erosion	26641.0	30
TOTAL	88551.6	100

Since open land only contributed a small part of high susceptibility to erosion (see Table 5-12), this means that high erosion susceptibility in this study area (29%) was caused more by steep slopes and easily eroded geological material. However, 43% of the land covers which have moderate potential to be eroded were distributed throughout the moderately low up to moderately high susceptibility unless the slope contribution to erosion susceptibility class was high.

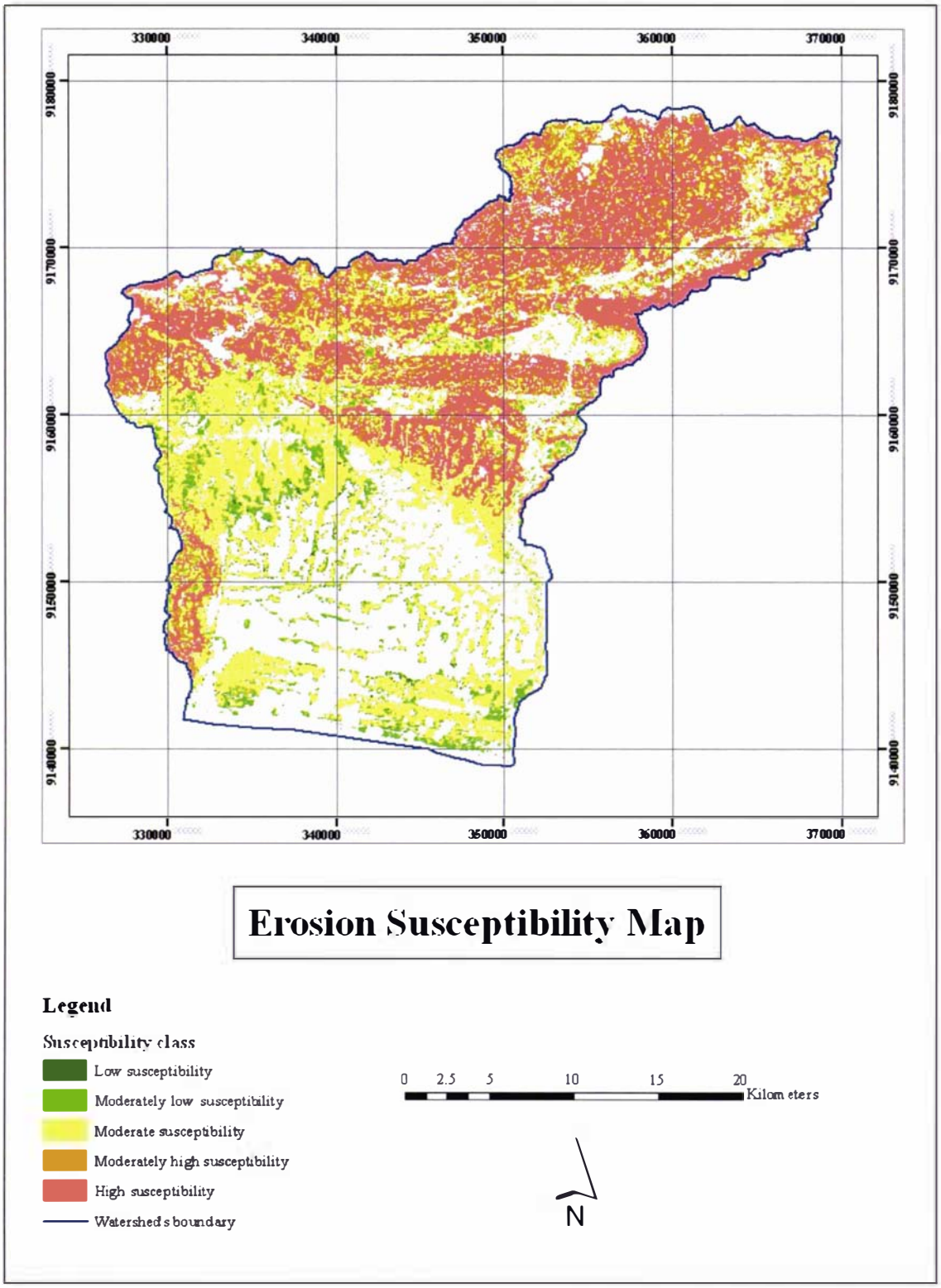

Figure 5-14 The distribution of erosion susceptibility classes in the study area

5.5.3 Erosion Likelihood

The likelihood of an area being eroded after a logging event is dependent on the damaging effect of rainfall. The damaging effect of rainfall is the management pressure which is presented in Figure 5-10 as the rainfall pressure. Combining the rainfall pressure with erosion susceptibility using the 2-D relationship (Figure 5-4) resulted in erosion likelihood and is presented in Figure 5-15.

Since the rainfall pressure is predominantly moderately high, the combination between it and erosion susceptibility resulted in many areas of 'moderately high' and 'high' erosion likelihood class (31% and 32% of the study area respectively). Figure 5-15 presents the distribution of erosion likelihood in the study area, while Table 5-14 presents the area (ha) and percentage of the total area in each erosion likelihood class.

Table 5-14 Area (ha) and percentage of each erosion likelihood class

Erosion likelihood class	**Area**	
	(ha)	**(%)**
Moderately low erosion likelihood	544.0	1
Moderate erosion likelihood	4989.8	6
Moderately high erosion likelihood	27775.6	31
High erosion likelihood	28601.2	32
No erosion likelihood	26641.0	30
TOTAL	88551.6	100

There are small areas (1 and 6% of the total study area) that have moderately low and moderate likelihood of being eroded. These areas are forest or mixed forest which are located in the flat lowland area and receive moderate rainfall. Since the locations of these areas were scattered around rice fields, they could be trees grown around houses in villages or markers of the owner's boundary around rice fields.

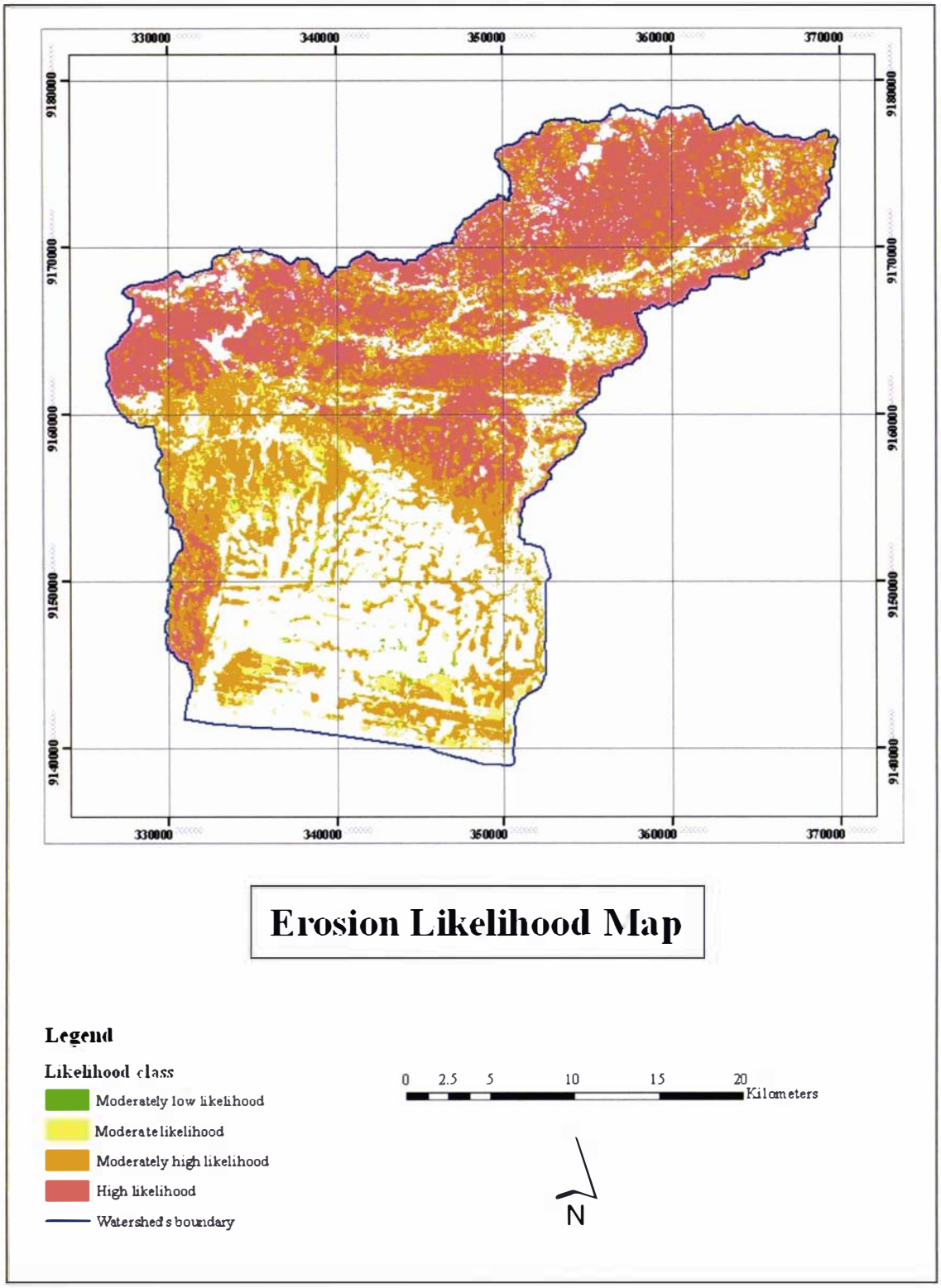

Figure 5-15 The distribution of erosion likelihood classes in the study area

Compared to erosion susceptibility, erosion likelihood in the study area shows worsening conditions. From less than 40% of moderately high and high susceptibility to erosion, it increases to more than 60% of the study area having moderately high to high erosion likelihood. This is because of the high rainfall pressure.

Using the result of this analysis it could be argued that more than 60% of the study area could become eroded after logging unless some measures are taken. This condition can only be improved by reducing the effect of rainfall pressure. This can be done by arranging the timing of the operation and amount of ground cover at times of the high rainfall pressure (see Section 5.3.5).

5.5.4 Environmental Consequences

Once the erosion likelihood is understood, it is also important to know the consequence of environmental damage caused by erosion. Until now most erosion studies have not included environmental evaluation in the erosion analysis; most only predict the likelihood of erosion by measuring the erosion factors and leave environmental consequence untouched although consequence is important information to resolve natural resource management issues.

In this study the environmental evaluation was assessed according to the flowchart presented in Figure 5-3 and Section 5.4.5. There were two consequences assessed when the forest is logged; productivity consequence and biodiversity consequence. Productivity consequence is assessed using land cover, soil type and soil depth factors while biodiversity consequence only used land cover and soil depth.

5.5.4.1 Short- and Long-term Productivity

The productivity class was derived from a combination of soil fertility and land cover productivity value. In the absence of direct information about soil fertility, the analysis was conducted by using soil type to infer soil fertility.

The potential productivity asset value of an area was determined as a combination of its short- and long-term productivity. The short-term productivity is the potential productivity of an area within a period of two to three years after logging. At this period of time it is assumed that stumps were removed, the land was cleared, and food

crops were cultivated together with planted forest trees in both formerly mixed and monotype forests. With the same food crop varieties, mixed and monotype forest were assessed as highly productive, while open land was assessed as moderately productive. This is because soils under forest and mixed forest were assessed as having a higher fertility resulting from mulch or organic material left after the forests were logged.

Land cover and soil fertility relationship (see Figure 2-14) were combined using the 2-D relationship shown in Figure 5-5. This relationship was then translated into ERmapper using 'if – then' statement as follows:

if land cover = 3 and soil fertility = 2 then 2 else
if land cover = 3 and soil fertility = 3 then 3 else
if land cover = 3 and soil fertility = 4 then 4 else
if land cover = 5 and soil fertility = 2 then 3 else
if land cover = 5 and soil fertility = 3 then 4 else
if land cover = 5 and soil fertility = 4 then 5 else 0

The result of this combination is presented in Figure 5-16a with 34% of the total study area having high short-term productivity.

In contrast to the short-term productivity, long-term productivity was assessed for the period when food crops are not permitted to be planted in the logged area. This period lasts until the forests are logged again. Within this period, monotype forest has potentially higher income or productivity compared to mixed forest and open land. Monotype forest, which in this study area is pine forests, is able to produce gums during this period while mixed forest is unproductive until the trees are logged. Open land, on the other hand, was the least productive because it is used only for food crop production and its fertility could be depleted due to erosion.

Areas and percentage of short- and long-term productivity are presented in Table 5-15 while Figure 5-16b shows the distribution of the long-term productivity.

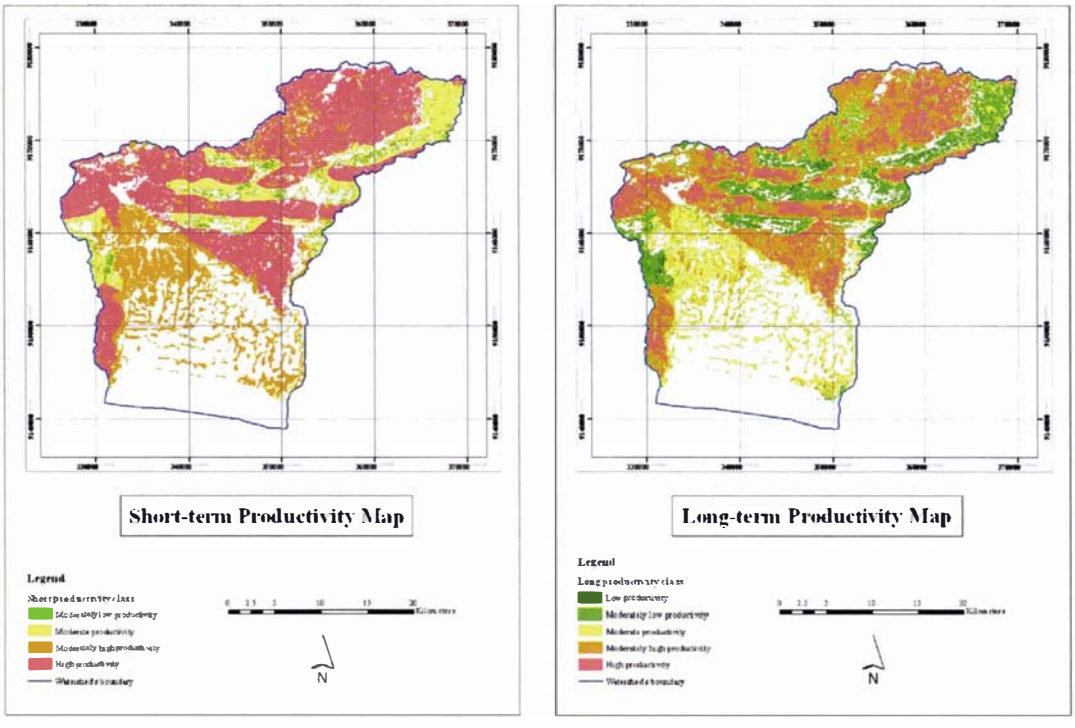

a b

Figure 5-16 The short- and long-term productivity class distribution within the study area

Table 5-15 Area (ha) and percentage of each productivity class

Productivity class	**Short-term productivity**	**Long-term productivity**
	Area in ha (%)	
Low productivity	--	1717.1 (2)
Moderately low productivity	1703.1 (2)	10182.5 (11)
Moderate productivity	9016.0 (10)	10376.9 (12)
Moderately high productivity	13566.4 (15)	18850.8 (21)
High productivity	30016.2 (34)	13174.3 (15)
No productivity	34250.0 (39)	34250.0 (39)
TOTAL	88551.6 (100)	88551.6 (100)

The productivity asset classes of the study area were created by combining the short- and long-term productivity and the result is presented in Figure 5-17. The combination followed the 2-D relationship presented in Figure 5-5.

The highly productive areas were located in the mixed and monotype forest, on Dystropept or Rendoll soils. They occupied 34% of the total study area. The low and moderately low classes (2 and 8% of the study area) were in the Tropudalf soil, since this soil had a moderately low fertility compared to other soils.

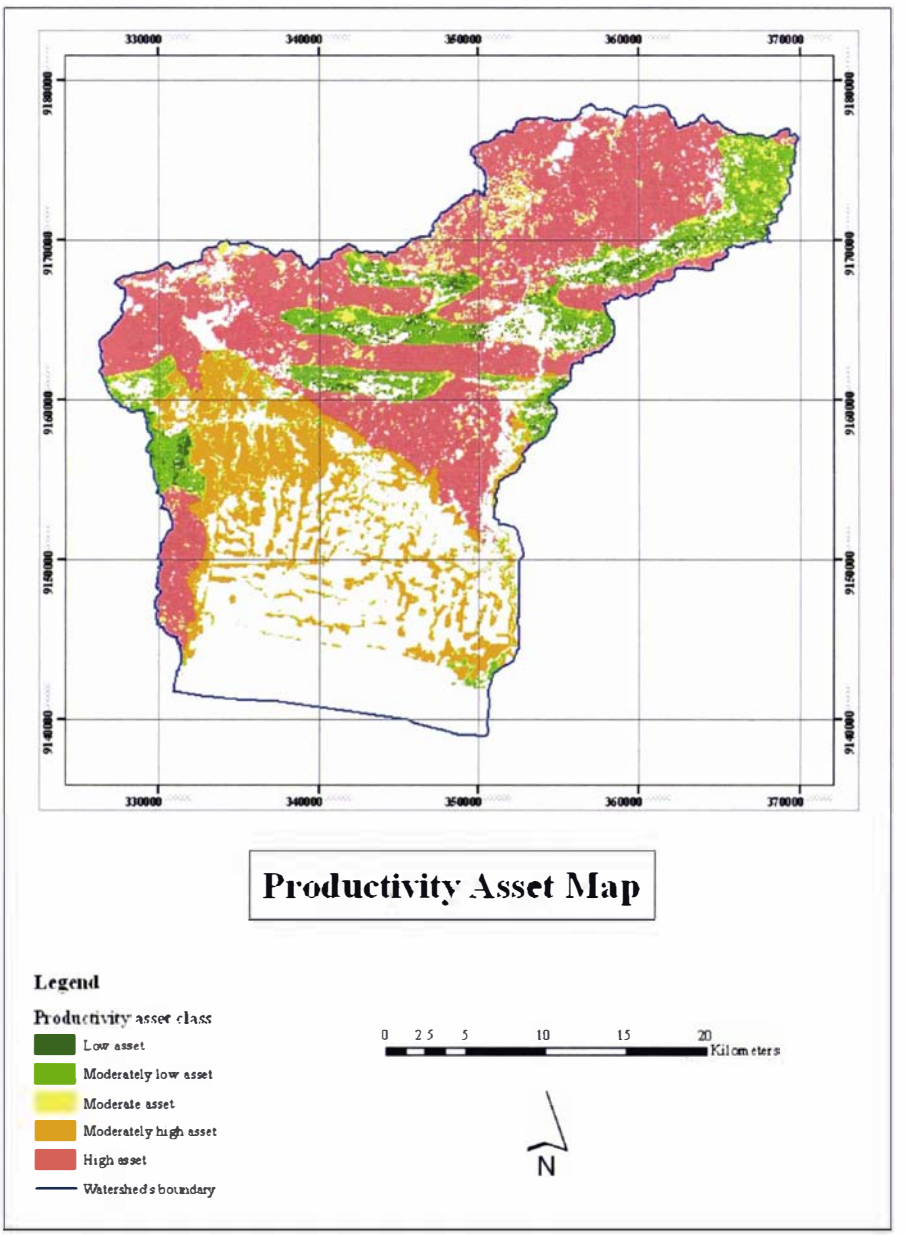

Figure 5-17 The distribution of productivity asset classes in the study area

5.5.4.2 Environmental Sensitivity

The soil database from South Java Flood Control Sector Project (SJFCSP, 2001) provided data on three different soil depths: top-soil, sub-soil, and effective soil depths. Top soil depth is the depth required for food crops production; while effective soil depth is that required by forest trees whose roots usually penetrate deeper to the ground. Due to the different requirements, effective soil depth and top soil depth were chosen to be used in this study. They were grouped according to the classification mentioned in Table 5-8 and the result of this combination can be seen in Figure 5-18.

Since the soil map used in this study was digitised from an existing 1:100000 soil map, the shapes of the water bodies were not the same as those maps derived from the imagery. Beaches and water bodies were not categorised as soil, so it was excluded from the analysis. This resulted in a different sized area that was categorised as 'no erosion' (villages, rice fields, cloud, shadows of cloud, water bodies and beach). It was larger than the previous analysis because of the addition of the beaches. With the addition of beaches, areas which were excluded from the analysis became 39% from previously 30% without beaches.

The map in Figure 5-18 showed that 49% of the study area has moderately low class of erosion sensitivity (more than 30% of low class of erosion sensitivity is occupied by rice fields, which were excluded from the analysis). Although most of the study area only has moderately low erosion sensitivity, it does not mean that this area will not be eroded. It means that within the study area, 49% was less sensitive to erosion compared to the moderate and high erosion sensitivity land, which occupied 10%. This data layer was then used for evaluating the consequence to erosion.

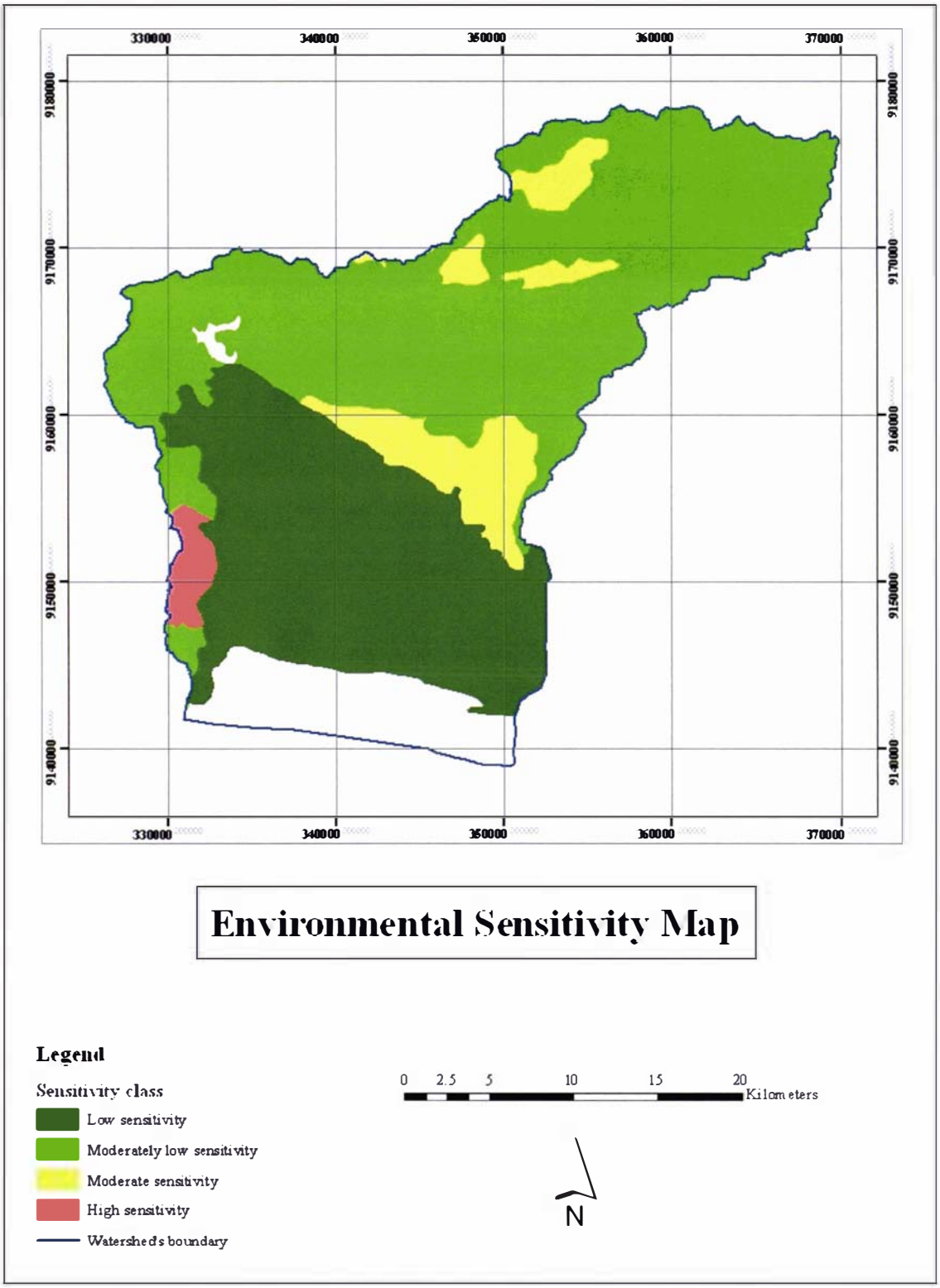

Figure 5-18 The distribution of environmental sensitivity to erosion as represented by soil depth

5.5.4.3 Productivity Consequence

Productivity consequence is a measure of the relative significance of the reduction in productive asset value arising from erosion. It is derived by combining the productivity asset value (Figure 5-17) with environmental sensitivity (Figure 5-18) (see flow chart in Figure 5-3) using the 2-D relationship shown in Figure 5-5. The productivity consequence will be realised if erosion is not controlled following logging.

Since most of the study area has only a moderately low sensitivity to erosion (49%), the productivity consequences of erosion in the logged areas are generally not severe. Fifty percent of the study area has moderately low (23%) and moderate (27%) productivity consequences if erosion is allowed to occur in the logged area. This means that 50% of the productivity consequence of the study area will be moderately low or moderately affected when the logged forest is eroded. Only two percent of the land gave high consequence because it had a high productivity asset, but in a high sensitive soil. Figure 5-19 shows the distribution of the productivity consequence of the study area.

5.5.4.4 Biodiversity Asset Value and Biodiversity Consequence

Biodiversity consequence is the consequence of biodiversity degradation in an area after logging. It was created by combining biodiversity asset value with environmental sensitivity. The biodiversity asset value was assessed on the basis of micro-organism activity in the soil, such as mulches or decayed plants, of the former land cover. This value is assumed to be depleted by the soil erosion process. Since we have no direct information on micro-organisms we use above-ground macro-biodiversity, as evidenced by land cover before the logging as a surrogate for the remaining below-ground micro-biodiversity that is left after logging.

Mixed forest was assigned the highest biodiversity class compared to the other land covers. This is due to the variety of trees planted in the mixed forest, which can support more diverse species. Monotype forest, however, while it supports more micro-organism activity than open land, does not support as much as mixed forest. Therefore mixed forest has the highest, monotype forest moderate, and open land the lowest biodiversity asset value. The distribution of these asset values is presented in Figure 5-20.

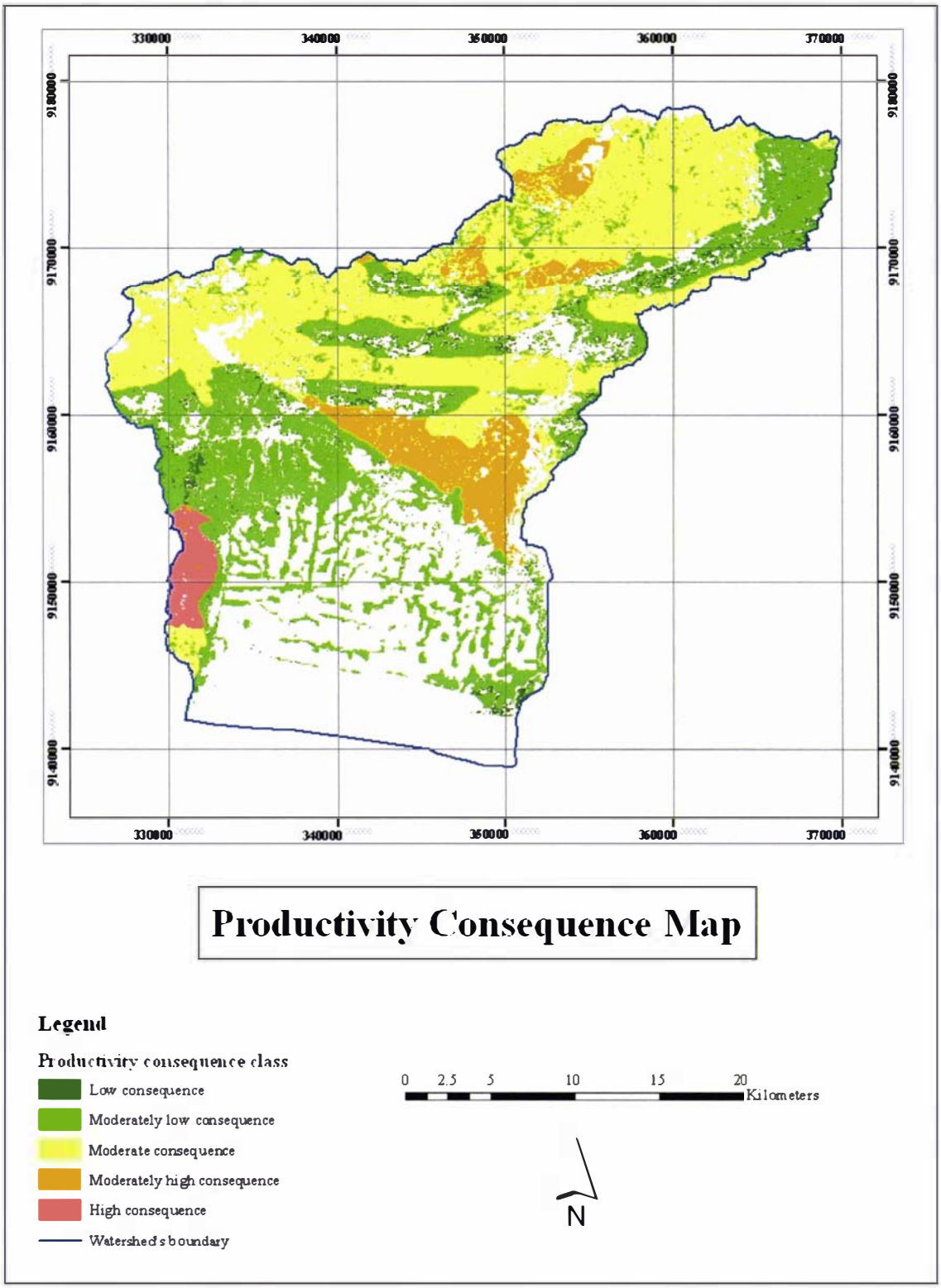

Figure 5-19 The distribution of productivity consequence classes in the study area

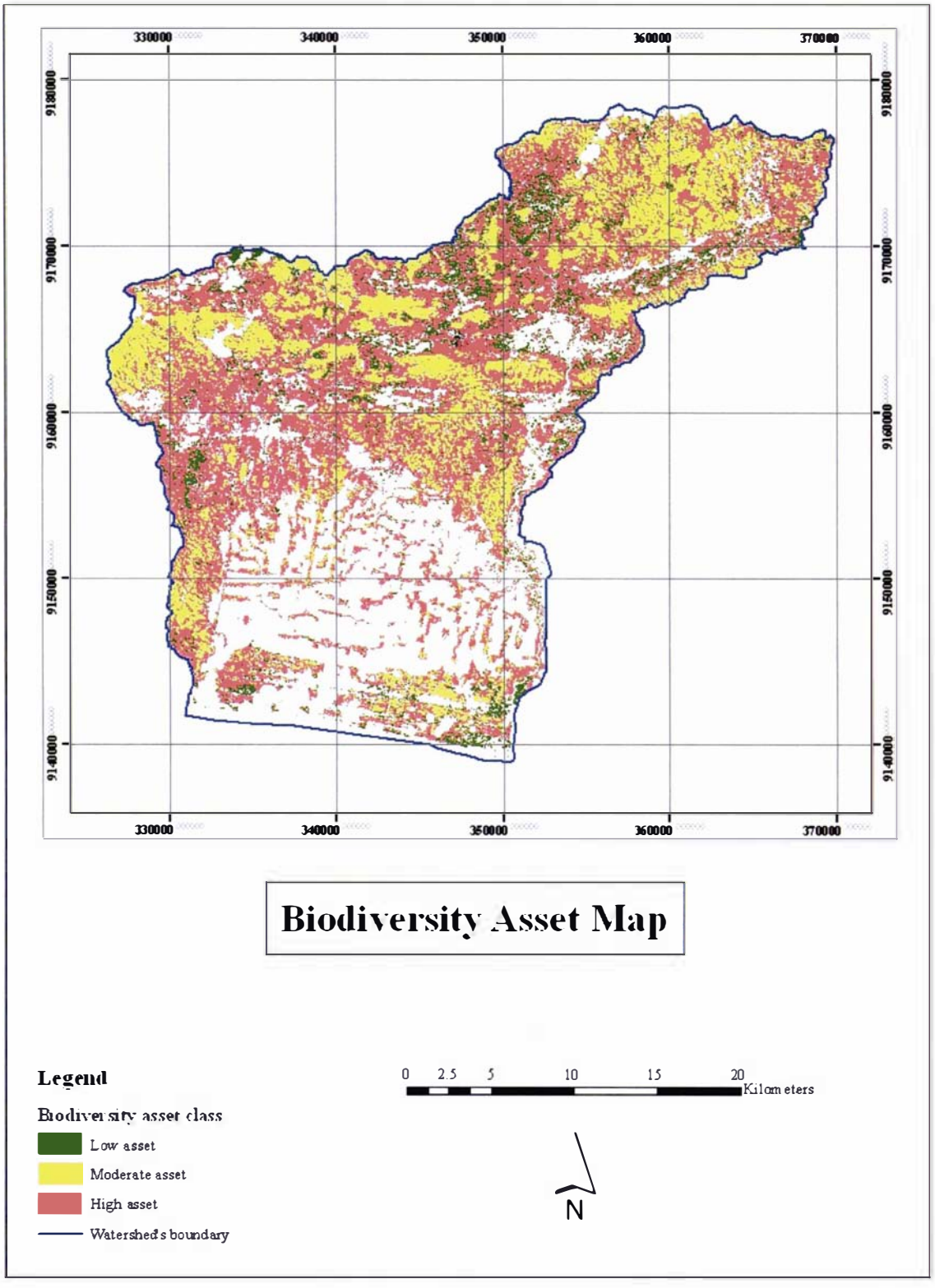

Figure 5-20 The distribution of biodiversity asset classes in the study area

Combining the biodiversity asset value with environmental sensitivity gives the consequence for biodiversity following erosion in the logging area. Biodiversity consequence is created using the 2-D relationship shown in Figure 5-5, and the result is presented in Figure 5-21.

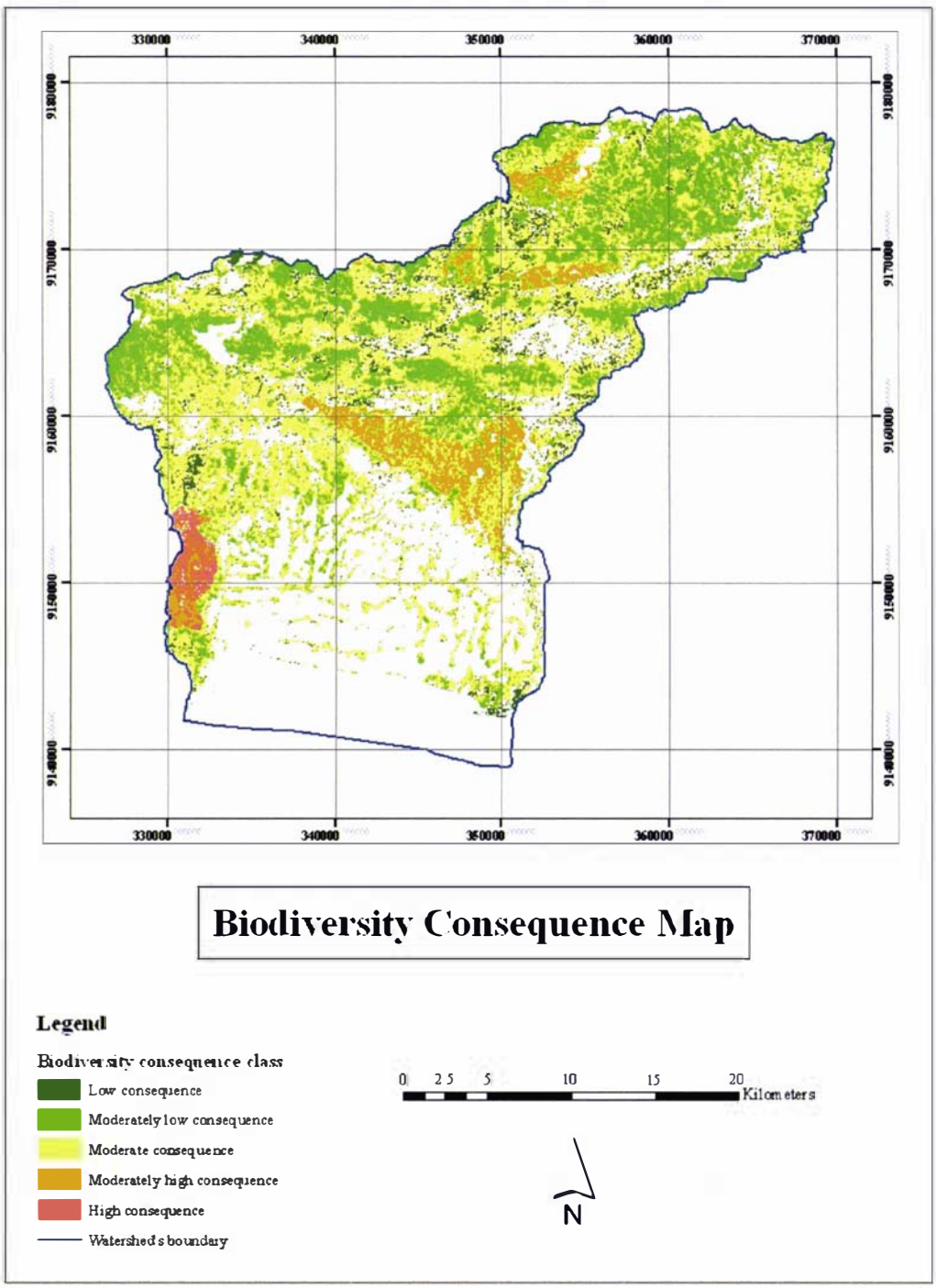

Figure 5-21 The distribution of biodiversity consequence classes in the study area

While the largest biodiversity consequence class was moderate consequence (33%), in total 50% of the study area had a biodiversity consequence that was either moderately low or moderate, the same as with the productivity consequence (Figure 5-19).

5.5.4.5 Consequence

The final consequence for this study area was derived from combining the potential productivity consequence and biodiversity consequence. Since a higher class of consequence will give higher risk, then combining both consequences used the worse scenario. Within both consequences, the higher class is kept, whether it was productivity or biodiversity consequences. The result of the combination is shown in Figure 5-22, while in Table 5-16 the area (ha) and percentage of all consequences are presented.

Table 5-16 Total area (ha) and percentage of each erosion consequence class in the study area

Erosion consequence class	**Productivity consequence**	**Biodiversity consequence**	**Total consequence**
		Area in ha (%)	
Low consequence to erosion (1)	2547.8 (3)	4620.5 (5)	2571.1 (3)
Moderately low consequence to erosion (2)	20647.5 (23)	15194.4 (17)	5524.9 (6)
Moderate consequence to erosion (3)	24082.7 (26)	29152.7 (33)	39177.0 (43)
Moderately high consequence to erosion (4)	5657.2 (6)	4561.6 (5)	5660.9 (6)
High consequence to erosion (5)	1366.4 (2)	772.3 (<1)	1367.7 (2)
No consequence to erosion	34250.0 (30)	34250.0 (30)	34250.0 (30)
TOTAL	88551.6 (100)	88551.6 (100)	88551.6 (100)

From Figure 5-22 it can be seen that most of the study area is dominated by moderate consequences (43%). The moderately low consequence class (6%) was smaller than both productivity and biodiversity consequences (23 and 17% respectively). This situation happened because the productivity and biodiversity consequences might not be

located in the same place. Therefore the moderately low productivity consequence might have moderate biodiversity consequence or vice versa.

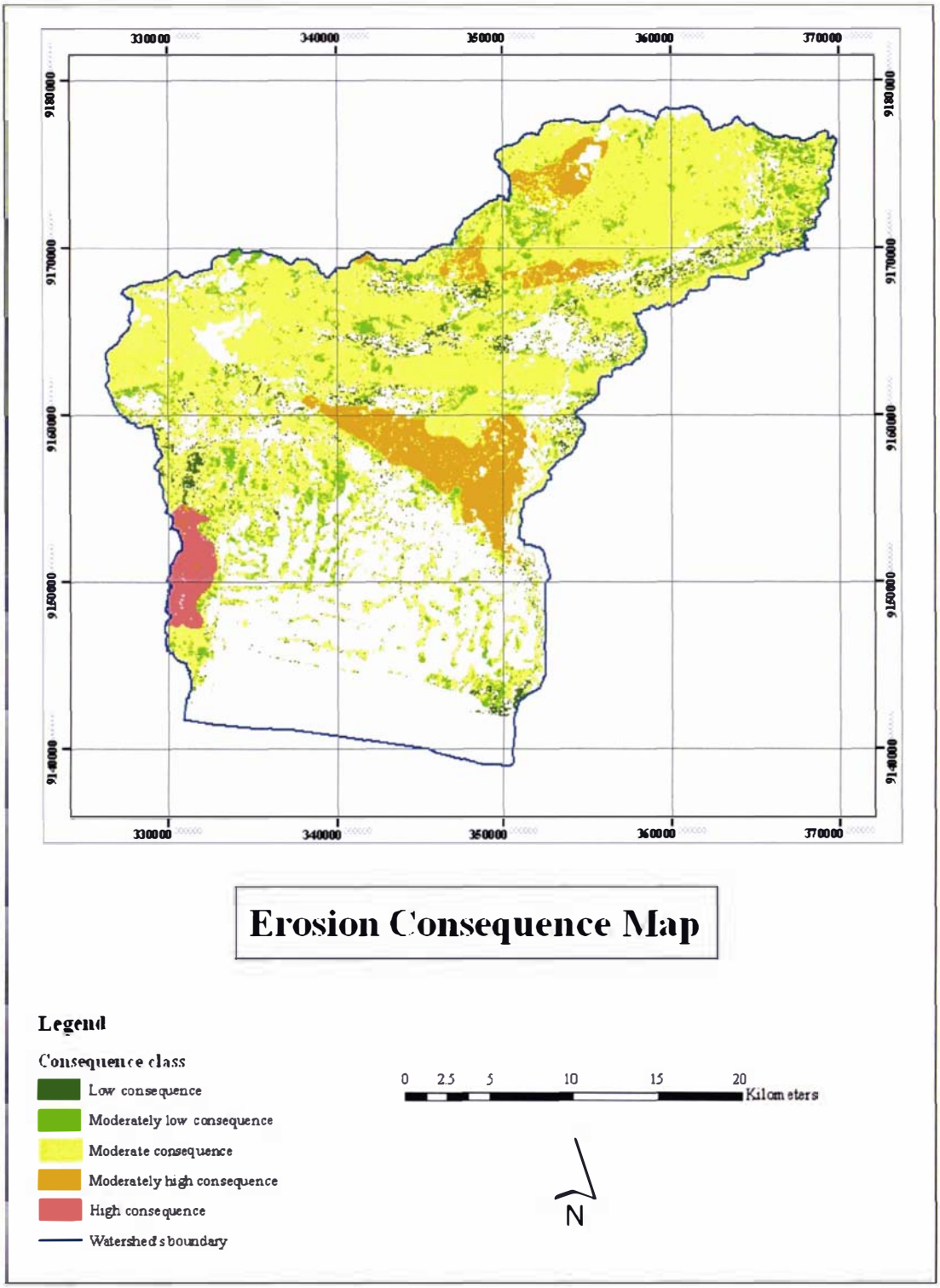

Figure 5-22 The distribution of erosion consequence classes in the study area

5.5.5 Erosion Risk

The usual erosion risk analyses only predict erosion through overlaying erosion factors such as rainfall, slope, soil and land cover. This predicts the likelihood of erosion, but erosion risk analysis needs more information than just four erosion factors. The risk analysis used here also derives the consequences following erosion, which are measures of the system and its ability continue to sustain the current land uses. The greater the consequence then the greater the risk to future use as well.

The erosion risk information is important when making decisions about managing natural resources (MacEwan *et al.*, 2004a); in this study the issue is logging the production forest. The decision makers have to be informed not only of the potential or likelihood of erosion, but also the risk when erosion occurs after logging is performed. Using this information, the decision makers are able to choose whether the logging is continued with conservation activities to reduce erosion, or the logging is totally cancelled due to unacceptably high risks.

The likelihood of erosion in this study area was mostly moderately high and high (see Table 5-14 and Figure 5-15). This situation shows that when the forest is logged, more than 60% of the study area will have moderately high or high erosion likelihood. Since the consequence of erosion happening in the logged area will have predominantly moderately low (36% of the total study area) or moderate (44% of the total study area) consequences, the risk is in effect lessened.

The erosion risk data layer produced combining erosion likelihood and consequences using a 2-D relationship, is presented in Figure 5-23. The high risk area occupied only 5% of the total study area on land which was formerly mixed and monotype forest. This land had a high risk because it had a high asset value, which means it has a potentially high productivity, but has a sensitive soil. Therefore when these areas are logged, without the implementation of soil conservation measures, they will degrade easily, and the high productivity potential in these areas will be depleted or lost.

To know the distribution of each erosion risk class on the existing land cover, the risk map was then overlaid on land cover map. The results are presented in Table 5-17.

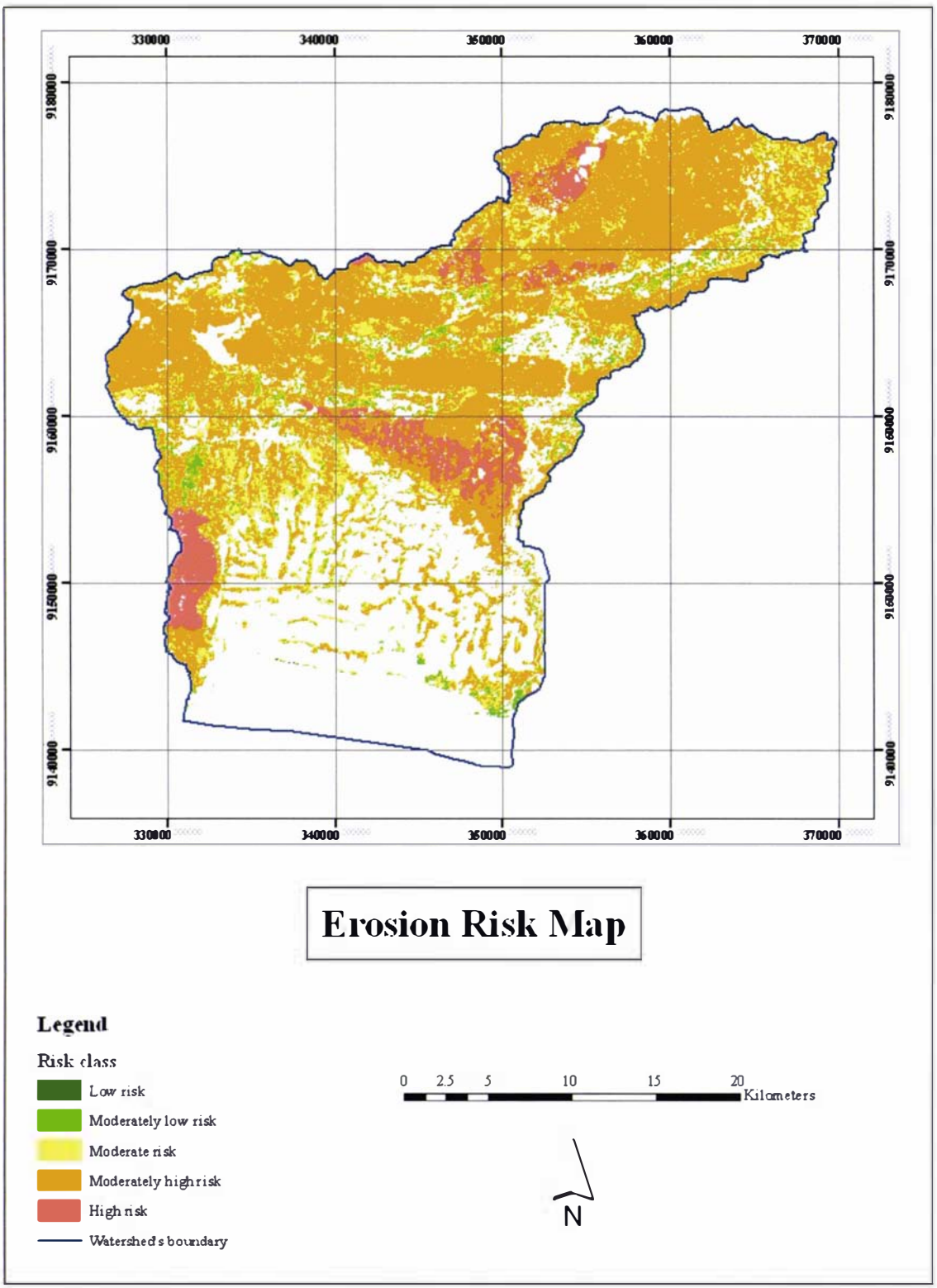

Figure 5-23 The erosion risk class distribution in the study area

Table 5-17 Erosion risk class for each land cover in hectares (number in the brackets show the percentage)

Land cover	Low risk	Moderately low	Moderate risk	Moderately high	High risk	No risk	Total
Open land	5.7 (0)	2119.3 (2)	2050.1 (2)	569.9 (1)	15.1 (0)	1209.8 (2)	5969.9 (7)
Mixed forest	-	33.8 (0)	2335.3 (3)	27989.4 (32)	3092.3 (3)	4228.5 (5)	37679.3 (43)
Forest	-	523.2 (1)	3053.9 (3)	11212.2 (12)	1204.4 (2)	2170.7 (2)	18261.4 (20)
Rice field and villages	-	-	-	-	-	26641.0 (30)	26641.0 (30)
Total	5.7 (0)	2776.3 (3)	7436.3 (8)	39771.5 (45)	4311.8 (5)	34250.0 (39)	88551.6 100

5.6 Implications

The technique for predicting erosion risk in this study is designed for forest managers to help them in preparing a logging management plan in a sustainable way. Information about the potential risk and the consequence is an important consideration when planning logging activities. Areas with high risk need more careful planning (and logging) than lower risk areas.

This method was carried out in a production forest in Java, which usually has more data available than outside Java. If the method was to be used to analyse erosion risk outside Java or even outside Indonesia, some adjustments to the classes of each factor would have to be made. This is because the general condition such as elevation (that affects slope and aspect), rainfall, geological type, land cover (that also affects productivity and biodiversity) might be different to the classes given in this study. To solve this problem, the planners and decision makers have to redesign the classes according to the local conditions but still keep the 'low', 'moderate', and 'high' definition for each class. In the future, it is suggested that this method be accompanied by lists of possibilities for every factor with each class. Such a list will help the decision makers and planners to use the method more easily.

Two important issues need addressing as a result of using this analysis for predicting the erosion risk. They are: improvement of the available information, and suggested logging method. Dealing with these two issues will help the forest manager to manage the forest more sustainably.

5.6.1 Improvement of Available Data

The risk area is dependent on the erosion likelihood and the consequence faced if erosion is permitted to happen. Land cover was one of the important factors used for both predicting the likelihood and assessing the consequence. Land cover maps derived from imagery classification, such as this study, are sufficient to predict erosion likelihood. However, for the consequence analysis, this map needs to be more detailed with tree species, since each tree species has its own productivity and biodiversity asset values. A more detailed land cover map for consequence analysis should be collected from higher resolution imagery and/or ground cover survey.

Another important suggestion is to assess biodiversity asset class for each tree species in each land cover. This information is also important since data like this is usually not available. The biodiversity asset in this study is the presence of micro-organisms living in the soil and mulches, which will disappear when the trees are logged.

Soil fertility, as one of the factors that determine potential productivity, is important information that should be made available as well. This information could be gathered by doing soil surveys and refining the available soil map. By having more comprehensive soil and land cover data, this analysis will be more accurate.

The recovery time is the time needed by soil to recover after logging activity. Every type of forest species needs different recovery time because it depends on the activity of the ground cover and the growth of the tree canopy as well. This information is also important because it will show when and how long the critical time will be after logging. By plotting the erosion risk class versus logging time, a risk chart is able to be drawn. Each tree species should have its own chart, and using this risk chart, soil conservation measures could be planned and implemented.

5.6.2 Suggested Logging Method

The clear cutting method applied by Perum Perhutani needs to be studied more, especially for areas with high erosion risk. Strip logging along the contour line is an alternative method for high risk areas. This is supported by Ziemer (1986) who said that when logging the forest in blocks, the un-logged blocks will become the buffers for the logged one, although this phenomenon still needs more studies as well.

There are other considerations in proposing strip logging. The width of the strip should be big enough for the tree to fall without destroying other strips. A tree height gap is adequate for a strip. When the slope is not a hindrance, a wider gap such as twice of tree height gap is convenient for logging, but when the slope is steep and a tree height gap is too risky then the gap has to be decreased.

The second consideration is soil depth. If the soil depth is already limited, soil loss during logging has to be addressed carefully. The strip next to the logged strip has to be able to trap the eroded material as much as possible. This strip has to be prepared by planting ground cover, especially for forests with no ground cover, long enough to make sure that the ground cover is ready to trap the eroded material during and after logging. Therefore planting ground covers should be added into the logging preparation, especially for areas where the soil sensitivity is high or moderately high.

The third concern is the order of the blocks to be logged. If the block is wide enough to make more than two strips, the third or fourth strip should be cut after the first strip is logged. This gives time for the eroded material which trapped in the second strip to settle down before it is logged. It is also suggested that logging start from the bottom of the slope and continue up-slope. Carrying out this method will also give time for the eroded material to be undisturbed for the next logging. If the block is not wide enough to make more than two strips, then the strip should be modified with a checker board pattern and the next logged area will be diagonal to the previously logged area.

According to the study done by Priyono & Savitri (1998) any erosion under the pine forest due to logging needed three years before it was under the class of tolerable erosion since it was logged. This is due more to the ground cover effectiveness than the canopy of the trees themselves (Kusumandari & Mitchell, 1997). It means that after three years the logged area is able to become an erosion buffer for its neighbouring

blocks which will be logged. This is another consideration to be included in the harvesting plan.

The determination of next species to be planted after logging needs more consideration. It is not only just matching plant requirement and land capability. Other considerations are soil sensitivity and the cumulative risk. When the soil sensitivity is high then the species chosen should be a combination of trees and cover crop that have the ability to reduce erosion risk quickly. Areas of high soil sensitivity also need a longer cycle species to give the soil the opportunity to recover after the last logging (Huth & Ditzer, 2001). In addition, fast growing species in a highly sensitive soil will only aggravate the soil condition.

5.7 Conclusion

From the erosion analysis done in this study, there are some main points to be highlighted. The first point is that, although erosion susceptibility in the forest is small to negligible, it does not mean that there will be no erosion risk when the forest is logged. Logging is one of the un-avoidable activities in the production forest that causes erosion, and to address this problem properly the forest managers and decision-makers should be well-informed about erosion and its effect on the environment.

The second point is that this method is robust enough to be used not only in the plantation forest in Java, but also outside Java, or even outside Indonesia with some adjustment in the given classes according to the local conditions. For the unavailable data, the planners and decision makers have to surrogate these from the available data.

Since this method is a prediction and the value for each erosion factor is qualitative, the result is only an indication of where erosion is likely to happen. Although it results in only medium-scale information, nevertheless this is needed by the managers and decision makers. They could use this information to make more sustainable logging plans.

For the predicted erosion there was almost no data taken straight from the field. Most of the information was derived from secondary data such as the Landsat image,

topographical maps, and soil maps. The only primary data was daily rainfall data. When available, more detailed maps, especially soil maps, will improve the prediction.

Until now soil conservation measures have been proposed according to soil prediction or erosion likelihood without considering the relative consequences of the erosion if it is allowed to happen. Knowing the consequence of erosion will lead to understanding the risk if erosion is let to happen. This information is important for the decision makers to decide whether a production forest will be logged or left standing due to high risk.

The method to predict erosion risk in this study used the minimum dataset that is usually available in Indonesia. Although it used a minimum dataset, the result is very useful for the decision makers and forest planners in planning soil conservation measures from erosion risk. Using already available data makes this method easy to be implemented by forestry companies.

Since Indonesia set a very risky threshold for removing forest from a watershed (Section 5.2 compared to Section 5.3.4), the rainfall threshold for this method has to be made lower than the usual threshold value. Using the wet and dry month ratio meant that the rainfall threshold was probably lower than the heavy rainfall or erosive rainfall indicators, but it was also based on Indonesian conditions and always available.

Using this analysis, it was found that 45% of the study area has moderately high risk from erosion, and these areas were under mixed forest (32%) and forest (12%). The land with a moderate erosion risk (8%) was under mixed forest (3%), forest (3%) and open land (2%). Since mixed forest and forest had a moderately high risk, a proper logging plan accompanied by soil conservation measures should be prepared before the forest in the study area is logged.

SCALING ISSUES

6.1 Introduction

The use of images as auxiliary data for predicting erosion has already been described in Chapter 5. Since aerial photographs are commonly used, especially by Perum Perhutani, for forest planning and monitoring, this is a good opportunity to compare and analyze the difference between results for Landsat images and aerial photographs.

It is already understood that different scales result in different levels of informational detail. This is a problem when the data collected are different to the previously available information. There may be aggregation, dis-aggregation, extrapolation, or interpolation to be done, and it is believed that any of these would imply a change in the model/measurement scale (Bloschl, 1999).

Since Perum Perhutani is still using aerial photos as its input as well as satellite images, it is pertinent to examine the possibility of different outcomes resulting from the different scales of Landsat images (30 metres resolution) and aerial photographs (1:20000). Comparing the analysis at different scales is necessary to see the robustness of the method described in Chapter 5.

Perum Perhutani is a State Forest Company in Indonesia that was given authority to manage forests in Java and some areas beyond Java. For forest management planning, Perum Perhutani generates several maps with different scales for different purposes in different offices. It uses at least four different map scales: the working map (1:10000) used by the planners in the sub-district level; the rotation map (1:25000) used by forest planners in the district level, the production map (1:100000) is used by provincial level planners, and the monitoring map (1:250000) used by the head office's planners (Sadhardjo Siswomartana, 2005).

The working map is derived from terrestrial field measurement. It contains information about the compartment, sub-compartment and sub-sub-compartment (if any) numbers, planting year, planting species, and forest type. The working map is regularly cross-checked with aerial photos to update the database.

The forest planners in the sub-district level have to plan forest management activities (such as planting, thinning, pruning, or logging) each year using the working map. Each year this map is updated according to the activities done. The extent of a working map is often different to the extent of administrative map, because administrative and forest boundaries are different. Therefore the working map usually covers more than one sub-district. Sometimes within one working map there are several forest species with different life cycles.

The rotation map is created from the working map, aerial photos and topographic maps. It is used by the forest district planners for planning the logging rotation which maintains the sustainability of each forest species. Each rotation map consists of several working maps covering 4000 – 8000 ha. The planners have to differentiate the logging rotation according to the life cycle of each tree species.

The rotation map usually has one or two dominant forest species as the main source of targeted income, with some minor species. This map is updated every five years unless there is a significant change within that period of time such as illegal logging or forest fire that destroys quite a significant area.

The production map is generated from the rotation map. This map is held in the provincial office to forecast and calculate forest production for 25 years. Using this map the planners at the provincial level set a targeted income for each district to achieve. This map is also used as a guideline for rotation and working maps, especially when there is a species change due to a certain policy.

The monitoring map is used by the head office to roughly predict the forest production trend and forest area left each year. This map is generated using satellite image and is used by the decision makers to make policies corresponding to the current forest condition. In a critical situation, the decision drawn from this map can change the forest species, undoing a policy which was decided previously in the production map.

By understanding the way Perum Perhutani develops forest planning, it can be seen that Landsat imagery is used as support information in the head office, while the aerial photos add information to working maps as well as rotation and production maps. The advantage of using Landsat images in head office is that the decision makers are able to determine the areas prone to erosion. They can then regulate those areas with specific

treatments before the logging has to be carried out. Approaches such as using strip logging instead of clear cutting, or employing soil conservation measures need to be added in those areas along with the normal management. If the head office management is aware of the erosion problems, they will anticipate lesser profits compared to other areas without problems.

The purpose of this chapter is to understand the different results gained from aerial photos compared to Landsat images. By understanding the differences, the method described in Chapter 5 might need adjustments.

6.2 Scale Issues

Analysing digital maps or images at different scales is not as difficult as doing the same thing with hard copies. Although it is not as difficult, nevertheless the problem of different information gathered at different scales still persists. The planners and decision makers have to be aware of this issue. To a decision maker, generalizations associated with scales can lead to the obscuring of information vital to a correct decision, especially when the information must be integrated from different sources (Goodchild & Quattrochi, 1996).

Since collecting data is the costly part within a project, this sometimes becomes a hindrance in deciding the scale of observation. It is then often largely outside the control of the scientists, who usually have already designed a particular data collection for entirely different or generic purposes (Goodchild & Quattrochi, 1996). When this happens, compromise is the only solution as long as the main objective of the project is not changed.

Bloschl (1999) acknowledged three factors that influence scale: spacing, extent and support. Spacing refers to the distance between samples, which is the pixel size of an image. Extent is the overall coverage of the data and refers to the overall size of the image, while support means the footprint of the sensor, sometimes called grain. It often is similar to pixel size, but is not necessarily identical. Support is responsible for the appearance of the map. Changing the size of the support can make the map look smoother or coarser.

Furthermore, Bloschl mentioned that spacing is an important factor in the analysis. If the data collection is too widely spaced for the process scale, the small-scale variability will not be captured, or will appear as noise. This fact should also be kept in mind when combining images with different spacing or resolution.

With the progress in technology, people need more opportunity to analyse data with multiple scales. Therefore the tools or techniques developed should cater for the ability to operate at multiple scales, to work with data whose scales are not necessarily ideal, and to produce results that can be aggregated or disaggregated in ways that suit the decision-making process (Goodchild & Quattrochi, 1996).

In a slope map derived from a DEM, its spacing or pixel size affects the level of slope detail. This also influences the areal extent of each slope class. The coarser the pixel size, the more detail in the slope is lost (Hancock, 2005). From his study, Hancock found that within a catchment, the hillslope detail was lost with a pixel size greater than 10 metres, although some information still could be gathered from a DEM at larger pixel size.

Zhang *et al.* (1999) also found that slope derived from DEMs with various spatial resolutions gave a different level of detail too. Using high resolution DEMs will result in high slope values, but slopes are under-estimated when using coarse resolution DEMs. This means that choosing the resolution for a DEM is crucial, because the accuracy of slope values depends greatly on the DEM. This is especially so when using slopes for soil erosion modelling.

Analogous to the slope affected by scales, soil variability is also influenced by scales (Lin *et al.*, 2005). Soil mapping typically divides the soil into map units. This map unit is based initially on aerial photo-interpretation of factors that influence soil development, such as landform and vegetation cover. Within each map unit the soil is relatively homogeneous. When the scale is increased the homogeneity of each map unit in the previous scale can be changed. For example, from the position of soil in the hillslope, the A-horizon thickness can show apparent differences at the 1:1000 scale. The bottom of the slope tends to have the thickest A-horizon, while the summit has the least (Lin *et al.*, 2005). Unfortunately this looks the same in a smaller scale. This condition is due presumably to erosion and deposition activities. Knowing this

phenomenon, a small-scale soil map could be made more detailed by differentiating soils according to the position on the hillslope.

Environmental ecosystems are another factor largely influenced by scale. This is because they are very heterogeneous due to the climatic variation, environmental disturbance and edaphic properties (Pickett & Cadenasso, 1995). This heterogeneity gives information on a small scale map which cannot easily be seen in larger areas, or vice versa (Bugmann *et al.*, 2000). The interpolation and extrapolation of the information should be done carefully since the ecosystem cannot be averaged.

Scale also affects the prediction of the rate of soil erosion and sediment transport processes (Kirkby *et al.*, 1996). Usually erosion is predicted using field scale or catchment scale models. There is no essential difference between both models in terms of general physical processes of erosion (Jetten *et al.*, 1999) but the dominant patterns and processes at each scale are different (Kirkby *et al.*, 1996).

Kirkby *et al.* found different important factors at each scale. At the field scale the important factors are the timing and volume of overland flow hydrographs. This model is generally for a small area within a short period of time (one to a few storms). At the catchment scale, topography, soil, and vegetation pattern are important factors. This model is used by the decision makers most of the time. For the coarser, national to global scale, climate and lithology are the critical parameters. Understanding the important parameters for each scale will help the researchers in focusing data gathering according to the scales they work on.

On the other hand, Amore *et al.* (2004) found that USLE (Universal Soil Loss Equation) and WEPP (Watershed Erosion Prediction Project) are not sensitive to the different sizes of hillslopes. A finer detail of a catchment does not improve the model's capability of predicting erosion although it is useful in developing an erosion model.

Often the data used for the erosion analysis in both field scale or catchment scale have been derived from a limited amount of field data followed by some assumptions, especially in areas that were difficult to access. When such data are implemented into the catchment scale model, there might be error propagation, particularly spatial error, which draws the result to an inaccurate conclusion. This is the reason why a catchment model should be calibrated before it is applied. Although catchment scale models need

time to be calibrated, they are good in dealing with heterogeneous catchments (Jetten *et al.*, 1999).

6.3 Description of Location

For the purpose of analysis, a location inside the study area was chosen. The location needed to be covered by the aerial photos and have some land cover varieties that were recognized easily. The chosen area consists of two sub-watersheds located next to each other in the upper part of the Luk Ulo – Telomoyo watershed (Figure 6-1). Binangun (757.7 ha) has four streams running into its main river. They are the Jlegong, Drawanganti, Penawangan and Kunir streams. Kedung Tangkil (510.5 ha) has at least two streams that run into its main river. Binangun and Kedung Tangkil rivers are then joined at Somagede River which continues to the Telomoyo River. These two watersheds were chosen because they have forest, mixed forest, open land, villages and rice fields. Within this chapter the study area means the Binangun and Kedung Tangkil sub-watershed, not Luk Ulo – Telomoyo watershed anymore.

Each sub-watershed includes more than one village; Binangun sub-watershed contains the greater part of Binangun village, a part of Somagede and a little bit of Glontor village. Kedung Tangkil has a similar political composition containing parts of both Ginandong and Kenteng villages.

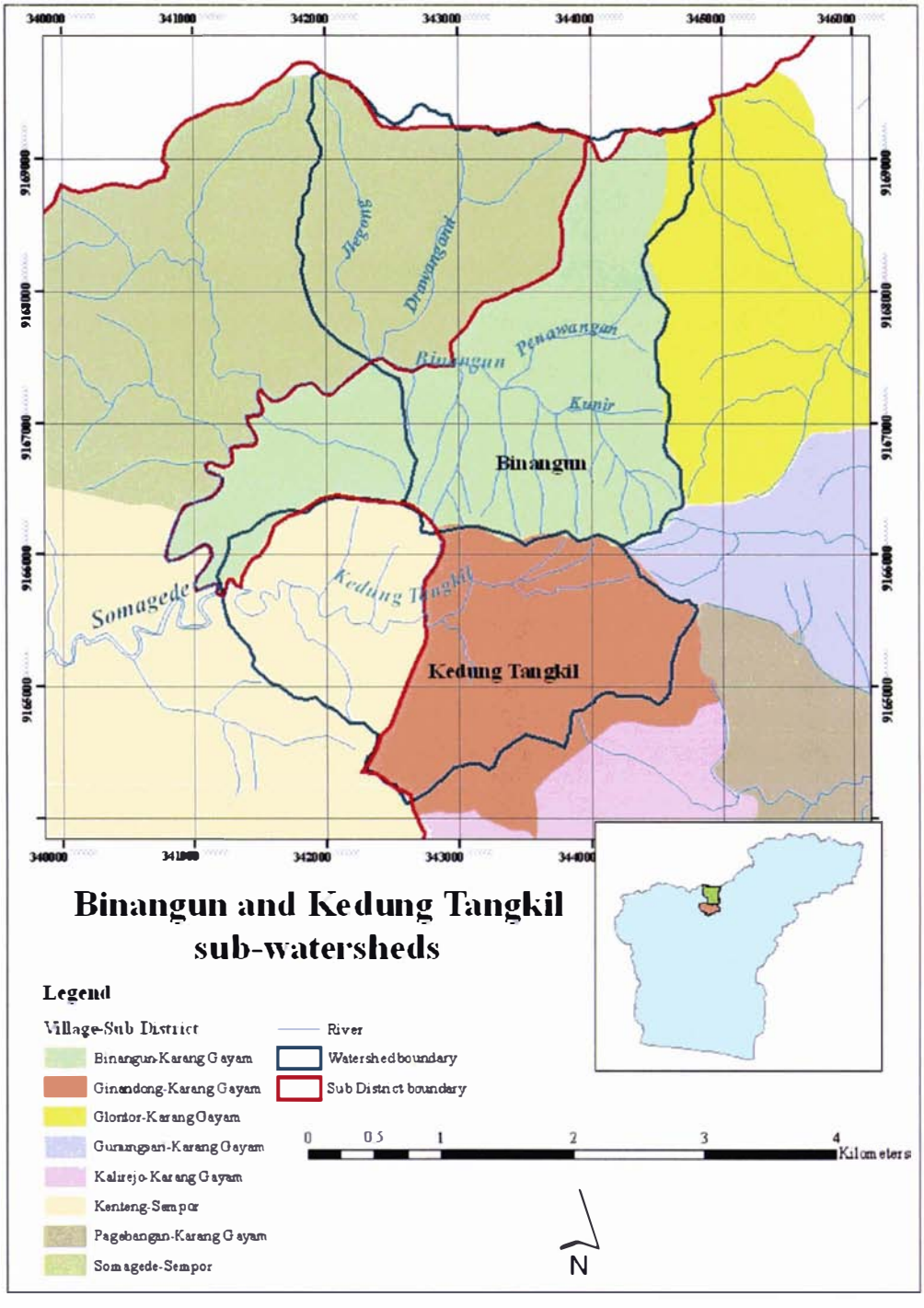

Figure 6-1 The Binangun and Kedung Tangkil sub-watersheds and their location in the Luk Ulo – Telomoyo watershed. The different watershed boundaries (in the upper part of the map) are because of different resolution of DEMs.

Since most watershed boundaries in Indonesia differ from the sub-district or village boundaries, watersheds can be difficult to manage properly. The issues related to boundary differences can make for inconsistency in watershed planning, because of

different district policies. For example, Binangun sub-watershed consists of two different sub-districts: Karang Gayam and Sempor. For Binangun sub-watershed to reduce the sediment yield in its river, soil conservation practices need to be done in both sub-districts. Village of Binangun is almost covered by the watershed. Furthermore because Binangun is in the upper part of the watershed, soil conservation practices in the village will significantly reduce sediment yield down stream. Soil conservation should be very high priority for the Binangun village authority. However, Somagede in the neighboring sub-district of Sempor, has a different situation. The sub-watershed only covers a small part of the village and has some other tributaries go to its river. Therefore, for Somagede, the sediment problem from two rivers (Jlegong and Drawanganti) is not as important issue as Binangun, and might not put these practices as the first priority of the village. If the rivers in Somagede but outside Binangun sub-watershed have another priority, it is likely that Somagede will stick to the plan influenced by those rivers. This situation is likely to lead inconsistent watershed management.

To make the management of Binangun and Kedung Tangkil sub-watersheds even more complicated, the forest in this area is under the management of Perum Perhutani which is located in Karanganyar, South Kedu compartment. Perum Perhutani also has their practices in managing the forest land, which might be different to sub-district and villages' practices for watershed management. This shows that within Binangun and Kedung Tangkil sub-watersheds there are many agencies having authority to manage the area.

6.4 Methodology

The method used to analyze erosion risk in this smaller study area is very similar to the procedure explained in Section 5.4 and Figures 5-2 and 5-3. When it was available, data of higher resolution was found that was appropriate for the smaller study area. These differences will now be explained, following the same sequence as in the methodology section Chapter 5.

6.4.1 Rainfall factor

While rainfall is affected by micro topography, no rainfall data was available to be able to model the behaviour of rainfall at any greater detail than was described in Section 5.4.1. So that rainfall data was used for the smaller study area.

6.4.2 Slope factor

A DEM was generated using all the 12.5 metre contours from the topographic data instead of only the 50 metre contours, as was used previously. The resolution of the DEM was chosen to match the scanned aerial photography and the technique used was the same as described in Section 5.4.2.

6.4.3 Geological factor

No greater detail geological data was available for the study area, and since geology tends to change relative slowly across the landscape this was thought not to be an issue, so the geology data described in Section 5.4.3 was used unchanged.

6.4.4 Land cover factor

The data used to derive land cover was completely different from that described in Section 5.4.4, though the same land cover classes were used. In place of satellite imagery, two aerial photos were used for this area: Run 24N, number 29 and Run 23F, number 16 from 5th July 1993. Further details of the aerial photos are described in Section 3.4. Fortunately, each photo covered one sub-watershed; Run 24N/29 covers Binangun, and Run 23F/16 covers Kedung Tangkil. These two photos were not mosaiced before the classification because the tone and texture for each photo was different and the image balancing wizard in ERMapper did not give sufficient correction to be useful. Since tonal differences affected the classification, the mosaic was assembled after the classification. Adjusting classified imagery is easier than balancing unclassified imagery.

The aerial photos were not topographically corrected, because the only available information was the date when the photo was taken and not the time. Therefore the

position of the sun when the photo was taken was not known. This means that the altitude and the solar azimuth angle cannot be determined sufficiently accurately.

The training areas for the supervised classification were villages, rice fields, open land, mixed forest, and pine forest. The symbol and colour used for each class were the same as those used for the satellite image analysis.

6.4.5 Environmental factors

Land cover, soil type and soil depth are required for the environmental consequence and sensitivity analyses. Land cover has been described in Section 6.4.4. Soil varies a great deal at the spatial scale of the aerial photography, but no additional soil data was available at any greater detail than was described in Section 5.4.5. Because of the particular importance of soil depth to the analysis a surrogate was needed that would provide additional spatial detail. While more detail for soil type would also have been useful, no surrogate was available. The surrogate that was chosen for soil depth was landform or position in the landscape.

Since landform information was not available for this study, position in the landscape, which is represented by slope class and altitude, was chosen. The erosion sensitivity class which is derived from soil depth is too general for this analysis. Following the statement of Lin *et al.* (2005) that the bottom of the slope has the thickest soil while the summit has the least, the soil depth was estimated according to its position in the terrain.

To divide the terrain position into summit, hillside and valley, slope and altitude classes were used to assist the division. Three altitudes were chosen to cover as much area of each slope class as possible; they were low, moderate, and high altitudes. The criteria for a summit are low to medium slopes but high altitude. The hillside is all high slopes and low to medium slopes at medium altitude, and the valley is all low to medium slopes at the low altitude. These combinations are presented in Figure 6-2.

High altitude	Summit	Summit	Hillside
Medium altitude	Hillside	Hillside	Hillside
Low altitude	Valley	Valley	Hillside
	Low slope	Medium slope	High slope

Figure 6-2 The combination of slope and altitude to model soil depth

The actual soil depths in the study area range from 100 to 140 cm (effective soil) with 10 to 20 cm top soil. From these combinations then soil depth for this study was classified into five classes:

- Class 5 with soil depth less than 100 cm
- Class 4 with 100 cm effective soil depth and 10 cm top soil
- Class 3 with 125 cm effective soil depth and 20 cm top soil
- Class 2 with 140 cm effective soil depth and 20 cm top soil
- Class 1 with soil depth deeper than 140 cm

Classes 1 and 5 were included in this classification since it is likely that in the study area there are soils that are shallower than 100 cm or deeper than 140 cm.

These soil depth classes were then assigned to the slope and elevation matrix (Figure 6-2). There are some assumptions in putting each soil depth class in the matrix. They are:

- Steeper summits have shallowest soils, because erosion will remove soil fastest and there is no deposition
- Other summits have shallow soils, because the soils will not be eroded so fast
- Hill sides have medium depth soils, because erosion will remove soil but there is also soil arriving from above, some of which will settle for short times as deposition

- Medium slope valleys will have deeper soils, because erosion will remove a very small amount of soil but there is also soil arriving from above much of which will settle as deposition
- Shallow to flat valleys will have deepest soils with relatively very little erosion, and most transported soil will accumulate as deposition

From those assumptions the soil depth division is presented in Figure 6-3, and the erosion sensitivity classes that follow are presented in Table 6-1.

High altitude	Summit Class 4	Summit Class 5	Hill side Class 4
Medium altitude	Hill side Class 3	Hill side Class 3	Hill side Class 4
Low altitude	Valley Class 1	Valley Class 2	Hill side Class 3
	Low slope	Medium slope	High slope

Figure 6-3 The new soil depth modelled from slope and altitude

After the analysis was done, the result was then compared with the result from the previous chapter to understand the different result given by different map scale. This information is important in choosing auxiliary data for predicting erosion risk.

Table 6-1 Soil erosion sensitivity class according to the soil depth in response to erosion

Soil erosion sensitivity class	**Soil depth (cm)**
High (5)	Soil depth less than 100 cm
Moderately high (4)	100 cm effective soil depth and 10 cm top soil
Moderate (3)	125 cm effective soil depth and 20 cm top soil
Moderately low (2)	140 cm effective soil depth and 20 cm top soil
Low (1)	soil depth deeper than 140 cm

6.5 Results and Discussion

6.5.1 Digital Elevation Model (DEM)

The DEM for this study was created using 12.5 metre interval contour lines and a pixel size of 1.69 meters. The pixel size was adjusted to the pixel size of the scanned photos which was 1.69 meters (see Section 3.4). Like the previous DEM generation, the DEM of this study area was made using TOPOGRID. It is presented in Figure 6-4a, while Figure 6-4b shows the DEM generated from 50 metre interval contour lines with 30 metre resolution (the same as Landsat resolution), which has been used for analysis in Chapter 5.

Since this DEM was more detailed, the watershed boundary of this study area was more detailed when compared to the Luk Ulo – Telomoyo study area. This is in line with the study done by Zhang *et al.* (1999) which said that the higher the DEM's resolution, the more detailed the DEM. This explains the different boundary between Luk Ulo – Telomoyo watershed and this study area (see Figure 6-1). Figure 6-4 shows the different level of detail (6-4a was more detailed than 6-4b) though in general these two DEMs have similar patterns.

With a more detailed DEM, the general soil depth information from a 1:100000 scale map is able to be remodelled according to its position in the slope.

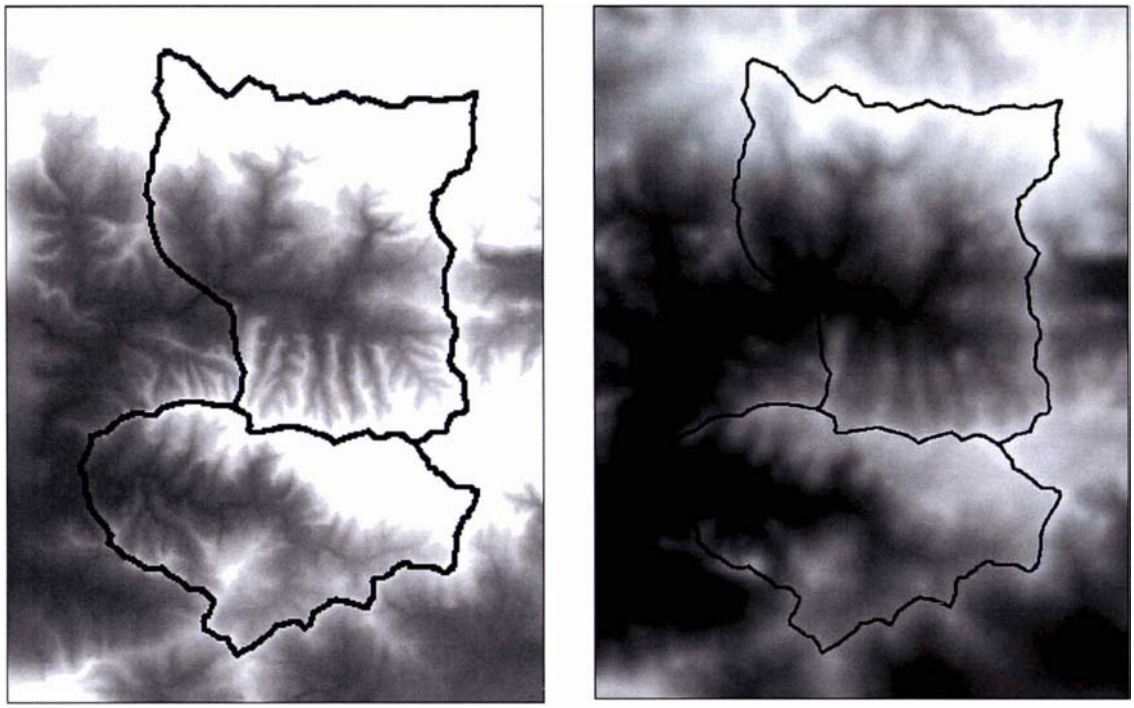

a b

Figure 6-4 DEMs generated from 12.5 metre contour data (a) and 50 metre contour data (b)

6.5.2 Aerial Photograph

The rectified aerial photos for both sub-watersheds are presented in Figure 6-5. Since the aerial photos were not topographically corrected, the result of the classification was much affected by the topographic factor, especially for areas in the hills.

Aerial photos are still a good resource for detailed information about forest cover (Smith, 1993). They are usually classified manually, using either pocket or mirror stereoscopes. Since visual interpretation is highly subjective and labour intensive (Coppin *et al.*, 2001), an attempt was made to classify the photos using supervised classification by employing the interpreter's knowledge in making training areas. Two primary factors will hinder an accurate classification outcome. These are lack of topographic correction and the inherent limitation of only having one spectral band in panchromatic imagery.

Land cover classification from the aerial photos was more difficult to do, in comparison to Landsat image, especially delineating the villages. Heterogeneous land covers such as villages surrounded by trees or open land with scattered trees were difficult to classify as either villages or open land. Usually they were classified as mixed forest. Figure 6-6 shows the appearance of a typical village in these aerial photos.

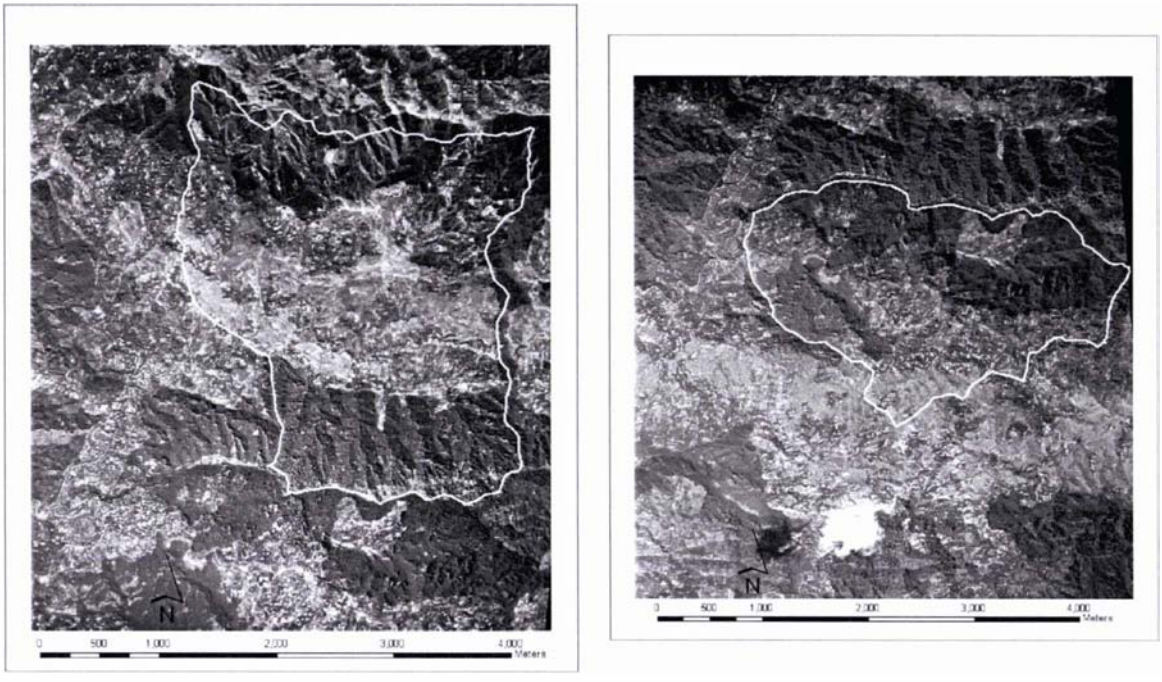

a b

Figure 6-5 The rectified aerial photo (a) Run 23F/16 with Binangun watershed's boundary and (b) Run 22N/29 with Kedung Tangkil watershed's boundary.

Due to the difficulty in separating villages from forest, especially in Run 23F (Binangun), the classification in this image was made in two passes. The first pass classified the following land covers: villages, rice field, open land, mixed forest and pine forest. The second pass was masking mixed and pine forests to further distinguish villages, rice fields and open land. The training areas were readjusted by deleting the mixed and pine forests and adding more training areas for these three land covers. By employing this step more villages and open land were captured.

Figure 6-6 A typical village (whitish colour) showing how it is built among trees for shelter. The darkest colour in the upper part of the photo is pine forest.

Since these two aerial photos (Run 22N and 23F) actually overlapped each other, the same training areas were used in the overlapped areas. From all training areas in Run 23F, pine forest occupied the smallest size, 13.8 ha (482,517 pixels), while mixed forest filled the largest area, 42.2 ha (1,475,524 pixels). Although the training area for villages occupied 41.3 ha (1,444,055 pixels) or 2% of the total area, nevertheless the classified map did not show many villages, especially in Run 23F (Binangun).

On the other hand, the largest training area in Run 22N (Kedung Tangkil) was pine forest (57.1 ha or 1,996,503 pixels) and the smallest was the mixed forest (7.9 ha or 276,223 pixels). The result of the classification is presented in Figure 6-7. The mosaic of both sub-watersheds is presented in Figure 6-8.

As shown in Figure 6-7, the classification results for each photo were slightly different, especially in the overlapping area. Run 22N gave too much pine forest and too little mixed forest, while Run 23F gave the opposite. This was not because Run 22N had relatively more pine trees in the training areas than did Run 23F, but actually Run 22N had more pine areas than Run 23F. Different tone and texture, especially at the edge of each photo make the difference more pronounced.

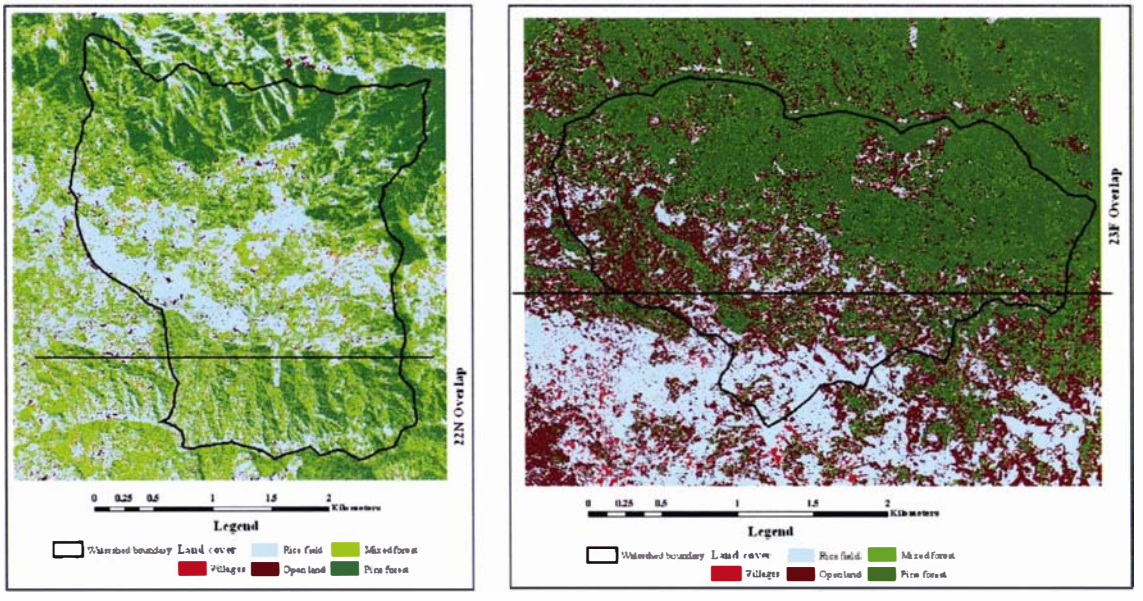

a b

Figure 6-7 The land cover classification derived from aerial photos. They are Run 23F (Binangun) (a) and Run 22N (Kedung Tangkil) (b). Black straight lines in the photos show the overlapped photos

According to Campbell (2002) each aerial photo has 50 – 60% overlap for each frame to minimize the effects of distortion made by the camera lens. This overlap is around the edge of each photo. When the edge of each photo is clipped leaving the middle part, the effect of distortion is lessened when the photos are joined. By applying this method, the problem of different textures due to distortion around the edge of the photos is minimized.

Tonal differences between the photos will still be present and these will result in different classification results that need to be addressed when the results are mozaiced. Run 22N over-classified pine forest. To correct this, pine forest in Run 22N was changed into mixed forest where Run 23F was mixed forest, but they remained as pine forest when Run 23F was pine forest.

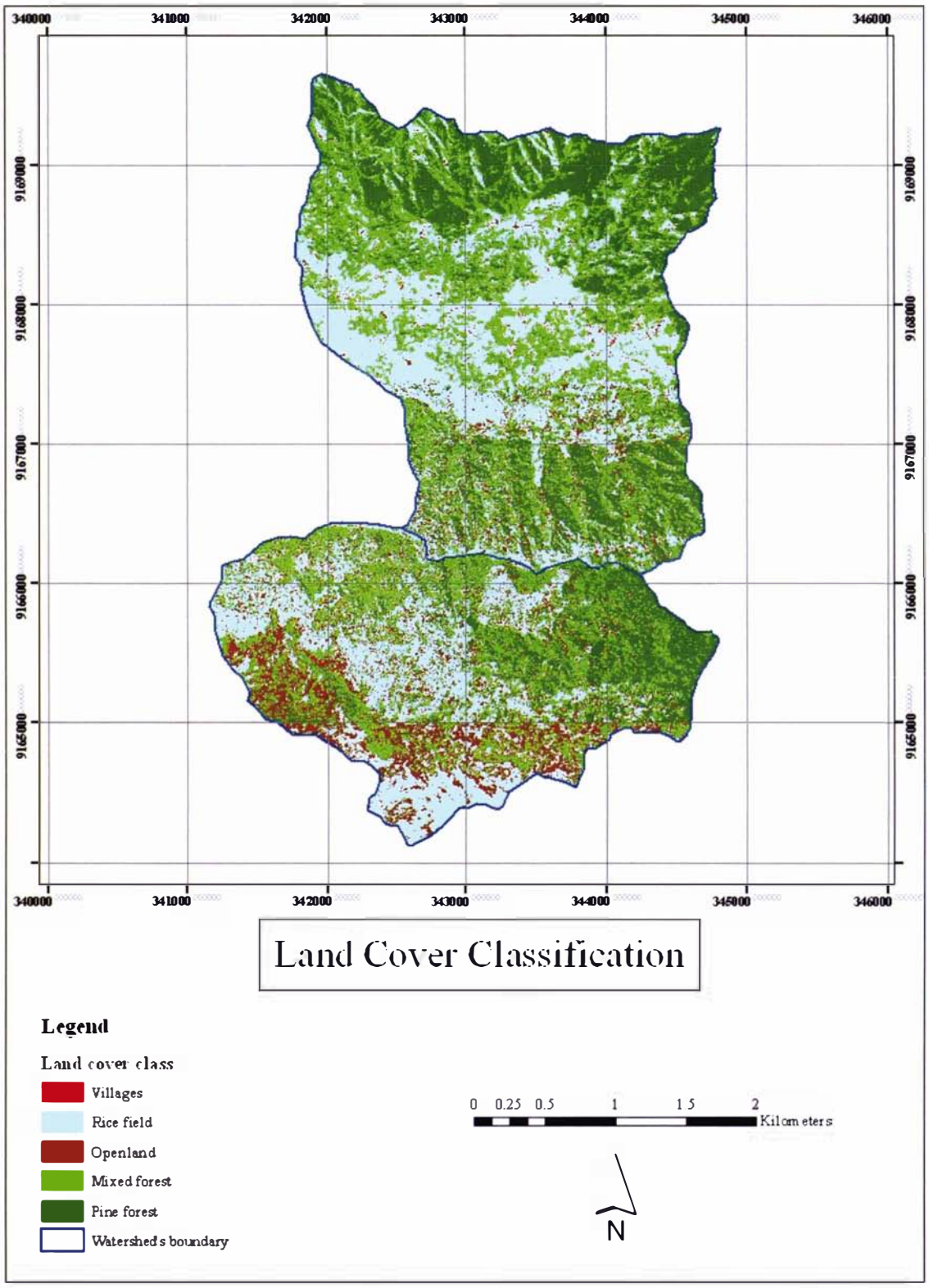

Figure 6-8 The distribution of land cover classification mosaicked from Runs 23F/16 and 22N/29.

The area (in ha and percentage) for each land cover across the watersheds is presented in Table 6-2. The pine forest spread out in the high altitude was mostly on the Binangun sub-watershed, while rice field occupied the lowest part of Binangun (around 150 meters a.s.l). In Kedung Tangkil, the rice fields occupied areas higher than Binangun (around 250 meters a.s.l). These rice fields were located on the southern part of Kedung Tangkil as rain-fed rice fields. At the time the photo was taken (July 1993), these rice fields looked more like open land.

Since there are difficulties in capturing villages due to the numbers of trees surrounding the houses, the total area of the villages is likely to be underestimated. In reality the area of the village for both sub-watersheds is probably more, but since it was difficult to separate the villages from mixed forest, some areas of the villages have probably been classified as mixed forest, leading to an overestimate in mixed forest area.

Even though the villages are underestimated and the mixed forest is overestimated, since the village in the topographical map showed small extent, the villages that were classified as mixed forest should not result in significant errors in the analysis.

Table 6-2 The land cover classification of Binangun and Kedung Tangkil sub-watersheds

Land cover type	**Area**	
	ha	**%**
Villages	35.9	3
Rice field	422.2	33
Open land	126.7	10
Mixed forest	330.5	26
Pine forest	352.9	28
Total	1268.2	100

The erosion prediction followed the flowchart presented in Figures 5-2 and 5-3. Land cover and slope data had 1.69 metre pixel resolution derived from aerial photo, while geology and rainfall pressure data had 30 metre resolution derived from Landsat imagery and then clipped to the study area (7.50^0 to 7.55^0S and 109.55^0 to 109.58^0 E).

The land cover data was derived from supervised classification of the aerial photo. Since the land cover was different, the environmental consequence of this area was different as well. The slope map was dissimilar to the previous analysis because it was derived from a higher resolution DEM, so it had more detail in it. The geology and rainfall pressure maps for this study were cut in the way already mentioned and then used straight away.

6.5.3 Erosion Susceptibility

The erosion susceptibility map was created by combining slope, geology and land cover maps. The criteria used to combine these maps were the same as in Section 5.4 and Figure 5-4. The slope map was derived from a high resolution DEM, the geology map was from Landsat image classification using RGB-531, and the land cover map was derived from the aerial photo. The contribution of slope, geology and land cover to erosion and the erosion susceptibility of the study area are shown in Figure 6-9.

As already discussed in Chapter 5, rice field and villages in this study were not included in the analysis because these land covers will never been cleared to the same extent as logged areas.

Figure 6-9 shows that high erosion susceptibility was widespread in the steep slopes of the sub-watersheds, except for a small part of the southern area of Kedung Tangkil. These small areas were covered with rainfed rice fields in the hills (altitude 150 – 200 meters a.s.l). Most of the land with high susceptibility to erosion occurred in forested areas. The extent of the land with high susceptibility to erosion was 415.2 ha or 33% of the total study area. This class was the most common in the study area while the least common was the land with low susceptibility (less than 1%).

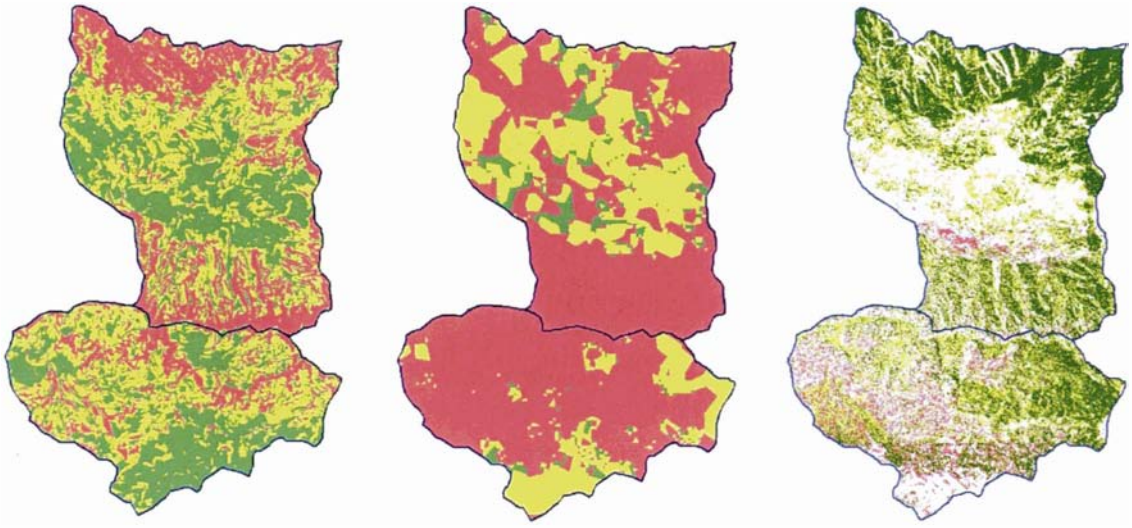

a. Slope class b. Geology class c. Land cover class

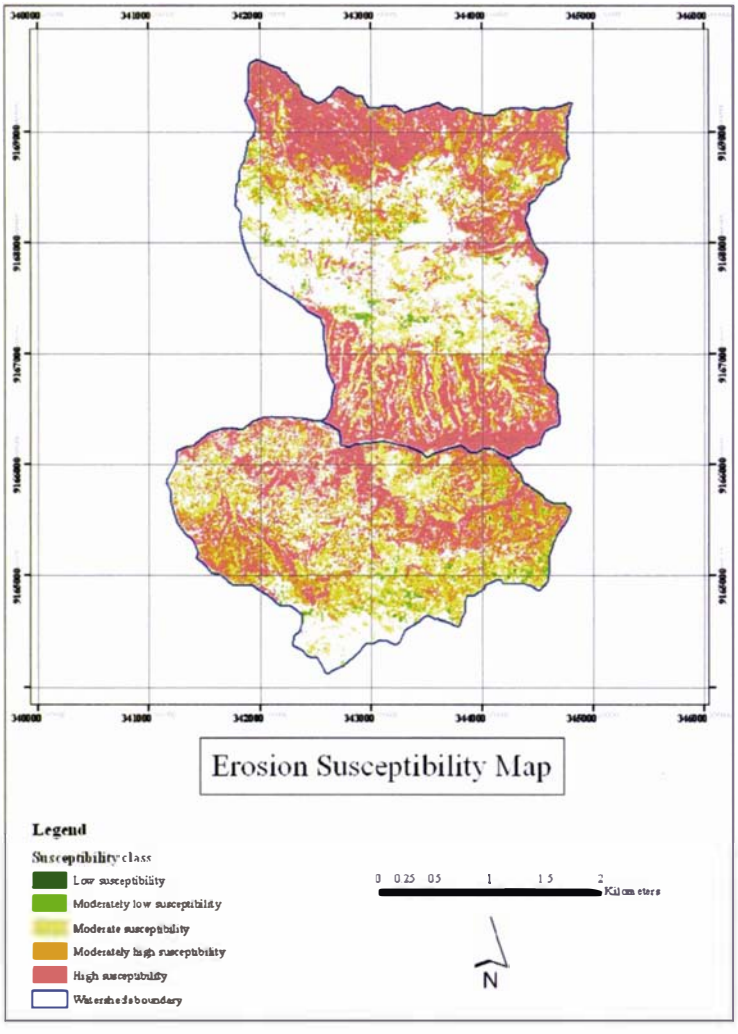

Figure 6-9 The erosion susceptibility class derived from (a) slope class, (b) geology class, and(c) land cover class.

6.5.4 Erosion Likelihood

The rainfall pressure data for this area was clipped from the original rainfall data derived in Chapter 5. By combining rainfall pressure with the erosion susceptibility (Figure 6-9), the erosion likelihood for these two sub-watersheds was determined. This is presented in Figure 6-10.

Figure 6-10 shows that more than 75% of the area had high rainfall (the rainfall ratio was 0 – 0.14%; Table 5-1). This means that the number of wet months was at least seven, with one dry month (Section 5.4.1).

The erosion likelihood was dominated by high likelihood (45% of the total area) especially in steeper areas, while areas of low to moderately low susceptibility became moderate or moderately high likelihood. This is as the result of high erosive rainfall pressures in the study area, which increased the likelihood of erosion.

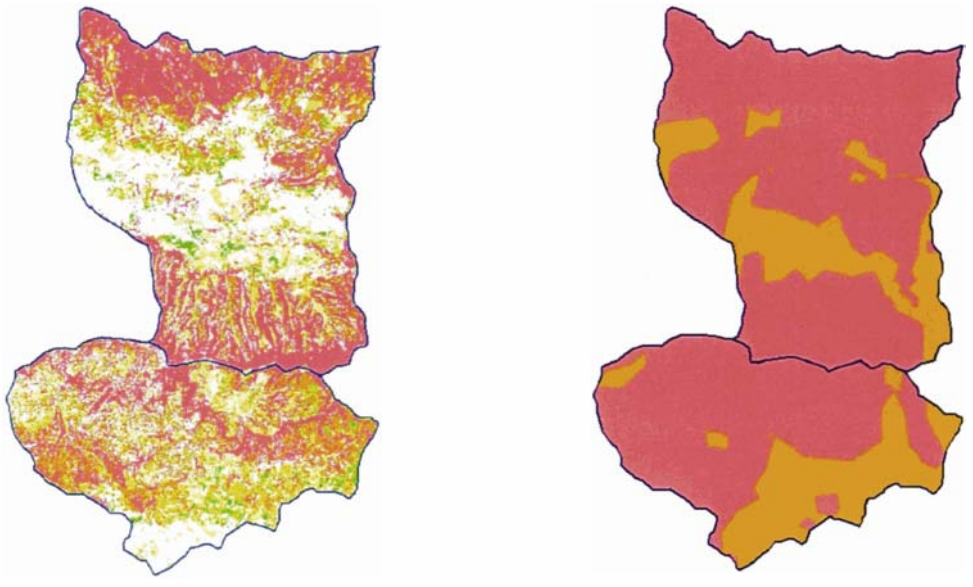

a. Erosion susceptibility class

b. Rainfall pressure class

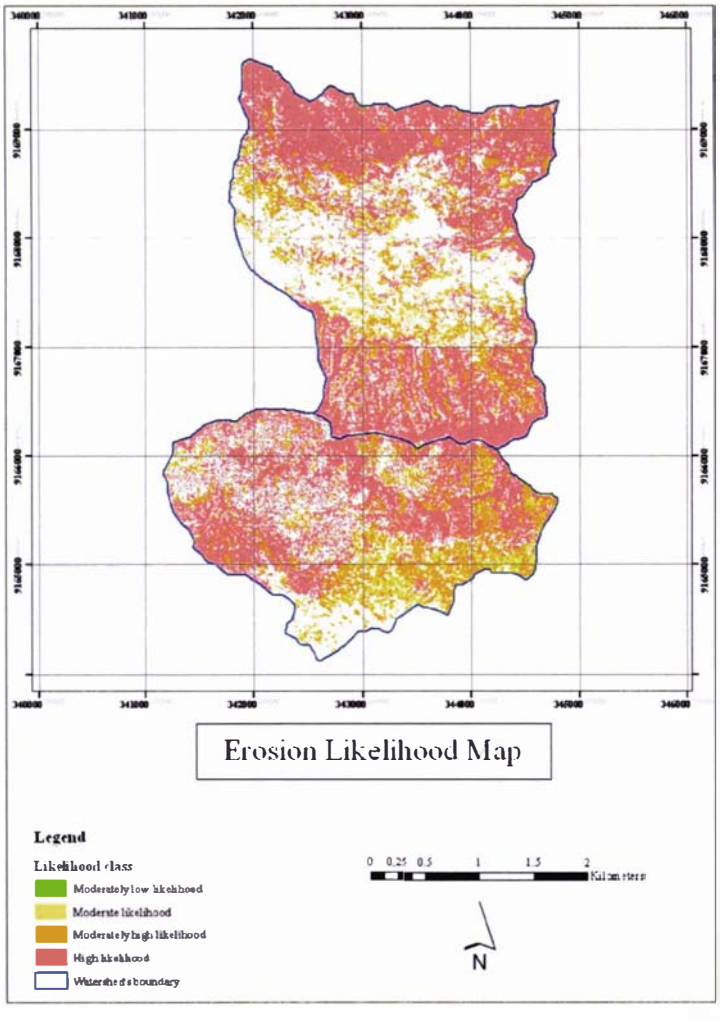

Figure 6-10 The erosion likelihood class derived from (a) erosion susceptibility and (b) rainfall pressure.

6.5.5 Environmental Consequence

6.5.5.1 Environmental Asset Value

As was already mentioned in Chapter 5 when discussing environmental asset and sensitivity, these factors were used to predict the relative environmental consequence of erosion in different areas.

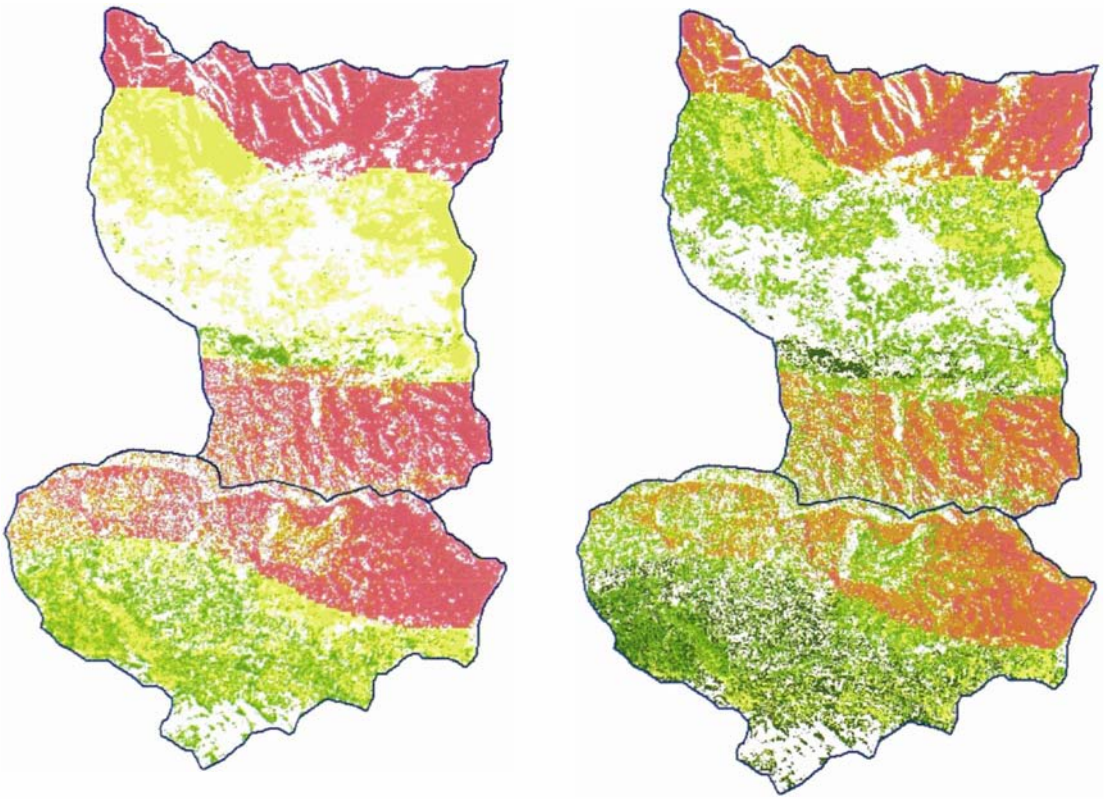

a. Short-term productivity class b. Long-term productivity class

Figure 6-11 The short- and long-term productivity classes in the study area

Figure 6-11a and b show the short- and long-term productive asset values in the study area. Short-term productivity was dominated by high productivity class (31%) in the steep slopes with Dystropept soil, and 21% moderate productivity in the moderately low soil fertility. The long-term productivity, on the other hand, distributed the moderately low, moderately high and high productivity classes in nearly similar amounts (17, 13, and 17% respectively).

The total productivity asset was a combination of short- and long-term productivity using a 2-D relationship as shown in Figure 5-6. The result is shown in Figure 6-12, while the areas (in ha) and percentages of the productivity classes are presented in Table 6-3.

Table 6-3 Areas (ha) and percentages of each productivity asset value class in the study area

Productivity class	**Short-term**	**Long-term**	**Total productivity**
		Area in ha (%)	
Low productivity (1)	--	100.4 (8)	100.4 (8)
Moderately low productivity (2)	98.6 (8)	212.1 (17)	158.5 (12)
Moderate productivity (3)	272.2 (21)	111.8 (9)	162.8 (13)
Moderately high productivity (4)	51.2 (4)	170.3 (13)	--
High productivity (5)	388.0 (31)	215.5 (17)	388.8 (31)
No productivity	458.1 (36)	458.1 (36)	458.1 (36)
TOTAL	1268.2 (100)	1268.2 (100)	1268.2 (100)

The distribution of total productivity asset classes shows that 31% of the study area was occupied by high productivity class. The high productivity asset classes were located in the higher altitude where most areas are under pine trees, while the low and moderately low are under open land.

The productivity asset class presented in Figures 6-11 and 6-12 shows sharp lines which separated the high and moderately high asset with the rest. These sharp lines were derived from soil type data which surrogate soil fertility. These lines are able to be avoided if more detailed soil fertility data are available. Since the soil fertility used a 1:100000 soil map, the result was too general. Agreeing with the comments made by Lin *et al.* (2005) and Zhang *et al.* (1999) about different level of detail from different map scale, this analysis needs soil fertility data from a more detailed map.

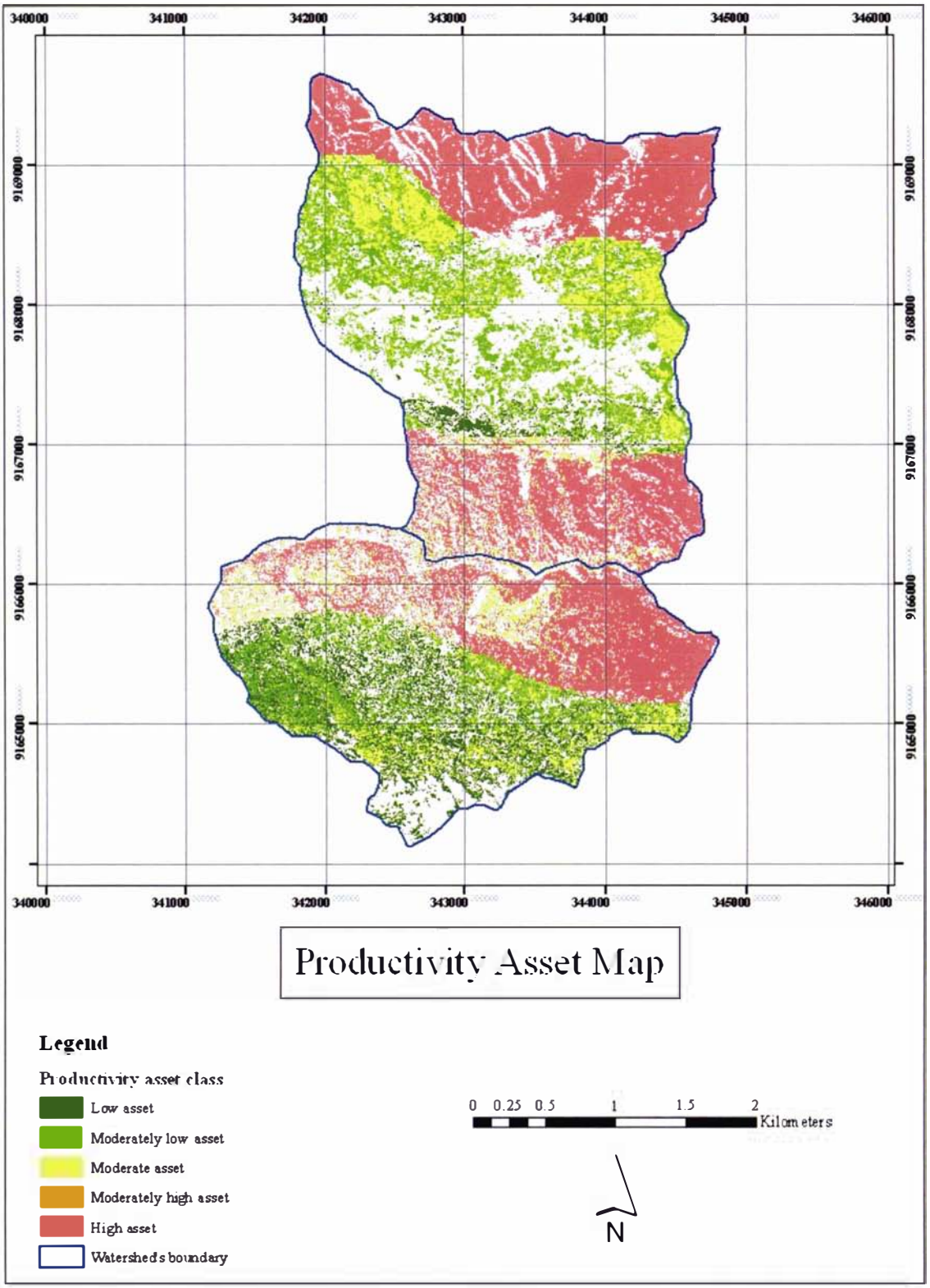

Figure 6-12 The distribution of productivity asset class in the study area

6.5.5.2 Environmental Sensitivity

Environmental sensitivity classes for this analysis were created by modelling soil depth according to assumptions of Lin *et al.* (2005). A combination of slope and altitude classes is used to divide the terrain into summit, hill-slope, and valley (Figure 6-3) Figure 6-13 shows the slope classes according to the slope classification mentioned in Table 5-2. Trial and error was used to find the contour lines that best separated slopes $<25^0$ that were summits and valleys. The chosen contour lines were 375 meters and over for summits and 225 meters and under for valleys. Using the matrix in Figure 6-3 the soil depth was modelled, and then based on the modelled soil depth, soil erosion sensitivity class was assigned using Table 6-1.

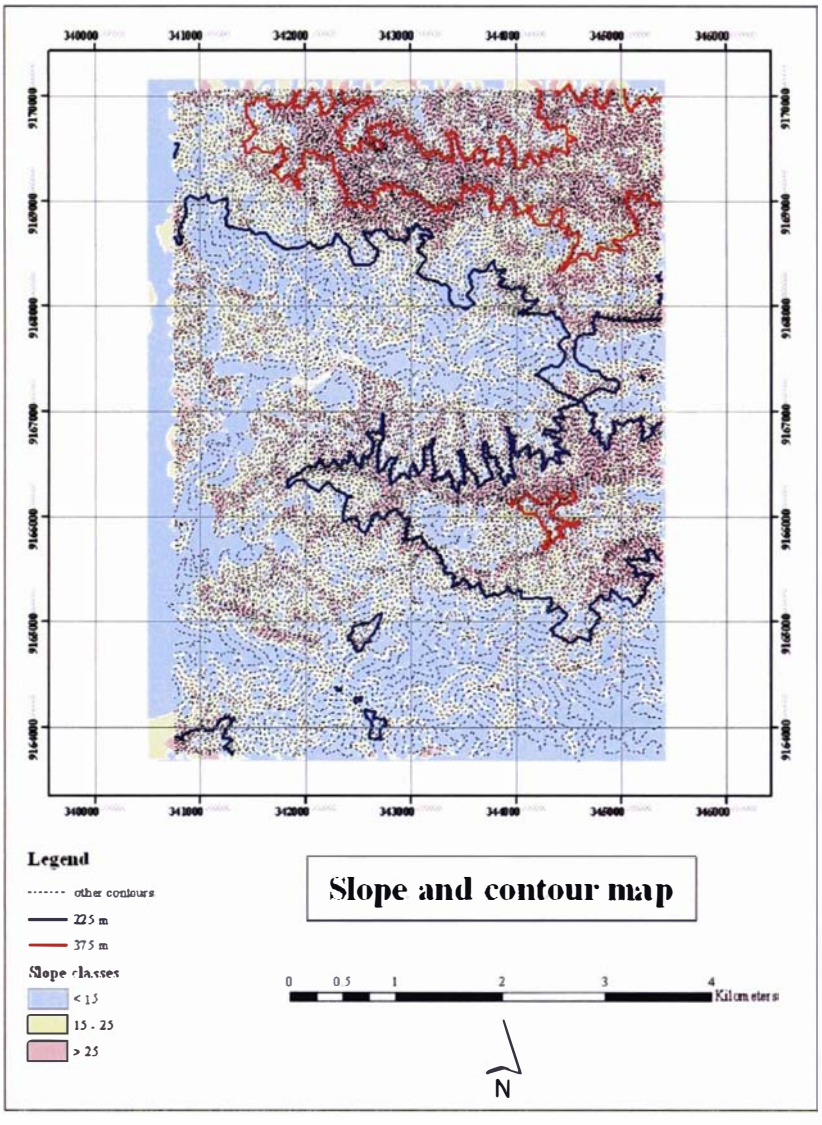

Figure 6-13 The contour lines and slope classes, to differentiate soil depths according to their hillslope position.

The soil erosion sensitivity class is presented in Figure 6-14a, while Figure 6-14b shows the original erosion sensitivity derived from soil depths in the 1:100000 soil map.

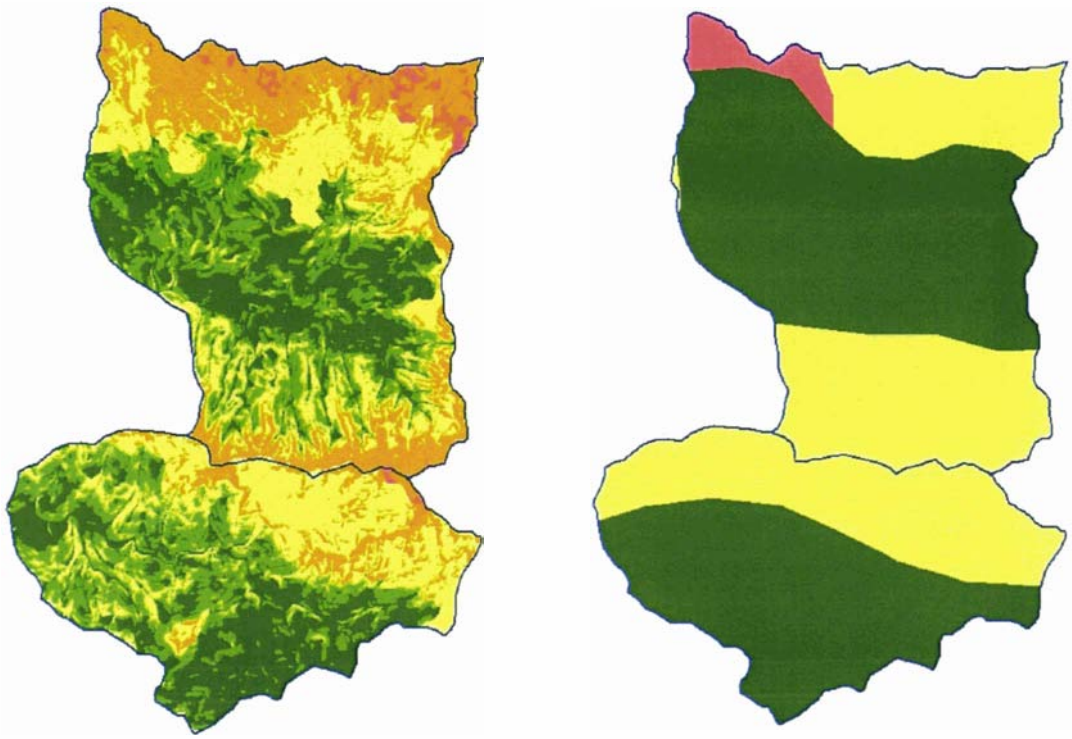

a b

Figure 6-14 Soil erosion sensitivity class modelled from slope and elevation (a) and soil depth (b) of the study area. The colours indicate the sensitivity to erosion. Red is high and green is low.

Compared to the erosion sensitivity from soil depth derived from a 1:100000 scale map, the new soil erosion sensitivity has more detail in it. Although it has more detail than the original both figures still have the same general pattern. Using the method presented in Section 6.4.5, overlaying two different map scales (1:100000 scanned soil map that has 11.8 metre resolution with DEM that has 1.69 metre resolution) is avoided.

Since the soil erosion sensitivity did not really use the soil map, the sharp line showing the soil boundaries will be less distinct for the later analysis, and this is more reasonable because in reality there are few abrupt changes in the environment.

6.5.5.3 Environmental Consequence

Combining the productivity asset class with environmental sensitivity using the 2-D relationship (Figure 5-5) resulted in the potential productivity consequence classes shown in Figure 6-15.

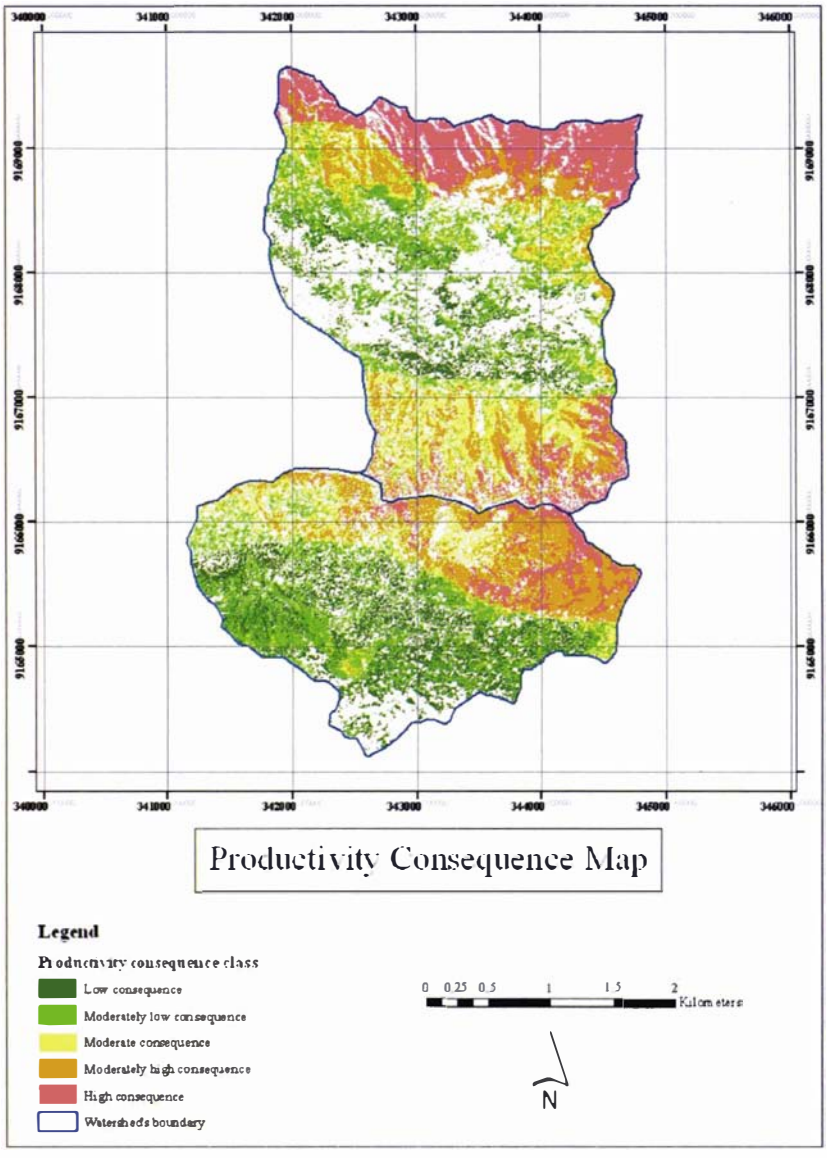

Figure 6-15 Distribution of productivity consequence classes in the study area

As already mentioned in Section 5.5.4.1, productivity consequence is represented by values that will reduce from a logged area if erosion is not controlled. The high class of productivity consequence (13% of this study area) is located in the northern part of Binangun sub-watershed. This area is under pine forests that sit in shallow soils with

moderately high environmental sensitivity, while other classes were low (12% of the total area), moderately low (14%), moderate (10%) and moderately high (14%).

The biodiversity consequence is dominated by moderate and moderately high classes, they occupy 19 and 20% respectively, with less than 10% of each low, moderately low and high class. Biodiversity consequence was derived by combining biodiversity asset class (see Figure 6-16a) and environmental sensitivity (Figure 6-16b). The result is presented in Figure 6-16.

The overall consequence was derived from combining potential productivity consequence and biodiversity consequence. Following the logic for deriving overall consequence in Chapter 5, the worst scenario from the two consequences was assigned to the overall consequence. This is presented in Figure 6-17 and Table 6-4.

Table 6-4 Areas (ha) and percentages of each erosion consequence class in the study area

Erosion consequence class	**Productivity consequence**	**Biodiversity consequence**	**Total consequence**
		Area in ha (%)	
Low consequence to erosion (1)	149.6 (12)	115.4 (9)	95.7 (8)
Moderately low consequence to erosion (2)	183.3 (15)	125.4 (10)	92.9 (7)
Moderate consequence to erosion (3)	131.6 (10)	238.3 (19)	220.8 (18)
Moderately high consequence to erosion (4)	180.1 (14)	250.1 (20)	219.5 (17)
High consequence to erosion (5)	165.5 (13)	80.9 (6)	181.1 (14)
No consequence to erosion	458.1 (36)	458.1 (36)	458.1 (36)
TOTAL	1268.2 (100)	1268.2 (100)	1268.2 (100)

Since the productivity consequence and biodiversity consequence for each pixel does not have to be in the same class, the total consequence is the total of both consequences or the highest percentage of each consequence (see Section 5.5.4.5).

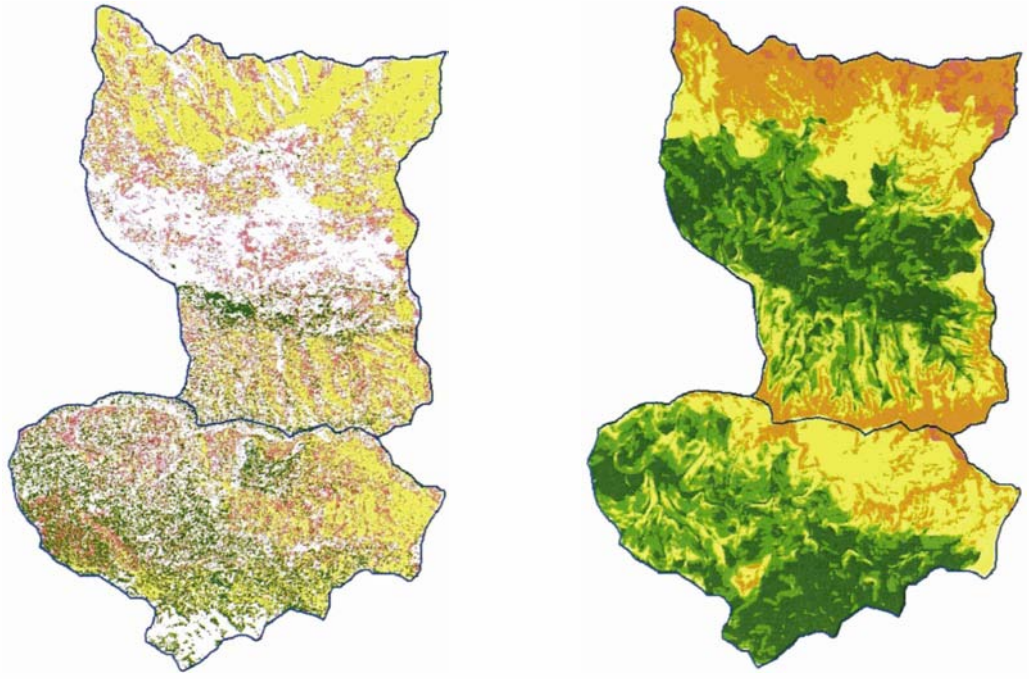

a. biodiversity asset b. soil sensitivity

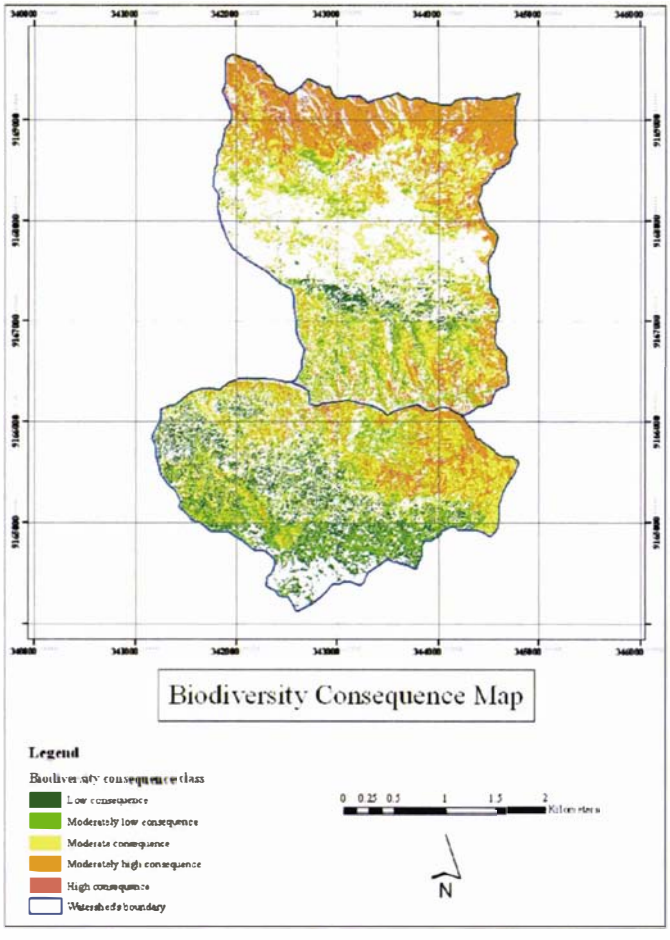

Figure 6-16 The distribution of biodiversity consequence in the study area

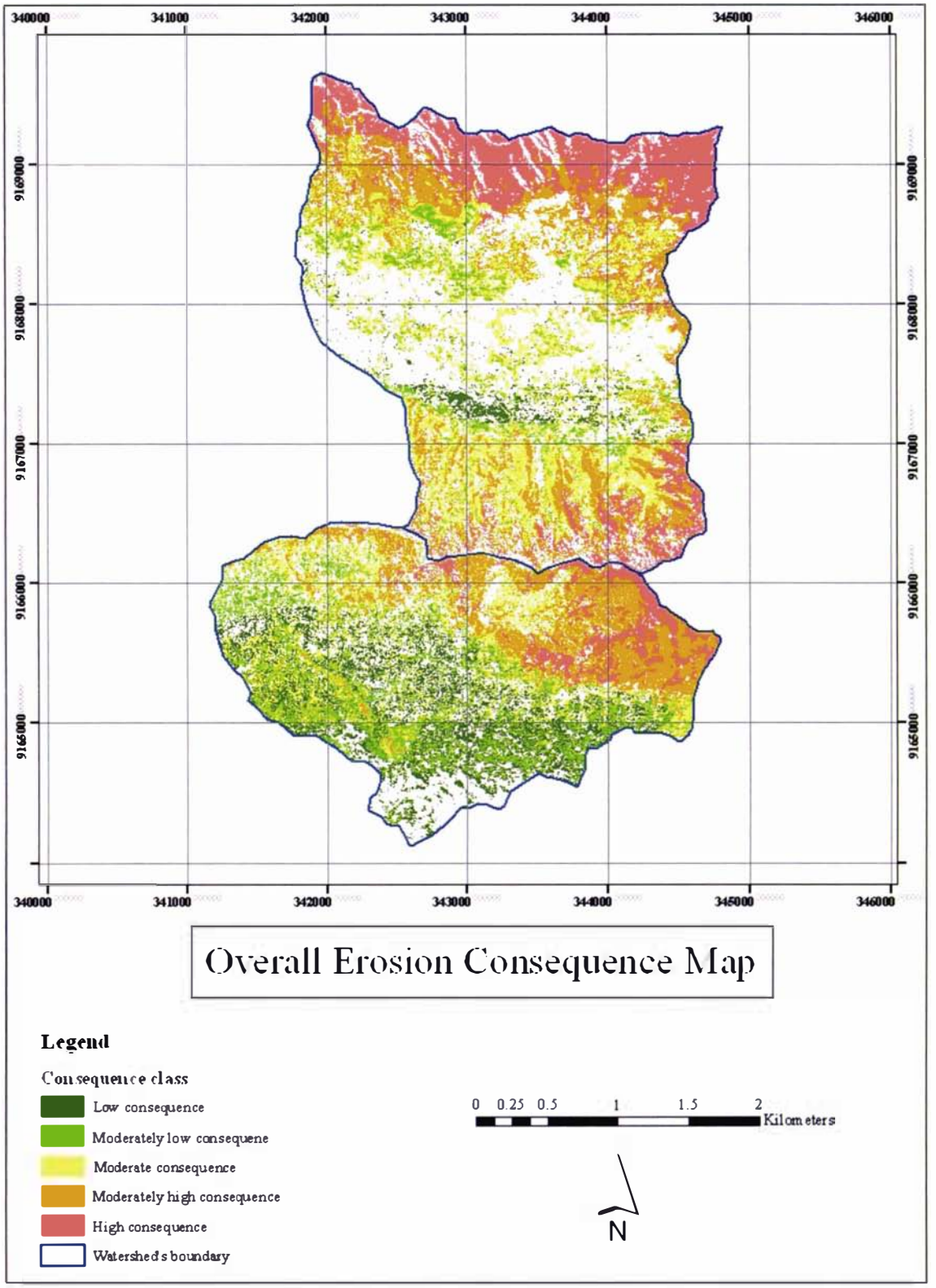

Figure 6-17 The distribution of erosion consequence class in the study area

6.5.6 Erosion Risk

Erosion risk of this area is obtained from erosion likelihood combined with consequence using 2-D relationship (Figure 5-5), and shown in Figure 6-18. Since erosion risk is important information for planners and decision makers, information about erosion risk for each land cover is needed to be understood. Table 6-5 shows the erosion risk class for each land cover.

Table 6-5 Areas (ha) and percentages of each erosion risk class in each land cover

Land cover	Moderately low risk	Moderate risk	Moderately high risk	High risk	No risk	Total
Open land	39.5 (3)	59.8 (5)	17.7 (1)	9.8 (1)	-	126.7 (10)
Mixed forest	1.2 (0)	12.2 (1)	152.7 (12)	164.4 (13)	-	330.5 (26)
Forest	21.5 (2)	61.2 (5)	95.8 (8)	174.4 (13)	-	352.9 (28)
Rice field and villages	-	-	-	-	458.1 (36)	458.1 (36)
Total	62.2 (5)	133.2 (11)	266.2 (21)	348.6 (27)	458.1 (36)	1268.2 (100)

From Table 6-5 it can be seen that 27% of the total study area has been assessed as having a high erosion risk. More than 95% of this land with a high erosion risk is either monotype or mixed forests. Of the 28% of the total area that is under pine forest, nearly half was predicted to have a high erosion risk. For the 26% of the total study area which is mixed forest, almost all of this land falls either in the high risk category (50%) or in the moderately high risk category (46%). In other words it can be said that 96% of mixed forest in this area has a moderately high or high erosion risk, while 75% of monotype forest is found in those categories. This condition suggests that a proper logging plan accompanied by soil conservation measures is a must when this area is logged.

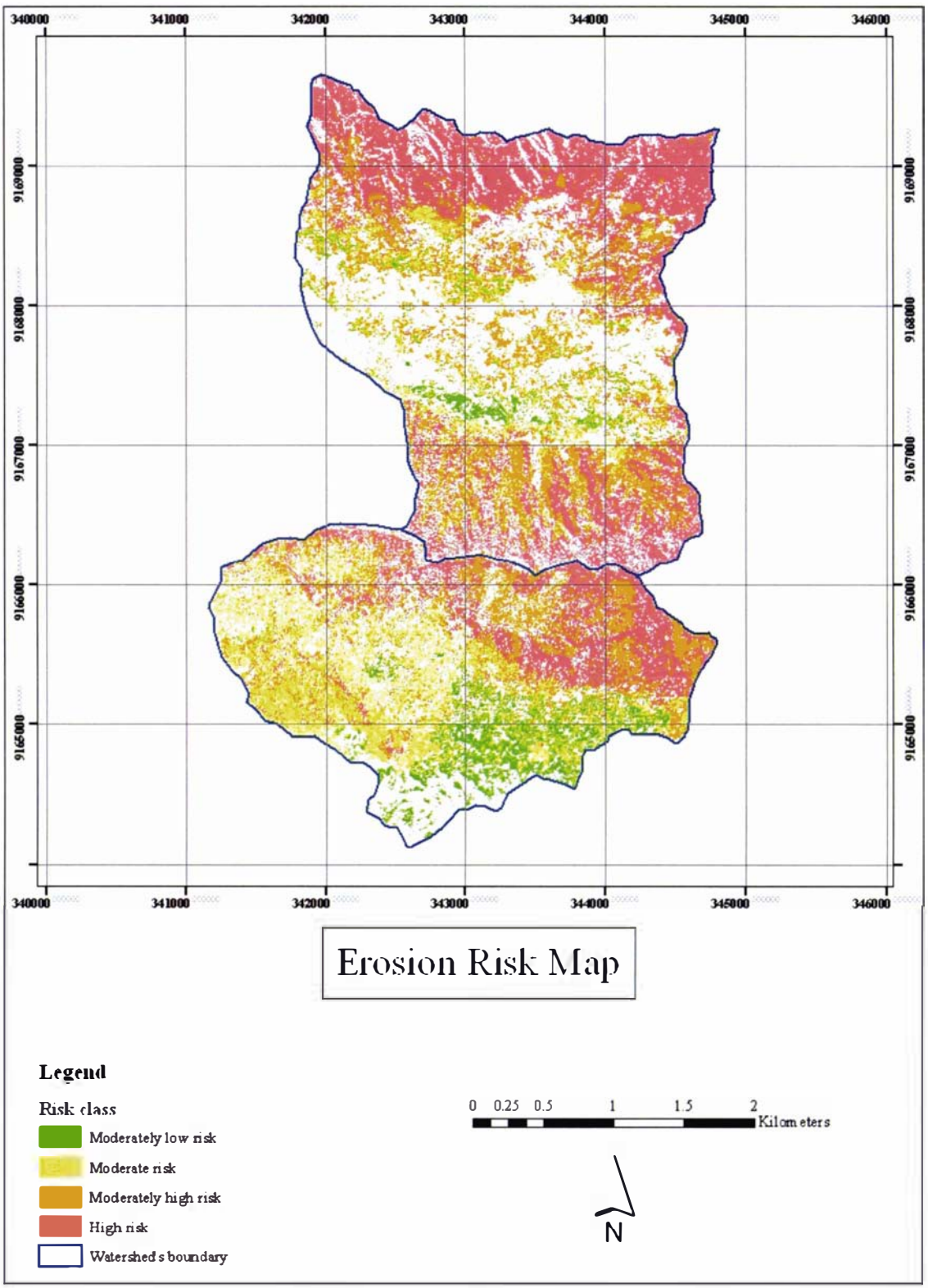

Figure 6-18 Distribution of erosion risk class of the study area

6.5.7 Comparison of the Different Scales

A comparison was made in order to understand the result of analyzing erosion using the same method but with different scales. The erosion prediction for Luk Ulo – Telomoyo watershed has already been described in Chapter 5, and the resultant images were clipped around the area of Binangun and Kedung Tangkil sub-watersheds for comparison. The comparison was done for the land cover classification and the effect of inserting slope and altitude for modelling soil depth.

6.5.7.1 Land cover Classification

Figure 6-19 presents the difference between land cover derived from an aerial photo and Landsat image. The land cover classification from aerial photo shows more detail in some parts, but loses it in some other parts. For example, open land (showed in brown) and villages (red) were two land covers that were difficult to distinguish in aerial photos, resulting in reduced areas when compared to Landsat image classification.

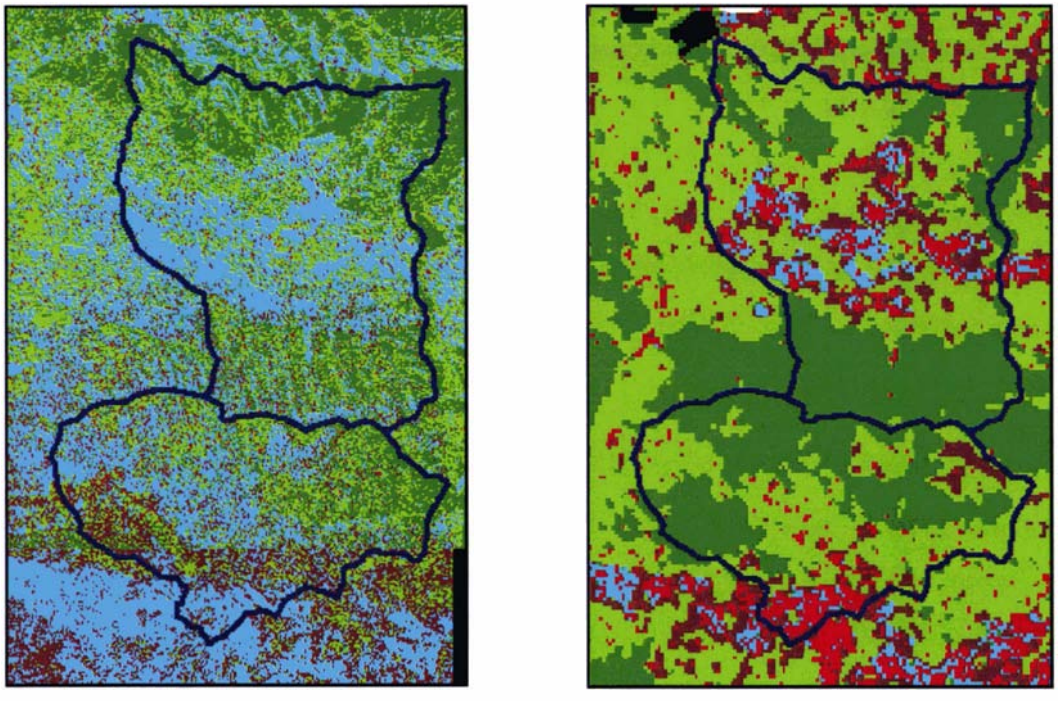

a. From aerial photos b. From Landsat image

Figure 6-19 The difference between land cover derived from (a) panchromatic aerial photo and (b) Landsat image (red = village, cyan = rice field, brown = open land, light green = mixed forest, dark green = forest)

Rice fields (cyan), on the contrary, were easier to find in aerial photos. Figure 6-19a shows where rice fields covered some part of mixed forests (light green) and villages in Figure 6-19b. This different result for rice field and mixed forest might be more because of the different times of capturing the images (aerial photo was captured on July 1993 while Landsat 7 was on April 2001). In dry season (July) rice fields and open land looked quite similar, especially rainfed rice fields or bare land. Therefore there is a possibility of misclassifying open land as rice fields, or vice versa. With the Landsat image, on the other hand, the difficult was on separating open land and mixed forest (see Section 4.7.4).

From both classifications it can be concluded that there is a possibility that open land is classified as mixed forest in Landsat image, but classified as rice field in aerial photo. To ensure what the real land cover is in the field, it is suggested that a more extensive ground check of these classes should be made after the classification has been done.

Since the pixel size for land cover (from aerial photos with 1.69 metres resolution) was different to the other maps, such as geological map (from an image with 30 metres resolution), or soil map (a 1:100000 map scanned with 300 DPI that made the resolution 11.8 metres), the land cover classification had higher variability which showed the reality in the ground (Figures 6-9c and 6-19a). Due to the scale difference, the aerial photos have more detailed information than the image has. This corresponds to the statement made by Bloschl (1999) about combining images with different spacing or pixel size.

The aerial photo classification in this study was not done manually so that the result of this classification is able to be compared to the image's result, since the image was classified automatically. Using the same method, it is found that although aerial photos gave more detailed information, but it was difficult to classify automatically and the result was strongly influenced by topographical effect. If the information needed to correct the topographical effect is available, the topographical effect will be reduced and the result of automatic classification will be better. However, when such data is unavailable, a mixture of manual and automatically classification will help.

Another way to reduce the error in classifying the land cover is by combining the classified land cover with land cover data from the working map or rotation map owned

by Perum Perhutani (see Section 6.1). The forest and non-forest land cover in the working map was always ground checked, therefore the accuracy is assured.

6.5.7.2 Result of Slope and Altitude Insertion

The soil data used for analyzing erosion risk in Binangun and Kedung Tangkil sub-watersheds was different to soil data used for Luk Ulo – Telomoyo watershed. Since the soil map used in Luk Ulo – Telomoyo watershed was too general for this analysis, a combination of slope and altitude were used to model soil depth (Section 6.4.5 and Figure 6-3). Soil erosion sensitivity was then created from the modelled soil depth. With different soil erosion sensitivity, the analysis involving erosion sensitivity will give different results compared with the analysis in Chapter 5 (see Figure 6-20).

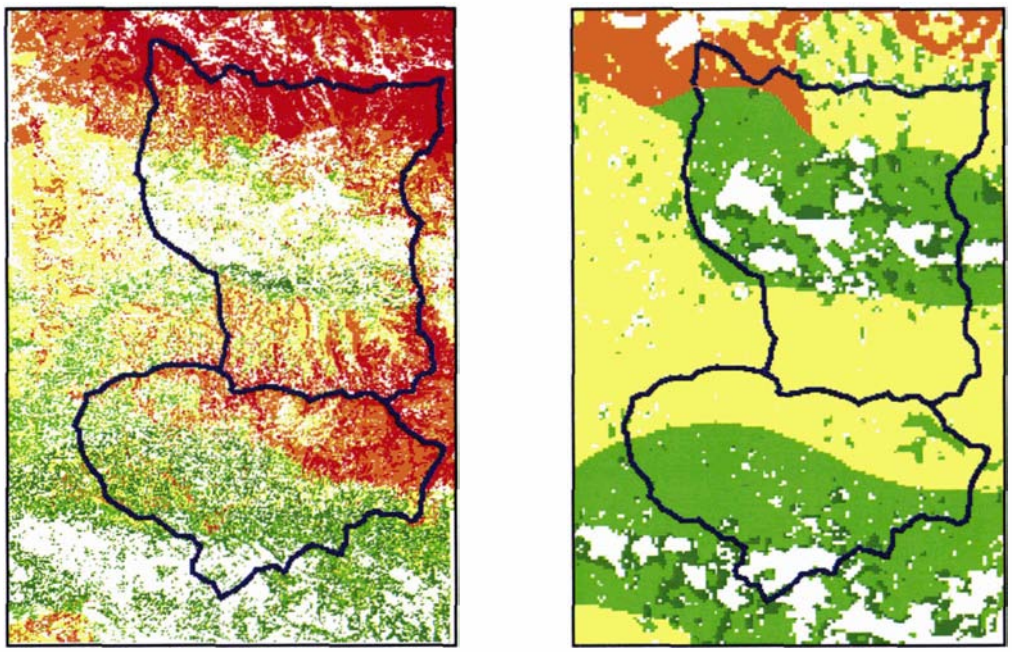

a. From a modelled soil depth b. From original soil map

Figure 6-20 The consequences using sensitivity from a modelled soil depth using altitude and slope to separate the hills into summit, hill-slope and valley (a), and from original soil map (b). (red = high consequence, orange = moderately high consequence, yellow = moderate consequence, light green = moderately low consequence, dark green = low consequence, white = not analysed)

In general, the patterns of both images were similar except that Figure 6-20a gave more moderately high (orange) and high consequences (red) compared to Figure 6-20b. This is due to the additional information from slope and altitude that made soil sensitivity

have more details. The moderately high and high consequences class in Figure 6-20a show areas with high altitude, which were ignored in the previous analysis. Similar to the moderate consequence (yellow) in Figure 6-20b, it was divided into moderately high and moderate in Figure 6-20a. From this comparison, it shows that soil sensitivity has an important role in improving the analysis of erosion consequences. The important issue in using aerial photo as another source of data is the variability of classes resulting from the analysis. There were more varied classes compared with Landsat image.

Using a modelled soil depth, it was found that within areas of moderate consequence as derived from Landsat analysis; there was more variability in the aerial photo analysis. Using a detailed DEM to model the soil depth, the analysis was able to subdivide the Landsat moderate class into moderate, moderately high and high classes.

Another comparison was made for erosion risk and its difference is presented in Figure 6-21. The erosion risk from the image was clipped from the Luk Ulo – Telomoyo watershed using coordinates of Binangun and Kedung Tangkil sub-watersheds. To see the differences between the risks for both images, the areas (in hectare and percentage) for each image are presented in Table 6-6.

Table 6-6 Comparison between erosion risk areas predicted from aerial photos and Landsat imagery (numbers in the brackets shows the percentage)

		Erosion risk from Aerial photos					
		0	**2**	**3**	**4**	**5**	**Total**
Erosion Risk from Landsat Image	**0**	107.7 (8)	14.6 (1)	5.9 (0)	23.5 (2)	6.9 (1)	158.6 (13)
	2	25.7 (2)	8.9 (1)	3.0 (0)	4.5 (0)	0.9 (0)	43.0 (3)
	3	61.5 (5)	4.9 (0)	46.4 (4)	51.6 (4)	55.7 (4)	220.1 (17)
	4	257.3 (20)	33.8 (3)	77.9 (7)	186.4 (15)	263.6 (20)	819.0 (65)
	5	5.9 (0)	0.0 (0)	0.0 (0)	0.2 (0)	21.5 (2)	27.6 (2)
	Total	458.1 (36)	62.2 (5)	133.2 (11)	266.2 (21)	348.6 (27)	1268.2 (100)

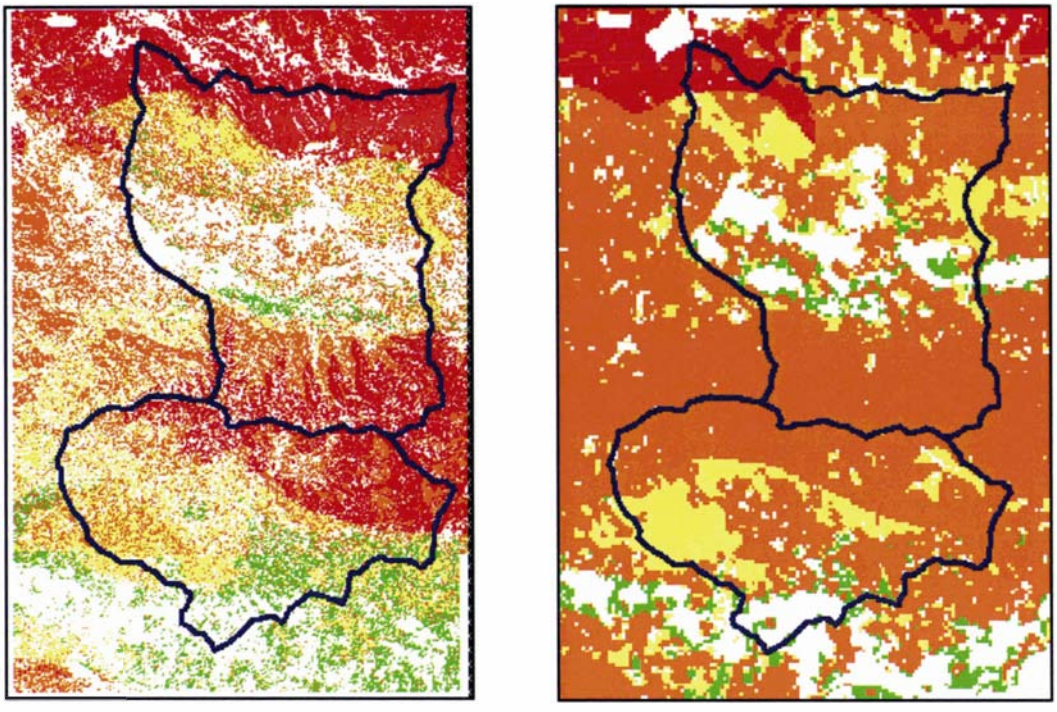

a. Erosion risk from aerial photo

b. Erosion risk from Landsat image

Figure 6-21 The difference between erosion risks using (a) aerial photo and (b) Landsat image. (red = high risk, orange = moderately high risk, yellow = moderate risk, light green = moderately low risk, dark green = low risk, white = not analysed)

Table 6-6 shows that 30% of erosion risk areas derived from the aerial photo had the same class as in the Landsat based analysis (the diagonal values). Moderately high risk areas were most extensive in the Landsat image (65%). For the areas with a moderately high risk, as determined from the Landsat image, 20% was in the no risk area (rice field and villages) according to aerial photo. It is likely that these areas were villages or rice fields that had been classified as mixed forest in the Landsat image. As mixed forests, these areas were in the moderately high risk, but as villages or rice field they were excluded from the analysis. This was because land cover classification in the aerial photo easily picked up rice fields (see Section 6.5.7.1); leading to more rice fields being found in the aerial photos.

Furthermore, of the areas with moderately high erosion risk from the Landsat image, 32% was predicted as having a high risk in the aerial photo. This happened because in the Landsat image the modelled soil depth from slope and altitude was not used, therefore classification of the Landsat image does not incorporate high altitude and

steep slope. These areas of high erosion risk in Figure 6-21a were located in the higher altitude and steeper slopes so it is understandable that the risk would be high. Since they are under pine forests, the planners will have to make sure that the logging plan is accompanied by soil conservation measures.

In the Landsat image this phenomenon was not clearly shown, since altitude was not included in the analysis. This means that the analysis for the whole catchment (Luk Ulo – Telomoyo) gave general information and the detail was explained in both Binangun and Kedung Tangkil sub-watersheds. If the exact location of high risk areas in the Landsat image needs to be known, an analysis using aerial photos and a modelled soil depth should be made; otherwise the result from Landsat image is sufficient for logging plan activities.

Although a modelled soil depth gave more information in this method, it does not mean that it has to be applied in the Landsat method as well. Landsat image has the appropriate scale for the forest planners and decision makers to determine logging plans. With a 30 metre resolution, it is impossible to locate most areas at risk to erosion. Aerial photo interpretation, on the other hand, shows more exact locations where the risks are identified. With a 1.69 metre resolution, this information is more appropriate for the forestry people in the field or researchers who want to design detailed soil conservation practices. Understanding this difference is important so that a suitable analysis is able to be made in the correct scale for the correct application.

6.6 Conclusion

Compared to the classification of the Landsat image, aerial photo classification is more difficult to do automatically, especially for classifying villages and open land. Although some difficulties were still found in separating open land, villages, mixed forest and forest in the Landsat image, these can be resolved by adjusting the NDVI threshold values. In the aerial photos, the solution may be to do it manually or a combination of manual and automatic interpretations, especially when classifying the villages and open land. Combining both methods will increase the chances to capture villages and open land, and, at the same time, decrease the subjectivity of the interpreter. When the

working map produced by Perum Perhutani is available, land cover data from this map can be used to correct the classification.

Another difficulty with aerial photos in automatic classification is topography influencing the classification. With manual classification this problem is avoided. Different tones and textures in the photos that affect the mosaic are prevented by postponing the mosaicing until the classification is already made. Another way is to crop the edges of the photo to remove the effect of distortion which influences the texture. Image balancing is yet another way to reduce the tonal difference between two or more photos.

The use of aerial photos in some parts of the classification shows more detail than Landsat images, but in other parts they lose some detail too. Villages and open land were examples of land cover that were not easy to identify in aerial photos, while rice fields were relatively easy to capture. Even though rice fields were easy to capture in the aerial photo, there is still possibility that rice fields were actually open land (or vice versa) depending on the time the photo was taken. The only way to determine for sure what the real land cover is, is by field checking.

Since the real soil map does not give much information about soils in the study area except soil name and soil depth, information derived from a combination of slope and altitude was able to model soil depth according to its position in the hillslope. This additional information distributes moderately high erosion risk in Landsat imagery into moderately high and high risk in the aerial photos (Figure 6-21).

Similar to the result in Chapter 5, mixed and pine forests experienced moderately high and high risk for erosion risk. The majority (76%) of forest are predicted to have moderately high (27%) and high (49%) erosion risks, while mixed forests have 46% of moderately high and 50% of high erosion risk. Those erosion risks show that logging activities have to include soil conservation measures to reduce the high class of risks in the production forest.

The different scales used in this chapter show that when the scale increases, the result of the analysis gave more detail, not only in the variability but location as well. Using Landsat imagery the planners will know the whereabouts of erosion risk and it may be sufficient for logging plan activities. However, when the planners want to make a more

detailed soil conservation plan in the areas of high erosion risk, an analysis using aerial photos and a modelled soil depth should be carried out.

CONCLUSIONS AND RECOMMENDATIONS

The previous chapters have presented a study of the use of remote sensing and geographic information systems to predict erosion risk in forest areas. The method used in this study has not yet been applied to other types of land use; the threshold values for other land uses will probably be different to those presented in this study and further research needs to be done to extend the technique to other areas.

The main objective of the study was to produce a method to identify areas most susceptible to erosion in the study area. It is intended that the method be used particularly by forestry planners and decision makers so that they can improve environmental management of the forest, especially during and after logging.

The study area was within the Kebumen and Banjarnegara districts of Central Java, Indonesia. It is an 88,551.6 ha catchment area with two major rivers: the Luk Ulo and the Telomoyo. Data used in this study were: topographical, soil, and geological maps, a satellite image, aerial photographs and rainfall data. The satellite image was from Landsat 7 ETM+ dated at 28th April 2001 and the panchromatic aerial photos were acquired on 5th July 1993. This study also analyzed 10 years of daily rainfall data from 17 rainfall stations surrounding the study area.

7.1 Conclusions

The general conclusion of this study is that remotely-sensed imagery with other auxiliary data can be used to identify areas at risk from erosion due to logging activities. The auxiliary data proposed in this method are topographical, soil and geological maps and rainfall data. Since all of these datasets are usually available in Indonesia, the methodology should be easy to implement by the forest companies. The resulting maps can be used to advantage when generating forest logging plans to comply with sustainable forest management. Some technical issues were identified during this study; they are discussed under three headings, namely: data preparation, data analysis and results.

7.1.1 Data Preparation

Adequate slope and rainfall maps are not readily available in Indonesia to assist with erosion prediction in remote forest areas. Therefore slope map are derived automatically from a DEM. When a DEM is unavailable, generating DEM using TOPOGRID command in ARCInfo solves the problem. Data used by this command was digitised from a topographical map. These were contour lines, spot heights, river network, and water body boundaries. The TOPOGRD command uses these input data to create a hydrologically consistent DEM that can be analysed further to create watershed boundary, slope and aspect data layers. These data layers are essential for erosion prediction and can also be used for correcting the topographic effect in imagery and for improving rainfall maps.

In Indonesia rainfall surfaces are usually created using methods based on Thiessen polygons or interpolated Isohyets neither of which considers altitude when estimating the rainfall in areas where the terrain is significantly different from the areas with rain-gauges. ANUSPLIN (software used to create rainfall surfaces), on the other hand, can be programmed to consider altitude and aspect for each gauging station, and use these data to predict rainfall in un-gauged areas. With this advantage, ANUSPLIN is able to model effects such as the rain shadow effect. With the available data, ANUSPLIN which interpolates using thin plate splines performed better that co-kriging, especially in predicting the rain shadow areas.

7.1.2 Data Analysis

Land cover, as one erosion factor, is classified using Landsat 7 ETM+ imagery and aerial photos. To eliminate the atmospheric and topographic effects particularly in the satellite imagery, Dark Object Subtraction (DOS) and Sun Canopy Sensor (SCS) methods were chosen. DOS was selected to correct the atmospheric effects due to its simplicity and ease of use. Since there were no *in-situ* and climatic data available for this study, DOS was preferred because it does not require information other than that provided by the image itself. SCS gave better results in correcting the topographic effect compared to other correction methods such as cosine and C. These latter two methods produced over- and under-corrected imagery, especially in hilly areas.

Since the panchromatic aerial photo only has one band, there is no method to decrease the topographic effect. When classifying aerial photos automatically, the topographic effects influenced the result of the classification and reduced accuracy. A combination of visual and automatic classifications is an alternative to improve the accuracy of this classification.

With a heterogeneous land cover such as this study area, a single classification is unable to capture all the land cover types in the area. Using a stratified classification the result was better, although this method still needs small adjustments. RGB-754, RGB-532, NDVI and RGB-721 were the band combinations used to classify villages, rice field, vegetation, and clouds respectively. At the end the results of each classification were combined to get a complete land cover type. Even though the land cover classifications were already stratified, the accuracy was not high (44%). The accuracy assessment was done by comparing the classified imagery with topographic maps using 770 randomised point samples. The low accuracy can be explained by the complexity of the area, the rate of change of land cover in the area, and the differences in time between the acquisition of the image and ground reference data.

In the erosion risk analysis, environmental factors (asset value and sensitivity) were taken into account; this is not usually the case in erosion analyses. This method gives a more complete picture of the effect of erosion on the environment especially during and after logging. Although this analysis provides only an indication of where the highest erosion risk is most likely, it is still very useful information for forest planners and decision makers to make their logging plans more sustainable. Information about erosion risk is important for the decision makers to determine whether an area is worth logging or if the risk is too high.

7.1.3 Results

The proposed erosion risk method is robust enough to be used not only in the plantation forest in Java, but also outside Java, or even outside Indonesia with some adjustment in the given classes according to the local conditions. Some of the values determined in this study also need adjustment when applied to other locations. These values are the thresholds used to differentiate vegetation after calculating NDVI. In this study they were 0.15 – 0.45 for open land; 0.65 – 0.8 for mixed forest; and > 0.8 for monotype

forest. Other threshold values used in this study were those for isolating cloud and cloud-shadow in the satellite image. These values might be different if this method is applied to other images.

Additional information about soil depth distribution in the sloped area improved the result of the analysis. When the analysis used aerial photos and soil depths inferred from hill-slope position, the high and moderately high risk areas were distributed more evenly compared to using Landsat imagery and more general soil depth data. Using Landsat the proportions of the Binangun and Kedung Tangkil catchments with a high or moderately high erosion risk were 64% and 2% respectively, while from the aerial photo they were 21% and 27%.

Using Landsat imagery it is possible to determine that, from 45% of the Luk Ulo and Telomoyo study area have moderately high risk (Table 5-17), 70% is predicted to occur in the mixed forest area, while the rest will happen in the monotype forest. Using more detailed information (aerial photos) however, the result is quite different. In the Binangun and Kedung Tangkil study area, from 65% area that are predicted to have moderately high erosion risk (Table 6-6), 15% were classified as moderately high erosion risk, 30% were classified as other classes (from moderately low to high erosion risk classes), and 20% is under rice field and villages which are excluded from the analysis. Within the later study area, it can be said that more detailed analysis resulted in more detail erosion risks being identified and in the more precise location.

Since both mixed and monotype forests were rated as moderately high and high risks, they need soil conservation measures especially during and after logging to minimize erosion. They also need carefully designed logging methods to minimize the risk.

7.2 Recommendations for Implementation of the Method

The techniques described in this thesis provide a means of identifying areas susceptible to erosion and evaluating the erosion risk for these areas. An important outcome from this research would be the implementation of the methodology, especially by agencies like forestry companies when logging operations are being planned.

Experience has shown that a method will not be implemented if it requires data which are difficult to collect. Therefore this method employs data that are readily available in Indonesia. If certain data are unavailable, this method also shows how to surrogate using the available data.

The recommendation below was made to help the forest companies to prepare before implementing this method. There are various programmes that will need to be carried out to ensure a wider acceptance of the scheme.

The recommendations cover two general areas: (1) Operational and (2) Policy and Management. Operational recommendations give more emphasis to data acquisition and analysis, while policy and management recommendations are more concerned with the supporting conditions that make this method work. A summary of the current practices, associated problems and suggested solutions for each category is presented in Table 7-1.

Table 7-1 Policy, management and operational recommendations

Category	Current practices	Current problems	Recommended solutions
Operational			
Rainfall data	Rainfall data gathered from selected sites	– Too few gauges – Poor distribution	– More rain gauges, with some automatic gauges – Better distribution
Soil data	Soil data are used to calculate erosion	– Wrong scale – No soil fertility data	– Acquire data from Indonesian Soil Research Institute (ISRI) – Carry out soil survey
Land cover data	Land cover data are used to calculate erosion	Land cover data are out of date	– Classify land cover data from the recent images – Improve the classification according to each forest species
DEM	Contours digitised manually	– Contour interval too large – Difficult to separate contours in hilly areas	– Acquire DEM from satellite provider – Generate DEM from topographical map
Imagery	Images are classified manually	High subjectivity	Do automatic classification, combine with manual classification if necessary

Category	Current practices	Current problems	Recommended solutions
Data management	Ministry of Forestry and forest companies collect their own data	– Duplicate data or no data for a certain erosion factor – Erosion is calculated with restricted data	– All of the important data have to be made available prior to the logging activity – Establish data collection responsibility among companies concerned and share the data
Hardware and software	Hardware and software are used for analyzing image	– Expensive – Not readily available	Establish agency to provide relevant products from imagery and ancillary data
Personnel	Forest companies' personnel do land cover survey	The personnel do not know how to predict erosion or to do soil survey	Conduct training for the forest companies' personnel
Agencies involved	Ministry of Forestry monitor erosion in watersheds	– Information about erosion is not reported to the forest companies – Forest companies do not make erosion calculation	– Ministry of Forestry still monitors erosion – Forest companies liaise with Ministry of Forestry – Researchers use erosion monitoring data to improve the method
Policy and management			
Policy	Ministry of Forestry make regulations for forest management	No enforcement to implement soil conservation practices in the forest	Ministry of Forestry to do more to encourage the adoption of this method
Funding	Funding is used for forest management	No funding is available for doing erosion/soil conservation research	Reallocate funding for erosion/soil conservation research and the implementation of this method
Networking	Researchers have a co-operation with some of forest companies	No communication about erosion problem between researchers and users (forestry planners)	Build a network for educators, researchers, planners and managers

7.2.1 Recommendations for Rainfall Data

It is recommended that more rain gauges be installed throughout the region to improve the accuracy of predicted rainfall. Some improvement to rainfall prediction might be achieved by enlarging the size of the study area to include all rainfall stations in Java and hence predict the whole island. A DEM for the whole island would have to be available to supply information about altitude and aspect of each rain gauge used.

The second recommendation is to build rainfall stations in more varied locations to collect data at a variety of altitudes, aspects and land cover types. A DEM, aspect map, and land cover map could be used as references to choose the sites. Where the chosen rainfall stations are not easily accessible, a fully automatic rain gauge recorder is recommended.

7.2.2 Recommendations for Soil Data

Two recommendations are given related to the soil data. The first recommendation is to acquire more soil information, especially soil fertility and soil depth from the Indonesian Soil Research Institute (ISRI) at various scales. However, if the data at a suitable scale are unavailable, a soil survey should be carried out. Land units, mapped in the largest available scale, should be used as guidelines in determining where to sample soils.

The second recommendation is to consider both food crop and forest trees when doing the soil fertility assessment, since food crops require more fertile soils than forest trees.

7.2.3 Recommendations for Land Cover Data

It is recommended that land cover be determined from more recent images. The stratified classification used in this study is recommended, although the difficulty of separating open land, mixed forest, monotype forest and villages will still exist, adjusting the threshold values in NDVI may provide at least a partial solution.

The next recommendation is to separate monotype forests according to species, since each species gives different productivity values. These data should be available in the forest companies' concession.

7.2.4 Recommendations for DEM

The DEM, which is used for correcting images, delineating watershed boundaries and determining slope and aspect, should, if possible, be derived from stereographic satellite imagery (ASTER or SPOT). However, if these more reliable DEMs are unavailable, it is recommended that contour lines be digitised from topographic maps with the largest

scale available before using interpolation techniques to generate the DEM. In most instances 12.5m contour intervals will be available.

7.2.5 Recommendations for Imagery

It is recommended that automatic classification techniques be used first on all imagery. Manual classification is an alternative but may be susceptible to a degree of subjectivity being introduced by the interpreter. A mixed classification procedure should be employed to take advantage of the efficiency of automatic classification and lessen the subjectivity of the interpreter.

7.2.6 Recommendation for Data Management

The important factor that makes this method work is the availability of data for the analysis; therefore it is critical to keep the data updated. If logging is to be implemented in a certain year, then the risk analysis, DEM creation, land cover survey, soil survey and rain gauge installation should be done in the previous five-year period. A second recommendation is to gather data collected by the Ministry of Forestry and the forest companies and to ensure access to these data by all parties.

7.2.7 Recommendation for Hardware and Software

Equipment needed to implement the proposed methodology successfully includes computers, scanners and colour printers. Since most of the forest companies usually analyse imageries, they already have the hardware and most of the software required. It is recommended that they ensure both the hardware and software are updated regularly. For companies that do not have the appropriate software, it is recommended that it be purchased.

7.2.8 Recommendation for Personnel

Forest company personnel often do land cover surveys, but not soil surveys or erosion analysis. Therefore the recommendation for this problem is to conduct training for them. The training should include analysing erosion risk using the method proposed in

this study and also how to conduct soil surveys. If those personnel do not understand image analysis, a practical training course in image analysis is recommended as well.

7.2.9 Recommendations for Agencies Involved

There are three recommendations for the agencies involved. Firstly the Ministry of Forestry, through the Directorate of Watershed Management, is still responsible for monitoring erosion in the forest areas at the catchment scale. It is recommended that the Ministry of Forestry publish the results of this monitoring for the benefit of forest companies and researchers. The second recommendation is to encourage the forest companies to use this method and thereby reduce erosion in the logging areas by applying soil conservation practices. The third recommendation is that the researchers look to improve the method especially after considering the erosion monitoring data from the Directorate of Watershed Management.

7.2.10 Recommendation for Policy

An important policy recommendation is that the Ministry of Forestry be pro-active in encouraging forest companies to adopt more sustainable forest management. All forest companies in Indonesia that manage production forests should be urged to apply the proposed method. If they do not have the capability then systems should be put in place to assist them in establishing the necessary facilities and training of personnel.

7.2.11 Recommendation for Funding

For this method to be adopted by all the forest companies, funding has to be allocated within forest companies' budgets. The expenses are mostly for collecting data, purchasing imagery, and applying soil conservation measures in the logging areas.

7.2.12 Recommendation for Networking

A recommendation to ensure that the method is always kept up-to-date is to build a network among the researchers, universities, users (forest companies), and software providers. This network should be used to provide feedback to the software developers

and to encourage dialogue between the researchers, Ministry of Forestry staff and forestry company planners.

7.3 Recommendations for Future Research

Although the study was able to produce a method to identify areas most susceptible to erosion and also evaluate the erosion risk, there are still some subjects that need to be studied in more detail. Chief among these are the recovery time, the use of heavy rain data, evaluation of the biodiversity factor and readjusting the land cover classification method.

7.3.1 Recovery Time

The time it takes for the soil to recover its stability after logging is an important piece of information that is still largely unknown because it is different for different landscapes and different forest covers. The recovery time could be displayed in cumulative risk charts which could represent the value of erosion risk since the forest was logged. This information could be used as the motivation to design adequate ground cover over the period of this critical time. By understanding the recovery process, proper soil conservation practices can be carried out.

Information about recovery time also influences the choice of the next species to be planted after logging. High or moderately high risk land with a long recovery time should preferably be planted with longer-cycle species instead of fast-growing ones. By planting trees with a longer cycle, disturbance to the environment will be minimized.

7.3.2 The Use of Heavy Rain Data

If heavy rain data are available, it is possible to determine more accurately areas that are prone to debris slides and landslides. Analysing areas prone to mass movement erosion is similar to analysing areas prone to soil erosion, but with more emphasis on geology and high intensity rainfall events. Adding this information to the already available erosion prediction will give a more complete picture to forest planners and decision makers about the vulnerability of an area.

7.3.3 Valuation of Biodiversity Factor

In this study, the biodiversity asset was valued using certain assumptions based on land cover type. In the future this value should be assessed using more detailed ground sampling. An inventory of micro-organism activities should be undertaken for mixed and monotype forests, and a comparison made with open land. Such activity tends to diminish when the soil is bare or subjected to disturbance like when it is being logged. The proposed technique does allow other values to be incorporated into the analysis. Mapping the biodiversity asset should increase the accuracy of the erosion risk analysis.

7.3.4 Readjustment of Land Cover Classification Method

The land cover classes may need to be adjusted after comparing them more closely with field conditions. For instance, since villages are most often surrounded by trees, it may be a good idea for villages to be classified using both RGB-754 and NDVI. Using both datasets to classify villages, it may be possible to separate villages from open land and mixed forest.

REFERENCES

Achard, F., Eva, H., & Mayaux, P. (2001). Tropical forest mapping from coarse spatial resolution satellite data: production and accuracy assessment issues. *International Journal of Remote Sensing, 22*(14), 2741-2762.

Aguma, R., & Hussin, Y. A. (2002). *The use of Remote Sensing and GIS to Support Sustainable Management of Tropical Forest in East Kalimantan, Indonesia.* Retrieved 15 September, 2004, from www.gisdevelopment.net/application/environment/conservation/geom0009pf.htm

Amore, E., Modica, C., Nearing, M. A., & Santoro, V. C. (2004). Scale effect in USLE and WEPP application for soil erosion computation from three Sicilian basins. *Journal of Hydrology, 293*(1-4), 100-114.

Aplin, P. (2004). Remote sensing: land cover. *Progress in Physical Geography, 28*(2), 283-293.

Asdak, C. (2002). *Hidrologi dan Pengelolaan Daerah Aliran Sungai [Hydrology and Watershed Management]* (2 ed.). Yogyakarta: Gadjah Mada University Press.

Barbier, E. B., & Bishop, J. T. (1995). Economic values and incentives affecting soil and water conservation in Developing-Countries. *Journal of Soil and Water Conservation, 50*(2), 133-137.

Bartsch, K. P., Van Miegroet, H., Boettinger, J., & Dobrowolski, J. P. (2002). Using empirical erosion models and GIS to determine erosion risk at Camp Williams, Utah. *Journal of Soil and Water Conservation, 57*(1), 29-37.

Bettinger, P., & Wing, M. G. (2004). *Geographic Information Systems. Applications in Forestry and Natural Resources Management.* New York: McGraw Hill Co.

Bhandari, S. P., & Hussin, Y. A. (2003). *A comparison of Sub-Pixel and maximum likelihood classification of Landsat ETM+ images to detect illegal logging in the tropical rain forest of Berau, east Kalimantan, Indonesia.* Retrieved 7 April, 2004, from http://www.gisdevelopment.net/technology/ip/ma03167pf.htm

Bhuyan, S. J., Marzen, L. J., Koelliker, J. K., Harrington, J. A., & Barnes, P. L. (2002). Assessment of runoff and sediment yield using remote sensing, GIS, and AGNPS. *Journal of Soil and Water Conservation, 57*(6), 351-364.

BIOTROP. (2003). *BIOTROP Training and Information Center.* Retrieved 15 September, 2004, from http://btic.biotrop.org/about.htm

Bloschl, G. (1999). Scaling issues in snow hydrology. *Hydrological Processes, 13*(14-15), 2149-2175.

Boggs, G., Devonport, C., Evans, K., & Puig, P. (2001). GIS-based rapid assessment of erosion risk in a small catchment in the wet/dry tropics of Australia. *Land Degradation & Development, 12*(5), 417-434.

Botanical Institute. (2002, 24 October). *Vegetation and Remote Sensing*. Retrieved 9 May, 2003, from www.uib.no/bot/kurs/bb209/correction.pdf

Brown, R. E., & Richardson, M. L. (1998). *Soil erosion risk mapping using remote sensing derived data in Eastern Paraguay*. Paper presented at the Conference and Exhibition of the Remote Sensing Society, The University of Greenwich, 9 - 11 September 1998.

Bruijnzeel, L. A. (2004). Hydrological functions of tropical forests: not seeing the soil for the trees? *Agriculture Ecosystems & Environment, 104*(1), 185-228.

Bugmann, H., Lindner, M., Lasch, P., Flechsig, M., Ebert, B., & Cramer, W. (2000). Scaling issues in forest succession modelling. *Climatic Change, 44*(3), 265-289.

Bureau of Meteorology. (2004). *Vegetation monitoring products derived from NOAA satelite data*. Retrieved 22 September, 2004, from www.bom.gov.au/sat/NDVI/NDVI12.shtml

California Department of Conservation. (1999). *Factors affecting landslides in forested terrain. Note 50*. Retrieved 12 July, 2005, from www.consrv.ca.gov/cgs/information/publications/cgs_notes/note_50/note50.pdf

Campbell, J. B. (2002). *Introduction to Remote Sensing* (3rd ed.). New York: The Guilford Press.

Carmel, Y., Dean, D. J., & Flather, C. H. (2001). Combining location and classification error sources for estimating multi-temporal database accuracy. *Photogrammetric Engineering and Remote Sensing, 67*(7), 865-872.

Central Board Statistics of Kebumen Regency. (2003). *Kebumen in Figures 2003*: Regional Development Planning Board of Kebumen Regency and Central Board Statistics of Kebumen Regency.

Chang, T. J., Bayes, T. D., & McKeever, S. (2003). Investigating reservoir sediment and watershed erosion using a geographical information system. *Hydrological Processes, 17*(5), 979-987.

Chavez, P. (1996). Image-based atmospheric correction - Revisited and improved. *Photogrammetric Engineering and Remote Sensing, 62*(9), 1025 - 1036.

Cheesman, J., Cutler, M., Douglas, I., McMorrow, J., Foody, G., & Walsh, R. (2000). Spatially modelling the soil erosion risk of tropical forest exploitation systems in South East Asia, *4th International Conference on Integrating GIS and Environmental Modeling (GIS/EM4): Problems, Prospects and Research Needs* (Vol. 217, pp. 1-9). Banff, Alberta: Canada.

Civco, D. L. (1989). Topographic normalization of Landsat Thematic Mapper digital imagery. *Photogrammetric Engineering and Remote Sensing, 55*(9), 1303-1309.

Cleaves, E. T. (2003). Conceptual model for transferring information between small watersheds. *Environmental Geology, 45*(2), 190-197.

Cohen, M. J., Shepherd, K. D., & Walsh, M. G. (2005). Empirical reformulation of the Universal Soil Loss Equation for erosion risk assessment in a tropical watershed. *Geoderma, 124*(3-4), 235-252.

Colby, J. D., & Keating, P. L. (1998). Land cover classification using Landsat TM imagery in the tropical highlands: the influence of anisotropic reflectance. *International Journal of Remote Sensing, 19*(8), 1479-1500.

Convention on Biological Diversity. (2002, 5 September 2002). *Forest Biodiversity Definitions*. Retrieved 16 February, 2004, from www.biodiv.org/programmes/areas/forest/definitions.asp

Coppin, P., Nackaerts, K., Queen, L., & Brewer, H. (2001). Operational monitoring of green biomass change for forest management. *Photogrammetric Engineering and Remote Sensing, 67*(5), 603-611.

Darmawan, M., Aniya, M., & Tsuyuki, S. (2001). *Forest fire hazard using remote sensing and geographic information systems: Toward understanding of land and forest degradation in lowland areas of East Kalimantan, Indonesia.* Retrieved 14 July, 2004, from www.crisp.nus.edu.sg/~acrs2001/pdf/234darmawan.pdf

de Barry, P. A. (2004). *Watersheds. Processes, Assessment, and Management*. New Jersey: John Wiley & Sons, Inc.

Dillaha, T. A., Wolfe, M. L., Shirmohammadi, A., & Byne, F. W. (2001). *ANSWERS History*. Retrieved 31 March, 2003, from http://dillaha.bse.vt.edu/answers/AnswersHistory.html

Dixon, J. A., & Easter, K. W. (1986). Integrated watershed management: An approach to resource management. In K. W. Easter, J. A. Dixon & M. M. Hufschmidt (Eds.), *Watershed Resources Management. An Integrated Framework with Studies from Asia and the Pacific* (pp. 3-15). Honolulu, Hawaii: East West Centre.

Donoghue, D. N. M. (2002). Remote sensing: environmental change. *Progress in Physical Geography, 26*(1), 144-151.

Dorren, L. K. A., Maier, B., & Seijmonsbergen, A. C. (2003). Improved Landsat-based forest mapping in steep mountainous terrain using object-based classification. *Forest Ecology and Management, 183*(1-3), 31-46.

Dwivedi, R. S., Kandrika, S., & Ramana, K. V. (2004). Comparison of classifiers of remote sensing data for land use/land cover mapping. *Current Science, 86*(2), 328 - 335.

Dymond, J. R., & Shepherd, J. D. (1999). Correction of the topographic effect in remote sensing. *IEEE Transactions on Geoscience and Remote Sensing, 37*(5), 2618 - 2620.

Dymond, J. R., & Shepherd, J. D. (2004). The spatial distribution of indigenous forest and its composition in the Wellington region, New Zealand, from ETM plus satellite imagery. *Remote Sensing of Environment, 90*(1), 116-125.

Dymond, J. R., Shepherd, J. D., & Qi, J. (2001). A simple physical model of vegetation reflectance for standardising optical satellite imagery. *Remote Sensing of Environment, 75*(3), 350 - 359.

Ekstrand, S. (1996). Landsat TM-based forest damage assessment: Correction for topographic effects. *Photogrammetric Engineering and Remote Sensing, 62*(2), 151 - 161.

Elliot, W. J., Foltz, R. B., & Robichaud, P. R. (2000). Measuring and Modelling Soil Erosion Processes in Forests. *Landwards, 55*(2), 18 - 25.

Elliot, W. J., Robichaud, P. R., Hall, D. E., Cuhaciyan, C. O., Pierson, F. B., & Wohlgemuth, P. M. (2001). *A Probabilistic Approach to Modeling Erosion for Spatially-Varied Conditions.* Paper presented at the ASAE Annual International Meeting, St Joseph, MI.

El-Swaify, S. A. (1993). Soil erosion and conservation in the humid tropics. In D. Pimentel (Ed.), *World soil erosion and conservation* (pp. 233 - 255). Cambridge: Cambridge University Press.

ESRI Support Centre. (2004, 30 November). *GIS Dictionary*. Retrieved 15 December, 2004, from http://support.esri.com/index.cfm?fa=knowledgebase.gisDictionary.gateway

Fahsi, A., Tsegaye, T., Tadesse, W., & Coleman, T. (2000). Incorporation of digital elevation models with Landsat-TM data to improve land cover classification accuracy. *Forest Ecology and Management, 128*(1-2), 57-64.

FAO. (1999). *State of the World's Forest.* Retrieved 4 October, 2005, from www.fao.org/documents/show_cdr.asp?url_file=///docrep/W9950E/w9950e00.htm

Fletcher, R. J., & Gibb, R. G. (1990). *Land Resource Survey Handbook for Soil Conservation Planning in Indonesia.* Jakarta : Ministry of Forestry, Directorate General Reforestation and Land Rehabilitation Indonesia ; Palmerston North: DSIR Land Resources.

Foody, G. M., & Hill, R. A. (1996). Classification of tropical forest classes from Landsat TM data. *International Journal of Remote Sensing, 17*(12), 2353-2367.

Forest Stewardship Council International Center. (2000). *FSC Principles and Criteria.* Retrieved 4 October, 2005, from www.forest-network.org/FSC/FSC-principles_and_criteria.htm

Franklin, S. E. (2001). *Remote Sensing for Sustainable Forest Management.* USA: Lewis Publisher.

Gao, J., Chen, H. F., Zhang, Y., & Zha, Y. (2004). Knowledge-based approaches to accurate mapping of mangroves from satellite data. *Photogrammetric Engineering and Remote Sensing, 70*(11), 1241-1248.

Giles, P. T. (2001). Remote sensing and cast shadows in mountainous terrain. *Photogrammetric Engineering and Remote Sensing, 67*(7), 833-839.

Goodchild, M. F., & Quattrochi, D. A. (1996). Scale, Multiscaling, Remote Sensing and GIS. In D. A. Quattrochi & M. F. Goodchild (Eds.), *Scale in Remote Sensing and GIS* (pp. 1-11). Boca Raton, Fla.: Lewis Publishers.

Goovaerts, P. (1999). Using elevation to aid the geostatistical mapping of rainfall erosivity. *Catena, 34*(3-4), 227-242.

Goovaerts, P. (2000). Geostatistical approaches for incorporating elevation into the spatial interpolation of rainfall. *Journal of Hydrology, 228*(1-2), 113-129.

Gopal, S., & Woodcock, C. (1994). Theory and Methods for Accuracy Assessment of Thematic Maps Using Fuzzy-Sets. *Photogrammetric Engineering and Remote Sensing, 60*(2), 181-188.

Gournellos, T., Evelpidou, N., & Vassilopoulos, A. (2004). Developing an erosion risk map using soft computing methods (case study at Sifnos Island). *Natural Hazards, 31*(1), 63-83.

Grossman, R., & Forrester, A. L. (2001, January). *Exploring Remote Sensing through Forestry Applications.* Retrieved 10 September, 2004, from www.csa.com/hottopics/remote/overview.html

Gu, D., & Gillespie, A. (1998). Topographic normalization of landsat TM images of forest based on subpixel Sun-canopy-sensor geometry. *Remote Sensing of Environment, 64*(2), 166-175.

Gu, D., Gillespie, A. R., Adams, J. B., & Weeks, R. (1999). A Statistical Approach for Topographic Correction of Satellite Images by Using Spatial Context Information. *IEEE Transactions on Geoscience and Remote Sensing, 37*(1), 236 - 246.

Guenni, L., & Hutchinson, M. F. (1998). Spatial interpolation of the parameters of a rainfall model from ground-based data. *Journal of Hydrology, 213*(1-4), 335-347.

Hamilton, L. S., & Pearce, A. J. (1986). Biophysical Aspects in Watershed Management. In K. W. Easter, J. A. Dixon & M. M. Hufschmidt (Eds.), *Watershed Resources Management. An Integrated Framework with Studies from Asia and the Pacific* (pp. 33 - 52). Honolulu, Hawaii: East West Centre.

Hancock, G. R. (2005). The use of digital elevation models in the identification and characterization of catchments over different grid scales. *Hydrological Processes, 19*(9), 1727-1749.

Hartanto, H., Prabhu, R., Widayat, A. S. E., & Asdak, C. (2003). Factors affecting runoff and soil erosion: plot-level soil loss monitoring for assessing sustainability of forest management. *Forest Ecology and Management, 180*(1-3), 361-374.

Haugland, M. (1998). *The Rain Shadow Effect.* Retrieved 24 May, 2005, from http://www.weatherpages.com/rainshadow/

Hegg, K. M., & Driscoll, R. S. (1982). Remote sensing applications to National Forest Inventories. In C. J. Johannsen & J. L. Sanders (Eds.), *Remote Sensing for Resource Management* (pp. 506 - 511). Ankeny, Iowa: Soil Conservation Socicty of America.

Hidayat, Y. (2002). *Aplikasi model ANSWERS dalam memprediksi erosi dan aliran permukaan di DTA Bodong Jaya dan DAS Way Besay Hulu, Lampung Barat (Using ANSWERS model in predicting erosion and surface runoff inBodong Jaya nad Way Besay Hulu watersheds, West Lampung).* Institut Pertanian Bogor, Bogor.

Higman, S., Bass, S., Judd, N., Mayers, J., & Nussbaum, R. (1999). *The Sustainable Forestry Handbook.* London: Earthscan Publication Ltd.

Hutchinson, M. F. (1995). Interpolating mean rainfall using thin plate smoothing splines. *International Journal of Geographical Information Systems, 9*(4), 385 - 403.

Hutchinson, M. F. (1998a). Interpolation of Rainfall Data with Thin Plate Smoothing Splines - Part I: Two Dimensional Smoothing of Data with Short Range Correlation. *Journal of Geographic Information and Decision Analysis, 2*(2), 139 - 151.

Hutchinson, M. F. (1998b). Interpolation of Rainfall Data with Thin Plate Smoothing Splines - Part II: Analysis of Topographic Dependence. *Journal of Geographic Information and Decision Analysis, 2*(2), 152 - 167.

Hutchinson, M. F. (2004). ANUSplin User Guide (Version 4.3). Canberra.

Hutchinson, M. F., & Gessler, P. E. (1994). Splines - More Than Just a Smooth Interpolator. *Geoderma, 62*(1-3), 45-67.

Huth, A., & Ditzer, T. (2001). Long-term impacts of logging in a tropical rain forest - a simulation study. *Forest Ecology and Management, 142*(1-3), 33-51.

Hyyppa, J., Hyyppa, H., Inkinen, M., Engdahl, M., Linko, S., & Zhu, Y. H. (2000). Accuracy comparison of various remote sensing data sources in the retrieval of forest stand attributes. *Forest Ecology and Management, 128*(1-2), 109-120.

Jensen, J. R. (1986). *Introductory Digital Image Processing. A Remote Sensing Perspective.* New Jersey: Prentice-Hall.

Jetten, V., de Roo, A., & Favis-Mortlock, D. (1999). Evaluation of field-scale and catchment-scale soil erosion models. *Catena, 37*(3-4), 521-541.

Kesteven, J. L., & Hutchinson, M. F. (1996). *Spatial Modelling of Climatic Variables on A Continental Scale. Paper presented at the The 3rd International Conference/Workshop on Integrating GIS and Environmental Modeling, Santa Fe, NM, Jan 21 - 25, 1996.* Retrieved 7 September, 2005, from www.ncgia.ucsb.edu/conf/SANTA_FE_CD-ROM/sf_papers/kesteven_jennifer/jlkpaper.html

King, R. B. (2002). Land cover mapping principles: a return to interpretation fundamentals. *International Journal of Remote Sensing, 23*(18), 3525-3545.

Kirkby, M. J., Imeson, A. C., & Cammeraat, L. H. (1996). Scaling up processes and models from the field plot to the watershed and regional areas. *Journal of Soil and Water Conservation, 51*(5), 391 - 396.

Kusumandari, A., & Mitchell, B. (1997). Soil Erosion and Sediment Yield in Forest and Agroforestry Areas in West Java, Indonesia. *Journal of Soil and Water Conservation, 52*(4), 376 - 380.

Lal, R. (1990a). *Soil Erosion in the Tropics. Principles and Management.* New York: McGraw-Hill, Inc.

Lal, R. (1990b). Trees and Soil Erosion. In *Soil Erosion in the Tropics: Principles and Management* (pp. 423 - 485). New York: McGraw-Hill, Inc.

Lal, R. (2001). Soil degradation by erosion. *Land Degradation & Development, 12*(6), 519-539.

Lee, S. (2004). Soil erosion assessment and its verification using the Universal Soil Loss Equation and Geographic Information System: A case study at Boun, Korea. *Environmental Geology, 45*(4), 457-465.

Lepoutre, D., Royer, A., & Lantieri, D. (1998, December). *Use of high-resolution satellite data for irrigation management and monitoring. Pilot study in Indonesia.* Retrieved 15 September, 2004, from www.fao.org/sd/Eldirect/Elre0009.htm

Liang, S. L., Fang, H. L., & Chen, M. Z. (2001). Atmospheric correction of landsat ETM plus land surface imagery. Part I: Methods. *IEEE Transactions on Geoscience and Remote Sensing, 39*(11), 2490 - 2498.

Liang, S. L., Fang, H. L., Morisette, J. T., Chen, M. Z., Shuey, C. J., Walthall, C. L., *et al.* (2002). Atmospheric correction of landsat ETM plus land surface imagery - Part II: Validation and applications. *IEEE Transactions on Geoscience and Remote Sensing, 40*(12), 2736-2746.

Lillesand, T. M., Kiefer, R. W., & Chipman, J. W. (2004). *Remote Sensing and Image Interpretation* (5 ed.). New York; Chichester: John Wiley & Sons, Inc.

Lin, H. S., Wheeler, D., Bell, J., & Wilding, L. (2005). Assessment of soil spatial variability at multiple scales. *Ecological Modelling, 182*(3-4), 271-290.

Liu, J. G., Mason, P., Hilton, F., & Lee, H. (2004). Detection of rapid erosion in SE Spain: A GIS approach based on ERS SAR coherence imagery. *Photogrammetric Engineering and Remote Sensing, 70*(10), 1179-1185.

Lu, D., Li, G., Valladares, G. S., & Batistella, M. (2004). Mapping soil erosion risk in Rondonia, Brazilian Amazonia: Using RULSE, remote sensing and GIS. *Land Degradation & Development, 15*(5), 499-512.

MacEwan, R., Bluml, M., McNeill, J., & Reynard, K. (2004a). *Land Use Impact Modelling for Native Biodiversity Risk* (No. ESAI Project 05116): Ecologically Sustainable Agriculture Initiative. Departmeny of Primary Industries.

MacEwan, R., McNeill, J., & Clarkson, T. D. (2004b). *Developing a regional soil health strategy using a land use impact model.* Paper presented at the SuperSoil 2004. International Soil Science Conference 5 - 9 December 2004, Sydney, Australia.

Masek, J. G., Honzak, M., Goward, S. N., Liu, P., & Pak, E. (2001). Landsat-7 ETM+ as an observatory for land cover Initial radiometric and geometric comparisons with Landsat-5 Thematic Mapper. *Remote Sensing of Environment, 78*(1-2), 118-130.

McKenney, D. W., Hutchinson, M. F., Kesteven, J. L., & Venier, L. A. (2001). Canada's plant hardiness zones revisited using modern climate interpolation techniques. *Canadian Journal of Plant Science, 81*(1), 129-143.

Metternicht, G., & Gonzalez, S. (2005). FUERO: foundations of a fuzzy exploratory model for soil erosion hazard prediction. *Environmental Modelling & Software, 20*(6), 715-728.

Metternicht, G. I., & Zinck, J. A. (1998). Evaluating the information content of JERS-1 SAR and Landsat TM data for discrimination of soil erosion features. *ISPRS Journal of Photogrammetry and Remote Sensing, 53*(3), 143-153.

Nasendi, B. D. (2000). Deforestation and Forest Policies in Indonesia. In M. Palo & H. Vanhanen (Eds.), *World Forests from Deforestation to Transition?* (pp. 167 - 182). Dordrecht ; Boston: Kluwer Academic Publishers.

The New International Atlas. (1996). Rand Mc Nally & Company.

Nezry, E., Yakam-Simen, F., Romeijn, P., Supit, I., & Demargne, L. (2000). *Advanced Remote Sensing Techniques for Forestry Applications: A Case Study in Sarawak (Malaysia).* Retrieved 17 April, 2003, from www.treemail.nl/download/sci-00.pdf

NOAA Coastal Service Center. (2005, 29 September). *What does accuracy mean in GIS and remote sensing.* Retrieved 3 November, 2005, from http://www.csc.noaa.gov/crs/lca/faq_tech.html

Oliver, C. J. (2000). Rain forest classification based on SAR texture. *IEEE Transactions on Geoscience and Remote Sensing, 38*(2), 1095-1104.

Pemerintah Kab. Banjarnegara. (2003). *Kabupaten Banjarnegara [Banjarnegara District]*. Retrieved 5 November, 2004, from www.banjarnegara.go.id/

Pemerintah Kab. Kebumen. (2002). *Kabupaten Kebumen [Kebumen District]*. Retrieved 5 November, 2004, from www.kebumen.go.id/

Petit, C. C., & Lambin, E. F. (2001). Integration of multi-source remote sensing data for land cover change detection. *International Journal of Geographical Information Science, 15*(8), 785-803.

Pickett, S. T. A., & Cadenasso, M. L. (1995). Landscape Ecology - Spatial Heterogeneity in Ecological-Systems. *Science, 269*(5222), 331-334.

Price, D. T., McKenney, D. W., Nalder, I. A., Hutchinson, M. F., & Kesteven, J. L. (2000). A comparison of two statistical methods for spatial interpolation of Canadian monthly mean climate data. *Agricultural and Forest Meteorology, 101*(2-3), 81-94.

Priyono, C. N. S., & Savitri, E. (1998). *Erosi Tanah-Limpasan Permukaan pada Peremajaan Hutan Pinus dan pada Alternatif Pola Penebangan Hutan Pinus [Soil erosion-runoff in the Pine Reforestation and on the logging alternative method area]*. Paper presented at the Prosiding Seminar Nasional Pengelolaan Hutan dan Produksi Air untuk Kelangsungan Pembangunan [*Proceeding on the Seminar on the forest management and water production for the sustainable development*], Jakarta.

Rao, D. P. (2001). A remote sensing-based integrated approach for sustainable development of land water resources. *IEEE Transactions on Systems Man and Cybernetics Part C-Applications and Reviews, 31*(2), 207-215.

Renschler, C. S. (2000). *Strategies for Implementing Natural Resource Management Tools. A Geographic Information Science Perspective on Water and Sediment Balance Assessment at Different Scales.* University of Bonn, Bonn.

Renschler, C. S., & Harbor, J. (2002). Soil erosion assessment tools from point to regional scales-the role of geomorphologists in land management research and implementation. *Geomorphology, 47*(2-4), 189-209.

Reynolds, S. G. (1990). The Influence of Forest Clearance Methods. Tillage and Slope Runoff on Soil Chemical Properties and Banana Plants Yield in the South Pacific. In J. Boardman, I. D. L. Foster & J. A. Dearing (Eds.), *Soil Erosion on Agricultural Land* (pp. 339 - 350). Chichester, West Sussex, England ; New York: John Wiley & Sons Ltd.

Riaño, D., Chuvieco, E., Salas, J., & Aguado, I. (2003). Assesment of Different Topographic Corrections in Landsat -TM Data for Mapping Vegetation Types. *IEEE Transactions on Geoscience and Remote Sensing, 41*(5), 1056 - 1061.

Richardson, B., Skinner, M. F., & West, G. (1999). The role of forest productivity in defining the sustainability of plantation forests in New Zealand. *Forest Ecology and Management, 122*(1-2), 125-137.

RSGISForum. (2005). *Indonesian Remote Sensing and GIS*. Retrieved 8 March, 2005, from http://inisiatif.rsgisforum.net/indexe.html

Sadhardjo Siswomartana. (2005). Production Director, Perum Perhutani. Jakarta.

Shepherd, J. D., & Dymond, J. R. (2003). Correcting satellite imagery for the variance of reflectance and illumination with topography. *International Journal of Remote Sensing, 24*(17), 3503-3514.

Short, N. M. (2004, 15 July). *Section 13: Collecting data at the surface - ground truth; the "multi" concept; Hyperspectral imaging spectroscopy*. Retrieved 2 November, 2005, from http://rst.gsfc.nasa.gov/Sect13/Sect13_3.html

SJFCSP. (2001). *Final Report. Component E : Upper Catchment Land Rehabilitation (Under ADB Loan : 1479 - INO)*. Indonesia.

Skidmore, A. K. (1989). An expert system classifies Eucalypt forest types using Thematic Mapper Data and a Digital Terrain Model. *Photogrammetric Engineering and Remote Sensing, 55*(10), 1449-1464.

Smith, G. S. (1993). Forestry and Remote Sensing. In H. J. Buiten & J. G. P. W. Clevers (Eds.), *Land Observation by Remote Sensing: Theory and Application* (pp. 451 - 457). Singapore: Gordon & Breach Science Publishers.

Standard Australia, & Standard New Zealand. (2004). *Risk Management Guidelines. Companion to AS/NZS 4360:2004*: Standards New Zealand.

Stott, T. (2005). Natural recovery from accelerated forest ditch and stream bank erosion five years after harvesting of plantation forest on Plynlimon, mid-Wales. *Earth Surface Processes and Landforms, 30*(3), 349-357.

Sumner, G. (1988). *Precipitation, Process and Analysis*. Great Britain: The Bath Press.

Sun, G., & McNulty, S. G. (1999). *Modeling Soil Erosion and Transport on Forest Landscape*. Retrieved 31 March, 2003, from www.srs.usda.gov/pubs/rpc/1999-06/rpc_99jun36.pdf

Suprapto, A. (2002, 3-5 October 2001). *Land and Water Resources Development in Indonesia*. Paper presented at the Investment in Land and Water, Bangkok, Thailand.

Sutikno. (2005). Pusat Study Bencana Alam (*Center of Disaster Studies*), Gadjah Mada University. Yogyakarta, Indonesia.

The Weather Channel. (no date). *Weather Glossary*. Retrieved 6 January, 2006, from http://www.weather.com/glossary/

Thomas, I. L., Benning, V. M., & Ching, N. P. (1987). *Classification of Remotely Sensed Images*. Bristol: Adam Higler.

Toy, T. J., Foster, G. R., & Renard, K. G. (2002). *Soil Erosion: Processes, Prediction, Measurement, and Control*. New York: John Wiley & Sons, Inc.

Tripathi, N. K., & Radiarta, N. (2003). *Mapping Coral Reef Habitat in Indonesia using Remote Sensing*. Retrieved 15 September, 2004, from www.gisdevelopment.net/application/nrm/ocean/ma03187abs.htm

Trippett, J. (2002, February - March). Forest in Crisis. *GIS User, 50,* 40 - 41.

UU No. 41 tentang Kehutanan [*The Law Number* 41 *on Forestry*], (1999).

Vieira, I. C. G., de Almeida, A. S., Davidson, E. A., Stone, T. A., de Carvalho, C. J. R., & Guerrero, J. B. (2003). Classifying successional forests using Landsat spectral properties and ecological characteristics in eastern Amazonia. *Remote Sensing of Environment, 87*(4), 470-481.

Vricling, A., Sterk, G., & Beaulieu, N. (2002). Erosion risk mapping: A methodological case study in the Colombian Eastern Plains. *Journal of Soil and Water Conservation, 57*(3), 158-163.

Wang, G., Gertner, G., Fang, S., & Anderson, A. B. (2003). Mapping Multiple Variables for Predicting Soil Loss by Geostatistical Methods with TM Images and a Slope Map. *Photogrammetric Engineering and Remote Sensing, 69*(8), 889-898.

Waryono, Rivai Ali, & Gunawan, D. H. (1987). *Pengantar Meteorologi dan Klimatologi [Introduction to Meteorology and Climatology]*. Surabaya: PT. Bina Ilmu.

Wischmeier, W. H. (1976). Use and Misuse of Universal Soil Loss Equation. *Journal of Soil and Water Conservation, 31*(1), 5-9.

Wischmeier, W. H., & Smith, D. D. (1978). *Predicting rainfall erosion losses - a guide to conservation planning*. Washington: U.S. Department of Agriculture, Agriculture Handbook No. 537.

Woodcock, C. E., Macomber, S. A., Pax-Lenney, M., & Cohen, W. B. (2001). Monitoring large areas for forest change using Landsat: Generalization across space, time and Landsat sensors. *Remote Sensing of Environment, 78*(1-2), 194-203.

Wulder, A. A., Skakun, R. S., Kurz, W. A., & White, J. C. (2004). Estimating time since forest harvest using segmented Landsat ETM+ imagery. *Remote Sensing of Environment, 93*(1-2), 179-187.

Xavier, A. C., & Vettorazzi, C. A. (2004). Monitoring Leaf Area Index at watershed level through NDVI from Landsat-7/ETM+ data. *Sci. Agric. (Piracicaba, Brazil), 61*(3), 243-252.

Xie, Y., Liu, B., & Nearing, M. A. (2002). Practical thresholds for separating erosive and non-erosive storms. *Transactions of the ASAE, 45*(6), 1843-1847.

Zhang, X. Y., Drake, N. A., Wainwright, J., & Mulligan, M. (1999). Comparison of slope estimates from low resolution DEMs: Scaling issues and a fractal method for their solution. *Earth Surface Processes and Landforms, 24*(9), 763-779.

Zhuang, X., Engel, B. A., Xiong, X. P., & Johannsen, C. J. (1995). Analysis of Classification Results of Remotely-Sensed Data and Evaluation of Classification Algorithms. *Photogrammetric Engineering and Remote Sensing, 61*(4), 427-433.

Ziemer, R. R. (1986). *Soil Erosion and Management Activities on Forested Slopes*. Retrieved 8 August, 2003, from www.rsl.psw.fs.fed.us/projects/water/yearag86.pdf

Ziemer, R. R., Lewis, J., Rice, R. M., & Lisle, T. E. (1991). Modelling the Cumulative Watershed Effects of Forest Management Stategies. *Journal of Environmental Quality, 20*, 36 - 42.

APPENDIX A. DESCRIPTION OF THE GEOLOGICAL UNIT

These descriptions are the extended legend of the 1:100000 geological map made by the Geological Research and Development Centre, Directorate General of Geology and Mineral Resources, Department of Mines and Energy on 1992.

Symbol	Explanation
Km	**SCHIST AND PHYLLITE:** Amphibol, mica, glaucophane schists and phyllite as tectonic inclusions
Kobe/Kose	**BASALT AND CHERT:** Basaltic pillowlava and radiolarian chert as tectonic inclusions
Kog	**GABBRO:** Gabbro as tectonic inclusions
Kose	**SERPENTINITE:** brecciated serpentinites, commonly angular, as tectonic inclusions
KTl	**LUK ULO COMPLEX:** Melange, consisting of various sizes of blocks and tectonically mixed, that embedded within broken and sheared shale and dark grey siltstone. Blocks comprise basalt, black and red cherts, mafics and ultramafics (Kog); schist and phyllite (Km); greywacke (KTs); granite, silicified tuff and grey and red limestone. Commonly, the blocks are elongate. Lithological boundary is a tectonic contact. Highly folded shert, sub-parallel to the bedding, alternates with red claystone. In some places, landslide evidences are recognised. Red limestone, containing cretaceous radiolaria and chert are presumed to be deposited biogenetically in shallow marine environment. Basalt, interfingering commonly with chert, is tectonically bounded. Presumably, granite and quartz- porphyry were originated from igneous rock. Within the rock, dominated by matrix, fish-structure is present. Northwards, matrix is dominant. The complex is Late Cretaceous-Paleocene in age.

Symbol	Explanation
KTm/Km	**BRECCIATED ROCKS:** Fragments, consisting of altered sediments and volcanics, granite, quartz-plagioclase porphyry, gabbro, amphibolite, serpentinite, and tuff; brecciated, tectonically intermixed, and upthrusted on the Cretaceous sediments. Some of granite and porphyry were presumedto be originated from igneous rock, and the rest from silicified tuff and metamorphosed sediments
KTog	**MAFICS AND ULTRAMAFICS:** Gabbro, amphibolite, basalt, and serpentinite. Gabbro, pale green, embedded with marl. Locally, it shows distinctive contact. The rocks are tectonically bounded within the Luk Ulo Complex. Basalt altered, as pillow lava, tholeitic (Asikin, 1974); directly contact with tuffaceous sediments and tuff. Serpentinite, as intercalation or lenses within gabbro and basalt, directly contact with schist, brecciated and highly sheared. Early Cretaceous in age.
KTs	**GREYWACKE:** Greywacke and conglomerate. Greywacke recognised as block or tectonically bounded, fine-coarse grained, greenish dark grey, graded-bedding; consists of quartz, feldspar, calcite, glass, and rock fragments; locally 'boundinage'; commonly, as fragments embedded within shaly matrix. Conglomerate is polymictic. Deposited as a turbidite in a fast subsiding basin, together with black claystone, siltstone, and mudstone. The age is Late Cretaceous-Paleocene.
Qa	**ALLUVIUM:** Pebbles, sands, silts, and clay; as river and swamp deposits. Thickness up to 150 m. (Clay, silt, sand, gravel and pebble)
QTlb	**BRECCIA MEMBER OF LIGUNG FORMATION:** Andesitic volcanic breccia (agglomerate), hornblende andesitic lava, and tuff; forming upper sequence of the Ligung Formation
Tekl	**REEF LIMESTONE:** Reef limestone as olistolith
Teok	**KARANG SAMBUNG FORMATION:** Scaly clay with fragments of limestone, conglomerates, sandstone, claystone and basalts
Tmd	**DIABASE:** Diabase, as sill with columnar jointing

Symbol	Explanation
Tmk	**KALIPUCUNG FORMATION:** Reef limestone, locally clastic limestone bituminous shale in the lower part
Tmp	**PENOSOGAN FORMATION:** Alternating conglomerate, sandstone, claystone, marl, tuff and rhyolite; well bedded. Lower part compromises polymict conglomerate, consisting of milky quartz, calcarenite fragments with Lepidocyclina. Sandstone is composed mainly of quartz, with minor biotite, tourmaline, rutile, and other heavy minerals; illsorted, calcareous and pebbly, locally. Upwards, gradually turns to be siltstone, thin beds-massive. Graded-bedding. Unit is a turbiditic deposit. Middle part of the sequence is composed of claystone, marl, and calcarenite with tuff intercalation. Calcarenite consists of foraminifera and coralline fragments, angular to sub-rounded, illsorted, cemented by calcite. Pebbley coarse sandstone is still found, thinning upwards. More upwards, predominantly, marl and tuffaceous marl, containing Globigerina, Globoquadrina, Orbulina, and large foraminifers are found. Former name is 'Fossiel Horizont' (Harloff, 1933). Dacitic, rhyolitic, and glassy tuff intercalations are recognised. Ripple-mark, mudrock, graded-bedding, bioturbation, parallel lamination, and flutecast, tend to show a shallow marine or tidal depositional environment. The unit is Middle Miocene age (Tf2-Tf3). Previous name is 'Tweede Mergeltuf Horizont' (Harloff, 1933) with thickness is up to 300 m. Upper part of the unit is made up of alternating tuff and tuffaceous marl. Glassy tuff with 5 – 10 m thick thins upwards. The formation overlies conformably the Waturanda Formation, and is overlain conformably by the Halang Formation. Until thickness is up to 1140 m (Iskandar, 1974)
Tmpb	**BRECCIA MEMBER OF HALANG FORMATION:** Breccia with components of andesite, basalt and limestone, matrix of coarse grained tuffaceous sandstone, intercalations of sandstone and basaltic lava
Tmph	**HALANG FORMATION:** Tuffaceous sandstone, conglomerate, marl and claystone; andesitic breccia in the lower part. Globigerina and other foraminiferas are found within upper sequence. The age is Middle Miocene-Early Pliocene. Thickness of andesitic breccia varies from 200 m in the south to 500 m in the north. Coarse rock debris does not exist within the upper sequence. Deposited as turbidites in upper bathyal zone. Thickness of the unit, thinning to the east up to 700 m.

Symbol	Explanation
Tmw	**WATURANDA FORMATION:** Sandstone, breccia, conglomerate, lahar, and claystone intercalation. Sandstone, greywacke, massive-bedded, 2 – 100 cm thick. Upwards, volcanic breccia, intercalated with greywacke, calcareous tuff, claystone, conglomerate, and lahar is found. Polymict breccia is composed of andesite and basalt, 3 cm – several meters, commonly 30 cm thick; matrix is sandstone and tuff, coarsening upwards. Greywacke intercalation, 50 – 200 cm thick, medium – very coarse grained; composed of plagioclase, pyroxene, glass, and mafic minerals. Claystone contains small foraminifers, Early-Middle Miocene in age. Gradded-beds, parallel lamination, and convolute are recognised. Depositional environment was deep marine, with some part of the unit was deposited by turbiditic current. Overlain conformably by Penosogan Formation, and overlies conformably or partly interfingers with the Totogan Formation. Previous name: 'Eerste Breccie Horizont' (Harloff, 1933). (In the lower part consists of coarse grained sandstone, changes into breccia to the upper part with andesitic-basaltic components; sandstone and tuff matrix)
Tmwt	**TUFF MEMBER, WATURANDA FORMATION:** Alternating glassy, crystal tuff, calcareous sandstone, and tuffaceous marl; compact, well bedded (2 – 80 cm); calcite fills in cracks. Tuff comprises feldspar, glass, quartz and ore minerals. Calcareous sandstone, 4 – 15 m thick, contains planktonic foraminifers, showing late N6 – early N8 (early Miocene) in age. Upper bathyal environment. Thickness from several metres up to 200 m. the unit, present as the lower part of the Waturanda Formation overlies conformably by the Totogan Formation. Former name: 'Eerste Margeltuf Horizont' (Harloff, 1933).
Tomg	**GABON FORMATION:** Breccia with andesitic components, tuff and coarse grained sandstone matrix; locally lapilli tuff, lava and laharic deposits; commonly altered.

Symbol	Explanation
Tomt	**TOTOGAN FORMATION:** Breccia, claystone, marl, sandstone, conglomerate, and tuff. Lower part consists of irregular alternating breccia, tuffaceous claystone intercalation locally. Polymict breccia, angular components, consisting of claystone, slate, sandstone, fossiliferous limestone, basalts, schist, granite, quartz, and radiolarian chert; matrix is tuffaceous calcareous claystone, red-brown-violet chert, cemented by carbonate; generally sheared. Upwards, breccia and sandstone clast are parallel to the bedding. Basaltic conglomerate, unsorted, intercalated within breccia. Upper part of the sequence consists of alternating claystone, sandstone, and tuff; well-bedded; contains quartz fragments. Planktonic foraminifers recognised show that the age of the unit is Oligocene to Early Miocene. Univergina sp. and Glyroldina sp. present show that the depositional environment was upper bathyal. The whole rock unit is an olistostrom deposit. Thickness is about 150 m, thinning to the intergingers with the upper part of the Reefal Limestone Unit.
Tpd	**DAMAR FORMATION:** Tuffaceous claystone, volcanic breccia, sandstone, tuff and conglomerate; lahar deposit, in places. Volcanic breccia and tuff are andesitic in composition, whereas, conglomerate is basaltic and locally compact. Mollusc is found, locally. Depositional environment was non-marine. Overlies conformably the Kalibiuk Formation
Tpp	**PENIRON FORMATION:** Breccia, with tuff intercalation; plant debris and silicified, locally. Breccia polymict; composed ofpyraxene andesite, claystone and limestone clatst; embedded in clayey-tuffaceous sandstone matrix; sandstone, tuff, and marl intercalations are found. Tuff, slightly weathered, silt-medium sand size, moderately sorted, thickness about 20 cm. Unit is present as turbidite, deposited in sub-marine upper fan zone (Suharyanto, 1982). Presumably: Pliocene in age (Suyanto and Kamil, 1975). Thickness is about 700 m. Overlies unconformably by Younger Sumbing Volcanics. Northwards can be correlated to breccia Member of Tapak Formation. As 'Derde Breccie Horizont' (Harloff, 1933)

APPENDIX B. DAILY RAINFALL (mm) FROM 17 STATIONS DURING 1991 – 2000

1991

Station	Jan	Feb	Mar	Apr	May	Jun	Jul	Aug	Sep	Oct	Nov	Dec	Total
Adimulyo	464	529	166	291	0	0	0	0	0	7	407	374	2238
Alian	626	516	119	230	0	0	0	0	0	0	277	279	2047
Karang Anyar	507	520	249	465	40	10	0	0	0	38	386	314	2529
Sempor	--	--	--	322	16	25	0	0	5	97	514	409	--
Rowokele	394	315	198	319	29	9	0	0	0	58	483	290	2095
Gombong	674	478	269	238	31	21	0	0	0	59	544	337	2651
Karang Gayam	467	576	236	312	25	5	0	0	0	42	259	183	2105
Puring	610	464	100	223	0	0	0	0	0	60	868	468	2793
Sadang	--	--	--	--	--	--	--	--	--	--	--	--	--
Wadas Lintang	--	--	--	--	--	--	--	--	--	--	--	--	--
Klirong	762	342	228	358	0	0	0	0	0	45	415	247	2397
Kuwarasan	347	253	269	352	16	9	0	0	0	62	502	379	2189
Kebumen	--	--	--	--	--	--	--	--	--	--	--	--	--
Petanahan	824	479	290	378	0	0	0	0	0	84	424	278	2757
Banjarnegara	261	367	460	376	104	0	0	0	0	167	359	386	2480
Purwanegara	--	--	120	289	0	0	13	0	0	--	393	616	--
Mandiraja	570	440	333	337	0	0	0	0	0	61	385	421	2547

-- = no data

1992

Station	Jan	Feb	Mar	Apr	May	Jun	Jul	Aug	Sep	Oct	Nov	Dec	Total
Adimulyo	209	244	182	237	126	255	0	300	177	821	607	228	3386
Alian	356	303	380	349	100	47	0	299	115	730	441	261	3381
Karang Anyar	206	422	230	244	92	216	39	197	127	665	635	177	3250
Sempor	489	445	330	577	273	144	154	435	268	759	710	419	5003
Rowokele	421	311	330	418	232	217	205	672	316	877	558	367	4924
Gombong	462	404	328	594	260	203	153	405	271	676	474	245	4550
Karang Gayam	151	367	177	327	121	153	65	387	441	504	474	245	3412
Puring	313	452	343	356	445	409	203	300	477	1050	1019	513	5880
Sadang	472	479	839	557	383	84	161	0	250	628	482	595	4930
Wadas Lintang	--	--	--	--	--	--	--	--	--	--	--	--	--
Klirong	380	474	286	655	302	225	130	268	224	845	624	373	4786
Kuwarasan	389	309	280	248	307	150	83	279	328	725	745	295	4138
Kebumen	--	--	--	--	--	--	--	--	--	--	--	--	--
Petanahan	435	519	331	763	302	437	0	210	405	936	806	332	5476
Banjarnegara	563	438	808	646	263	155	100	497	131	606	564	715	5486
Purwanegara	403	317	604	523	180	71	25	240	120	533	750	520	4286
Mandiraja	443	389	464	414	278	160	51	290	130	474	679	476	4248

-- = no data

1993

Station	Jan	Feb	Mar	Apr	May	Jun	Jul	Aug	Sep	Oct	Nov	Dec	Total
Adimulyo	156	329	144	255	148	107	0	12	0	0	399	430	1980
Alian	360	380	241	362	0	166	0	11	0	25	454	264	2263
Karang Anyar	156	325	211	307	100	48	0	15	5	26	441	487	2121
Sempor	560	320	437	372	146	125	0	66	35	31	431	927	3450
Rowokele	265	232	309	262	140	92	0	82	56	54	460	580	2532
Gombong	292	157	251	256	138	75	0	56	32	42	415	584	2298
Karang Gayam	267	400	90	261	49	48	0	0	4	16	305	356	1796
Puring	604	327	426	374	73	214	0	209	90	99	220	575	3211
Sadang	521	--	355	574	242	273	0	0	0	0	637	--	--
Wadas Lintang	677	673	447	400	145	0	0	0	2	127	639	468	3578
Klirong	397	166	277	212	159	132	0	176	64	48	235	491	2357
Kuwarasan	361	268	354	287	64	80	0	98	47	29	448	553	2589
Kebumen	278	209	269	191	100	106	0	27	12	10	408	501	2111
Petanahan	269	467	381	237	123	116	0	178	79	85	581	387	2901
Banjarnegara	716	412	831	761	360	200	0	10	1	116	816	690	4913
Purwanegara	425	193	0	0	0	59	0	75	72	0	0	334	1158
Mandiraja	639	239	458	412	245	119	0	18	72	18	503	469	3192

-- = no data

1994

Station	Jan	Feb	Mar	Apr	May	Jun	Jul	Aug	Sep	Oct	Nov	Dec	Total
Adimulyo	508	240	545	57	38	0	0	0	0	59	108	203	1758
Alian	363	543	809	377	0	0	0	0	0	0	280	174	2546
Karang Anyar	473	174	579	153	77	0	0	0	0	0	48	249	1753
Sempor	636	424	670	383	46	0	5	0	0	39	243	350	2796
Rowokele	564	297	476	360	69	4	0	0	0	3	96	162	2031
Gombong	412	233	615	251	34	0	5	0	0	8	129	196	1883
Karang Gayam	385	161	281	176	6	3	0	0	0	3	100	135	1250
Puring	791	398	533	178	0	0	0	0	0	30	141	264	2335
Sadang	388	632	869	489	140	0	0	0	0	48	263	431	3260
Wadas Lintang	364	362	782	324	100	5	0	0	0	34	390	503	2864
Klirong	592	346	659	356	126	0	0	0	0	41	218	290	2628
Kuwarasan	494	417	574	212	43	10	0	0	0	37	128	154	2069
Kebumen	494	241	589	70	51	6	0	0	0	25	146	313	1935
Petanahan	519	353	594	239	84	0	0	0	0	26	108	251	2174
Banjarnegara	585	426	557	589	18	106	0	1	0	60	465	571	3378
Purwanegara	450	303	381	135	0	39	0	0	0	19	509	277	2113
Mandiraja	583	359	476	250	52	52	3	0	0	46	441	209	2471

-- = no data

1995

Station	Jan	Feb	Mar	Apr	May	Jun	Jul	Aug	Sep	Oct	Nov	Dec	Total
Adimulyo	320	772	237	186	21	283	124	0	0	216	441	390	2990
Alian	589	320	724	218	0	349	0	0	0	369	841	646	4056
Karang Anyar	471	587	113	2484	16	208	27	0	0	305	490	221	2686
Sempor	591	716	657	317	276	361	65	5	4	645	696	535	4868
Rowokele	504	579	390	238	151	453	123	0	0	698	590	340	4066
Gombong	481	671	458	271	204	403	81	0	9	636	470	381	4065
Karang Gayam	288	333	399	258	108	322	22	0	0	386	630	412	3158
Puring	469	684	441	165	147	283	191	0	5	364	469	640	3858
Sadang	525	419	494	361	86	210	75	0	0	235	689	564	3658
Wadas Lintang	451	725	572	253	211	224	123	0	8	472	1094	339	4472
Klirong	468	614	247	72	0	234	165	0	0	113	535	630	3078
Kuwarasan	449	751	326	142	73	345	87	0	8	572	510	411	3674
Kebumen	426	579	301	174	25	134	27	2	0	224	472	387	3802
Petanahan	364	630	236	167	54	217	196	0	0	255	414	376	2909
Banjarnegara	429	917	839	329	369	254	138	0	3	440	955	440	5113
Purwanegara	507	775	439	148	139	239	101	10	0	422	565	405	3750
Mandiraja	459	549	462	240	188	286	74	0	21	522	684	428	3913

-- = no data

1996

Station	Jan	Feb	Mar	Apr	May	Jun	Jul	Aug	Sep	Oct	Nov	Dec	Total
Adimulyo	361	410	428	155	89	0	26	0	0	570	385	575	2999
Alian	787	708	723	101	76	0	0	0	0	873	584	570	4422
Karang Anyar	288	353	354	126	17	0	19	0	0	609	430	303	2499
Sempor	451	681	647	253	55	36	59	21	18	940	745	579	4485
Rowokele	456	654	583	162	92	28	41	64	0	1074	581	501	4236
Gombong	481	522	447	167	33	31	51	23	0	923	457	324	3459
Karang Gayam	333	439	493	86	53	9	13	5	3	509	462	252	2657
Puring	469	647	344	150	62	0	4	0	0	471	647	343	3228
Sadang	--	--	--	--	--	--	--	--	--	--	--	--	--
Wadas Lintang	628	624	451	197	66	117	68	92	7	906	884	381	4421
Klirong	557	789	357	178	69	0	41	0	0	478	543	508	3520
Kuwarasan	349	647	449	257	63	8	29	16	15	899	606	501	3839
Kebumen	--	521	494	160	18	4	41	7	2	609	480	593	--
Petanahan	415	487	341	139	52	77	2	0	0	--	457	510	--
Banjarnegara	450	545	552	517	69	163	46	117	3	864	894	273	4493
Purwanegara	434	473	--	--	--	--	--	--	--	--	--	--	--
Mandiraja	425	406	545	138	15	66	78	137	31	654	579	304	3378

-- = no data

1997

Station	Jan	Feb	Mar	Apr	May	Jun	Jul	Aug	Sep	Oct	Nov	Dec	Total
Adimulyo	174	335	6022	103	0	0	0	0	0	0	82	165	941
Alian	245	472	0	0	119	0	0	0	0	0	59	95	990
Karang Anyar	216	419	94	40	131	0	0	0	0	0	9	248	1157
Sempor	237	620	68	122	76	0	3	0	16	21	104	277	1544
Rowokele	264	377	145	72	144	0	0	0	0	0	45	137	1184
Gombong	209	516	45	54	69	0	0	0	0	7	75	247	1222
Karang Gayam	201	375	76	77	70	0	0	0	0	0	--	--	--
Puring	245	226	80	0	46	0	0	0	0	0	77	132	806
Sadang	--	301	--	--	--	--	--	--	--	--	102	--	--
Wadas Lintang	196	465	162	222	196	31	0	0	0	0	178	418	1868
Klirong	370	395	27	31	97	0	0	0	0	0	144	180	1244
Kuwarasan	207	304	97	50	46	0	0	0	0	0	64	225	993
Kebumen	243	380	96	0	112	0	0	0	0	4	86	195	1116
Petanahan	--	--	--	--	--	--	--	--	--	--	--	--	--
Banjarnegara	366	403	171	364	396	7	0	0	0	2	206	335	2250
Purwanegara	275	--	--	--	--	--	--	--	--	--	--	--	--
Mandiraja	283	355	99	0	0	0	0	0	0	0	--	--	--

-- = no data

1998

Station	Jan	Feb	Mar	Apr	May	Jun	Jul	Aug	Sep	Oct	Nov	Dec	Total
Adimulyo	396	189	305	596	131	310	137	72	184	552	728	428	4028
Alian	291	449	--	597	185	419	400	57	86	608	767	246	--
Karang Anyar	362	341	439	524	144	459	232	66	231	808	569	--	--
Sempor	277	438	489	438	173	502	457	159	251	627	896	643	5350
Rowokele	270	229	431	396	215	503	283	72	129	542	531	470	4071
Gombong	265	305	561	501	117	442	251	79	217	538	650	533	4459
Karang Gayam	173	348	267	507	108	552	282	95	179	539	653	550	4253
Puring	338	260	--	420	--	222	423	138	206	511	382	541	--
Sadang	181	332	5787	702	133	213	263	68	375	732	624	460	4661
Wadas Lintang	123	582	600	1024	117	446	253	115	168	760	561	511	5260
Klirong	438	313	334	496	198	384	256	148	237	352	416	473	4045
Kuwarasan	--	224	516	414	120	257	345	110	210	352	698	485	--
Kebumen	209	274	240	607	100	161	184	56	171	579	606	615	3802
Petanahan	396	274	211	491	59	372	228	163	256	338	393	493	3674
Banjarnegara	474	837	474	327	287	519	471	133	132	540	575	521	5290
Purwanegara	--	--	--	--	--	--	--	--	--	--	--	--	--
Mandiraja	--	--	--	--	--	--	--	--	--	--	--	--	--

-- = no data

1999

Station	Jan	Feb	Mar	Apr	May	Jun	Jul	Aug	Sep	Oct	Nov	Dec	Total
Adimulyo	695	218	315	326	385	35	0	0	0	184	167	464	2789
Alian	445	412	--	--	--	30	0	10	0	394	235	--	--
Karang Anyar	703	307	485	317	297	42	0	0	0	167	200	428	2946
Sempor	--	--	--	--	--	--	--	--	--	--	--	--	--
Rowokele	399	183	707	178	303	16	19	27	5	171	277	261	2546
Gombong	731	243	515	369	398	94	0	5	18	245	446	372	3436
Karang Gayam	563	320	424	273	334	64	0	0	0	231	226	374	2809
Puring	886	145	472	331	137	5	0	0	11	52	193	394	2626
Sadang	140	73	309	145	386	43	0	9	5	404	298	431	2243
Wadas Lintang	772	333	443	1029	218	14	29	26	7	288	702	519	4380
Klirong	610	243	379	523	142	0	0	0	0	108	376	495	2876
Kuwarasan	433	219	496	348	351	17	0	11	45	103	250	321	2594
Kebumen	578	274	299	323	118	18	14	10	9	173	177	394	2387
Petanahan	594	224	366	537	124	0	0	0	0	124	334	497	2800
Banjarnegara	753	490	418	139	229	82	33	42	2	515	554	576	3833
Purwanegara	--	--	--	--	--	--	--	--	--	--	--	--	--
Mandiraja	--	--	--	270	336	43	48	55	0	399	308	235	--

-- = no data

2000

Station	Jan	Feb	Mar	Apr	May	Jun	Jul	Aug	Sep	Oct	Nov	Dec	Total
Adimulyo	459	364	192	206	152	64	27	37	129	839	699	314	3482
Alian	278	653	586	260	196	10	0	8	88	--	785	411	--
Karang Anyar	294	397	336	286	127	38	0	73	128	654	826	181	3340
Sempor	288	467	525	392	211	96	0	112	121	829	688	341	4070
Rowokele	152	354	337	315	240	60	0	40	107	364	361	179	2509
Gombong	345	422	450	468	238	60	0	27	202	736	879	302	4129
Karang Gayam	311	265	410	518	174	42	2	72	166	566	595	228	3349
Puring	173	244	243	244	120	32	0	39	151	668	841	268	3023
Sadang	353	--	--	--	--	--	--	--	--	--	--	--	--
Wadas Lintang	436	402	739	334	287	113	33	5	68	470	787	395	4069
Klirong	351	378	198	221	171	26	0	26	144	653	842	268	3278
Kuwarasan	182	352	274	452	182	52	0	94	103	658	821	201	3371
Kebumen	492	242	277	182	137	32	0	51	171	722	772	417	3495
Petanahan	347	384	280	207	170	14	0	41	148	677	775	202	3245
Banjarnegara	--	--	--	--	--	--	--	--	--	--	--	--	--
Purwanegara	--	--	--	--	--	--	--	--	--	--	--	--	--
Mandiraja	--	--	--	--	--	--	--	--	--	--	--	--	--

-- = no data

APPENDIX C. RAINFALL SURFACES FOR THREE YEARS (1992, 1995 AND 1998)

Rainfall surfaces in the study area are developed using the ANUSPLIN software. Each rainfall map is created from 24 stations: 17 actual stations and 7 simulated stations to make the rain shadow effect recognised by the software. The values in each map show the actual rainfall intensity in a month (mm/month); 0 (zero) means no rain and 9999 means no data. The colour in the map is arranged from red (the lowest value) to blue (the highest value).

1992

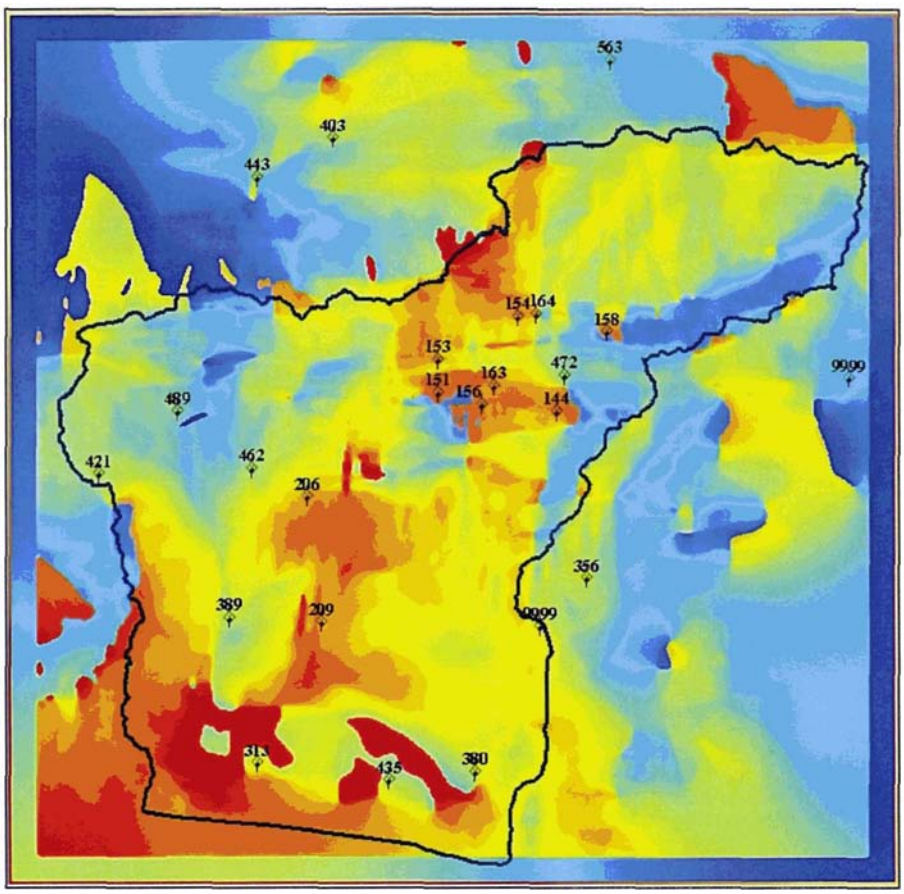

January

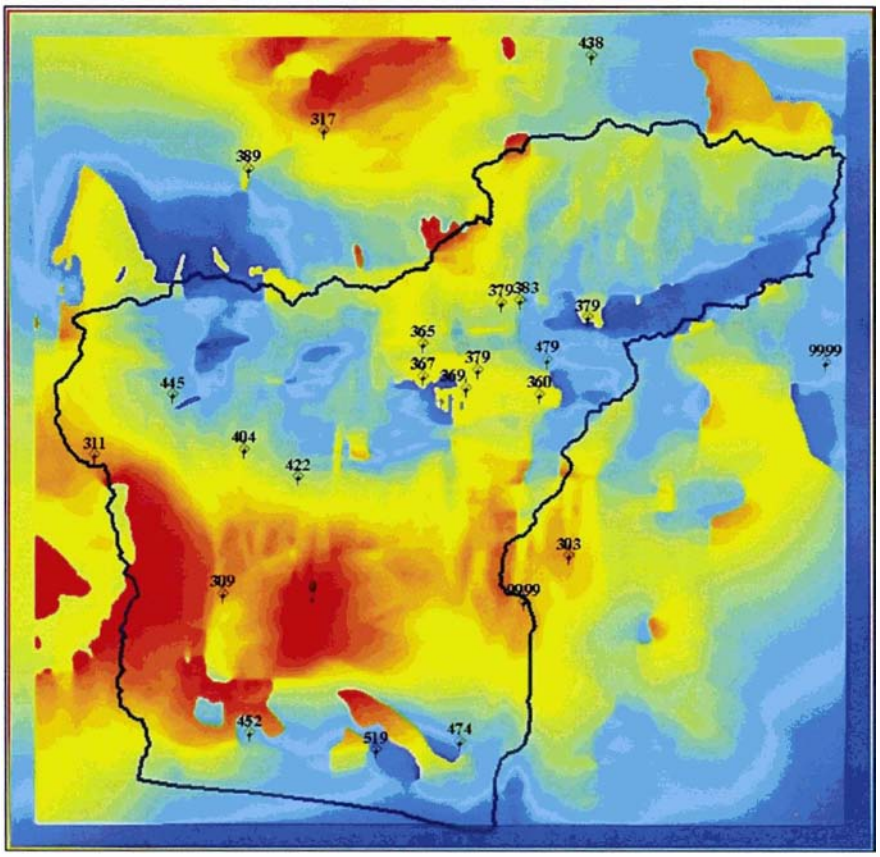

February

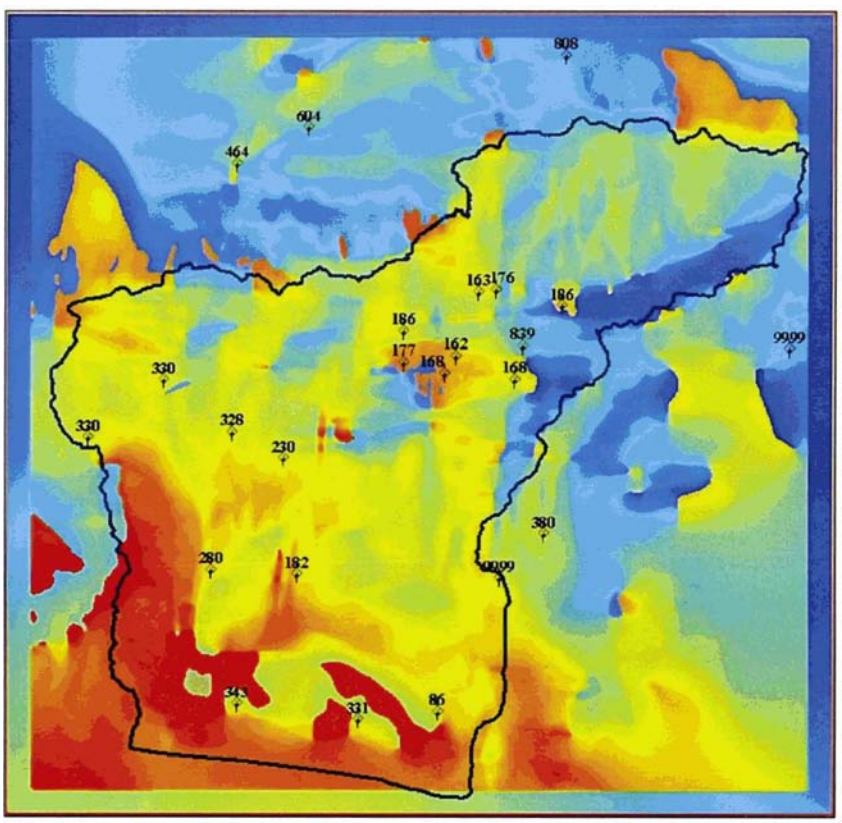

March

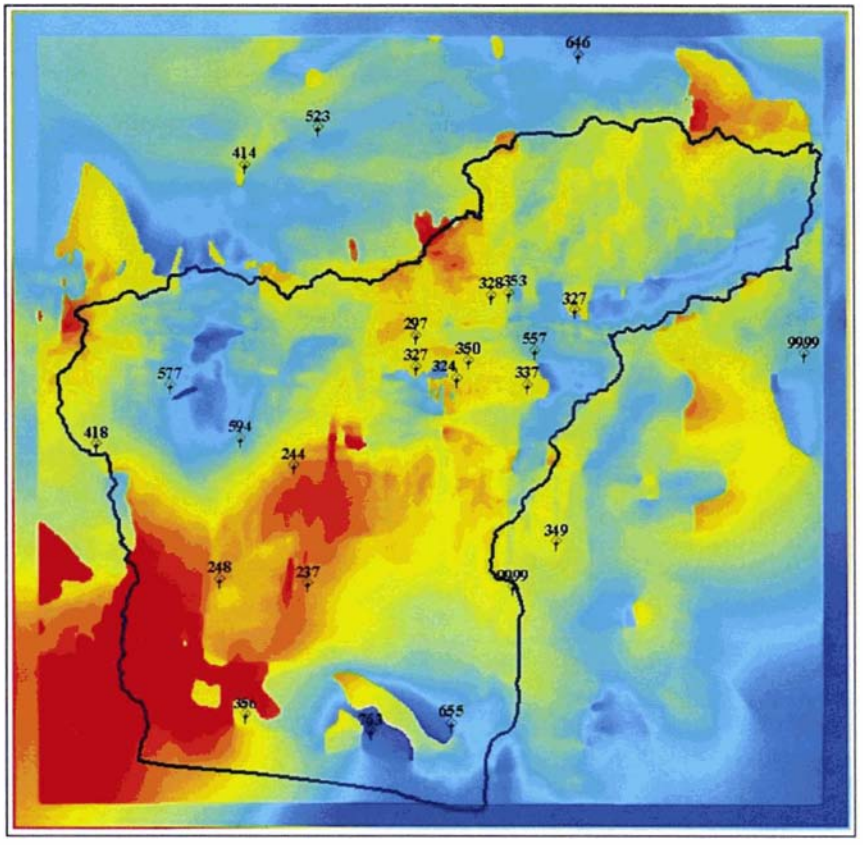
646
523
414
328
353
327
297
327
350
324
557
337
9999
577
418
594
244
349
248
237
9999
356
655

April

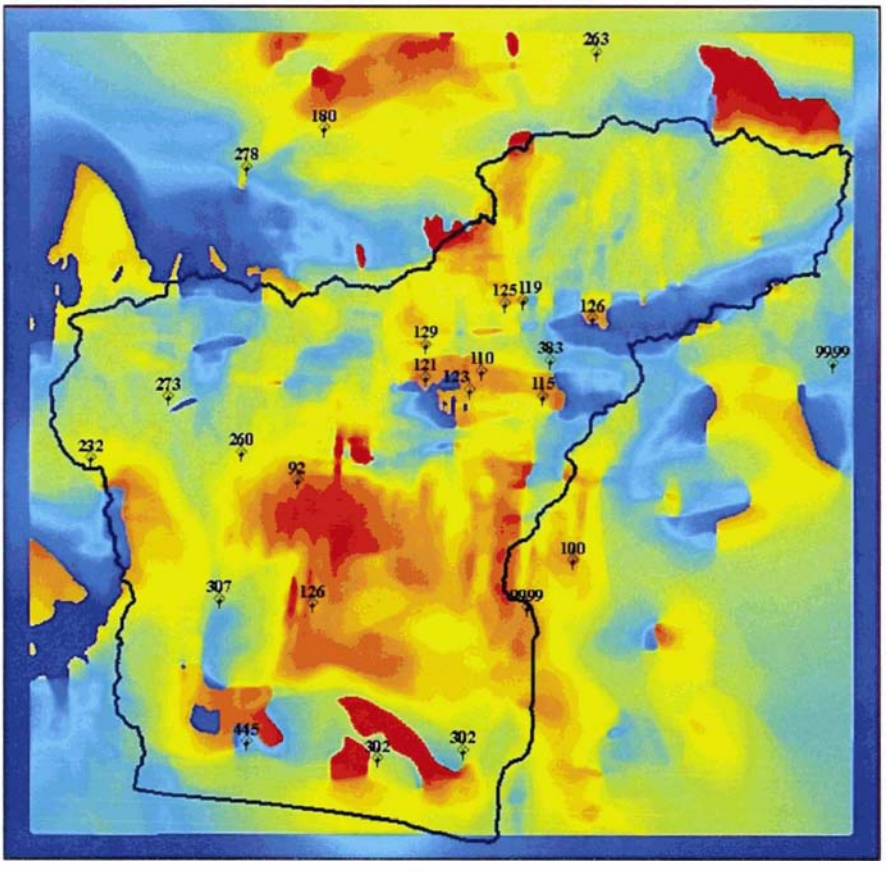
263
180
278
125
119
126
129
121
123
110
383
9999
273
115
232
260
92
100
307
126
9999
445
302
302

May

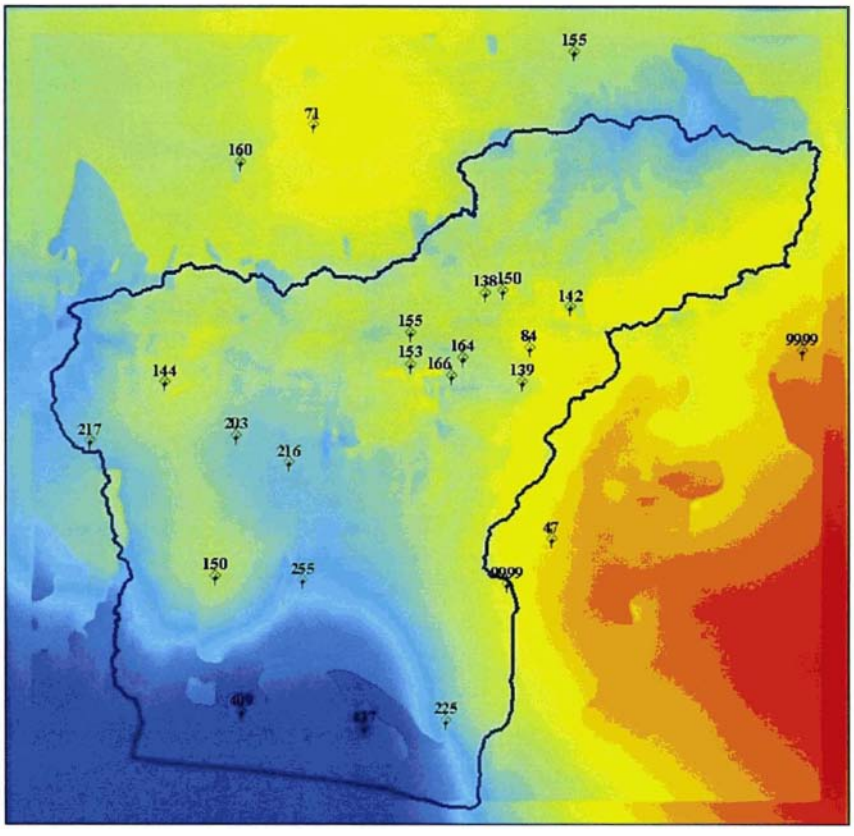
155
71
160
138
150
142
155
84
153
164
166
139
144
9999
217
203
216
47
150
255
9999
225

June

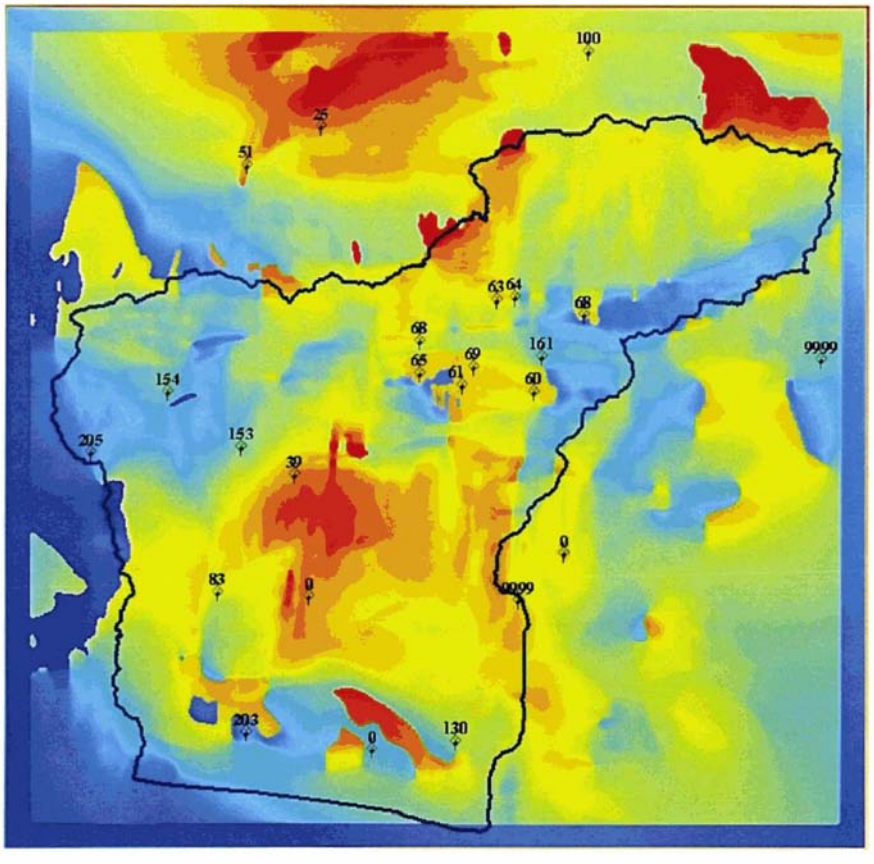
100
25
51
63
64
68
68
161
65
69
61
60
154
9999
153
205
39
0
83
0
9999
203
0
130

July

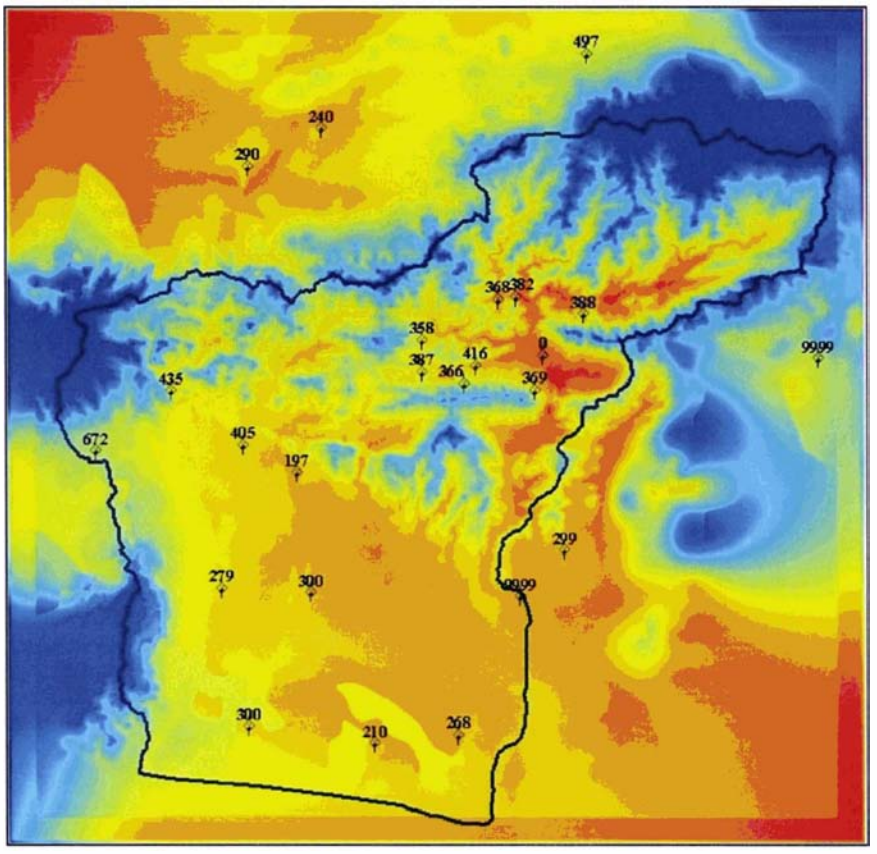

August

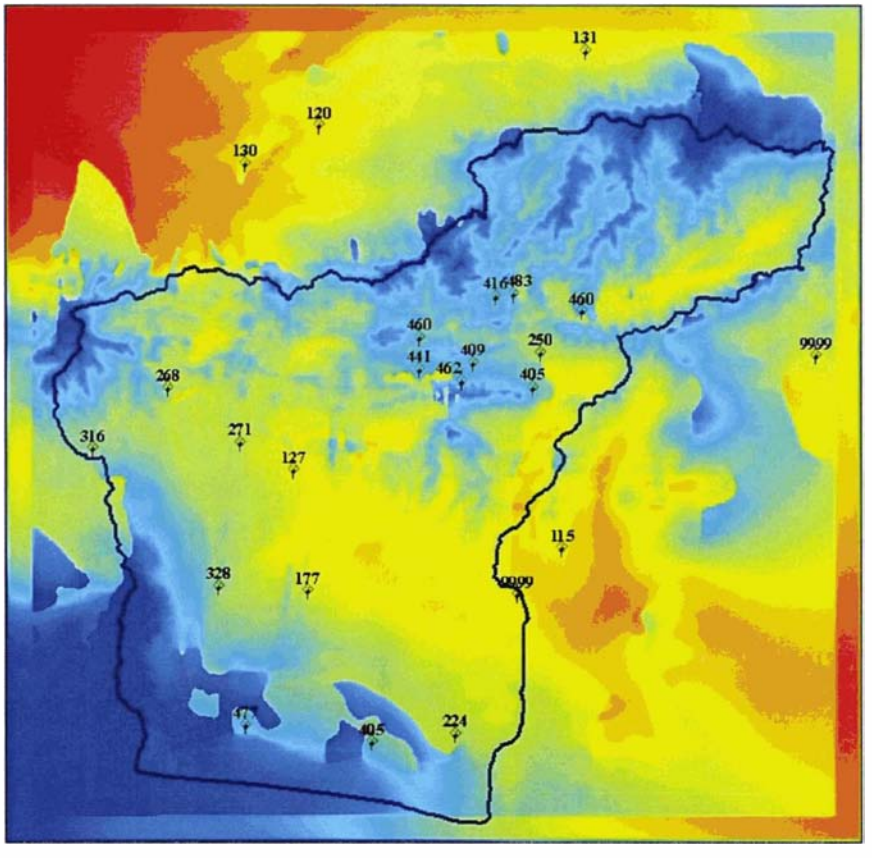

September

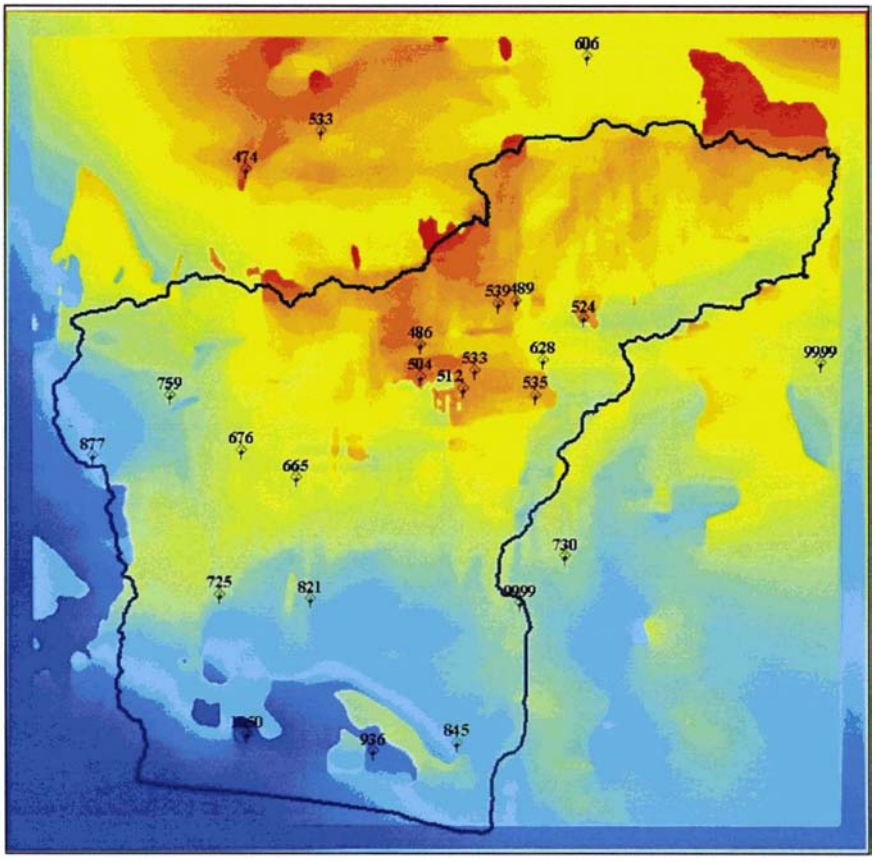

October

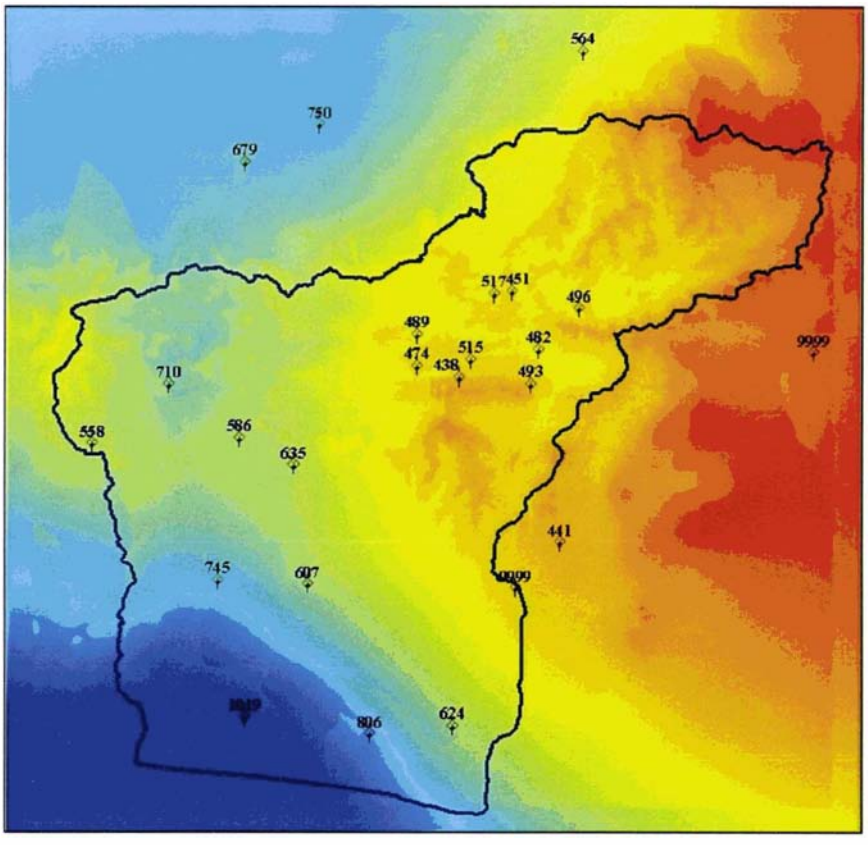

November

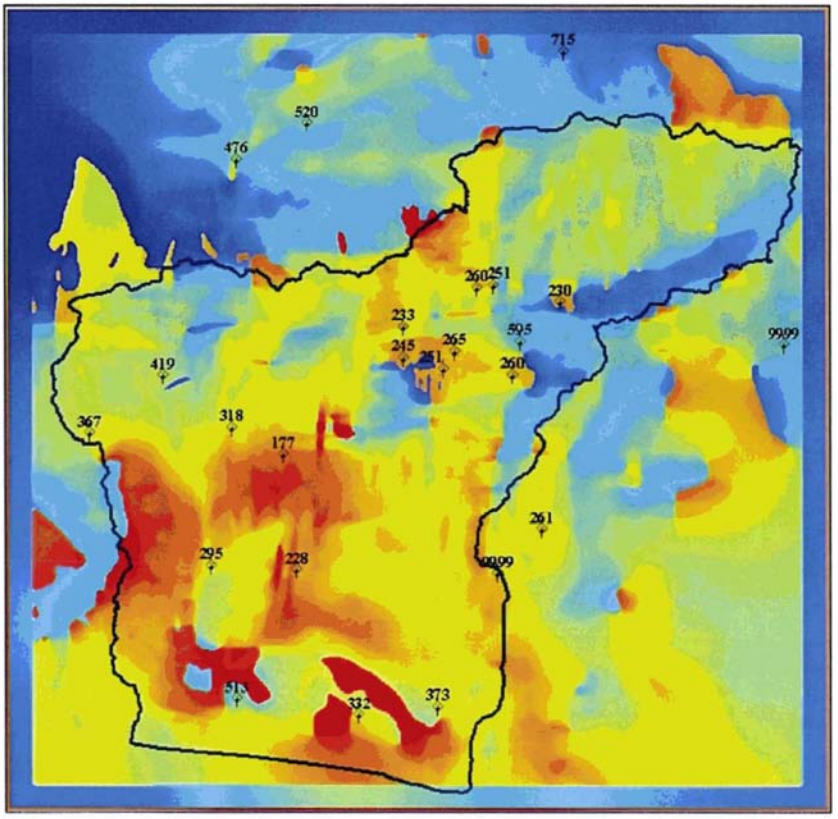

December

1995

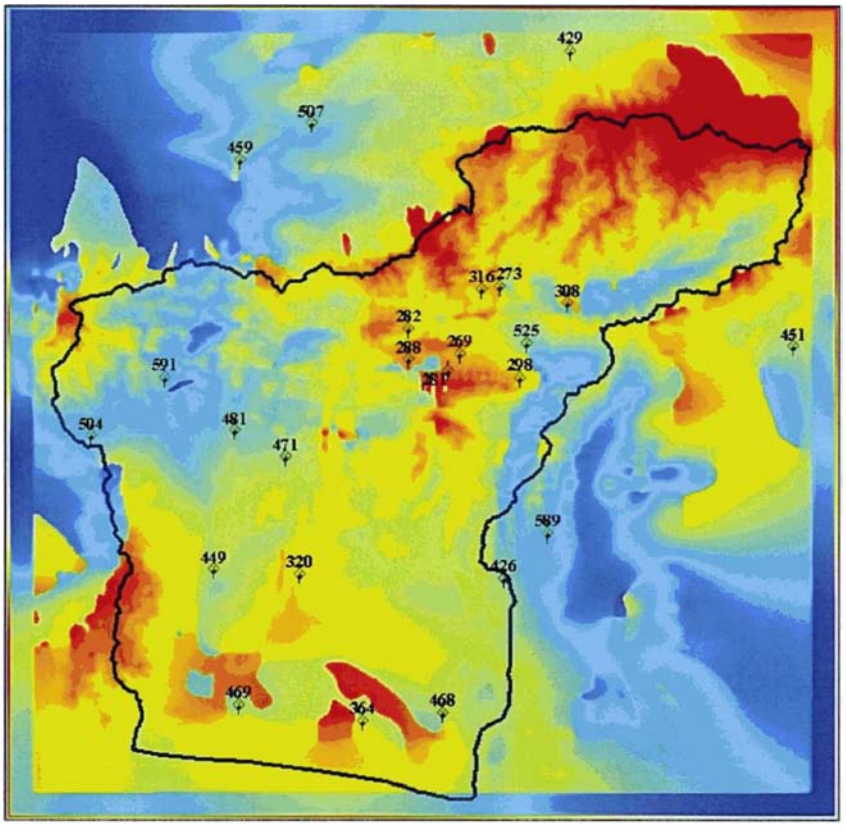

January

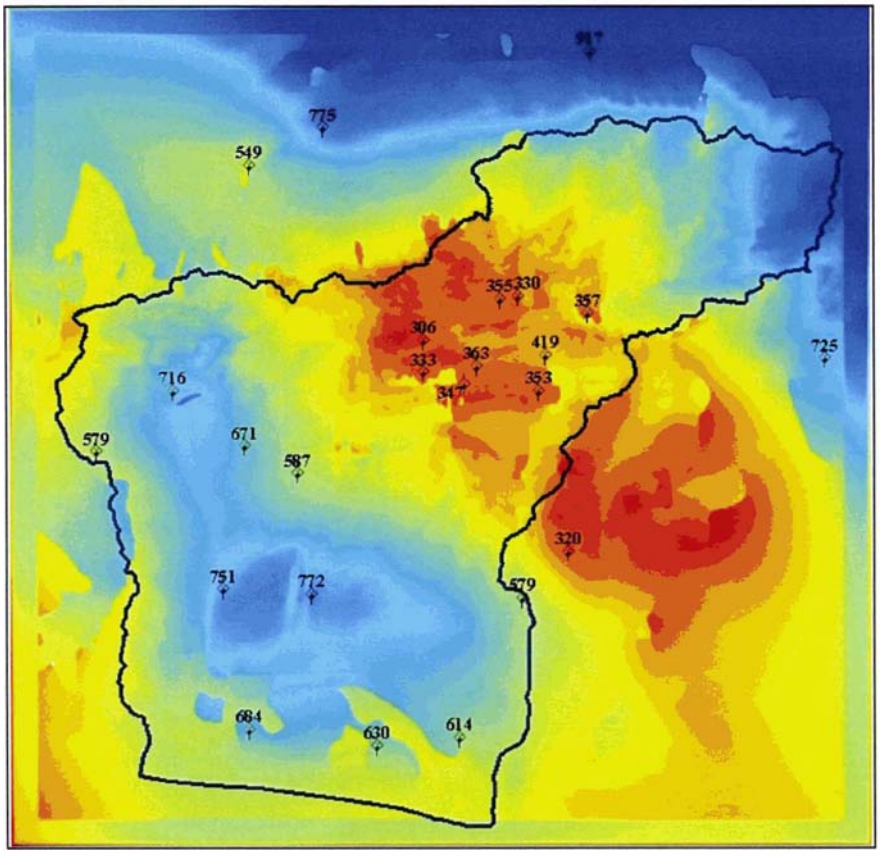

February

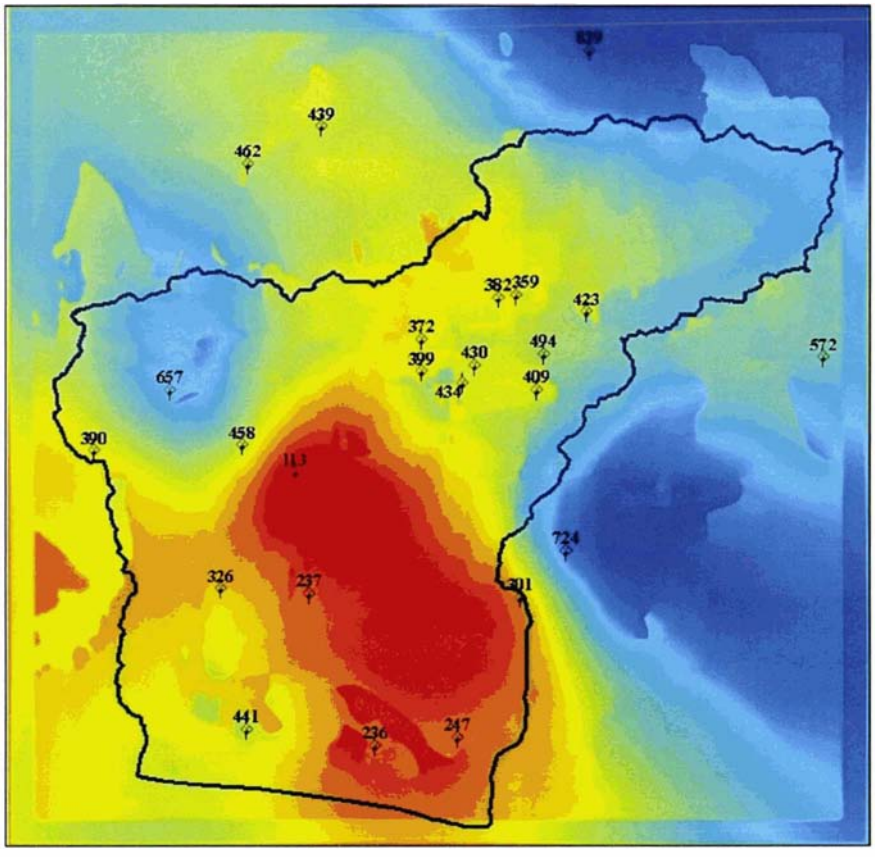

March

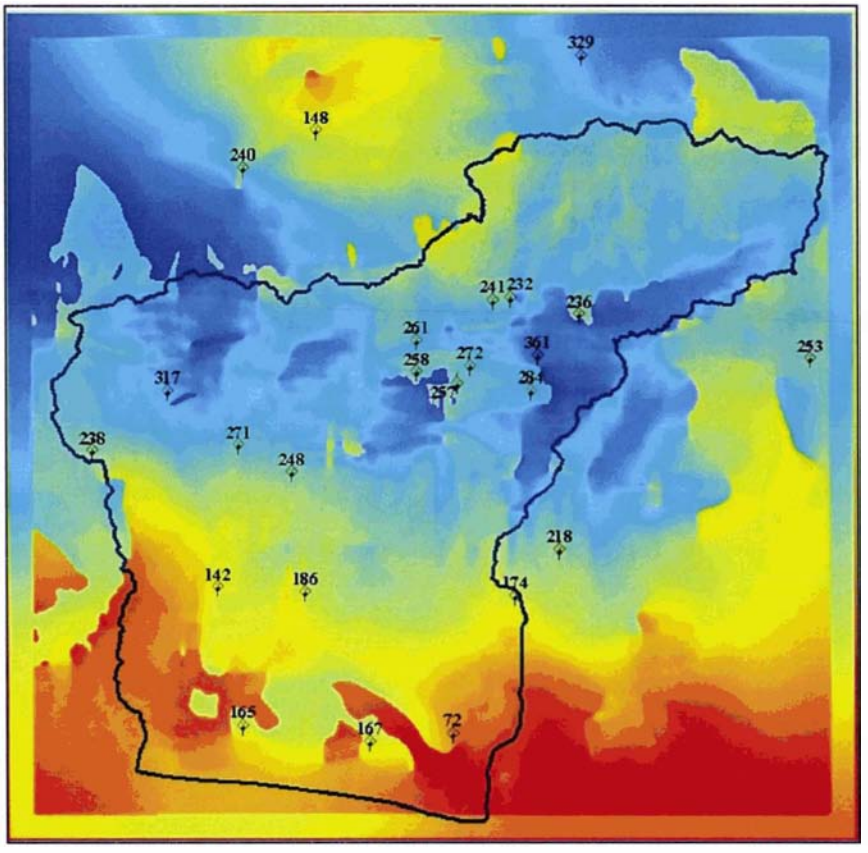
329
148
240
241
232
236
261
258
272
361
284
253
317
271
238
248
218
142
186
174
165
167
72

April

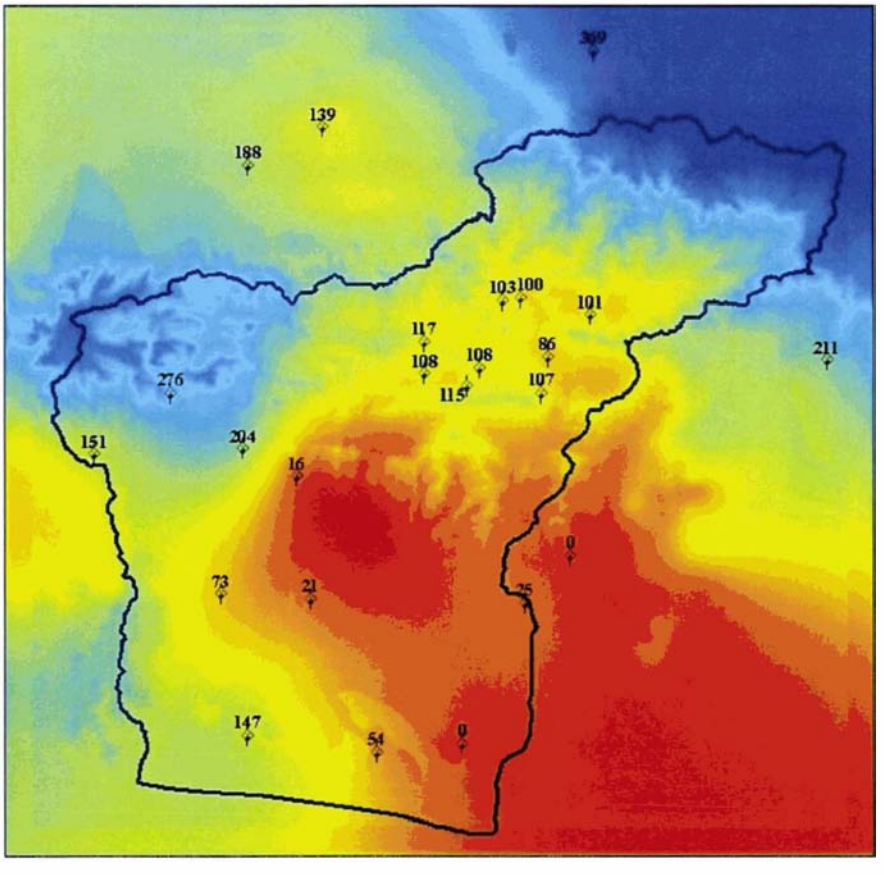
369
139
188
103
100
101
117
108
108
86
211
276
115
107
151
204
16
0
73
21
25
147
54
0

May

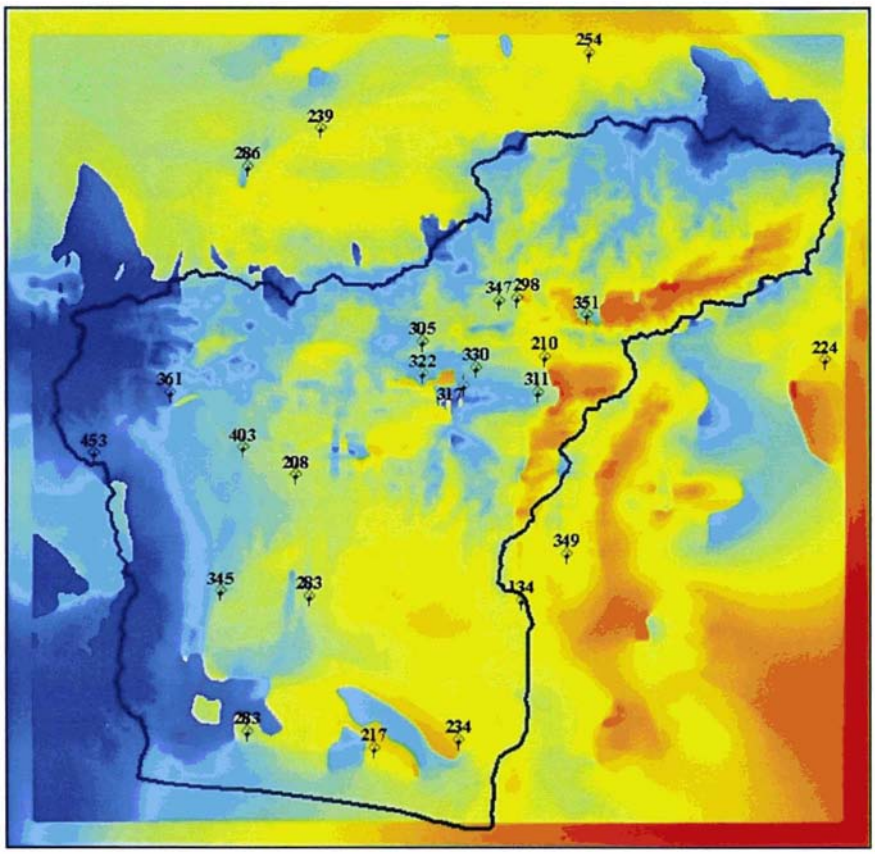
254
239
286
347
298
351
305
322
330
210
224
361
317
311
453
403
208
349
345
283
134
283
217
234

June

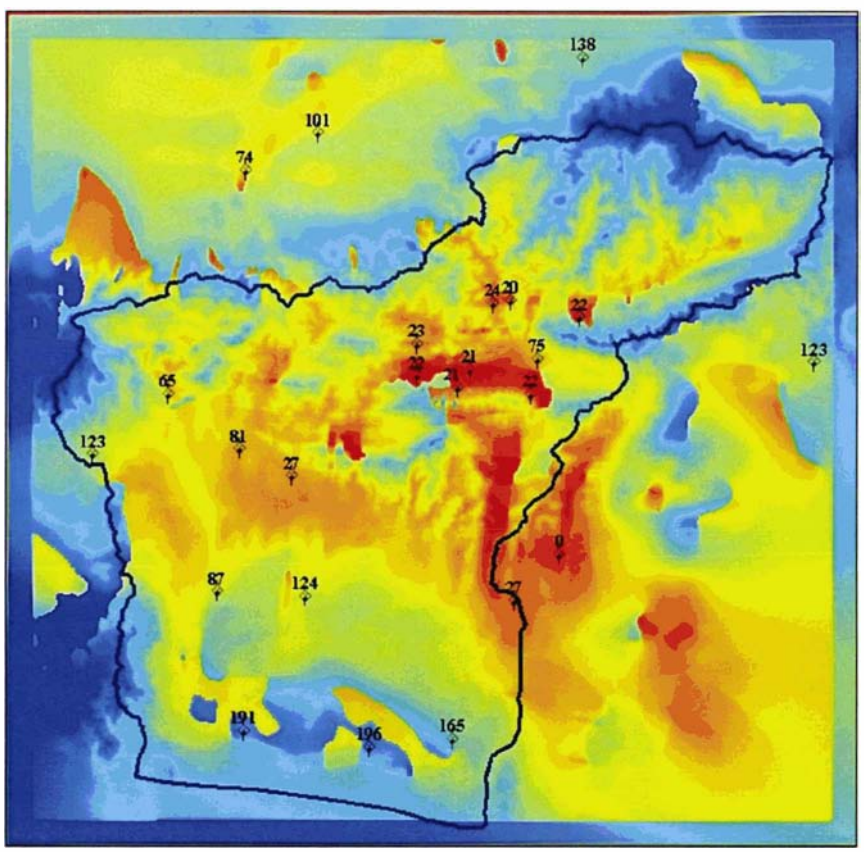
138
101
74
24
20
22
23
22
21
75
123
65
81
123
27
9
87
124
27
191
196
165

July

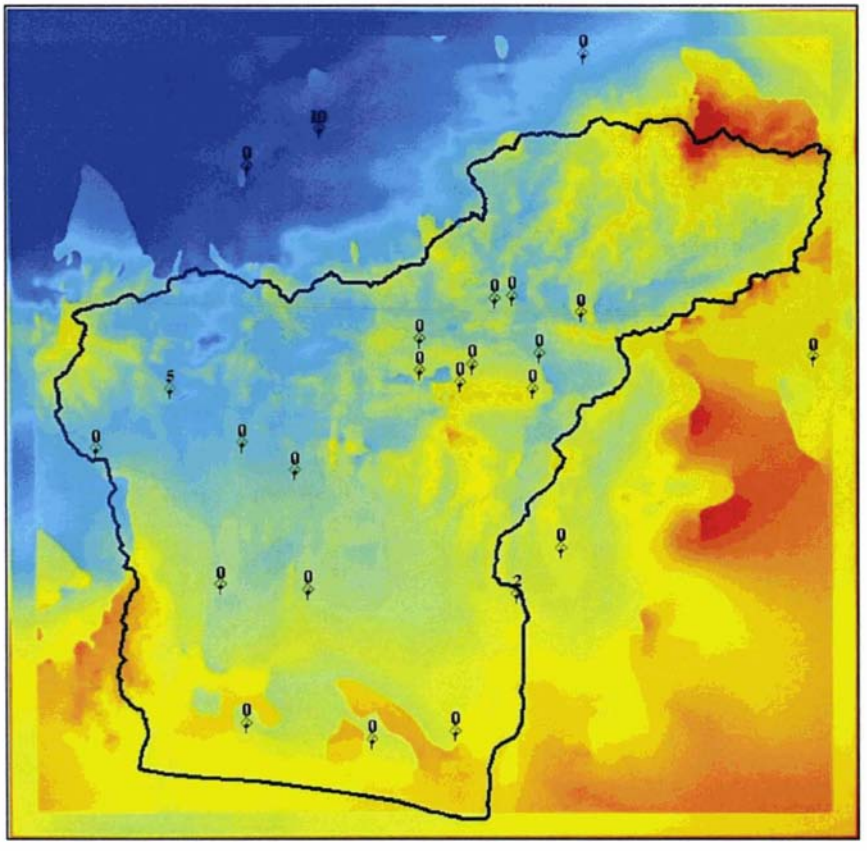

August

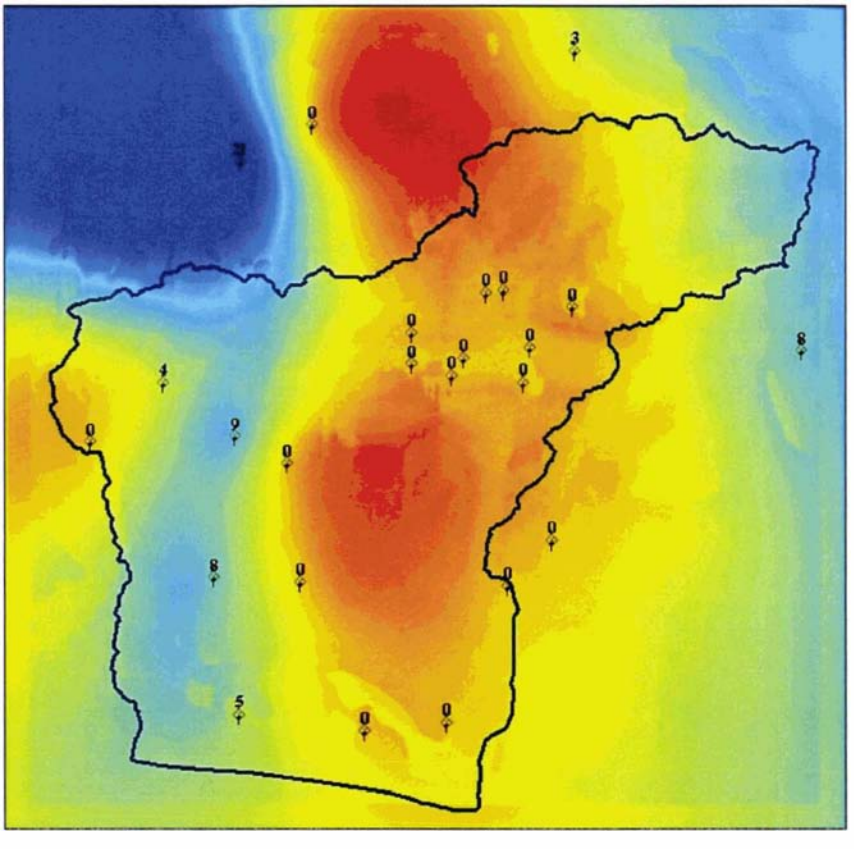

September

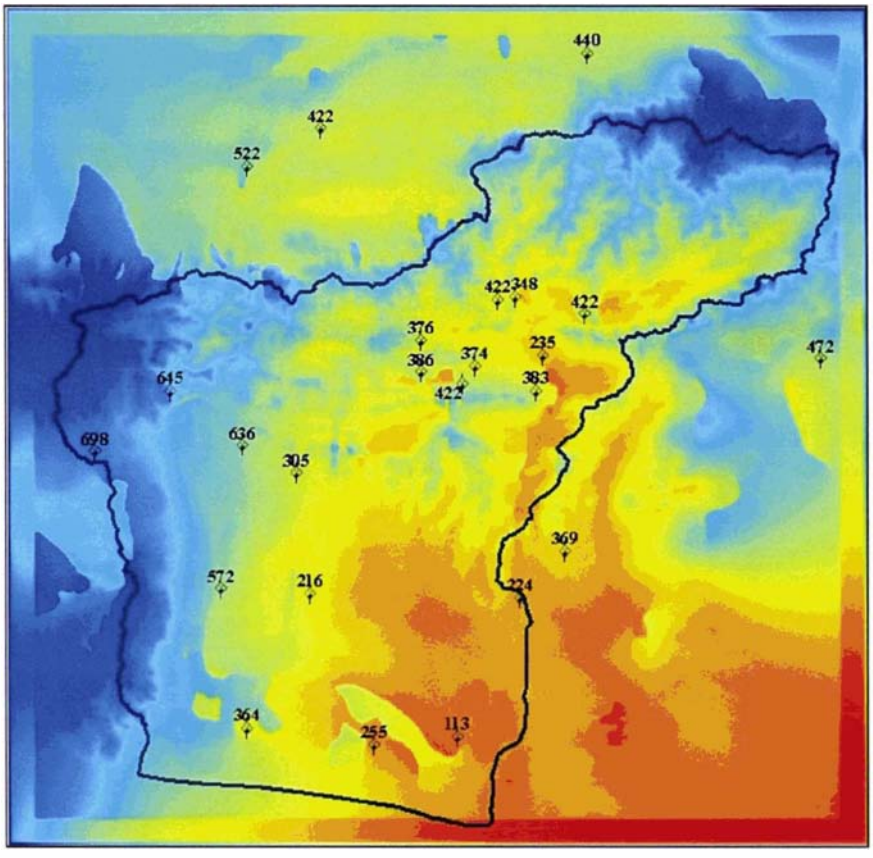

October

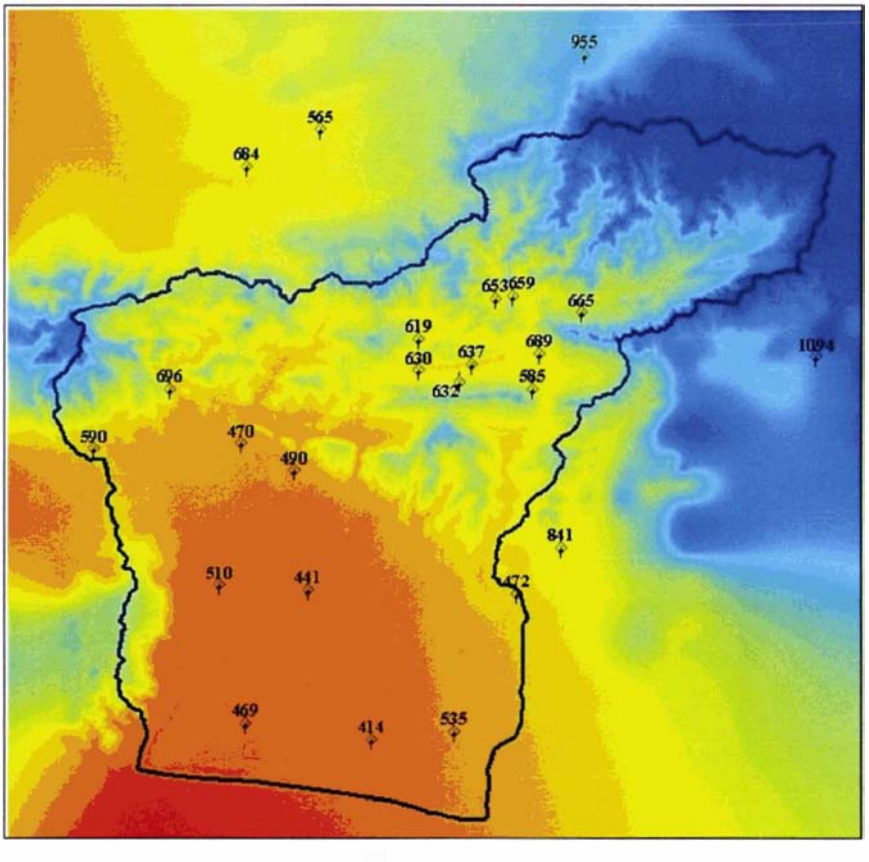

November

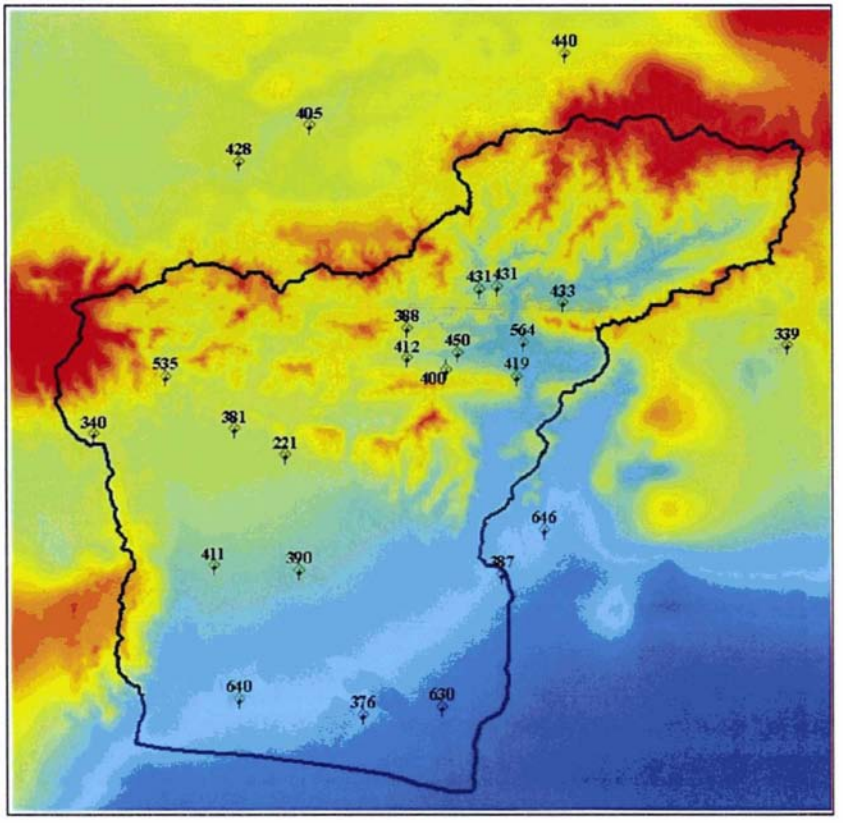

December

1998

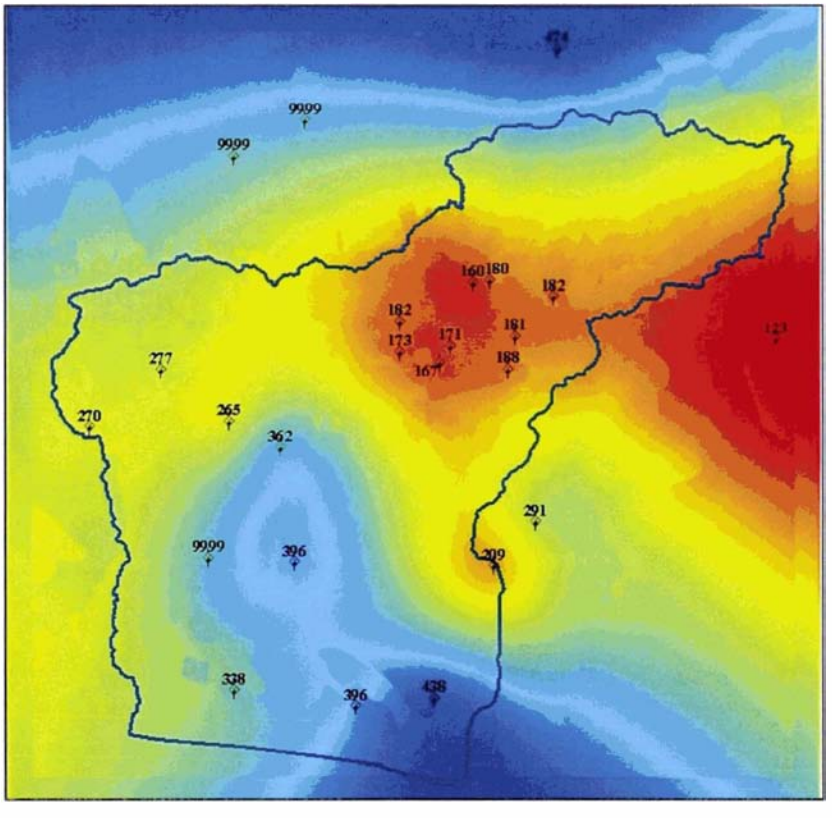

January

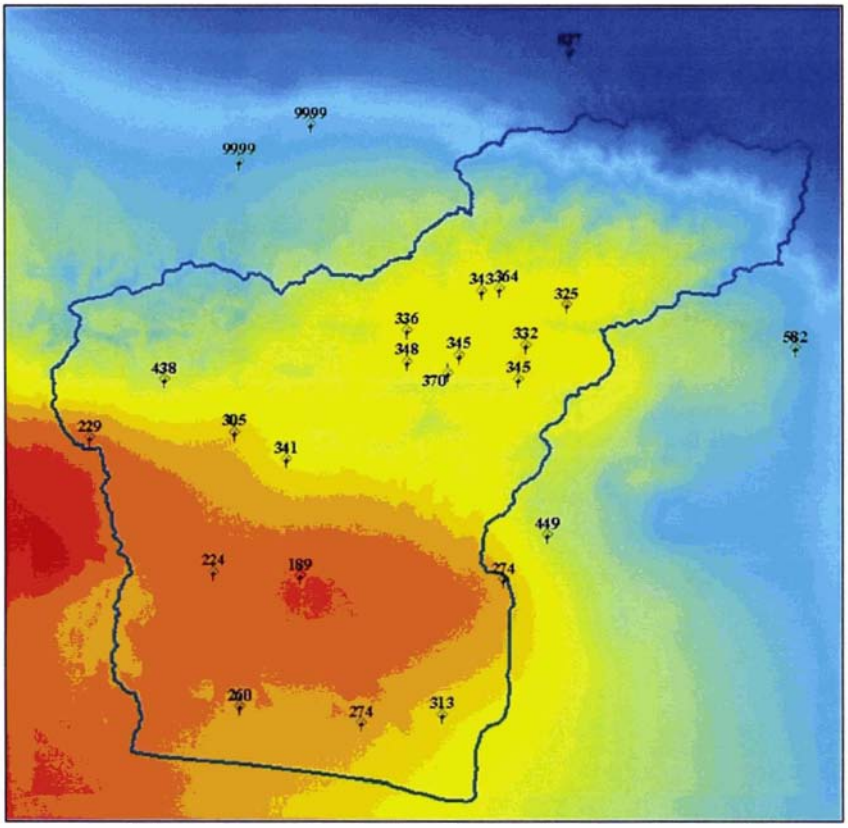

February

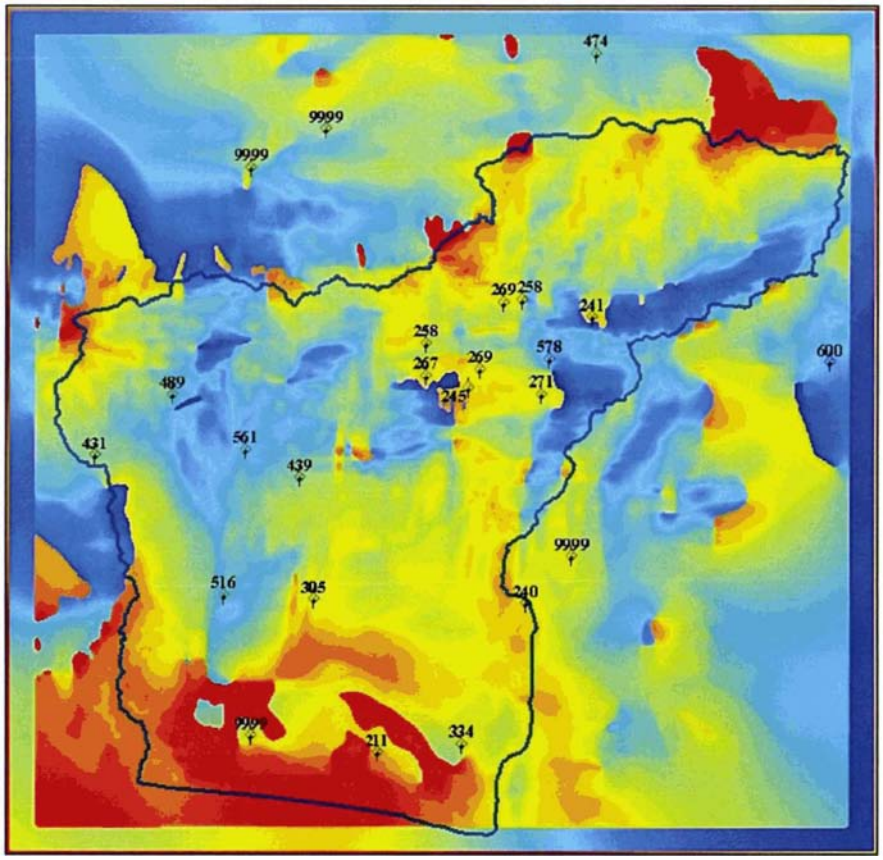

March

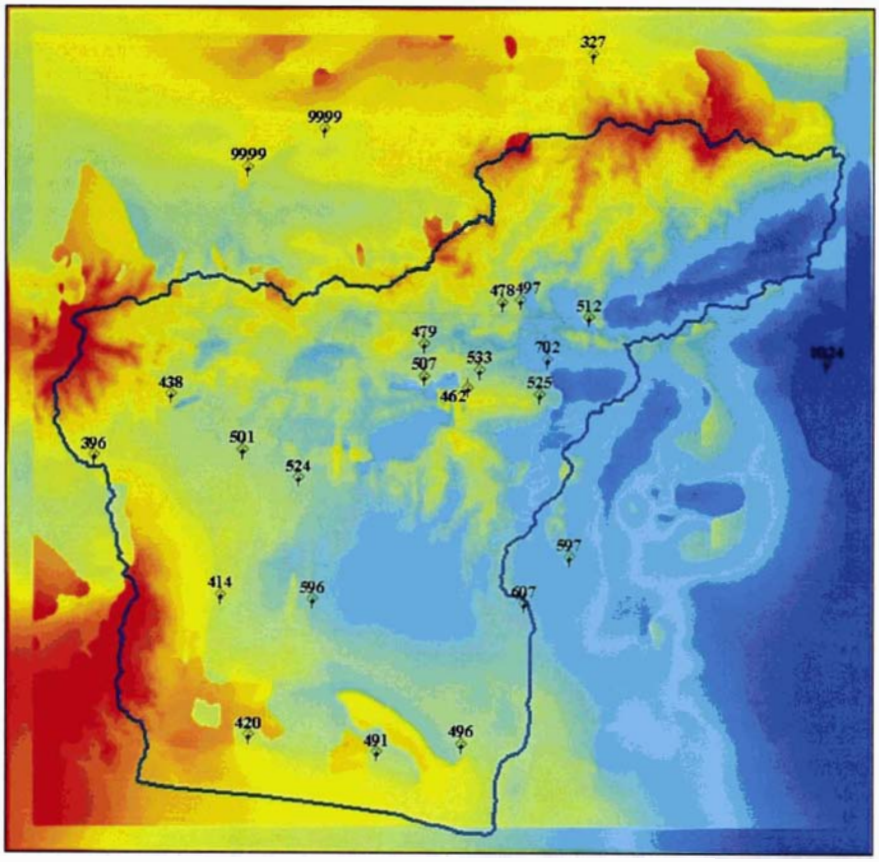
327
9999
9999
478
497
512
479
507
533
702
438
462
525
396
501
524
597
414
596
607
420
491
496

April

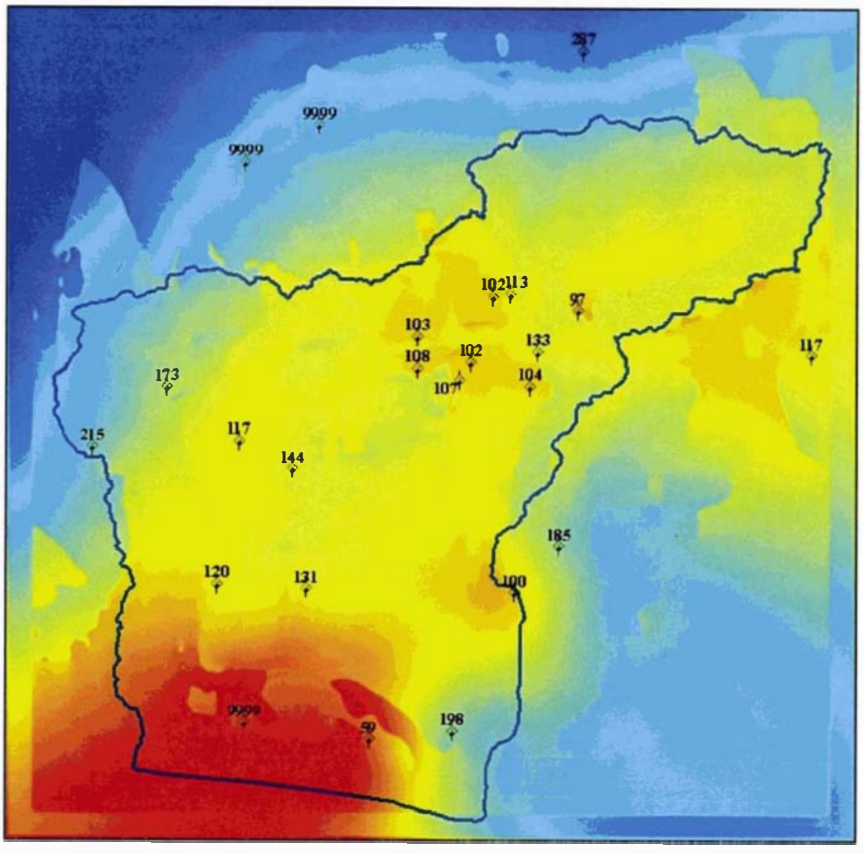
287
9999
9999
102
113
97
103
108
102
133
117
173
107
104
117
215
144
185
120
131
100
9999
92
198

May

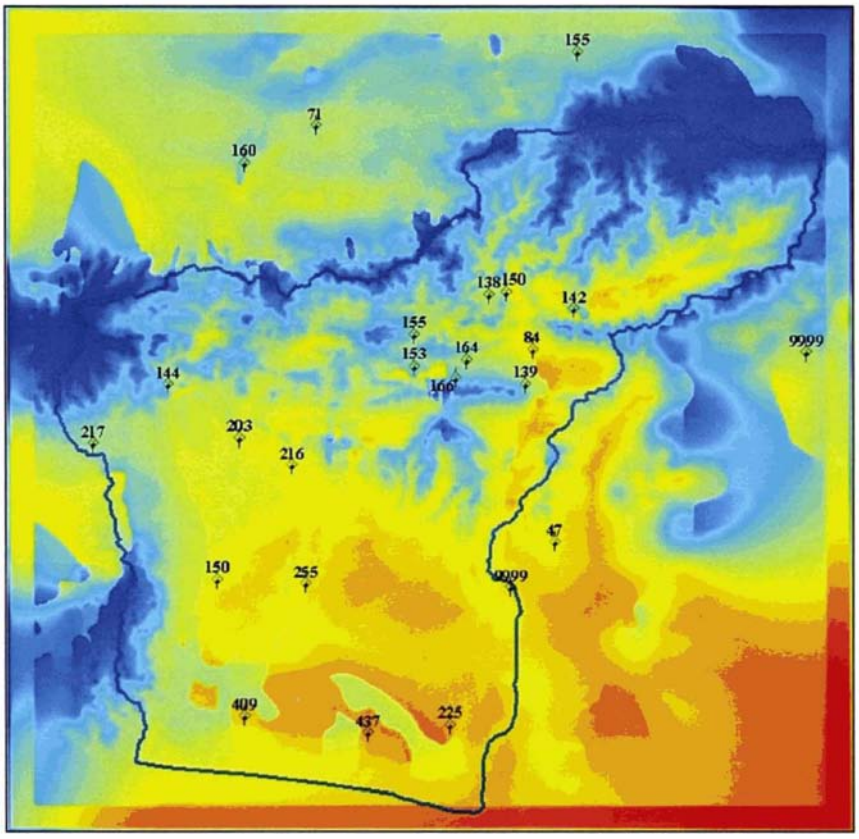
155
71
160
138
150
142
155
153
164
84
9999
144
166
139
217
203
216
47
150
255
9999
409
437
225

June

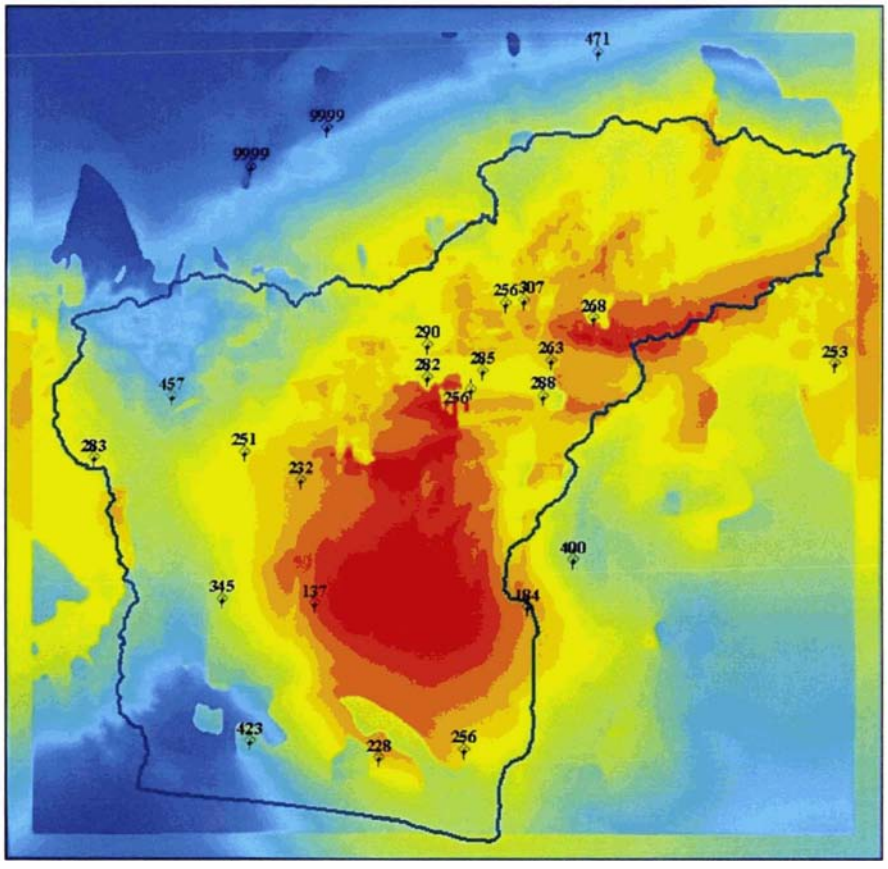
471
9999
9999
256
307
268
290
263
253
282
285
457
288
256
283
251
232
400
345
137
184
423
228
256

July

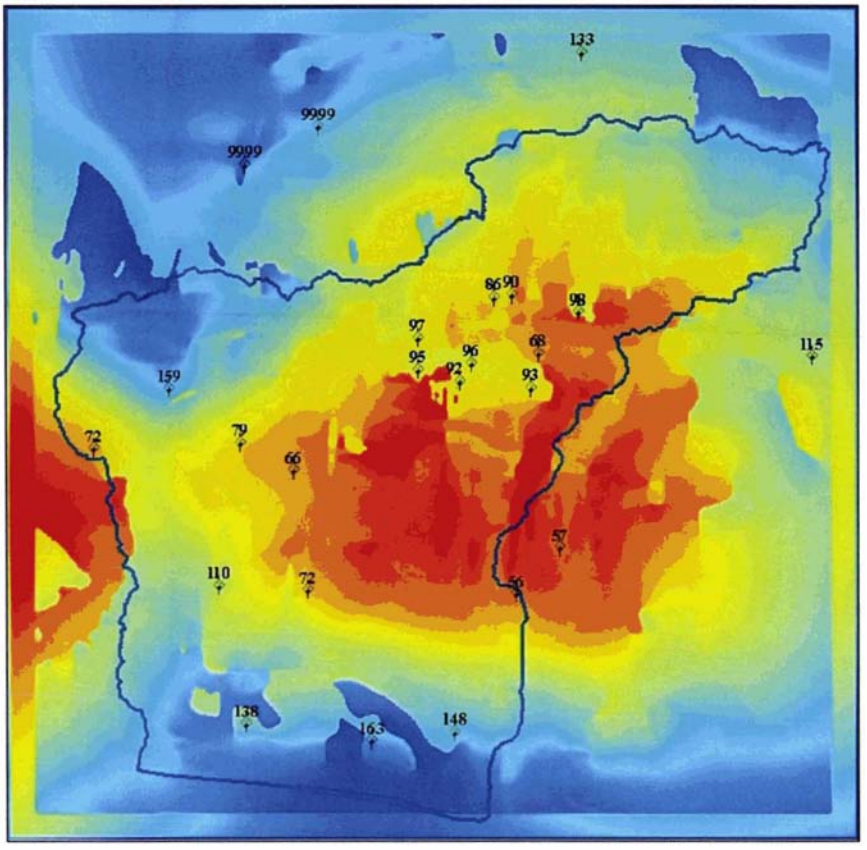

August

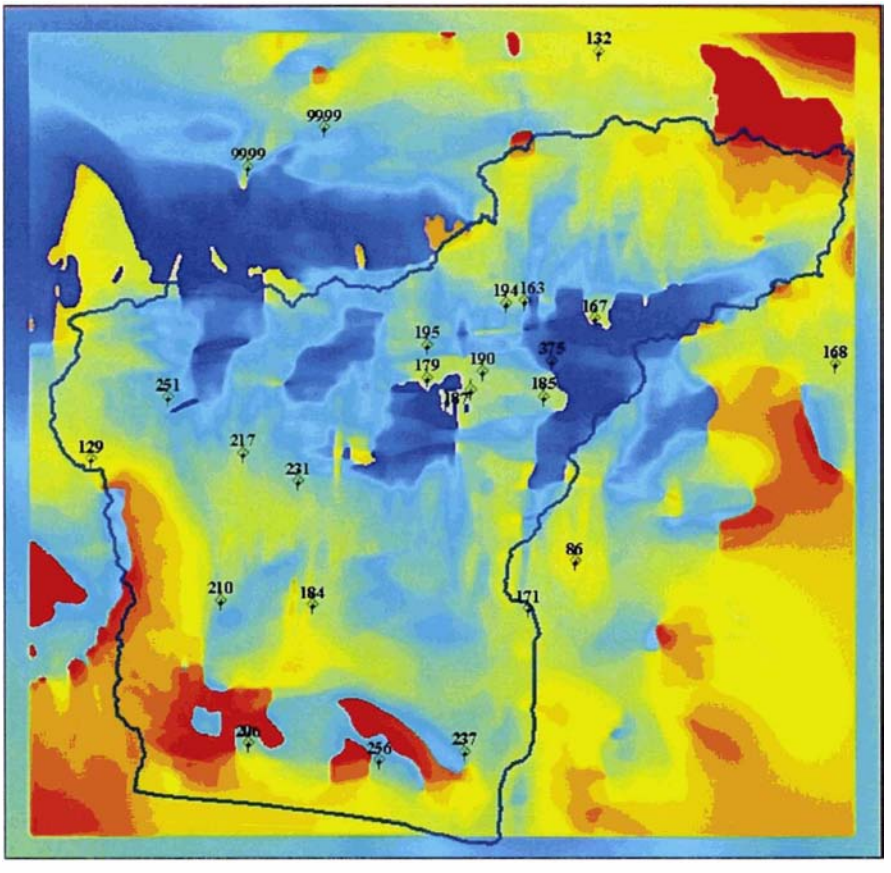

September

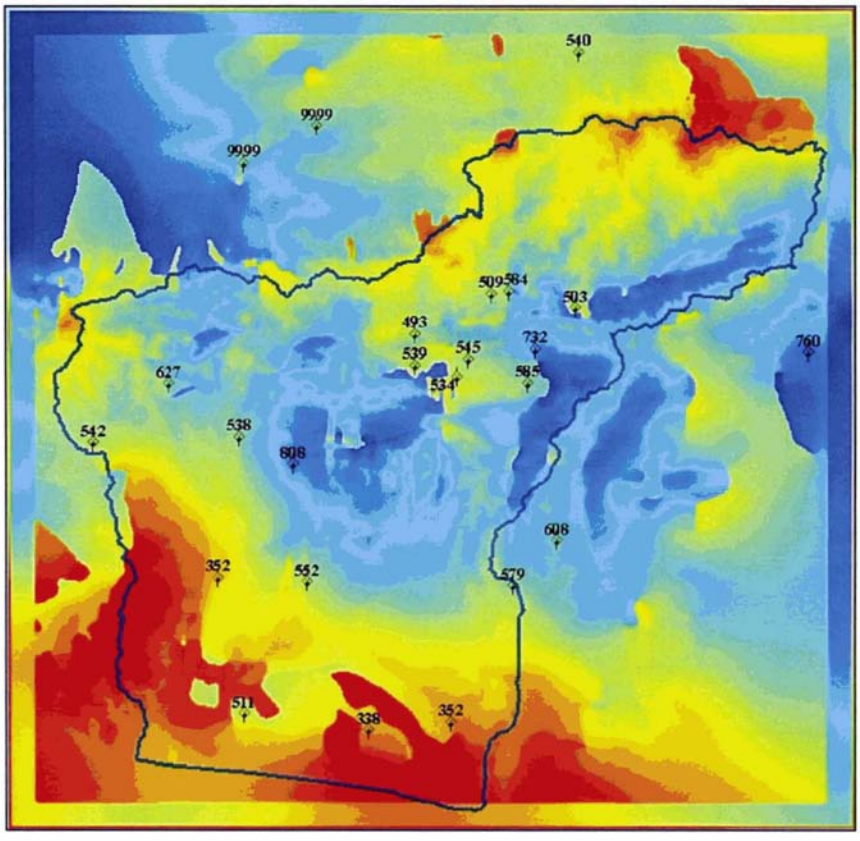

October

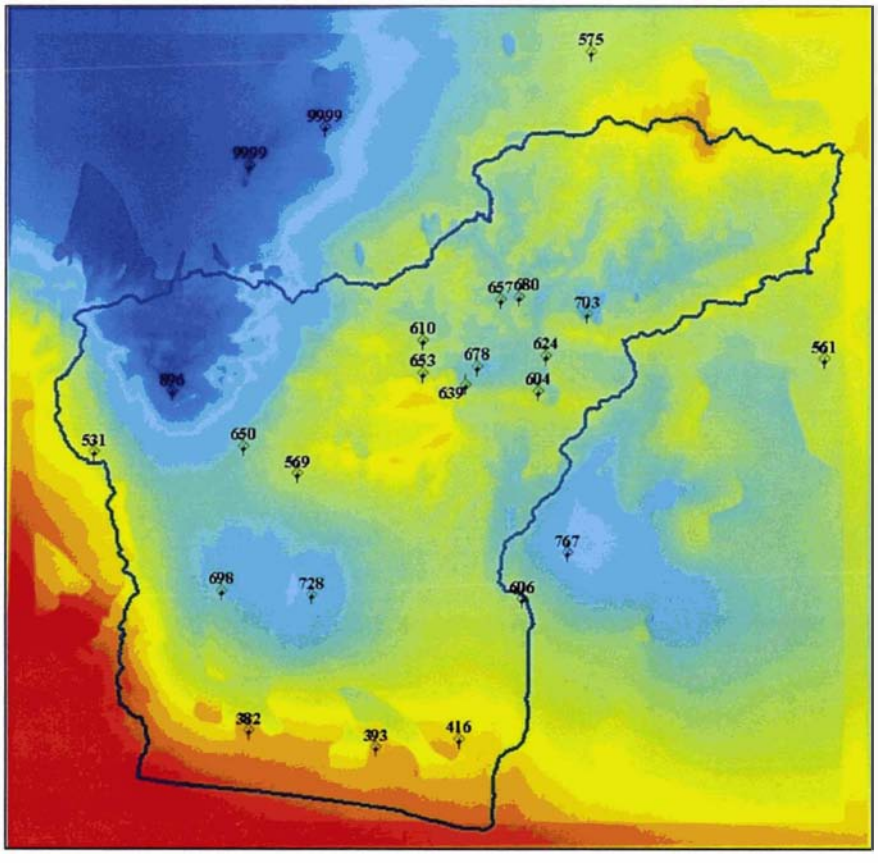

November

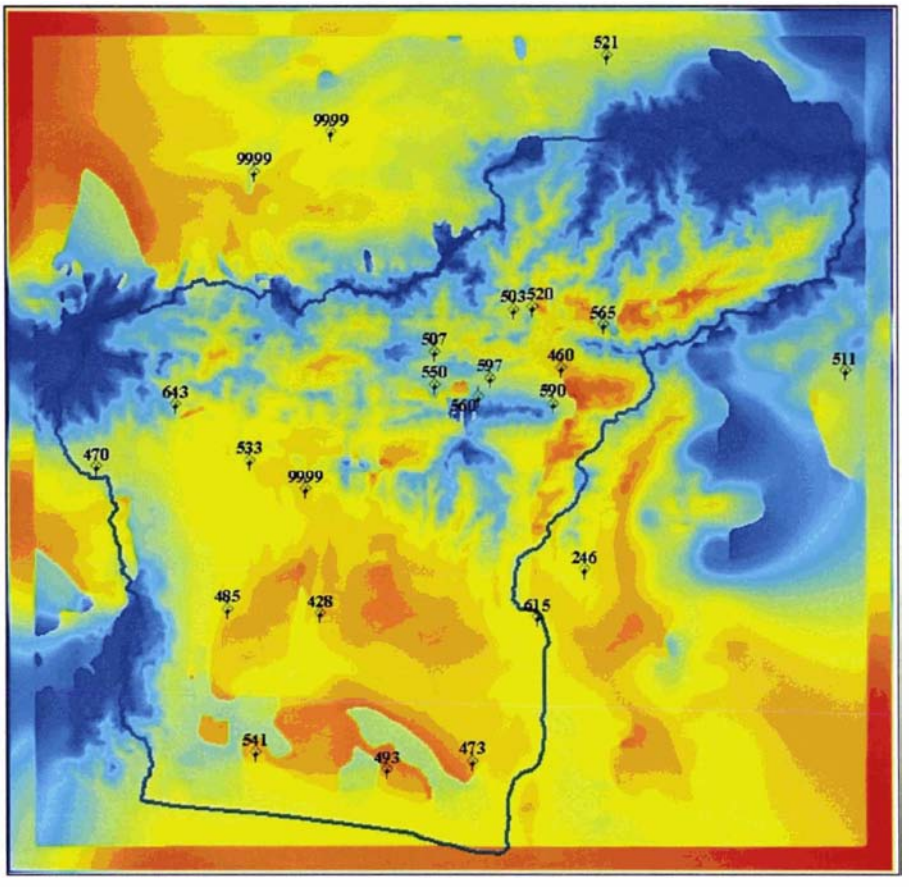
521
9999
9999
503
520
565
507
550
597
460
511
643
590
560
470
533
9999
246
485
428
615
541
493
473

December

APPENDIX D. SPLINA AND LAPGRD COMMANDS OF ANUSPLIN

ANUSPLIN is software distributed by the Centre for Resource and Environmental Studies (CRES), the Australian National University Canberra, Australia. It is a FORTRAN program that the user has to type in the input data.

The commands used for this study are SPLINA and LAPRGD and the log files are shown as follows:

SPLINA:

```
E:\Endang\anusplin\raintext>splina rain.cmd enda.log
SPLINA VERSION 4.3 13/04/04
COPYRIGHT AUSTRALIAN NATIONAL UNIVERSITY

TITLE OF FITTED SURFACES (60 CHARS):
------------------------------------1992, 24 stations 10 months
1992, 24 stations 10 months

SURFACE VALUE UNITS CODE AND MISSING DATA VALUE:
------------------------------------------------
  0 - UNDEFINED
  1 - METRES
  2 - FEET
  3 - KILOMETRES
  4 - MILES
  5 - DEGREES
  6 - RADIANS
  7 - MILLIMETRES
  8 - MEGAJOULES7
    7

INDEPENDENT VARIABLES
---------------------
NUMBER OF INDEPENDENT SPLINE VARIABLES (0 TO 10):2
    2

NUMBER OF INDEPENDENT COVARIATES (0 TO  8):2
    2

NUMBER OF SURFACE SPLINE VARIABLES (0 TO  6):0
    0

NUMBER OF SURFACE COVARIATES (0 TO  6):0
    0

TRANSFORMATION CODES            REFERENCE UNIT CODES
--------------------            --------------------
```

```
  0 - NO TRANSFORMATION          0 - UNDEFINED
  1 - X/A                        1 - METRES
  2 - X*A                        2 - FEET
  3 - A*LOG(X + B)               3 - KILOMETRES
  4 - (X/B)**A                   4 - MILES
  5 - A*EXP(X/B)                 5 - DEGREES
  6 - A*TANH(X/B)                6 - RADIANS
  7 - ANISOTROPY ANGLE           7 - MILLIMETRES
  8 - ANISOTROPY FACTOR          8 - MEGAJOULES

LOWER & UPPER LIMITS, TRANSF CODE, REF UNIT, MARGIN(S) FOR
VARIABLE  1:323500 372000 0 1 1
   323500.       372000.        0         1   1.000

LOWER & UPPER LIMITS, TRANSF CODE, REF UNIT, MARGIN(S) FOR
VARIABLE  2:9137000 9185000 0 1 1
  0.913700E+07  0.918500E+07    0         1   1.000

LOWER & UPPER LIMITS, TRANSF CODE, REF UNIT, MARGIN(S) FOR
VARIABLE  3:-6.28 286.24 0 1
  -6.28000       286.240        0         1

LOWER & UPPER LIMITS, TRANSF CODE, REF UNIT, MARGIN(S) FOR
VARIABLE  4:7.19 332.35 0 5
   7.19000       332.350        0         5

SURFACE DIRECTIVES
------------------
DEPENDENT VARIABLE TRANSFORMATION:
  0 - NO TRANSFORMATION
  1 - NATURAL LOGARITHM
  2 - SQUARE ROOT0
    0

ORDER OF SPLINE (AT LEAST 2):2
    2

NUMBER OF SURFACES (AT LEAST 1):10
   10

NUMBER OF RELATIVE VARIANCES (0, 1 OR  10):0
    0

OPTIMIZATION DIRECTIVE (NORMALLY 1):
  0 - COMMON SMOOTHING PARAMETER FOR ALL SURFACES
  1 - COMMON SMOOTHING DIRECTIVE FOR ALL SURFACES
  2 - DIFFERENT SMOOTHING DIRECTIVE FOR EACH SURFACE1
    1

SMOOTHING DIRECTIVE (NORMALLY 1):
  0 - FIXED SMOOTHING PARAMETER FOR EACH SURFACE
  1 - MINIMIZE GCV FOR EACH SURFACE
  2 - MINIMIZE TRUE MEAN SQUARE ERROR FOR EACH SURFACE
  3 - FIXED SIGNAL FOR EACH SURFACE
  4 - MINIMIZE GML FOR EACH SURFACE1
    1

DATA FILE NAME:
--------------e:\endang\anusplin\1992\jan_dec92.dat
e:\endang\anusplin\1992\jan_dec92.dat
```

```
MAXIMUM NUMBER OF DATA POINTS (AT LEAST  5):25
      25

NO. OF CHARACTERS IN SITE LABEL (0 TO 20):14
   14
DATA FORMAT (SITE LABEL,  4 INDEP VARS, 10 SURFACES,  0 REL
VARIANCES):(a14,2f11.2,2f7.2/10f6.0)
(a14,2f11.2,2f7.2/10f6.0)

OUTPUT LARGE RESIDUAL FILE NAME (BLANK IF NOT REQUIRED):enda.res
enda.res

OUTPUT OPTIMIZATION PARAMETERS FILE NAME (BLANK IF NOT
REQUIRED):enda.opt
enda.opt

OUTPUT SURFACE COEFFICIENTS FILE NAME (BLANK IF NOT
REQUIRED):enda.sur
enda.sur

OUTPUT DATA LIST FILE NAME (BLANK IF NOT REQUIRED):enda.lis
enda.lis

OUTPUT ERROR COVARIANCE FILE NAME (BLANK IF NOT REQUIRED):enda.cov
enda.cov

VALIDATION DATA FILE NAME (BLANK IF NOT REQUIRED):
-------------------------------------------------
```

LAPGRD:

```
E:\Endang\anusplin\raintext>lapgrd raingrd enda.log
LAPGRD  VERSION  4.3  13/04/04
COPYRIGHT AUSTRALIAN NATIONAL UNIVERSITY

SURFACE FILE NAME:
-----------------enda.sur
enda.sur

SURFACE TITLE =
SURFACE UNITS = mm

NUMBER OF SURFACES  =   10
ORDER OF DERIVATIVE =    2
NUMBER OF KNOTS     =   22

NUMBER OF SPLINE INDEPENDENT VARIABLES =   2
NUMBER OF INDEPENDENT COVARIATES       =   2

VAR   LOWER LIMIT   UPPER LIMIT  TRANSF UNITS   MARGINS
  1    323500.       372000.      0      m       1.000       1.000
  2  0.913700E+07  0.918500E+07  0      m       1.000       1.000
  3  -6.28000       286.240      0      m       0.000       0.000
  4   7.19000       332.350      0      deg     0.000       0.000

SURFACE NUMBERS (0 TO 10):0
    0
```

```
TYPE OF SURFACE CALCULATION (0-1):
  0 - SUMMARY STATISTICS ONLY
  1 - ALL SURFACE VALUES1
    1

ERROR COVARIANCE FILE (BLANK IF NO ERRORS REQUIRED):
-------------------------------------------------enda.cov
enda.cov
TYPE OF ERROR CALCULATION (0-4):
  0 - STANDARD ERROR OF AVERAGE ONLY
  1 - MODEL STANDARD ERRORS
  2 - PREDICTION STANDARD ERRORS
  3 - 95% MODEL CONFIDENCE INTERVALS
  4 - 95% PREDICTION CONFIDENCE INTERVALS2
    2

MAXIMUM STANDARD ERRORS (BLANK OR 10 STANDARD ERRORS):


GRID SPECIFICATIONS
-------------------
POSITION OPTION (0 - AT CELL CORNERS, 1 - AT CELL CENTRES):1
    1

INDEX OF FIRST GRID VARIABLE (NORMALLY 1):1
    1

LOWER LIMIT, UPPER LIMIT AND SPACING OF FIRST GRID
VARIABLE:323623.47 371533.47 30
   323623.47000000       371533.47000000       30.00000

INDEX OF SECOND GRID VARIABLE (NORMALLY 2):2
    2

LOWER LIMIT, UPPER LIMIT AND SPACING OF SECOND GRID
VARIABLE:9137850.87 9184590.87 30
   9137850.8700000       9184590.8700000       30.00000

NUMBER OF COLUMNS =  1597
NUMBER OF  ROWS   =  1558

INPUT INDEPENDENT VARIABLE GRIDS
--------------------------------
MODE OF MASK GRID (0-3):
  0 - MASK GRID NOT SUPPLIED
  1 - GENERIC MASK GRID
  2 - ARC/INFO MASK GRID
  3 - IDRISI MASK IMAGE0
    0

MODE OF 3RD INDEPENDENT VARIABLE (0-3):
  0 - USER SUPPLIED CONSTANT
  1 - GENERIC INDEPENDENT VARIABLE GRID
  2 - ARC/INFO INDEPENDENT VARIABLE GRID
  3 - IDRISI INDEPENDENT VARIABLE IMAGE2
    2
INPUT GRID FILE NAME:e:\endang\anusplin\rastert_dem_new1.flt
e:\endang\anusplin\rastert_dem_new1.flt

MODE OF 4TH INDEPENDENT VARIABLE (0-3):
  0 - USER SUPPLIED CONSTANT
```

```
  1 - GENERIC INDEPENDENT VARIABLE GRID
  2 - ARC/INFO INDEPENDENT VARIABLE GRID
  3 - IDRISI INDEPENDENT VARIABLE IMAGE2
    2

INPUT GRID FILE NAME:e:\endang\anusplin\aspect.flt
e:\endang\anusplin\aspect.flt

OUTPUT SURFACE GRIDS
--------------------
MODE OF OUTPUT GRIDS (0-3):
  0 - X,Y,Z FORMAT
  1 - GENERIC GRID BY ROWS
  2 - ARC/INFO GRID
  3 - IDRISI IMAGE2
    2

SPECIAL VALUE FOR OUTPUT GRIDS:-9999
  -9999.00

NAME OF OUTPUT GRID FILE FOR SURFACE 1:jan.flt
jan.flt

NAME OF OUTPUT GRID FILE FOR SURFACE 2:feb.flt
feb.flt

NAME OF OUTPUT GRID FILE FOR SURFACE 3:mar.flt
mar.flt

NAME OF OUTPUT GRID FILE FOR SURFACE 4:apr.flt
apr.flt

NAME OF OUTPUT GRID FILE FOR SURFACE 5:may.flt
may.flt

NAME OF OUTPUT GRID FILE FOR SURFACE 6:jun.flt
jun.flt

NAME OF OUTPUT GRID FILE FOR SURFACE 7:sep.flt
sep.flt

NAME OF OUTPUT GRID FILE FOR SURFACE 8:oct.flt
oct.flt

NAME OF OUTPUT GRID FILE FOR SURFACE 9:nov.flt
nov.flt

NAME OF OUTPUT GRID FILE FOR SURFACE 10:dec.flt
dec.flt

OUTPUT ARC/INFO GRID FORMAT (BLANK FOR BINARY):


OUTPUT ERROR GRIDS
------------------
MODE OF OUTPUT GRIDS (0-3):
  0 - X,Y,Z FORMAT
  1 - GENERIC GRID BY ROWS
  2 - ARC/INFO GRID
  3 - IDRISI IMAGE2
    2
```

```
SPECIAL VALUE FOR OUTPUT GRIDS:-9999
  -9999.00

NAME OF OUTPUT GRID FILE FOR SURFACE 1:jan1.flt
jan1.flt


NAME OF OUTPUT GRID FILE FOR SURFACE 2:feb1.flt
feb1.flt

NAME OF OUTPUT GRID FILE FOR SURFACE 3:mar1.flt
mar1.flt

NAME OF OUTPUT GRID FILE FOR SURFACE 4:apr1.flt
apr1.flt

NAME OF OUTPUT GRID FILE FOR SURFACE 5:may1.flt
may1.flt

NAME OF OUTPUT GRID FILE FOR SURFACE 6:jun1.flt
jun1.flt

NAME OF OUTPUT GRID FILE FOR SURFACE 7:sep1.flt
sep1.flt

NAME OF OUTPUT GRID FILE FOR SURFACE 8:oct1.flt
oct1.flt

NAME OF OUTPUT GRID FILE FOR SURFACE 9:nov1.flt
nov1.flt

NAME OF OUTPUT GRID FILE FOR SURFACE 10:dec1.flt
dec1.flt

OUTPUT ARC/INFO GRID FORMAT (BLANK FOR BINARY):
```

APPENDIX E. RESULTS OF ANUSPLIN FOR EACH RAINFALL SURFACE

The result of each command from ANUSPLIN (SPLINA and LAPRGD) for each month is shown as follows:

January – June 1992 and September – December 1992

```
DATA SUMMARY
------------
NUMBER OF DATA POINTS READ     =     22
NUMBER OF POINTS WITHIN LIMITS =     22

 SURF  MEAN RELATIVE VARIANCE  ROOT MEAN REL VAR
    1                 1.00               1.00

SURFACE STATISTICS
------------------
SURF RHO        NPTS   ERROR    SIGNAL    SURF   MEAN     STD DEV
   1 0.162E-01   22     0.0     22.0 *     1     308.36   142.3
   2 0.162E-01   22     0.0     22.0 *     2     385.77   66.02
   3 0.224E+07   22     9.5     12.5       3     323.68   197.1
   4 0.162E-01   22     0.0     22.0 *     4     419.27   150.8
   5 0.162E-01   22     0.0     22.0 *     5     205.05   103.0
   6 0.162E-01   22     0.0     22.0 *     6     180.91   92.30
   7 0.513E+06   22     5.3     16.7       7     312.50   135.6
   8 0.359E+06   22     4.4     17.6       8     656.68   166.2
   9 0.898E+06   22     6.8     15.2       9     594.50   144.2
  10 0.162E-01   22     0.0     22.0 *    10     344.73   139.5
 AVG 0.401E+06   22     2.6     19.4              373.15   138.4

SURF GCV        MSR        VAR       SURF  RTGCV  RTMSR      RTVAR
   1 0.662E+04 0.342E-11 0.150E-03   1    81.3  0.185E-05 0.123E-01
   2 830.      0.429E-12 0.189E-04   2    28.8  0.655E-06 0.434E-02
   3 0.182E+05 0.340E+04 0.787E+04   3    135.  58.3       88.7
   4 0.795E+04 0.411E-11 0.181E-03   4    89.2  0.203E-05 0.134E-01
   5 0.457E+04 0.236E-11 0.104E-03   5    67.6  0.154E-05 0.102E-01
   6 0.135E+04 0.700E-12 0.308E-04   6    36.8  0.837E-06 0.555E-02
   7 0.343E+04 199.      826.        7    58.6  14.1       28.7
   8 0.257E+04 103.      514.        8    50.7  10.1       22.7
   9 0.585E+04 565.      0.182E+04   9    76.5  23.8       42.6
  10 0.578E+04 0.299E-11 0.131E-03  10    76.0  0.173E-05 0.115E-01
 AVG 0.571E+04 427.      0.110E+04         75.6  20.7       33.2

SURF GML        MSE        VAR       SURF  RTGML  RTMSE      RTVAR
   1 0.113E+05 0.150E-03 0.115E-03   1    107.  0.123E-01 0.107E-01
   2 0.286E+04 0.189E-04 0.290E-04   2    53.5  0.434E-02 0.538E-02
   3 0.161E+05 0.447E+04 0.743E+04   3    127.  66.8       86.2
   4 0.156E+05 0.181E-03 0.158E-03   4    125.  0.134E-01 0.126E-01
   5 0.861E+04 0.104E-03 0.873E-04   5    92.8  0.102E-01 0.934E-02
   6 0.327E+04 0.308E-04 0.331E-04   6    57.1  0.555E-02 0.575E-02
   7 0.492E+04 627.      981.        7    70.1  25.0       31.3
```

```
   8 0.314E+04 411.      485.       8    56.0  20.3       22.0
   9 0.621E+04 0.125E+04 0.178E+04  9    78.8  35.4       42.2
  10 0.108E+05 0.131E-03 0.109E-03 10    104.  0.115E-01 0.104E-01
 AVG 0.828E+04 676.      0.107E+04       91.0  26.0       32.7

SURF   COVARIATES AND STANDARD ERRORS
   1   -0.156       1.63        0.217E-03  0.954E-04
   2   -0.675E-01   0.532       0.769E-04  0.338E-04
   3   -0.159       2.45        0.885      0.449
   4   -0.357       1.02        0.238E-03  0.105E-03
   5    0.186       1.32        0.181E-03  0.793E-04
   6    0.157      -0.216       0.983E-04  0.432E-04
   7    0.844      -0.842       0.384      0.181
   8   -0.676E-01   0.569       0.321      0.148
   9   -0.179       0.988E-01   0.513      0.249
  10   -0.159       1.68        0.203E-03  0.892E-04

RANKED ROOT MEAN SQUARE RESIDUALS
---------------------------------
     1      9  SADANG            57.5
     2      3  KARANG ANYAR      29.4
     3     21  ST8               27.6
     4     16  ST1               22.6
     5      1  ADIMULYO          22.1

RANKED ROOT MEAN SQUARE RESIDUALS FOR SURFACE  1
     1      3  KARANG ANYAR     0.351E-05        206.0    206.0
     2     18  ST3             -0.301E-05        156.0    156.0
     3      9  SADANG          -0.300E-05        472.0    472.0
     4     16  ST1              0.295E-05        144.0    144.0
     5     21  ST8              0.260E-05        154.0    154.0
     6      6  GOMBONG         -0.252E-05        462.0    462.0
     7     17  ST2              0.244E-05        153.0    153.0
     8      7  KARANG GAYAM    -0.232E-05        151.0    151.0
     9     20  ST7             -0.216E-05        164.0    164.0
    10     22  ST4              0.147E-05        163.0    163.0

RANKED ROOT MEAN SQUARE RESIDUALS FOR SURFACE  2
     1      1  ADIMULYO         0.131E-05        244.0    244.0
     2      3  KARANG ANYAR    -0.975E-06        422.0    422.0
     3      4  SEMPOR          -0.963E-06        445.0    445.0
     4     17  ST2              0.925E-06        365.0    365.0
     5      9  SADANG          -0.872E-06        479.0    479.0
     6      6  GOMBONG          0.858E-06        404.0    404.0
     7     18  ST3             -0.848E-06        369.0    369.0
     8     16  ST1              0.756E-06        360.0    360.0
     9     21  ST8              0.664E-06        379.0    379.0
    10     20  ST7             -0.610E-06        383.0    383.0

RANKED ROOT MEAN SQUARE RESIDUALS FOR SURFACE  3
     1      9  SADANG           -181.            839.0    658.0
     2      3  KARANG ANYAR      85.2            230.0    315.2
     3     21  ST8               82.1            163.0    245.1
     4     16  ST1               68.1            168.0    236.1
     5      7  KARANG GAYAM     -67.7            177.0    109.3
     6     18  ST3              -62.4            168.0    105.6
     7      1  ADIMULYO          59.9            182.0    241.9
     8      4  SEMPOR           -49.3            330.0    280.7
     9     17  ST2               46.3            186.0    232.3
```

10	11	KUWARASAN	-41.3	280.0	238.7
RANKED ROOT MEAN SQUARE RESIDUALS FOR SURFACE 4					
1	3	KARANG ANYAR	0.455E-05	244.0	244.0
2	6	GOMBONG	-0.437E-05	594.0	594.0
3	21	ST8	0.347E-05	328.0	328.0
4	20	ST7	-0.307E-05	353.0	353.0
5	7	KARANG GAYAM	-0.296E-05	327.0	327.0
6	17	ST2	0.276E-05	297.0	297.0
7	9	SADANG	-0.187E-05	557.0	557.0
8	15	PETANAHAN	-0.164E-05	763.0	763.0
9	18	ST3	-0.153E-05	324.0	324.0
10	16	ST1	0.128E-05	337.0	337.0
RANKED ROOT MEAN SQUARE RESIDUALS FOR SURFACE 5					
1	9	SADANG	-0.308E-05	383.0	383.0
2	18	ST3	-0.258E-05	123.0	123.0
3	3	KARANG ANYAR	0.253E-05	92.0	92.0
4	7	KARANG GAYAM	-0.244E-05	121.0	121.0
5	22	ST4	0.227E-05	110.0	110.0
6	17	ST2	0.222E-05	129.0	129.0
7	16	ST1	0.216E-05	115.0	115.0
8	6	GOMBONG	-0.165E-05	260.0	260.0
9	15	PETANAHAN	0.113E-05	302.0	302.0
10	11	KUWARASAN	-0.984E-06	307.0	307.0
RANKED ROOT MEAN SQUARE RESIDUALS FOR SURFACE 6					
1	22	ST4	-0.165E-05	164.0	164.0
2	21	ST8	0.129E-05	138.0	138.0
3	20	ST7	-0.129E-05	150.0	150.0
4	11	KUWARASAN	0.119E-05	150.0	150.0
5	15	PETANAHAN	-0.118E-05	437.0	437.0
6	9	SADANG	0.115E-05	84.0	84.0
7	18	ST3	0.991E-06	166.0	166.0
8	10	KLIRONG	0.901E-06	225.0	225.0
9	7	KARANG GAYAM	0.850E-06	153.0	153.0
10	4	SEMPOR	0.806E-06	144.0	144.0
RANKED ROOT MEAN SQUARE RESIDUALS FOR SURFACE 7					
1	20	ST7	-31.0	483.0	452.0
2	6	GOMBONG	-28.9	271.0	242.1
3	15	PETANAHAN	-27.7	405.0	377.3
4	3	KARANG ANYAR	24.2	127.0	151.2
5	10	KLIRONG	17.5	224.0	241.5
6	17	ST2	-14.8	460.0	445.2
7	21	ST8	14.0	416.0	430.0
8	1	ADIMULYO	13.2	177.0	190.2
9	4	SEMPOR	11.1	268.0	279.1
10	18	ST3	6.52	462.0	468.5
RANKED ROOT MEAN SQUARE RESIDUALS FOR SURFACE 8					
1	11	KUWARASAN	21.9	725.0	746.9
2	20	ST7	19.1	489.0	508.1
3	21	ST8	-18.6	539.0	520.4
4	17	ST2	14.4	486.0	500.4
5	1	ADIMULYO	-13.1	821.0	807.9
6	8	PURING	-11.8	1050.0	1038.2
7	4	SEMPOR	-11.2	759.0	747.8
8	14	MANDIRAJA	9.42	474.0	483.4
9	22	ST4	-9.28	533.0	523.7
10	16	ST1	7.83	535.0	542.8

```
RANKED ROOT MEAN SQUARE RESIDUALS FOR SURFACE  9
     1      4  SEMPOR           -45.7            710.0    664.3
     2      5  ROWOKELE          37.9            558.0    595.9
     3     20  ST7               37.9            451.0    488.9
     4      1  ADIMULYO          31.2            607.0    638.2
     5     22  ST4              -30.6            515.0    484.4
     6      6  GOMBONG           30.1            586.0    616.1
     7      8  PURING           -29.8           1019.0    989.2
     8      3  KARANG ANYAR     -28.1            635.0    606.9
     9     18  ST3               24.5            438.0    462.5
    10     13  PURWANEGARA      -20.9            750.0    729.1

RANKED ROOT MEAN SQUARE RESIDUALS FOR SURFACE 10
     1      7  KARANG GAYAM   -0.350E-05         245.0    245.0
     2      9  SADANG         -0.348E-05         595.0    595.0
     3     17  ST2             0.334E-05         233.0    233.0
     4      3  KARANG ANYAR    0.251E-05         177.0    177.0
     5     18  ST3            -0.247E-05         251.0    251.0
     6     16  ST1             0.229E-05         260.0    260.0
     7     15  PETANAHAN       0.182E-05         332.0    332.0
     8     22  ST4             0.170E-05         265.0    265.0
     9     10  KLIRONG        -0.119E-05         373.0    373.0
    10      4  SEMPOR         -0.107E-05         419.0    419.0


LAPGRD SUMMARY STATISTICS
-------------------------
OUTPUT SURFACE AND ERROR GRIDS FOR SURFACE   1
NUMBER OF CELLS = 2488126      MEAN ERROR      =    0.35E-01
MINIMUM ERROR   =    0.14E-01  MAXIMUM ERROR   =    0.17
MINIMUM VALUE   =   -183.      MAXIMUM VALUE   =    910.
MEAN SURF VALUE =    441.      STANDARD ERROR  =    0.19E-01

OUTPUT SURFACE AND ERROR GRIDS FOR SURFACE   2
NUMBER OF CELLS = 2488126      MEAN ERROR      =    0.12E-01
MINIMUM ERROR   =    0.50E-02  MAXIMUM ERROR   =    0.60E-01
MINIMUM VALUE   =    147.      MAXIMUM VALUE   =    692.
MEAN SURF VALUE =    415.      STANDARD ERROR  =    0.67E-02

OUTPUT SURFACE AND ERROR GRIDS FOR SURFACE   3
NUMBER OF CELLS = 2488126      MEAN ERROR      =    0.18E+03
MINIMUM ERROR   =     97.      MAXIMUM ERROR   =    0.72E+03
MINIMUM VALUE   =   -492.      MAXIMUM VALUE   =   0.113E+04
MEAN SURF VALUE =    487.      STANDARD ERROR  =     82.

OUTPUT SURFACE AND ERROR GRIDS FOR SURFACE   4
NUMBER OF CELLS = 2488126      MEAN ERROR      =    0.38E-01
MINIMUM ERROR   =    0.15E-01  MAXIMUM ERROR   =    0.19
MINIMUM VALUE   =   -199.      MAXIMUM VALUE   =    987.
MEAN SURF VALUE =    465.      STANDARD ERROR  =    0.21E-01


OUTPUT SURFACE AND ERROR GRIDS FOR SURFACE   5
NUMBER OF CELLS = 2488126      MEAN ERROR      =    0.29E-01
MINIMUM ERROR   =    0.12E-01  MAXIMUM ERROR   =    0.14
MINIMUM VALUE   =   -245.      MAXIMUM VALUE   =    782.
MEAN SURF VALUE =    312.      STANDARD ERROR  =    0.16E-01
```

```
OUTPUT SURFACE AND ERROR GRIDS FOR SURFACE   6
NUMBER OF CELLS = 2488126      MEAN ERROR      =    0.16E-01
MINIMUM ERROR   =    0.64E-02  MAXIMUM ERROR   =    0.76E-01
MINIMUM VALUE   =    -132.     MAXIMUM VALUE   =    616.
MEAN SURF VALUE =     158.     STANDARD ERROR  =    0.86E-02

OUTPUT SURFACE AND ERROR GRIDS FOR SURFACE   7
NUMBER OF CELLS = 2488126      MEAN ERROR      =     69.
MINIMUM ERROR   =      33.     MAXIMUM ERROR   =    0.30E+03
MINIMUM VALUE   =    -341.     MAXIMUM VALUE   =   0.114E+04
MEAN SURF VALUE =     279.     STANDARD ERROR  =     34.

OUTPUT SURFACE AND ERROR GRIDS FOR SURFACE   8
NUMBER OF CELLS = 2488126      MEAN ERROR      =     56.
MINIMUM ERROR   =      26.     MAXIMUM ERROR   =    0.25E+03
MINIMUM VALUE   =     368.     MAXIMUM VALUE   =   0.132E+04
MEAN SURF VALUE =     729.     STANDARD ERROR  =     28.

OUTPUT SURFACE AND ERROR GRIDS FOR SURFACE   9
NUMBER OF CELLS = 2488126      MEAN ERROR      =     96.
MINIMUM ERROR   =      48.     MAXIMUM ERROR   =    0.41E+03
MINIMUM VALUE   =     300.     MAXIMUM VALUE   =   0.119E+04
MEAN SURF VALUE =     595.     STANDARD ERROR  =     46.

OUTPUT SURFACE AND ERROR GRIDS FOR SURFACE  10
NUMBER OF CELLS = 2488126      MEAN ERROR      =    0.33E-01
MINIMUM ERROR   =    0.13E-01  MAXIMUM ERROR   =    0.16
MINIMUM VALUE   =    -213.     MAXIMUM VALUE   =   0.101E+04
MEAN SURF VALUE =     465.     STANDARD ERROR  =    0.18E-01
```

July 1992

```
DATA SUMMARY
------------
NUMBER OF DATA POINTS READ     =     19
NUMBER OF POINTS WITHIN LIMITS =     19

 SURF  MEAN RELATIVE VARIANCE  ROOT MEAN REL VAR
    1                1.00              1.00

SURFACE STATISTICS
------------------
SURF RHO        NPTS   ERROR  SIGNAL    SURF   MEAN      STD DEV
   1 0.317E-01  19      0.0   19.0 *      1   95.895       54.63

SURF GCV     MSR         VAR         SURF  RTGCV  RTMSR      RTVAR
   1 700.    0.155E-11 0.330E-04     1   26.5   0.125E-05 0.574E-02

SURF GML        MSE         VAR       SURF RTGML  RTMSE      RTVAR
   1 0.175E+04 0.330E-04 0.365E-04   1   41.9  0.574E-02 0.604E-02


SURF   COVARIATES AND STANDARD ERRORS
   1   -0.277E-01  0.479         0.103E-03  0.450E-04

RANKED ROOT MEAN SQUARE RESIDUALS
---------------------------------
     1      1  KARANG ANYAR     0.283E-05
```

```
     2      4  GOMBONG          0.274E-05
     3      5  KARANG GAYAM     0.184E-05
     4      7  SADANG           0.173E-05
     5     13  ST1              0.148E-05
RANKED ROOT MEAN SQUARE RESIDUALS FOR SURFACE  1
     1      1  KARANG ANYAR     0.283E-05        39.0      39.0
     2      4  GOMBONG         -0.274E-05       153.0     153.0
     3      5  KARANG GAYAM    -0.184E-05        65.0      65.0
     4      7  SADANG          -0.173E-05       161.0     161.0
     5     13  ST1              0.148E-05        60.0      60.0
     6     14  ST2              0.132E-05        68.0      68.0
     7     18  ST8              0.117E-05        63.0      63.0
     8     15  ST3             -0.889E-06        61.0      61.0
     9     17  ST7             -0.737E-06        64.0      64.0
    10      9  KUWARASAN        0.489E-06        83.0      83.0
    11      2  SEMPOR           0.469E-06       154.0     154.0
    12     11  PURWANEGARA      0.439E-06        25.0      25.0
    13     19  ST4              0.339E-06        69.0      69.0
    14      6  PURING          -0.334E-06       203.0     203.0
    15     12  MANDIRAJA       -0.251E-06        51.0      51.0
    16     16  ST6              0.173E-06        68.0      68.0
    17      3  ROWOKELE        -0.136E-06       205.0     205.0
    18     10  BANJAR NEGARA   -0.655E-07       100.0     100.0
    19      8  KLIRONG          0.987E-08       130.0     130.0

LAPGRD SUMMARY STATISTICS
-------------------------
OUTPUT SURFACE AND ERROR GRIDS FOR SURFACE   1
NUMBER OF CELLS = 2488126      MEAN ERROR      =    0.16E-01
MINIMUM ERROR   =    0.66E-02  MAXIMUM ERROR   =    0.80E-01
MINIMUM VALUE   =   -124.      MAXIMUM VALUE   =    398.
MEAN SURF VALUE =    128.      STANDARD ERROR  =    0.84E-02
```

August 1992

```
DATA SUMMARY
------------
NUMBER OF DATA POINTS READ     =     21
NUMBER OF POINTS WITHIN LIMITS =     21

 SURF  MEAN RELATIVE VARIANCE  ROOT MEAN REL VAR
    1               1.00              1.00

SURFACE STATISTICS
------------------
SURF RHO         NPTS  ERROR    SIGNAL    SURF   MEAN      STD DEV
   1 0.230E+07    21    9.0      12.0       1   353.62     105.5

SURF GCV         MSR         VAR         SURF   RTGCV     RTMSR      RTVAR
   1 0.581E+04 0.107E+04 0.249E+04    1    76.2      32.7       49.9


SURF GML         MSE         VAR         SURF  RTGML     RTMSE      RTVAR
   1 0.564E+04 0.142E+04 0.262E+04    1    75.1      37.7       51.2

SURF    COVARIATES AND STANDARD ERRORS
   1     0.505     -0.424        0.512       0.276
```

```
RANKED ROOT MEAN SQUARE RESIDUALS
---------------------------------
     1       3  KARANG ANYAR       66.0
     2       5  ROWOKELE           63.9
     3       6  GOMBONG            56.4
     4      21  ST4                49.2
     5      10  KUWARASAN          46.9

RANKED ROOT MEAN SQUARE RESIDUALS FOR SURFACE  1
     1       3  KARANG ANYAR       66.0            197.0    263.0
     2       5  ROWOKELE          -63.9            672.0    608.1
     3       6  GOMBONG           -56.4            405.0    348.6
     4      21  ST4               -49.2            416.0    366.8
     5      10  KUWARASAN          46.9            279.0    325.9
     6       4  SEMPOR             37.4            435.0    472.4
     7      17  ST3                35.9            366.0    401.9
     8       1  ADIMULYO          -33.3            300.0    266.7
     9      12  PURWANEGARA        22.1            240.0    262.1
    10      11  BANJAR NEGARA     -20.5            497.0    476.5
    11      18  ST6                20.1            388.0    408.1
    12      14  PETANAHAN          15.8            210.0    225.8
    13       9  KLIRONG           -14.6            268.0    253.4
    14       7  KARANG GAYAM      -13.2            387.0    373.8
    15      13  MANDIRAJA          12.8            290.0    302.8
    16      19  ST7               -9.20            382.0    372.8
    17      20  ST8               -8.04            368.0    360.0
    18      15  ST1                7.38            369.0    376.4
    19      16  ST2                7.13            358.0    365.1
    20       2  ALIAN             -1.80            299.0    297.2
    21       8  PURING            -1.23            300.0    298.8

LAPGRD SUMMARY STATISTICS
-------------------------
OUTPUT SURFACE AND ERROR GRIDS FOR SURFACE   1
NUMBER OF CELLS = 2488126      MEAN ERROR      =    0.10E+03
MINIMUM ERROR   =     55.      MAXIMUM ERROR   =    0.41E+03
MINIMUM VALUE   =    149.      MAXIMUM VALUE   =    953.
MEAN SURF VALUE =    395.      STANDARD ERROR  =     45.
```

January – December 1995

```
DATA SUMMARY
------------
NUMBER OF DATA POINTS READ     =     24
NUMBER OF POINTS WITHIN LIMITS =     24

 SURF  MEAN RELATIVE VARIANCE  ROOT MEAN REL VAR
    1                 1.00               1.00

SURFACE STATISTICS
------------------
SURF RHO         NPTS  ERROR    SIGNAL   SURF    MEAN      STD DEV
   1 0.172E+07   24     9.6      14.4       1   409.08      103.6
   2 0.194E-01   24     0.0      24.0 *     2   543.00      185.7
   3 0.194E-01   24     0.0      24.0 *     3   422.67      158.8
   4 0.194E-01   24     0.0      24.0 *     4   232.08      65.04
   5 0.194E-01   24     0.0      24.0 *     5   117.46      87.45
   6 0.419E+08   24    17.3       6.7       6   294.33      70.95
```

```
   7 0.241E+07   24   10.6      13.4        7   73.833     59.32
   8 0.107E+09   24   18.2       5.8        8   0.70833    2.255
   9 0.194E-01   24    0.0      24.0 *      9   2.4167     4.934
  10 0.673E+07   24   13.6      10.4       10   400.88     142.8
  11 0.179E+08   24   15.9       8.1       11   624.79     159.9
  12 0.550E+08   24   17.6       6.4       12   437.38     100.4
 AVG 0.194E+08   24    8.6      15.4            296.55     110.7

SURF GCV        MSR        VAR         SURF RTGCV  RTMSR      RTVAR
   1 0.655E+04 0.104E+04 0.261E+04     1  80.9   32.3       51.1
   2 0.332E+04 0.234E-11 0.881E-04     2  57.7   0.153E-05  0.939E-
   3 0.973E+04 0.684E-11 0.258E-03     3  98.6   0.261E-05  0.161E-
   4 221.      0.155E-12 0.586E-05     4  14.9   0.394E-06  0.242E-
   5 827.      0.582E-12 0.219E-04     5  28.8   0.763E-06  0.468E-
   6 0.370E+04 0.191E+04 0.266E+04     6  60.8   43.7       51.6
   7 557.      110.      247.          7  23.6   10.5       15.7
   8 6.10      3.51      4.63          8  2.47   1.87       2.15
   9 6.54      0.460E-14 0.173E-06     9  2.56   0.678E-07  0.416E-
  10 0.844E+04 0.271E+04 0.478E+04    10  91.8   52.1       69.2
  11 0.989E+04 0.432E+04 0.654E+04    11  99.4   65.7       80.8
  12 0.136E+05 0.731E+04 0.998E+04    12  117.   85.5       99.9
 AVG 0.474E+04 0.145E+04 0.224E+04        68.8   38.1       47.3

SURF GML        MSE        VAR         SURF RTGML  RTMSE      RTVAR
   1 0.640E+04 0.157E+04 0.246E+04     1  80.0   39.6       49.6
   2 0.848E+04 0.881E-04 0.950E-04     2  92.1   0.939E-02  0.975E-
   3 0.229E+05 0.258E-03 0.256E-03     3  151.   0.161E-01  0.160E-
   4 0.147E+04 0.586E-05 0.164E-04     4  38.3   0.242E-02  0.406E-
   5 0.272E+04 0.219E-04 0.305E-04     5  52.2   0.468E-02  0.552E-
   6 0.298E+04  748.     0.268E+04     6  54.6   27.3       51.7
   7 572.      137.      257.          7  23.9   11.7       16.0
   8 4.85      1.12      4.63          8  2.20   1.06       2.15
   9 23.4     0.173E-06 0.262E-06     9  4.83   0.416E-03  0.512E-
  10 0.771E+04 0.207E+04 0.501E+04    10  87.8   45.5       70.8
  11 0.826E+04 0.222E+04 0.668E+04    11  90.9   47.1       81.7
  12 0.109E+05 0.266E+04 0.998E+04    12  104.   51.6       99.9
 AVG 0.603E+04  784.     0.226E+04        77.7   28.0       47.5

SURF   COVARIATES AND STANDARD ERRORS
   1   -0.532      0.733        0.504       0.261
   2   -0.250      0.405        0.164E-03   0.711E-04
   3   -0.542E-01  0.348        0.280E-03   0.122E-03
   4   -0.921E-01  0.472        0.422E-04   0.183E-04
   5    0.245     -0.648E-01    0.816E-04   0.355E-04
   6    0.306     -0.453        0.307       0.150
   7    0.282      0.344        0.143       0.760E-01
   8   -0.489E-02  0.449E-02    0.122E-01   0.563E-02
   9   -0.381E-02 -0.445E-02    0.725E-05   0.315E-05
  10    0.684     -0.549        0.513       0.277
  11    0.950     -0.345E-02    0.520       0.269
  12   -0.338     -0.258E-01    0.585       0.279

RANKED ROOT MEAN SQUARE RESIDUALS
---------------------------------
     1      2  ALIAN              81.3
     2      3  KARANG ANYAR       65.3
     3     13  KEBUMEN            55.9
     4      4  SEMPOR             53.0
     5      6  GOMBONG            50.1
```

RANKED ROOT MEAN SQUARE RESIDUALS FOR SURFACE 1

1	2	ALIAN	-68.8	589.0	520.2
2	4	SEMPOR	-57.1	591.0	533.9
3	9	SADANG	-54.3	525.0	470.7
4	1	ADIMULYO	49.3	320.0	369.3
5	14	PETANAHAN	46.7	364.0	410.7
6	13	KEBUMEN	42.0	426.0	468.0
7	22	ST7	34.6	273.0	307.6
8	18	ST1	32.4	298.0	330.4

RANKED ROOT MEAN SQUARE RESIDUALS FOR SURFACE 2

1	22	ST7	0.364E-05	330.0	330.0
2	23	ST8	-0.292E-05	355.0	355.0
3	2	ALIAN	0.275E-05	320.0	320.0
4	13	KEBUMEN	-0.248E-05	579.0	579.0
5	19	ST2	0.246E-05	306.0	306.0
6	4	SEMPOR	-0.168E-05	716.0	716.0
7	3	KARANG ANYAR	0.155E-05	587.0	587.0
8	16	PURWANEGARA	-0.154E-05	775.0	775.0

RANKED ROOT MEAN SQUARE RESIDUALS FOR SURFACE 3

1	3	KARANG ANYAR	0.538E-05	113.0	113.0
2	2	ALIAN	-0.509E-05	724.0	724.0
3	13	KEBUMEN	0.441E-05	301.0	301.0
4	18	ST1	0.406E-05	409.0	409.0
5	22	ST7	0.395E-05	359.0	359.0
6	6	GOMBONG	-0.345E-05	458.0	458.0
7	9	SADANG	-0.299E-05	494.0	494.0
8	23	ST8	-0.286E-05	382.0	382.0

RANKED ROOT MEAN SQUARE RESIDUALS FOR SURFACE 4

1	16	PURWANEGARA	0.841E-06	148.0	148.0
2	9	SADANG	-0.729E-06	361.0	361.0
3	4	SEMPOR	-0.643E-06	317.0	317.0
4	7	KARANG GAYAM	-0.640E-06	258.0	258.0
5	17	MANDIRAJA	-0.529E-06	240.0	240.0
6	22	ST7	0.499E-06	232.0	232.0
7	11	KLIRONG	0.492E-06	72.0	72.0
8	14	PETANAHAN	-0.428E-06	167.0	167.0

RANKED ROOT MEAN SQUARE RESIDUALS FOR SURFACE 5

1	3	KARANG ANYAR	0.230E-05	16.0	16.0
2	6	GOMBONG	-0.222E-05	204.0	204.0
3	13	KEBUMEN	-0.750E-06	25.0	25.0
4	2	ALIAN	0.636E-06	0.0	0.0
5	5	ROWOKELE	0.628E-06	151.0	151.0
6	24	ST4	-0.585E-06	108.0	108.0
7	22	ST7	0.479E-06	100.0	100.0
8	21	ST6	0.469E-06	101.0	101.0

RANKED ROOT MEAN SQUARE RESIDUALS FOR SURFACE 6

1	13	KEBUMEN	109.	134.0	243.2
2	2	ALIAN	-90.0	349.0	259.0
3	6	GOMBONG	-85.9	403.0	317.1
4	3	KARANG ANYAR	74.1	208.0	282.1
5	23	ST8	-52.8	347.0	294.2
6	5	ROWOKELE	-50.1	453.0	402.9
7	20	ST3	36.8	317.0	353.8
8	17	MANDIRAJA	33.8	286.0	319.8

RANKED ROOT MEAN SQUARE RESIDUALS FOR SURFACE 7

1	3	KARANG ANYAR	29.2	27.0	56.2
2	1	ADIMULYO	-16.9	124.0	107.1
3	6	GOMBONG	-16.0	81.0	65.0
4	19	ST2	15.6	23.0	38.6
5	12	KUWARASAN	13.6	87.0	100.6
6	2	ALIAN	12.9	0.0	12.9
7	11	KLIRONG	-12.3	165.0	152.7
8	9	SADANG	-10.5	75.0	64.5

RANKED ROOT MEAN SQUARE RESIDUALS FOR SURFACE 8

1	16	PURWANEGARA	-6.63	10.0	3.4
2	4	SEMPOR	-3.46	5.0	1.5
3	17	MANDIRAJA	3.04	0.0	3.0
4	15	BANJAR NEGARA	2.19	0.0	2.2
5	13	KEBUMEN	-2.19	2.0	-0.2
6	5	ROWOKELE	1.48	0.0	1.5
7	6	GOMBONG	1.37	0.0	1.4
8	3	KARANG ANYAR	1.16	0.0	1.2

RANKED ROOT MEAN SQUARE RESIDUALS FOR SURFACE 9

1	6	GOMBONG	-0.174E-06	9.0	9.0
2	17	MANDIRAJA	-0.153E-06	21.0	21.0
3	16	PURWANEGARA	0.140E-06	0.0	0.0
4	3	KARANG ANYAR	0.129E-06	0.0	0.0
5	4	SEMPOR	0.810E-07	4.0	4.0
6	20	ST3	-0.584E-07	0.0	0.0
7	12	KUWARASAN	-0.503E-07	8.0	8.0
8	24	ST4	0.455E-07	0.0	0.0

RANKED ROOT MEAN SQUARE RESIDUALS FOR SURFACE 10

1	6	GOMBONG	-135.	636.0	500.8
2	1	ADIMULYO	103.	216.0	319.4
3	12	KUWARASAN	-92.4	572.0	479.6
4	3	KARANG ANYAR	81.5	305.0	386.5
5	2	ALIAN	-73.2	369.0	295.8
6	11	KLIRONG	65.0	113.0	178.0
7	23	ST8	-61.5	422.0	360.5
8	14	PETANAHAN	-46.5	255.0	208.5

RANKED ROOT MEAN SQUARE RESIDUALS FOR SURFACE 11

1	2	ALIAN	-190.	841.0	650.7
2	13	KEBUMEN	113.	472.0	584.7
3	4	SEMPOR	-107.	696.0	588.5
4	16	PURWANEGARA	91.7	565.0	656.7
5	18	ST1	91.3	585.0	676.3
6	21	ST6	64.4	665.0	729.4
7	14	PETANAHAN	61.9	414.0	475.9
8	9	SADANG	-55.2	689.0	633.8

RANKED ROOT MEAN SQUARE RESIDUALS FOR SURFACE 12

1	3	KARANG ANYAR	194.	221.0	414.9
2	8	PURING	-161.	640.0	478.9
3	2	ALIAN	-157.	646.0	488.6
4	4	SEMPOR	-135.	535.0	399.8
5	11	KLIRONG	-120.	630.0	510.0
6	14	PETANAHAN	118.	376.0	493.9
7	9	SADANG	-105.	564.0	459.4
8	13	KEBUMEN	103.	387.0	489.9

```
LAPGRD SUMMARY STATISTICS
-------------------------
OUTPUT SURFACE AND ERROR GRIDS FOR SURFACE   1
NUMBER OF CELLS = 2488126      MEAN ERROR      =     96.
MINIMUM ERROR   =     56.      MAXIMUM ERROR   =    0.38E+03
MINIMUM VALUE   =   -150.      MAXIMUM VALUE   =    809.
MEAN SURF VALUE =    446.      STANDARD ERROR  =     36.


OUTPUT SURFACE AND ERROR GRIDS FOR SURFACE   2
NUMBER OF CELLS = 2488126      MEAN ERROR      =    0.24E-01
MINIMUM ERROR   =    0.11E-01  MAXIMUM ERROR   =    0.12
MINIMUM VALUE   =    238.      MAXIMUM VALUE   =   0.114E+04
MEAN SURF VALUE =    587.      STANDARD ERROR  =    0.11E-01

OUTPUT SURFACE AND ERROR GRIDS FOR SURFACE   3
NUMBER OF CELLS = 2488126      MEAN ERROR      =    0.42E-01
MINIMUM ERROR   =    0.18E-01  MAXIMUM ERROR   =    0.21
MINIMUM VALUE   =    63.0      MAXIMUM VALUE   =    930.
MEAN SURF VALUE =    506.      STANDARD ERROR  =    0.19E-01

OUTPUT SURFACE AND ERROR GRIDS FOR SURFACE   4
NUMBER OF CELLS = 2488126      MEAN ERROR      =    0.63E-02
MINIMUM ERROR   =    0.28E-02  MAXIMUM ERROR   =    0.31E-01
MINIMUM VALUE   =   -128.      MAXIMUM VALUE   =    443.
MEAN SURF VALUE =    213.      STANDARD ERROR  =    0.28E-02

OUTPUT SURFACE AND ERROR GRIDS FOR SURFACE   5
NUMBER OF CELLS = 2488126      MEAN ERROR      =    0.12E-01
MINIMUM ERROR   =    0.54E-02  MAXIMUM ERROR   =    0.61E-01
MINIMUM VALUE   =   -34.2      MAXIMUM VALUE   =    613.
MEAN SURF VALUE =    152.      STANDARD ERROR  =    0.54E-02

OUTPUT SURFACE AND ERROR GRIDS FOR SURFACE   6
NUMBER OF CELLS = 2488126      MEAN ERROR      =     74.
MINIMUM ERROR   =     54.      MAXIMUM ERROR   =    0.25E+03
MINIMUM VALUE   =    77.5      MAXIMUM VALUE   =    641.
MEAN SURF VALUE =    293.      STANDARD ERROR  =     25.

OUTPUT SURFACE AND ERROR GRIDS FOR SURFACE   7
NUMBER OF CELLS = 2488126      MEAN ERROR      =     28.
MINIMUM ERROR   =     17.      MAXIMUM ERROR   =    0.11E+03
MINIMUM VALUE   =   -19.1      MAXIMUM VALUE   =    364.
MEAN SURF VALUE =    126.      STANDARD ERROR  =     10.

OUTPUT SURFACE AND ERROR GRIDS FOR SURFACE   8
NUMBER OF CELLS = 2488126      MEAN ERROR      =     3.0
MINIMUM ERROR   =      2.2     MAXIMUM ERROR   =     10.
MINIMUM VALUE   =    -3.39     MAXIMUM VALUE   =    6.41
MEAN SURF VALUE =    0.532     STANDARD ERROR  =     1.0

OUTPUT SURFACE AND ERROR GRIDS FOR SURFACE   9
NUMBER OF CELLS = 2488126      MEAN ERROR      =    0.11E-02
MINIMUM ERROR   =    0.48E-03  MAXIMUM ERROR   =    0.54E-02
MINIMUM VALUE   =    -5.86     MAXIMUM VALUE   =    24.7
MEAN SURF VALUE =     4.51     STANDARD ERROR  =    0.48E-03

OUTPUT SURFACE AND ERROR GRIDS FOR SURFACE  10
NUMBER OF CELLS = 2488126      MEAN ERROR      =    0.11E+03
MINIMUM ERROR   =     74.      MAXIMUM ERROR   =    0.40E+03
```

```
MINIMUM VALUE   =     24.1      MAXIMUM VALUE  =   0.120E+04
MEAN SURF VALUE =     457.      STANDARD ERROR =     39.

OUTPUT SURFACE AND ERROR GRIDS FOR SURFACE  11
NUMBER OF CELLS = 2488126       MEAN ERROR     =    0.12E+03
MINIMUM ERROR   =     85.       MAXIMUM ERROR  =    0.42E+03
MINIMUM VALUE   =     352.      MAXIMUM VALUE  =   0.171E+04
MEAN SURF VALUE =     741.      STANDARD ERROR =     42.


OUTPUT SURFACE AND ERROR GRIDS FOR SURFACE  12
NUMBER OF CELLS = 2488126       MEAN ERROR     =    0.14E+03
MINIMUM ERROR   =     0.10E+03  MAXIMUM ERROR  =    0.48E+03
MINIMUM VALUE   =     144.      MAXIMUM VALUE  =    590.
MEAN SURF VALUE =     419.      STANDARD ERROR =     49.
```

January 1998

```
DATA SUMMARY
------------
NUMBER OF DATA POINTS READ     =     23
NUMBER OF POINTS WITHIN LIMITS =     21
 SURF  MEAN RELATIVE VARIANCE  ROOT MEAN REL VAR
    1                 1.00              1.00

SURFACE STATISTICS
------------------
SURF RHO         NPTS  ERROR    SIGNAL    SURF     MEAN      STD DEV
   1 0.433E+04    21    0.1     20.9 *     1      258.24      104.3

SURF GCV        MSR         VAR     SURF   RTGCV     RTMSR      RTVAR
   1 0.192E+04 0.722E-01  11.8      1      43.9      0.269      3.43

SURF GML         MSE       VAR     SURF   RTGML     RTMSE      RTVAR
   1 0.346E+04  11.7       9.51     1      58.8      3.42       3.08

SURF   COVARIATES AND STANDARD ERRORS
   1   -0.337E-01  0.556E-01    0.602E-01  0.263E-01

RANKED ROOT MEAN SQUARE RESIDUALS
---------------------------------
     1     20  ST8              0.595
     2     19  ST7              0.500
     3     12  KEBUMEN          0.487
     4      3  KARANG ANYAR     0.371
     5      2  ALIAN            0.369

RANKED ROOT MEAN SQUARE RESIDUALS FOR SURFACE  1
     1     20  ST8              0.595            160.0    160.6
     2     19  ST7             -0.500            180.0    179.5
     3     12  KEBUMEN          0.487            209.0    209.5
     4      3  KARANG ANYAR    -0.371            362.0    361.6
     5      2  ALIAN           -0.369            291.0    290.6
     6      6  GOMBONG          0.369            265.0    265.4
     7     21  ST4             -0.233            171.0    170.8
     8      9  KLIRONG         -0.219            438.0    437.8
     9      7  KARANG GAYAM     0.214            173.0    173.2
```

```
    10      16  ST2              -0.179            182.0    181.8
    11      17  ST3               0.171            167.0    167.2
    12      14  SADANG            0.121            181.0    181.1
    13       4  SEMPOR           -0.107            277.0    276.9
    14      11  PETANAHAN         0.962E-01        396.0    396.1
    15       1  ADIMULYO         -0.861E-01        396.0    395.9
    16      15  ST1              -0.721E-01        188.0    187.9
    17      10  BANJAR NEGARA    -0.535E-01        474.0    473.9
    18      13  WADAS LINTANG     0.495E-01        123.0    123.0
    19       8  PURING            0.414E-01        338.0    338.0
    20      18  ST6               0.249E-01        182.0    182.0
    21       5  ROWOKELE          0.210E-01        270.0    270.0
LAPGRD SUMMARY STATISTICS
-------------------------
OUTPUT SURFACE AND ERROR GRIDS FOR SURFACE   1
NUMBER OF CELLS = 2488126      MEAN ERROR      =     9.2
MINIMUM ERROR   =     3.9      MAXIMUM ERROR   =    45.
MINIMUM VALUE   =    98.3      MAXIMUM VALUE   =   516.
MEAN SURF VALUE =    305.      STANDARD ERROR  =     3.8
```

February, April, June - November 1998

```
DATA SUMMARY
------------
NUMBER OF DATA POINTS READ      =     22
NUMBER OF POINTS WITHIN LIMITS =     22

 SURF  MEAN RELATIVE VARIANCE  ROOT MEAN REL VAR
    1                 1.00               1.00

SURFACE STATISTICS
------------------
SURF  RHO         NPTS  ERROR    SIGNAL     SURF     MEAN      STD DEV
   1 0.172E-01    22     0.0      22.0 *     1     355.59      136.1
   2 0.123E+06    22     2.3      19.7       2     523.91      137.4
   3 0.155E+15    22    17.0       5.0 *     3     429.14      123.5
   4 0.176E+06    22     3.0      19.0       4     290.36      83.24
   5 0.172E-01    22     0.0      22.0 *     5     99.227      31.65
   6 0.421E+05    22     1.1      20.9 *     6     196.05      56.49
   7 0.403E+06    22     4.8      17.2       7     551.41      117.3
   8 0.172E-01    22     0.0      22.0 *     8     615.00      119.7
 AVG 0.194E+14    22     3.5      18.5               382.59      107.2

SURF GCV         MSR         VAR        SURF  RTGCV   RTMSR      RTVAR
   1 0.229E+04 0.141E-11 0.568E-04      1   47.9   0.119E-05 0.753E-02
   2 0.189E+04 21.5      201.           2   43.5   4.64      14.2
   3 0.956E+04 0.571E+04 0.739E+04      3   97.8  75.6       86.0
   4 0.538E+04 98.6      728.           4   73.3   9.93      27.0
   5 156.      0.960E-13 0.387E-05      5   12.5   0.310E-06 0.197E-02
   6 0.201E+04 4.61      96.3           6   44.9   2.15      9.81
   7 0.114E+05 543.     0.248E+04       7   107.  23.3       49.8
   8 0.470E+04 0.288E-11 0.116E-03      8   68.6   0.170E-05 0.108E-01
 AVG 0.467E+04 797.     0.136E+04           68.3  28.2       36.9

SURF GML         MSE         VAR        SURF  RTGML   RTMSE      RTVAR
   1 0.454E+04 0.568E-04 0.499E-04      1    67.4   .753E-02 0.706E-02
   2 0.325E+04 180.      214.           2    57.0     13.4      14.6
   3 0.739E+04 0.168E+04 0.739E+04      3    86.0     41.0      86.0
   4 0.709E+04 630.      634.           4    84.2     25.1      25.2
```

```
   5 513.       0.387E-05 0.564E-05  5     22.7    .197E-02 0.237E-02
   6 0.298E+04 91.7       74.8       6     54.6       9.58       8.65
   7 0.116E+05 0.194E+04 0.196E+04  7     108.       44.1       44.3
   8 0.105E+05 0.116E-03 0.115E-03  8     102.    .108E-01 0.107E-01
 AVG 0.598E+04 565.      0.128E+04          77.3      23.8       35.8

SURF   COVARIATES AND STANDARD ERRORS
   1    0.244       0.553E-01    0.132E-03  0.574E-04
   2   -0.792       0.744        0.224      0.995E-01
   3     1.03      -0.595        0.478      0.220
   4   -0.212      -0.352        0.411      0.184
   5    0.317E-02  -0.159        0.345E-04  0.150E-04
   6   -0.237E-01   0.954        0.165      0.723E-01
   7   -0.429       0.814        0.673      0.314
   8   -0.332      -0.274        0.189E-03  0.822E-04

RANKED ROOT MEAN SQUARE RESIDUALS
---------------------------------
     1     13  KEBUMEN           59.9
     2     15  SADANG            48.9
     3     12  PETANAHAN         43.4
     4     10  KUWARASAN         39.5
     5      9  KLIRONG           38.7

RANKED ROOT MEAN SQUARE RESIDUALS FOR SURFACE  1
     1     20  ST7             -0.277E-05        364.0    364.0
     2     21  ST8              0.229E-05        343.0    343.0
     3      2  ALIAN           -0.178E-05        449.0    449.0
     4     13  KEBUMEN          0.177E-05        274.0    274.0
     5      6  GOMBONG          0.159E-05        305.0    305.0
     6      4  SEMPOR          -0.144E-05        438.0    438.0
     7      3  KARANG ANYAR    -0.141E-05        341.0    341.0
     8     19  ST6              0.117E-05        325.0    325.0
     9     17  ST2              0.104E-05        336.0    336.0
    10      1  ADIMULYO         0.809E-06        189.0    189.0
    11      5  ROWOKELE         0.793E-06        229.0    229.0
    12     18  ST3             -0.638E-06        370.0    370.0

RANKED ROOT MEAN SQUARE RESIDUALS FOR SURFACE  2
     1     21  ST8               10.8            478.0    488.8
     2      7  KARANG GAYAM     -9.05            507.0    498.0
     3      1  ADIMULYO         -7.38            596.0    588.6
     4     20  ST7              -6.65            497.0    490.3
     5      3  KARANG ANYAR      5.93            524.0    529.9
     6     15  SADANG           -5.72            702.0    696.3
     7     10  KUWARASAN         4.88            414.0    418.9
     8     16  ST1               4.34            525.0    529.3
     9     22  ST4              -3.64            533.0    529.4
    10     18  ST3               3.07            462.0    465.1
    11      2  ALIAN             3.05            597.0    600.1
    12     17  ST2               3.05            479.0    482.1

RANKED ROOT MEAN SQUARE RESIDUALS FOR SURFACE  3
     1     13  KEBUMEN           169.            161.0    329.6
     2     15  SADANG            138.            213.0    350.8
     3     12  PETANAHAN        -121.            372.0    251.3
     4      9  KLIRONG          -109.            384.0    274.5
     5     10  KUWARASAN         107.            257.0    363.7
     6      3  KARANG ANYAR     -89.9            459.0    369.1
```

7	8	PURING	89.5	222.0	311.5
8	20	ST7	-76.3	541.0	464.7
9	17	ST2	-71.9	606.0	534.1
10	18	ST3	68.1	506.0	574.1
11	2	ALIAN	-53.0	419.0	366.0
12	21	ST8	-53.0	507.0	454.0

RANKED ROOT MEAN SQUARE RESIDUALS FOR SURFACE 4

1	21	ST8	19.2	256.0	275.2
2	2	ALIAN	-18.5	400.0	381.5
3	13	KEBUMEN	16.7	184.0	200.7
4	20	ST7	-16.5	307.0	290.5
5	4	SEMPOR	-14.0	457.0	443.0
6	6	GOMBONG	12.7	251.0	263.7
7	1	ADIMULYO	10.3	137.0	147.3
8	5	ROWOKELE	9.85	283.0	292.9
9	10	KUWARASAN	-8.53	345.0	336.5
10	3	KARANG ANYAR	-7.43	232.0	224.6
11	19	ST6	6.66	268.0	274.7
12	18	ST3	6.65	256.0	262.6

RANKED ROOT MEAN SQUARE RESIDUALS FOR SURFACE 5

1	4	SEMPOR	-0.692E-06	159.0	159.0
2	6	GOMBONG	0.545E-06	79.0	79.0
3	22	ST4	-0.542E-06	96.0	96.0
4	21	ST8	0.466E-06	86.0	86.0
5	18	ST3	0.433E-06	92.0	92.0
6	5	ROWOKELE	0.429E-06	72.0	72.0
7	10	KUWARASAN	-0.364E-06	110.0	110.0
8	1	ADIMULYO	0.283E-06	72.0	72.0
9	12	PETANAHAN	-0.259E-06	163.0	163.0
10	20	ST7	-0.207E-06	90.0	90.0
11	3	KARANG ANYAR	-0.190E-06	66.0	66.0
12	16	ST1	-0.168E-06	93.0	93.0

RANKED ROOT MEAN SQUARE RESIDUALS FOR SURFACE 6

1	20	ST7	4.13	163.0	167.1
2	15	SADANG	-3.88	375.0	371.1
3	18	ST3	-3.64	187.0	183.4
4	21	ST8	-2.86	194.0	191.1
5	4	SEMPOR	-2.83	251.0	248.2
6	22	ST4	2.62	190.0	192.6
7	17	ST2	2.50	195.0	197.5
8	2	ALIAN	2.19	86.0	88.2
9	16	ST1	2.07	185.0	187.1
10	10	KUWARASAN	-1.78	210.0	208.2
11	6	GOMBONG	1.76	217.0	218.8
12	5	ROWOKELE	1.67	129.0	130.7

RANKED ROOT MEAN SQUARE RESIDUALS FOR SURFACE 7

1	3	KARANG ANYAR	-57.2	808.0	750.8
2	6	GOMBONG	50.7	538.0	588.7
3	20	ST7	-38.8	584.0	545.2
4	21	ST8	32.5	509.0	541.5
5	10	KUWARASAN	31.1	352.0	383.1
6	8	PURING	-25.0	511.0	486.0
7	17	ST2	22.0	493.0	515.0
8	4	SEMPOR	-21.9	627.0	605.1
9	12	PETANAHAN	21.7	338.0	359.7
10	19	ST6	13.4	503.0	516.4
11	15	SADANG	-9.84	732.0	722.2

```
    12     18  ST3              -9.40            534.0    524.6

RANKED ROOT MEAN SQUARE RESIDUALS FOR SURFACE  8
     1      7  KARANG GAYAM      0.400E-05       563.0    563.0
     2     16  ST1               0.274E-05       604.0    604.0
     3     21  ST8               0.253E-05       657.0    657.0
     4      4  SEMPOR           -0.252E-05       896.0    896.0
     5      2  ALIAN            -0.200E-05       767.0    767.0
     6     18  ST3              -0.199E-05       639.0    639.0
     7     17  ST2              -0.189E-05       610.0    610.0
     8     22  ST4              -0.177E-05       678.0    678.0
     9      5  ROWOKELE          0.160E-05       531.0    531.0
    10     20  ST7              -0.159E-05       680.0    680.0
    11     13  KEBUMEN           0.150E-05       606.0    606.0
    12      1  ADIMULYO         -0.125E-05       728.0    728.0

LAPGRD SUMMARY STATISTICS
-------------------------
OUTPUT SURFACE AND ERROR GRIDS FOR SURFACE   1
NUMBER OF CELLS = 2488126      MEAN ERROR      =    0.20E-01
MINIMUM ERROR   =    0.86E-02  MAXIMUM ERROR   =    0.98E-01
MINIMUM VALUE   =    108.      MAXIMUM VALUE   =   0.107E+04
MEAN SURF VALUE =    475.      STANDARD ERROR  =    0.83E-02

OUTPUT SURFACE AND ERROR GRIDS FOR SURFACE   2
NUMBER OF CELLS = 2488126      MEAN ERROR      =     35.
MINIMUM ERROR   =     16.      MAXIMUM ERROR   =    0.17E+03
MINIMUM VALUE   =   -243.      MAXIMUM VALUE   =   0.118E+04
MEAN SURF VALUE =    487.      STANDARD ERROR  =     14.

OUTPUT SURFACE AND ERROR GRIDS FOR SURFACE   3
NUMBER OF CELLS = 2488126      MEAN ERROR      =    0.12E+03
MINIMUM ERROR   =     88.      MAXIMUM ERROR   =    0.40E+03
MINIMUM VALUE   =    58.9      MAXIMUM VALUE   =   0.136E+04
MEAN SURF VALUE =    484.      STANDARD ERROR  =     41.

OUTPUT SURFACE AND ERROR GRIDS FOR SURFACE   4
NUMBER OF CELLS = 2488126      MEAN ERROR      =     66.
MINIMUM ERROR   =     31.      MAXIMUM ERROR   =    0.31E+03
MINIMUM VALUE   =    58.6      MAXIMUM VALUE   =    761.
MEAN SURF VALUE =    356.      STANDARD ERROR  =     26.

OUTPUT SURFACE AND ERROR GRIDS FOR SURFACE   5
NUMBER OF CELLS = 2488126      MEAN ERROR      =    0.53E-02
MINIMUM ERROR   =    0.23E-02  MAXIMUM ERROR   =    0.26E-01
MINIMUM VALUE   =    18.3      MAXIMUM VALUE   =    255.
MEAN SURF VALUE =    118.      STANDARD ERROR  =    0.22E-02

OUTPUT SURFACE AND ERROR GRIDS FOR SURFACE   6
NUMBER OF CELLS = 2488126      MEAN ERROR      =     26.
MINIMUM ERROR   =     11.      MAXIMUM ERROR   =    0.12E+03
MINIMUM VALUE   =   -292.      MAXIMUM VALUE   =    514.
MEAN SURF VALUE =    191.      STANDARD ERROR  =     10.

OUTPUT SURFACE AND ERROR GRIDS FOR SURFACE   7
NUMBER OF CELLS = 2488126      MEAN ERROR      =    0.11E+03
MINIMUM ERROR   =     57.      MAXIMUM ERROR   =    0.51E+03
MINIMUM VALUE   =    27.2      MAXIMUM VALUE   =    908.
MEAN SURF VALUE =    548.      STANDARD ERROR  =     44.
```

```
OUTPUT SURFACE AND ERROR GRIDS FOR SURFACE   8
NUMBER OF CELLS = 2488126       MEAN ERROR      =    0.29E-01
MINIMUM ERROR   =    0.12E-01   MAXIMUM ERROR   =    0.14
MINIMUM VALUE   =    -151.      MAXIMUM VALUE   =   0.102E+04
MEAN SURF VALUE =    583.       STANDARD ERROR  =    0.12E-01
```

March 1998

```
DATA SUMMARY
------------
NUMBER OF DATA POINTS READ      =     20
NUMBER OF POINTS WITHIN LIMITS =     20

 SURF  MEAN RELATIVE VARIANCE  ROOT MEAN REL VAR
    1                1.00              1.00

SURFACE STATISTICS
------------------
SURF RHO       NPTS   ERROR    SIGNAL   SURF   MEAN      STD DEV
   1 0.324E-01  20    0.0     20.0 *     1   362.80      132.2

SURF GCV       MSR        VAR       SURF RTGCV  RTMSR      RTVAR
   1 0.346E+04 0.806E-11 0.167E-03 1    58.8  0.284E-05 0.129E-01

SURF GML       MSE        VAR        SURF RTGML  RTMSE      RTVAR
   1 0.835E+04 0.167E-03 0.176E-03  1   91.4  0.129E-01 0.133E-01

SURF   COVARIATES AND STANDARD ERRORS
   1   -0.480       1.50        0.224E-03  0.952E-04

RANKED ROOT MEAN SQUARE RESIDUALS
---------------------------------
     1     16  ST3              0.544E-05
     2     13  SADANG           0.544E-05
     3     20  ST4              0.435E-05
     4     15  ST2              0.379E-05
     5      8  KUWARASAN        0.326E-05

RANKED ROOT MEAN SQUARE RESIDUALS FOR SURFACE  1
     1     16  ST3             -0.544E-05        245.0    245.0
     2     13  SADANG          -0.544E-05        578.0    578.0
     3     20  ST4              0.435E-05        269.0    269.0
     4     15  ST2              0.379E-05        258.0    258.0
     5      8  KUWARASAN       -0.326E-05        516.0    516.0
     6     14  ST1              0.322E-05        271.0    271.0
     7      1  ADIMULYO         0.312E-05        305.0    305.0
     8      7  KLIRONG         -0.300E-05        334.0    334.0
     9     10  PETANAHAN        0.270E-05        211.0    211.0
    10      6  KARANG GAYAM    -0.264E-05        267.0    267.0
    11      5  GOMBONG          0.186E-05        561.0    561.0
    12      3  SEMPOR          -0.176E-05        489.0    489.0
    13      2  KARANG ANYAR    -0.175E-05        439.0    439.0
```

```
    14      4  ROWOKELE          0.128E-05        431.0    431.0
    15     11  KEBUMEN           0.120E-05        240.0    240.0
    16     17  ST6               0.105E-05        241.0    241.0
    17     19  ST8               0.937E-06        269.0    269.0
    18     18  ST7              -0.197E-06        258.0    258.0
    19     12  WADAS LINTANG    -0.112E-06        600.0    600.0
    20      9  BANJAR NEGARA     0.716E-07        474.0    474.0


LAPGRD SUMMARY STATISTICS
-------------------------
OUTPUT SURFACE AND ERROR GRIDS FOR SURFACE   1
NUMBER OF CELLS = 2488126       MEAN ERROR      =    0.34E-01
MINIMUM ERROR   =    0.15E-01   MAXIMUM ERROR   =    0.17
MINIMUM VALUE   =   -315.       MAXIMUM VALUE   =    871.
MEAN SURF VALUE =    397.       STANDARD ERROR  =    0.14E-01
```

May 1998

```
DATA SUMMARY
------------
NUMBER OF DATA POINTS READ      =     21
NUMBER OF POINTS WITHIN LIMITS  =     21

 SURF  MEAN RELATIVE VARIANCE  ROOT MEAN REL VAR
    1                 1.00               1.00

SURFACE STATISTICS
------------------
SURF RHO        NPTS  ERROR    SIGNAL    SURF     MEAN      STD DEV
   1 0.165E-01  21     0.0      21.0 *     1    134.05       51.47

SURF GCV    MSR        VAR       SURF  RTGCV     RTMSR      RTVAR
   1 867.  0.513E-12 0.211E-04    1     29.4     0.716E-06 0.459E-02


SURF  GML        MSE        VAR      SURF RTGML   RTMSE      RTVAR
   1 0.193E+04 0.211E-04 0.211E-04  1  43.9   0.459E-02 0.459E-02

SURF   COVARIATES AND STANDARD ERRORS
   1   -0.136E-01  0.151         0.806E-04  0.350E-04

RANKED ROOT MEAN SQUARE RESIDUALS
---------------------------------
     1     12  KEBUMEN           0.140E-05
     2     19  ST7               0.133E-05
     3     20  ST8               0.132E-05
     4      8  KLIRONG           0.112E-05
     5      2  ALIAN             0.109E-05

RANKED ROOT MEAN SQUARE RESIDUALS FOR SURFACE  1
     1     12  KEBUMEN           0.140E-05        100.0    100.0
     2     19  ST7              -0.133E-05        113.0    113.0
     3     20  ST8               0.132E-05        102.0    102.0
     4      8  KLIRONG          -0.112E-05        198.0    198.0
     5      2  ALIAN            -0.109E-05        185.0    185.0
     6     11  PETANAHAN         0.935E-06         59.0     59.0
```

```
      7      6  GOMBONG            0.714E-06        117.0    117.0
      8     15  ST1                0.543E-06        104.0    104.0
      9     14  SADANG            -0.533E-06        133.0    133.0
     10     17  ST3               -0.448E-06        107.0    107.0
     11      3  KARANG ANYAR      -0.428E-06        144.0    144.0
     12     18  ST6                0.390E-06         97.0     97.0
     13      1  ADIMULYO          -0.325E-06        131.0    131.0
     14     21  ST4                0.259E-06        102.0    102.0
     15     16  ST2                0.249E-06        103.0    103.0
     16      7  KARANG GAYAM      -0.236E-06        108.0    108.0
     17      5  ROWOKELE          -0.157E-06        215.0    215.0
     18      4  SEMPOR            -0.143E-06        173.0    173.0
     19     13  WADAS LINTANG      0.990E-07        117.0    117.0
     20     10  BANJAR NEGARA     -0.971E-07        287.0    287.0
     21      9  KUWARASAN          0.509E-08        120.0    120.0

LAPGRD SUMMARY STATISTICS
-------------------------
OUTPUT SURFACE AND ERROR GRIDS FOR SURFACE   1
NUMBER OF CELLS = 2488126      MEAN ERROR     =    0.12E-01
MINIMUM ERROR   =    0.53E-02  MAXIMUM ERROR  =    0.60E-01
MINIMUM VALUE   =   -35.0      MAXIMUM VALUE  =    434.
MEAN SURF VALUE =    179.      STANDARD ERROR =    0.52E-02
```

December 1998

```
DATA SUMMARY
------------
NUMBER OF DATA POINTS READ     =     21
NUMBER OF POINTS WITHIN LIMITS =     21

 SURF  MEAN RELATIVE VARIANCE  ROOT MEAN REL VAR
    1                 1.00               1.00

SURFACE STATISTICS
------------------
SURF RHO       NPTS   ERROR    SIGNAL    SURF     MEAN     STD DEV
   1 0.775E+14  21    16.0       5.0 *     1     506.24     77.01


SURF GCV       MSR       VAR       SURF  RTGCV     RTMSR     RTVAR
   1 0.871E+04 0.506E+04 0.664E+04   1    93.3      71.1      81.5

SURF GML       MSE       VAR       SURF  RTGML     RTMSE     RTVAR
   1 0.664E+04 0.158E+04 0.664E+04   1    81.5      39.8      81.5

SURF   COVARIATES AND STANDARD ERRORS
   1    0.336     -0.208        0.464      0.214

RANKED ROOT MEAN SQUARE RESIDUALS
---------------------------------
     1      2  ALIAN             253.
     2     12  KEBUMEN           127.
     3     21  ST4               74.6
     4      7  PURING            63.6
     5     15  ST1               58.7

RANKED ROOT MEAN SQUARE RESIDUALS FOR SURFACE  1
     1      2  ALIAN             253.           246.0    499.1
```

2	12	KEBUMEN	-127.	615.0	488.0
3	21	ST4	-74.6	597.0	522.4
4	7	PURING	-63.6	541.0	477.4
5	15	ST1	-58.7	590.0	531.3
6	3	SEMPOR	56.6	463.0	519.6
7	1	ADIMULYO	48.5	428.0	476.5
8	4	ROWOKELE	44.8	470.0	514.8
9	5	GOMBONG	-43.4	533.0	489.6
10	18	ST6	-32.3	565.0	532.7
11	11	PETANAHAN	-28.7	493.0	464.3
12	16	ST2	25.2	507.0	532.2
13	14	SADANG	17.7	460.0	477.7
14	13	WADAS LINTANG	16.5	511.0	527.5
15	6	KARANG GAYAM	-12.2	550.0	537.8
16	10	BANJAR NEGARA	-10.2	521.0	510.8
17	19	ST7	-8.94	520.0	511.1
18	17	ST3	-8.56	560.0	551.4
19	20	ST8	3.71	503.0	506.7
20	8	KLIRONG	3.15	473.0	476.2
21	9	KUWARASAN	-0.921	485.0	484.1

```
LAPGRD SUMMARY STATISTICS
-------------------------
OUTPUT SURFACE AND ERROR GRIDS FOR SURFACE   1
NUMBER OF CELLS = 2488126      MEAN ERROR      =    0.11E+03
MINIMUM ERROR   =     84.      MAXIMUM ERROR   =    0.38E+03
MINIMUM VALUE   =    427.      MAXIMUM VALUE   =    799.
MEAN SURF VALUE =    521.      STANDARD ERROR  =     38.
```